Peroxisome Abundance and Lipid-Toxicity of Pancreatic β-Cells in Response to Saturated Fats

Helen Ruth Blair

B.Sc. (Hons) Newcastle University

Thesis submitted in partial fulfilment of the requirements for the degree of Doctor of Philosophy at Newcastle University

Faculty of Medical Sciences

Institute of Cellular Medicine

September 2014

Abstract

Lipotoxicity results from the accumulation of fats within non-adipose tissue, and is one of the causes of insulin resistance and β-cell dysfunction in type 2 diabetes. Recently candidate gene studies have identified a gene variant at the *PEX11*α gene locus which is associated with reduced β-cell function. *PEX11*α and *PEX11*β encode proteins involved in the division and proliferation of peroxisomes, which are responsible for the initial oxidation of very long chain and long chain fatty acids prior to complete oxidation in the mitochondria. The aim of this thesis was to explore the impact of altered *PEX11*α and *PEX11*β expression on peroxisome abundance and insulin secretion in cultured pancreatic β-cells. siRNAs specific for *PEX11*α and *PEX11*β were used to knock down expression in MIN6 cells.

Transfection resulted in 70% knockdown of *PEX11*α at all time points examined. There was no significant difference in the levels of insulin secreted at 25mM glucose between the *PEX11*α knockdown and the scrambled control cells. At 25mM glucose, 250μM palmitate decreased insulin secretion by 50% compared with the BSA control in the scrambled control cells. This was unchanged by *PEX11*α knockdown. Transfection with siRNA specific for *PEX11*β resulted in >80% reduction in expression at all time points examined. At 96hrs a 35% reduction in PMP-70 protein levels, a marker of peroxisome abundance, was also seen. Incubation with palmitate in the *PEX11*β knockdowns resulted in a significant increase in insulin secretion at 25mM glucose compared with the scrambled palmitate control.

Palmitate incubation decreased insulin secretion at 25mM glucose in untransfected control cells. However, *PEX11*α knockdown did not alter insulin secretion in the presence or absence of palmitate. *PEX11*β knockdown resulted in a decrease in PMP-70 protein. Unexpectedly, *PEX11*β knockdown led to the partial recovery of the inhibitory effect of palmitate on insulin secretion.

I would like to dedicate this thesis to my parents,

Harold and Patricia Blair

"*Great are the works of the Lord, studied by all who have pleasure in them.*"

Ps. 111

Acknowledgements

Firstly, I would like to thank my supervisor, Professor Mark Walker for giving me the opportunity to undertake my PhD within his research group, and allowing me to develop my passion for research. Thank you for your help, guidance and encouragement over the last 4 years.

Next, I would like to thank Audrey Brown, primarily for putting up with me! But especially for being there as someone, I could talk to, to bounce ideas off, and for helping me learn new techniques in the lab.

I would also like to thank all the members of lab M4.095 who have been there throughout my PhD. Thank you for making work a pleasurable place to be. I would especially like to thank Donna Nile for her continued support throughout my entire PhD. My thanks must also go to Helen Marshall, Catherine Arden and Michael White for all their help and expertise whilst I've carried out my project. Thanks to Amy Arran and Alison Heggie for your continued friendship.

I am grateful to the BBSRC their funding.

I owe Unilever a debt of gratitude for sponsoring my PhD and allowing me to further my research in their laboratories at Colworth Science Park. Special thanks to Dave Gunn, my industrial supervisor for his friendship and support. Thanks to Katrina MacAulay, Alan Heath, Alison Russell, Michael Van Grinkel and Tony Dadd for furthering my skills and knowledge. Thank you to everyone at Unilever Discover who helped to make my time there enjoyable.

Finally, I would like to thank my dad Harold, my mum Tricia and my brother Graham. Thank you for all your support and encouragement, and for listening to numerous phone calls, whether you knew what I was talking about or not.

Table of Contents

List of Tables

List of Figures

Abbreviations

4-PBA	4-Phenylbutyrate
ABC	ATP-binding cassette
ABCD1	ATP-binding cassette, sub-family D (ALD), member 1
ACAA1	acetyl-Coenzyme A acyltransferase 1
ACOX	Acyl-Coenzyme A oxidase
ADAMTS9	ADAM metallopeptidase with thrombospondin type 1 motif, 9
ADCY5	Adenylate cyclase 5
ADP	Adenosine Diphosphate
Akt	Protein kinase B
AMACR	Alpha-methylacyl-CoA racemase
APS	Ammonium Persulfate
ATP	Adenosine triphosphate
BCL11A	B-cell lymphoma/leukemia 11A
BCL2	B-cell CLL/lymphoma 2
bp	Base pairs
BSA	Bovine Serum Albumin
Ca^{2+}	Calcium
$CaCL_2$	Calcium Chloride
CAPS	N-cyclohexyl-3-aminopropanesulfonic acid
CDC123-CAMK1D	Cell division cycle 123 homolog (Saccharomyces cerevisiae)-Calcium/calmodulin-dependent protein kinase type 1D
CDKAL1	CDK5 regulatory subunit associated protein 1-like 1
CDKN2A/B	Cyclin-dependent kinase inhibitor 2A/2B
cDNA	Complementary DNA
CENTD2 (ARAP1)	ArfGAP with RhoGAP domain, ankyrin repeat and PH domain 1
CO_2	Carbon dioxide
CoA	Coenzyme A
COOH	Carboxylic acid
COS-7	Fibroblast-like cell line derived from monkey kidney tissue
CPT1	Carnitine palmitoyl transferase 1

Cy3	Cyanine3
DAG	Diacylglycerol
DAPI	4'.6-diamidino-2-phenylindole
DBP	D-bifunctional protein
DGKB/TMEM195	Diacylglycerol kinase, β 90 kDa/ Transmembrane protein 195
dH_2O	Distilled Water
DHCA	3α,7α-dihydroxy-5β-cholestanoic acid
DLP1	Dynamin like protein 1
DMEM	Dulbecco's Modified Eagle's Medium
DMSO	Dimethyl sulphoxide
DNA	Deoxyribonucleic acid
Dnase	Deoxyribonuclease
DRP	Dynamin-related proteins
dsRNA	Double-stranded DNA
DUSP9	Dual specificity phosphatase 9
ECL	Enhanced chemiluminescent
EDTA	Ethylene diamine tetraacetic acid
ELISA	Enzyme-linked immunosorbent assay
ER	Endoplasmic reticulum
ETC	Electron transport chain
FA	Fatty acid
FATP4	Fatty acid transport protein 4 (very-long-chain acyl-CoA synthetase)
FBS	Foetal Bovine Serum
Fe^{2+}	Iron (II) ion
FFA	Free fatty acid
Fis1	Mitochondrial fission protein 1
FITC	Fluorescein isothiocyanate
FTO	Fat mass and obesity-associated protein
GATAD2A	GATA zinc finger domain containing 2A
GCK	Glucokinase (Hexokinase 4)
GCKR	Glucokinase (hexokinase 4) regulator
GLUT	Glucose transporter

GSIS	Glucose stimulated insulin secretion
GTP	Guanosine triphosphate
GWAS	Genome wide association study
H_2O	Water
H_2O_2	Hydrogen Peroxide
HCl	Hydrogen Chloride
Hepes	4-(2-hydroxyethyl)-1-piperazineethanesulfonic acid
HepG2	Human liver cell line
HGP	Hepatic glucose production
HHEX/IDE	Hematopoietically expressed homeobox/Insulin-degrading enzyme
HMGA2	High mobility group AT-hook 2
HNF1A	HNF1 homeobox A
HNF1B (TCF2)	Hepatocyte nuclear factor 1-β
HO•	Hydroxyl radical
hr	Hours
HRP	Horse-radish peroxidase
IGF2BP2	Insulin-like growth factor 2 mRNA binding protein 2
iNOS	Inducible nitric oxide synthase
INS-1/1E	Rat insulinoma cell line
IRD	Infantile Refsum disease
IRS-1	Insulin receptor substrate 1
JAZF1	Juxtaposed with another zinc finger protein 1
KCl	Potassium chloride
KCNJ11	K inwardly-rectifying channel, subfamily J, member 11
KCNQ1	K voltage-gated channel, KQT-like subfamily, member 1
KF	Potassium fluoride
KH_2PO_4	Potassium dihydrogen phosphate
KLF14	Kruppel-like factor 14
LBP	L-bifunctional protein
LCFA	Long chain fatty acid
LD	Linkage disequilibrium
LDH	Lactate dehydrogenase

LPC	Lysophosphatidylcholine
MEF	Mouse embryonic fibroblasts
$MgCl_2$	Magnesium chloride
MIN6	Mouse insunlinoma cell line
Mn^{2+}	Manganese (II) ions
mRNA	Messenger RNA
MTNR1B	Melatonin receptor 1B
NaCl	Sodium Chloride
NADPH	Nicotinamide adenine dinucleotide phosphate
NAFLD	Non-alcoholic Fatty Liver disease
$NaHCO_3$	Sodium bicarbonate
NALD	Neonatal adrenoleukodystrophy
NEFA	Nonesterified fatty acid
NH_2	Amino group
NO	Nitric oxide
NOTCH2	Neurogenic locus notch homolog protein 2
$O_2\bullet$-	S anion
OD	Optical density
PBD	Peroxisomal biogenesis disorders
PBS	Phosphate buffered saline
PCR	Polymerase chain reaction
PEDs	Peroxisomal enzyme/transporter deficiencies
PEX	Peroxin (peroxisomal membrane protein)
PKB	Protein kinase B
PMP	Peroxisomal membrane protein
PPAR	Peroxisome proliferator-activated receptor
PPRE	Peroxisome Proliferator Response Element
PRC1	Protein regulator of cytokinesis 1
PROX1	Prospero homeobox 1
RA	Retinoic acid
RBMS1	RNA binding motif, single stranded interacting protein 1
RCDP1	Rhizomelic chondrodysplasia punctata Type 1

RINm5F	Rat insulinoma cell line
RISC	Relationship between Insulin Sensitivity and Cardiovascular Disease
RLU	Relative luminescence units
RNA	Ribonucleic acid
ROS	Reactive oxygen species
rpm	Revolutions per minute
RXR	Retinoid X receptor
SCPx	Sterol carrier protein X
Scr	Scrambled
SD	Standard deviation
SDS	Sodium dodecyl sulfate
SDS-PAGE	Sodium dodecyl sulfate polyacrylamide gel electrophoresis
SEM	Standard error of the mean
siRNA	Small Interfering RNA
SLC30A8	Solute carrier family 30 (zinc transporter), member 8
SNP	Single nucleotide polymorphism
TBE	Tris-borate-EDTA buffer
TCF7L2	Transcription factor 7 like 2
TE	Tris-EDTA buffer
TEMED	Tetramethylethylenediamine
TFAM	Transcription factor A, mitochondrial
THADA	Thyroid adenoma associated
TLE4 (CHCHD9)	Transducin-like enhancer protein 4
TNF-α	Tumor necrosis factor alpha
TP53INP1	Tumor protein p53 inducible nuclear protein 1
Tris	2-Amino-2-(hydroxymethyl)-1,3-propanediol
TRITC	Tetramethylrhodamine isothiocyanate
TSPAN8-LGR5	Tetraspanin 8-Leucine-rich repeat-containing G protein-coupled receptor 5
UCP	Uncoupling protein
UV	Ultra violet
VLCFA	Very long chain fatty acid

Vps1p	Dynamin-related protein in yeast
WFS1	Wolfram syndrome 1 (wolframin)
Wy14,643	4-Chloro-6-(2,3-xylidino)-2-pyrimidinylthioacetic acid (Pirinixic acid)
X-ALD	X-linked adrenoleukodystropy
Ykt6	YKT6 v-SNARE homolog
ZBED3	Zinc finger, BED-type containing 3
ZDF	Zucker Diabetic Fatty rat
ZFAND6	Zinc finger, AN1-type domain 6

Chapter 1

Introduction

1 Introduction

1.1 Diabetes Mellitus

Diabetes Mellitus is the most common disease of the pancreatic endocrine system. It is a complex disease characterised by high blood glucose levels (hyperglycaemia). Chronic hyperglycaemia (increased levels of blood glucose over a long period of time) can result in symptoms such as excessive passage of urine (polyuria), which can lead to an increase in thirst (polydipsia). Blurred vision can result from the swelling of the lens inside the eye, often due to osmolality changes with fluctuating blood glucose levels (WHO, 1999; Hernandez *et al.*, 2010). Weight loss can also occur as the body cells are unable to get the energy needed from glucose due to inadequate amounts of insulin. The body uses muscle and fat as an energy source which leads to the reduction in weight. This breakdown of other body tissues can lead to ketoacidosis which in turn can lead to coma, and without treatment, death. If diabetes continues long term without diagnosis and treatment, it can give rise to complications such as nephropathy which can result in kidney failure, retinopathy which can cause blindness, and neuropathy where in severe cases the nerve damage can lead to amputations. In patients with diabetes the risk of cerebrovascular, peripheral vascular and cardiovascular disease is also increased (WHO, 1999).

It is rapidly becoming a major global health problem (Figure 1), and in 2007 the Centers for Disease Control and Prevention in the USA classified the increase in diabetes incidence as an epidemic, an uncommon procedure for a non-infectious disease. In the UK alone, 3.8 million of the adult population are estimated to be diagnosed with the disease, and in 2013 it was estimated that as many as 630,000 people were yet to be diagnosed. It is thought that the number of people with the disease in the UK could rise to 5 million by 2025. (National Collaborating Centre for Chronic Conditions, 2008; Diabetes UK, 2014a; Diabetes UK, 2014b).

Diabetes is currently diagnosed when fasting blood glucose reaches high levels of ≥7.0mM (126mg/dl) (WHO, 2006). Normal blood glucose levels for adult diabetic patients before a meal tend to be between 4.0 and 7.0mM while in healthy individuals it is recommended to be between 3.5 and 5.5mM (Diabetes UK, 2009). Outside of the

normal range, high blood glucose levels, usually >8.5mM, is termed hyperglycaemia and low blood glucose levels, <4mM, hypoglycaemia (Diabetes UK, 2012).

There are two types of diabetes mellitus. Type 1 diabetes mellitus, predominantly arising in young people and children, is an autoimmune disease which results from the destruction of β-cells and leads to a complete absence of insulin. Patients are treated with injections of exogenous insulin to prevent the breakdown of fats and proteins which can lead to ketoacidosis. Type 2 diabetes mellitus is characterised by insulin resistance where target cells are unable to respond normally to the insulin and abnormal insulin secretion from the pancreatic β-cells. Patients can often control the diabetes through diet and oral therapies, but sometimes exogenous insulin may be required (Bell and Polonsky, 2001; Mathis *et al.*, 2001; Zimmet *et al.*, 2001).

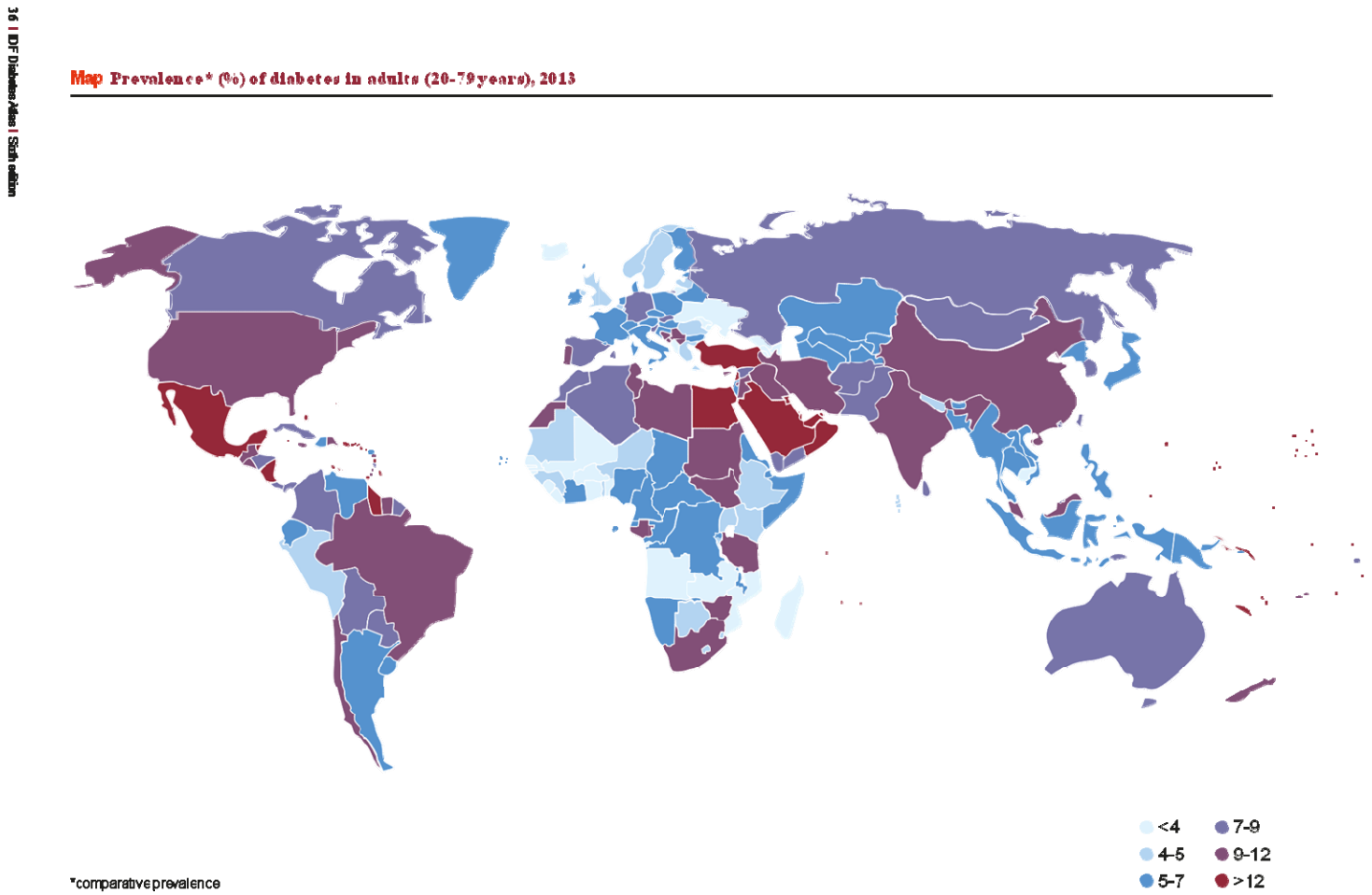

Figure 1 The estimated percentage of adult diabetes in the world in 2013

Map taken from Diabetes Atlas showing the estimated percentage worldwide diabetes in adults for 2013 (International Diabetes Federation, 2013).

1.1.1 Glucose Homeostasis

Metabolic control is tightly regulated, primarily by the endocrine system, with some influence from the nervous system. Regulation depends on the ratio of insulin to glucagon hormone levels both secreted by the islets of Langerhans in the pancreas (Pancreatic endocrine cells). Pancreatic islets (which make up less than 2% of total pancreatic tissue mass) consist of 4 specific cell types which secrete different peptide hormones. The majority of islet cells are insulin secreting β-cells. Alpha cells are responsible for secreting glucagon. The other cells, of which there are few, are D cells which secrete somatostatin, and some rare pancreatic polypeptide producing cells known as PP cells or F cells (Silverthorn, 2007).

In normal individuals blood glucose levels are controlled in a narrow range of between 4mM and 7mM by the balance of glucose absorption from food in the intestine, release of stored glucose from e.g. the liver, and glucose uptake and metabolism. Insulin is secreted by pancreatic β-cells in response to increases in blood glucose concentration (Figure 2). Secretion of insulin causes an increase in glucose uptake in storage tissues such as the muscles, adipose tissue and the liver, as well as inhibiting the release of glucose from the liver (Saltiel and Kahn, 2001).

In resting muscles and adipose tissue insulin activates a series of signalling cascades (Figure 3), some of which lead to the translocation of the GLUT4 glucose transporter to the cell surface from intracellular sites. The cells can then take up glucose by facilitated diffusion. When insulin is not present the GLUT4 transporters are not present on the membrane, and instead are stored within vesicles in the cytoplasm. In the liver glucose enters the cells via GLUT2 transporters with are continually expressed on the cell membrane. Insulin activates the enzyme hexokinase which phosphorylates glucose to glucose-6-phosphate thus ensuring the glucose concentration is lower on the inside of the cell, so glucose is able to be continually transported into the hepatocyte (liver cell) (Silverthorn, 2007).

As well as increasing glucose transport into cells, insulin activates enzymes for glycolysis (glucose metabolism), glycogenesis (glycogen synthesis) and lipogenesis (fat synthesis). At the same time glyogenolysis and lipolysis (glycogen and fat break down) as well as gluconeogenesis (glucose synthesis) are inhibited. Insulin also carries out

several other important roles, such as the support of cell growth and differentiation through the stimulation of protein synthesis. Dysregulation of these various processes due to insulin resistance and β-cell dysfunction can contribute to type 2 diabetes mellitus (Silverthorn, 2007).

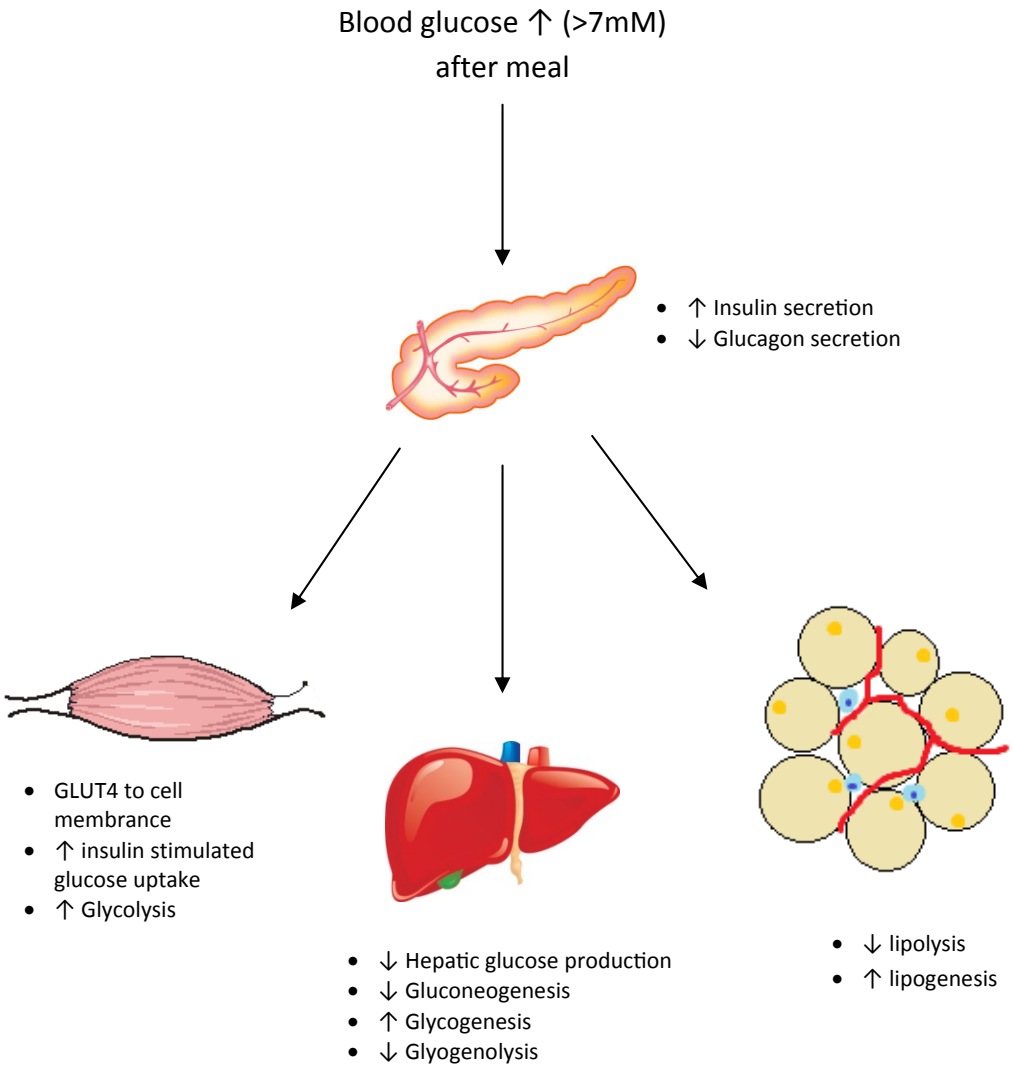

Figure 2 The role of insulin in glucose homeostasis

When glucose levels rise after a meal insulin is secreted which can inhibit or stimulate a variety of processes in order to stabilise the blood plasma levels. An increase in insulin causes GLUT4 to translocate to the cell membrane in muscle cells so glucose can be easily taken up which leads to an increase in the breakdown of glucose. In the liver, glucose synthesis and secretion, as well as glycogen breakdown are inhibited and glycogen synthesis is activated. Adipocytes reduce their fat breakdown so the body can use up glucose instead of fat, and the enzymes for fat synthesis are activated so any excess glucose can be stored as fat.

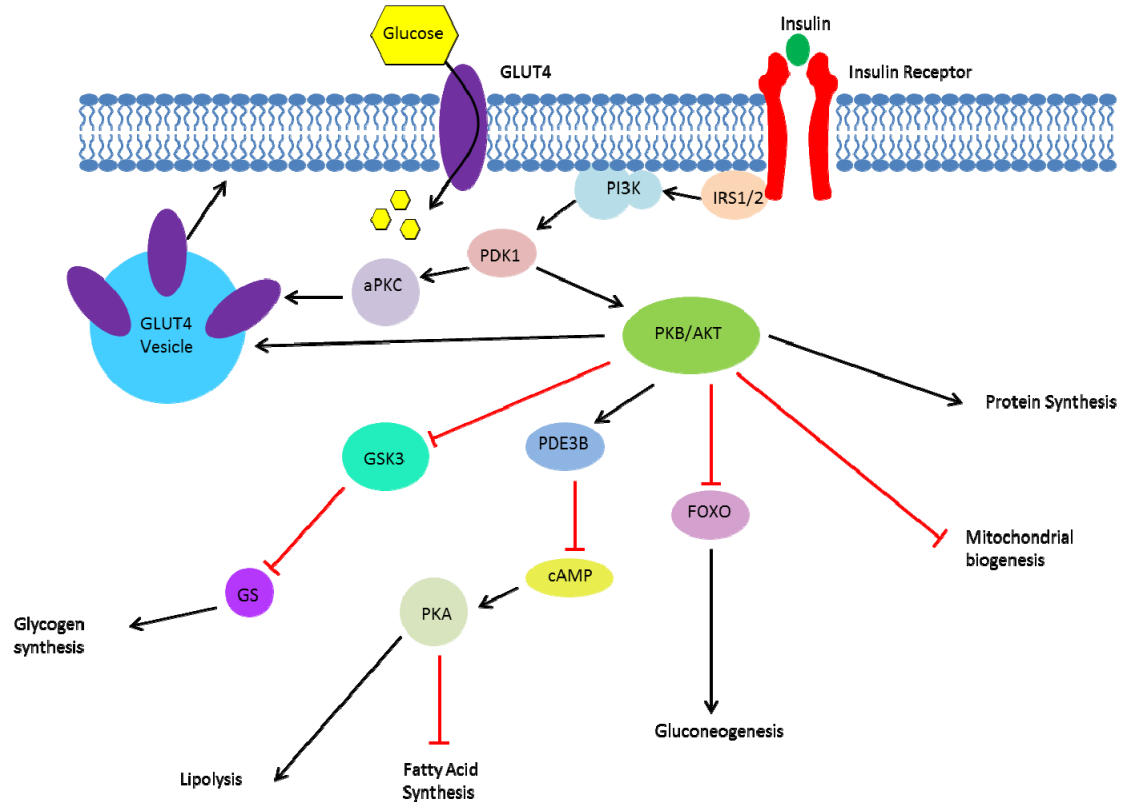

Figure 3 Insulin signalling pathway

Upon binding to its receptor, insulin initiates a series of signalling cascades. This shows some of the steps involved in insulin signalling which leads to decreases in gluconeogenesis and lipolysis, and increases in glycogen synthesis (glycogenesis), fatty acid synthesis (lipogenesis) as well as GLUT4 translocation to the cell membrane. (Adapted from (King, 2014))

1.1.2 Regulation of Insulin Secretion

Insulin is one of the most essential hormones of the pancreatic endocrine system, and is the only hormone capable of lowering blood glucose levels. When glucose levels rise following a meal, the pancreatic β-cells within the islets respond by secreting insulin. The mechanism involved in this begins with the transport of glucose across the cell membrane through the GLUT transporters (Figure 4). It has been reported that this is likely to be through GLUT1 and GLUT3 in human β-cells, while in rodent β-cells, it is GLUT2 that appears to be predominant (Rorsman and Braun, 2013).

Once inside the cell, glucose is subject to glycolysis which begins with the phosphorylation of glucose to glucose-6-phosphate by glucokinase. Glucokinase is the rate limiting step in GSIS. It acts as a glucose sensor, and activity is rapidly increased in response to glucose, with no increase in activity being seen following insulin stimulation. This enzyme is not inhibited by its product, glucose-6-phosphate which allows it to continually result in insulin secretion in response to rising glucose levels through the following process; after the production of glucose-6-phosphate, a series of metabolism steps leads to the production of pyruvate. Pyruvate is converted to acetyl-CoA in the mitochondrial matrix by pyruvate dehydrogenase. Acetyl-CoA can then enter the tricarboxylic acid (TCA) (Kreb's) cycle. During the TCA cycle, the electron carriers NADH and $FADH_2$ are produced, and from there are used to shuttle electrons across the electron transport chain (ETC). Following the ETC, ATP synthase generates ATP from ADP, thus causing an increase in the ATP/ADP ratio within the cytosol. The increase in the ATP/ADP ratio results in closure of the K_{ATP} channels which are a major determining factor of the cell membrane potential. The membrane depolarisation leads to the opening of voltage-dependent Ca^{2+} channels. Ca^{2+} influx upon opening of the channels results in the shuttling of insulin granules to the cell surface and a large increase in the rate of exocytosis of insulin (Matschinsky, 2002; Komatsu *et al.*, 2013; Rorsman and Braun, 2013).

Insulin secretion can also be regulated by neurotransmitters and other hormones. Upon activation of the parasympathetic nervous system, acetylcholine (Ach) can bind to the M3 muscarinc receptors on the cell surface membrane, causing a mild membrane depolarisation, and enhancement of glucose stimulated insulin secretion (GSIS) (Komatsu *et al.*, 2013; Rorsman and Braun, 2013). Glucagon-like peptide-1 (GLP-

1) is an incretin hormone secreted by the L-cells of the intestine upon stimulation by glucose or fat. GLP-1 is able to bind G-protein coupled receptors on the β-cell membrane and increase intracellular cAMP levels, elevating GSIS (Lim and Brubaker, 2006; Komatsu *et al.*, 2013; Rorsman and Braun, 2013). Somatostatin, released from the pancreatic δ-cells, and adrenaline which activates the α_2-adrenergic receptors can produce similar inhibitory effects on insulin secretion through membrane repolarisation (Rorsman and Braun, 2013). Pancreatic islets also contain the neurotransmitter GABA. Both $GABA_A$ and $GABA_B$ receptors are expressed on the β-cell surface and once activated can have stimulatory and inhibitory effects on insulin secretion respectively.

Free fatty acids (FFA) can also regulate insulin secretion. Although long term exposure of β-cells to fats results in lipotoxicity (discussed in section 1.4) and an inhibition of GSIS, short term exposure has been reported to be stimulatory. Although the mechanism resulting in the increase in insulin secretion is not fully determined, it is thought to be through an increase in intracellular Ca^{2+} which results in augmentation of exocytosis (Komatsu *et al.*, 2013; Rorsman and Braun, 2013).

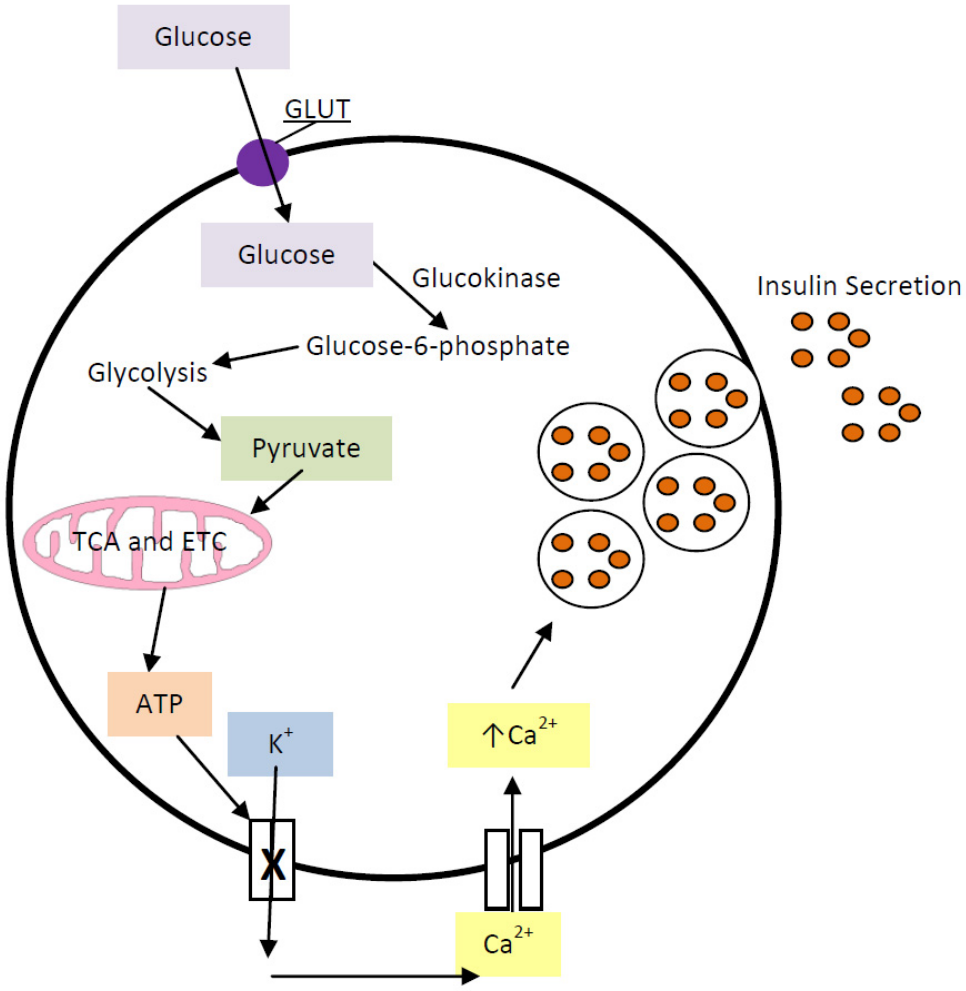

Figure 4 Glucose Stimulated Insulin secretion

Glucose is taken into the β-cell through the GLUT proteins expressed on the cell surface, and is metabolised by glycolysis to produce pyruvate. Pyruvate is converted to acetyl-CoA in the mitochondrial matrix and can then enter the TCA cycle which generates electron carriers NADH and FADH2. The electron transport chain (ETC) (oxidative phosphorylation) uses the electron carriers to shuttle electrons across the respiratory chain, producing ATP. The increase in ATP/ADP ratio results in the closure of ATP-gated K+ channels (KATP). Closure of KATP channels results in plasma membrane depolarisation, and therefore opening of voltage gated Ca^{2+} channels. The increase in cytosolic Ca^{2+} induces the migration of intracellular insulin granules to the cell surface. Fusion of insulin vesicles with the plasma membrane promotes exocytosis and secretion of insulin from the β-cell. (Adapted from (Gribble, 2009; Komatsu *et al.*, 2013))

1.1.3 Type 2 Diabetes Mellitus

Type 2 diabetes is primarily responsible for the diabetes epidemic seen in recent years. Not only is this epidemic occurring in developed countries but in developing countries as well. This increase in disease is partly due to people living longer, but also due to population growth and urbanisation, the increase in incidence of obesity and the reduction in the number of people carrying out physical activity. Currently 347 million people worldwide suffer with diabetes, with type 2 diabetes accounting for over 90% of these cases (Zimmet *et al.*, 2001; Wild *et al.*, 2004; WHO, 2013). Type 2 diabetes is also becoming increasing frequent in children and teenagers. Although type 1 is found more commonly in children, already in certain countries type 2 diabetes is beginning to predominate. The problem is added to by the fact that little is known about the diseases in children, and the use of type 2 diabetes therapies in children has not been approved. This issue needs to be resolved as the number of cases increase (Zimmet *et al.*, 2001; Hussain *et al.*, 2007).

Type 2 diabetes is not simply the lifestyle disease it is considered to be. It has strong genetic components with multiple gene effects and environmental factors contributing to whether the disease will develop. Despite the genetic influence, hyperglycaemia, when it does occur, is often seen later in life, but it is possible that diabetes may never arise (Bell and Polonsky, 2001; Scobie and Samaras, 2009).

The pathophysiology of type 2 diabetes is characterised by insulin resistance at target tissues, deterioration of insulin production from the pancreatic β-cells which can eventually lead to β-cell failure and death, and an inability to regulate hepatic glucose production (Mahler and Adler, 1999; Cherrington, 2005).

1.1.4 Insulin resistance

Obesity is primarily responsible for the insulin resistance seen in humans, with a weight reduction being associated with an improvement in insulin sensitivity (Bell and Polonsky, 2001; Chiasson and Rabasa-Lhoret, 2004). Insulin levels usually increase in obese subjects to uphold the normal glucose tolerance. Insulin secretion can be found to be three to four times greater in obese insulin resistant subjects compared with healthy controls. Excess insulin in the blood due to the hyper-secretion seen in obese insulin resistant subjects is often through an increase in β-cell mass as well as changes

in the expression of enzymes involved in β-cell glucose metabolism. These characteristics highlight the fundamental compensatory mechanisms involved in maintaining the normal glucose tolerance (Bell and Polonsky, 2001). It is the failure of these compensatory mechanisms that leads to the development of type 2 diabetes.

1.1.4.1 Mechanisms of Insulin Resistance

The insulin resistance seen in type 2 diabetes and obesity can result from a number of different mechanisms. TNF-α, a pro-inflammatory cytokine secreted by adipose tissue, has been found to be excessively expressed in obese subjects. Insulin signalling is impaired by exposure to TNF-α. It has been shown that TNF-α interferes directly with insulin signalling by causing a decrease in the tyrosine kinase activity of the insulin receptor, as measured by insulin-stimulated autophosphorylation of the receptor, and also reduces the successive phosphorylation of IRS-1 (insulin receptor substrate 1). IRS-1 is believed to play an important role in the insulin signal transduction pathway as a mediator of the tyrosine kinase activity of the insulin receptor, and is therefore essential for insulin action. It is thought that TNF-α may contribute to insulin resistance through local actions of the paracrine or autocrine systems. Inflammatory pathways are also activated in response to TNF-α, and thought to contribute to insulin resistance. TNF-α has additionally been shown to down-regulate various genes, including those for adiponectin, and the GLUT-4 glucose transporter, where decreased levels are associated with decreased insulin sensitivity. (Hotamisligil *et al.*, 1994; Yamauchi *et al.*, 2001; Nieto-Vazquez *et al.*, 2008).

Another mechanism insulin resistance can occur by is reduced expression of adiponectin. Adiponectin is an adipokine secreted from the adipose tissue which is involved in insulin sensitivity and glucose metabolism (Ziemke and Mantzoros, 2010). Adiponectin levels have been shown to be lower in obese subjects, and murine models with altered insulin sensitivity have shown that decreased expression of this adipokine is associated with insulin resistance. In addition to this, it has been reported that in murine models of obesity and type 2 diabetes, insulin resistance was reverse by restoration of adiponectin further supporting this method of insulin resistance (Yamauchi *et al.*, 2001).

It is also possible that circulating free fatty acids (FFA's) may contribute to insulin resistance as they are found to be raised in various insulin resistant conditions. One way in which they might contribute to diabetes and obesity is through the Randle glucose fatty acid cycle whereby the increase in fat oxidation is thought to inhibit glucose uptake and oxidation. In addition, glycogen synthesis is thought to be inhibited through elevated levels of FFA's and may induce insulin resistance (Kelley and Mandarino, 2000; Saltiel and Kahn, 2001; Boden and Shulman, 2002). Alternatively, it has been shown that increases in FFA in muscles can lead to large increases in incomplete β-oxidation of fatty acids in addition to the normal rates of complete fatty acid oxidation. This increase in incomplete fatty acid oxidation can lead to increases in ceramide and diacylglycerol (DAG) which impair insulin action. It is possible that ceramide works through the inhibition of Akt/PKB activation which is involved in the insulin signalling cascade, whereas DAG appears to lead to the activation of protein kinase C which results in a decrease in the tyrosine phosphorylation of IRS-1, inhibiting insulin action (Yu *et al.*, 2002; Holland *et al.*, 2007; Koves *et al.*, 2008).

Genetic factors can contribute to the sensitivity of tissues to insulin from reductions in receptor concentration, and glucose transporter translocation to decreases in kinase activity. As diabetes is a complex disease many polymorphisms in several genes involved in signalling, secretion and metabolism of insulin may influence the severity of the insulin resistance. The most severe forms of insulin resistance are often due to mutations within the insulin receptor, however, these are quite rare (Saltiel and Kahn, 2001).

1.1.5 Regulation of Hepatic glucose production

A problem caused by insulin resistance is the inability of insulin to suppress hepatic glucose production (HGP). Under normal circumstances this is possible through both direct and indirect mechanisms.

Insulin is able to reduce the secretion of glucagon (a hormone which stimulates the release of glucose) from pancreatic α-cells which, leading to a reduction in HGP. Insulin also leads to a reduction in the release of nonesterified fatty acids (NEFAs) from adipocytes, which reduces the supply of NEFAs to the liver. This allows the intermediate glucose-6-phosphate to be converted to lactate instead of glucose

(Nordlie *et al.*, 1999; Cherrington, 2005). In type 2 diabetes, where there is hepatic insulin resistance, there is a failure of insulin to regulate this gluconeogenesis, leading to uncontrolled hepatic glucose production, which contributes to hyperglycaemia.

1.1.6 Pancreatic β-Cell Dysfunction

Usually, as insulin resistance increases, the normal glucose tolerance is maintained as the insulin response from the pancreatic β-cells increases in proportion. However, in type 2 diabetes this mechanism falters. The insulin secretion is unable to balance the presiding level of insulin resistance leading to rising blood glucose levels and glucose intolerance (Bell and Polonsky, 2001).

The failure in the mechanism maintaining normal glucose levels could be due to long term exposure of pancreatic islet cells to free fatty acids (lipotoxicity). Insulin secretion rises in response to short term exposure of free fatty acids to the islet cells, however, there is evidence that long term exposure is toxic. Adipose tissue cannot cope with the high levels of fatty acids accumulating as they become saturated. This can lead to lipids being 'spilled' into non-adipose tissue such as the pancreas. This accumulation of fat within ectopic tissues leads to alternative toxic reactions and the formation of lipid moieties, which in turn can give rise to cellular dysfunction and programmed cell death (apoptosis) (Bell and Polonsky, 2001; Robertson *et al.*, 2004; Kusminski *et al.*, 2009).

It has also been shown that proliferation of β-cells is suppressed after long term exposure to elevated glucose levels (glucotoxicity). Over time glucose was shown to cause apoptosis of β-cells but there was large variation between cells indicating a genetic influence (Donath *et al.*, 2005).

Some forms of type 2 diabetes can be due to mutations within the mitochondrial genome which can cause reduced function of pancreatic β-cells, and therefore a reduction in the secretion of insulin. Although this information shows that mitochondrial function is important in the secretion of insulin, diabetes due to a primarily mitochondrial cause is very rare (Maechler and Wollheim, 2001).

1.1.7 Genetic Risk Factors in Diabetes

Type 2 diabetes is a complex disease with a strong genetic influence, with many susceptibility genes affecting β-cell function. Several genome-wide association studies (GWAS) have been carried out in recent years and have led to rapid progress in type 2 diabetes research.

Studies carried out in 2007 identified six new gene regions resulting in a total of 11 known gene regions altering the risk of developing type 2 diabetes (Diabetes Genetics Initiative of Broad Institute of *et al.*, 2007; Frayling, 2007; Frayling *et al.*, 2007; Scott *et al.*, 2007; Sladek *et al.*, 2007; Steinthorsdottir *et al.*, 2007; The Wellcome Trust Case Control Consortium, 2007; Zeggini *et al.*, 2007). The GWAS confirmed that the previously identified genes *TCF7L2* (transcription factor 7 like 2), *PPARG* (peroxisome proliferator-activated receptor-γ) and *KCNJ11* (potassium inwardly-rectifying channel, subfamily J, member 11) are involved in type 2 diabetes as well as identifying the 6 novel susceptibility loci. These novel associations were found close by, or within *CDKN2A-2B* (gene locus encoding cyclin-dependent kinase inhibitor genes), *HHEX-IDE* (haematopoietically expresses homeobox), *CDKAL1* (CDK5 regulatory-subunit-associated protein 1-like 1), *IG2BP2* (insulin-like growth factor 2 mRNA-binding protein 2), *SLC30A8* (solute carrier family 4, member 8 - zinc transporter), and *FTO* (fat mass and obesity-associated) (Sladek *et al.*, 2007; Steinthorsdottir *et al.*, 2007; Zeggini *et al.*, 2007). Although little is known of how *TCF7L2* predisposes to diabetes, *HHEX*, which is one of its targets, seems to be an acceptable candidate within the *HHEX-IDE* locus, as the transcription factor it encodes has a crucial role in pancreatic development. This association, in combination with: *CDKN2A*; encoding p16INK which when over-expressed lead to reduced islet proliferation in aging mice, and *CDKAL1*; expressed in high numbers in human islets and shares homology with a known inhibitor of CDK5 activation (CDK5 is associated with reduced β-cells function), points to an underlying risk associated with altered β-cell function (Krishnamurthy *et al.*, 2006; Pascoe *et al.*, 2007; Steinthorsdottir *et al.*, 2007).

The GWAS studies of 2007 led onto the meta-analysis of three GWAS (Diabetes, Genetics, Replication and Meta-analysis (DIAGRAM) consortium) which were able to identify a further 6 type 2 diabetes susceptibility loci affecting β-cell function. The six gene regions detected that reached genome wide significant levels for association

were *JAZF1*, *CDC123-CAMK1D*, *TSPAN8-LGR5*, *THADA*, *ADAMTS9* and *NOTCH2* (Zeggini *et al.*, 2008; McCarthy and Zeggini, 2009). In 2010 another meta-analysis carried out by the Meta-analysis of Glucose and Insulin related traits Consortium (MAGIC), using the data from 21 GWAS, identified another 5 type 2 diabetes associated risk genes which included *ADCY5*, *PROX1*, *GCK*, *GCKR* and *DGKB-TMEM195* further increasing the numbers of associated risk loci (Dupuis *et al.*, 2010). With the updated meta-analysis from the DIAGRAM consortium and data from other independent GWAS, more susceptibility loci have been discovered bringing the total that have an associated type 2 diabetes risk to almost 60, some of which can be seen in Table 1. Most of these genetic variants have been shown to affect pancreatic β-cell function (Qi and Hu, 2012).

Locus	SNP	Chr	Protein	Probable mechanism
Candidate and large-scale association				
PPARG	rs1801282	3	Peroxisome proliferator-activated receptor-γ	Insulin action
KCNJ11	rs5219	11	K inwardly-rectifying channel, subfamily J, member 11	β-cell function
TCF7L2	rs7903146	10	Transcription factor 7-like 2	β-cell function
WFS1	rs10010131	4	Wolfram syndrome 1 (wolframin	β-cell function
HNF1B (TCF2)	rs4430796	17	Hepatocyte nuclear factor 1-β	unknown
BCL2	rs12454712	18	B-cell CLL/lymphoma 2	Unknown
GATAD2A	rs3794991	19	GATA zinc finger domain containing 2A	Unknown
GWAS				
IGF2BP2	rs4402960	3	Insulin-like growth factor 2 mRNA binding protein 2	β-cell function
CDKAL1	rs10946398	6	CDK5 regulatory subunit associated protein 1-like 1	β-cell function
SLC30A8	rs13266634	8	Solute carrier family 30 (zinc transporter), member 8	β-cell function
CDKN2A/B	rs10811661	9	Cyclin-dependent kinase inhibitor 2A/2B	β-cell function
HHEX/IDE	rs1111875	10	Hematopoietically expressed homeobox/Insulin-degrading enzyme	β-cell function
FTO	rs8050136	16	Fat mass and obesity-associated protein	Obesity
NOTCH2	rs10923931	1	Neurogenic locus notch homolog protein 2 (Drosophila)	Unknown
THADA	rs7578597	2	Thyroid adenoma associated	β-cell function
ADAMTS9	rs4607103	3	ADAM metallopeptidase with thrombospondin type 1 motif, 9	Insulin action
JAZF1	rs864745	7	Juxtaposed with another zinc finger protein 1	β-cell function
CDC123-CAMK1D	rs1277979032	10	Cell division cycle 123 homolog (Saccharomyces cerevisiae)-Calcium/calmodulin-dependent protein kinase type 1D	β-cell function
TSPAN8-LGR5	rs7961581	12	Tetraspanin 8-Leucine-rich repeat-containing G protein-coupled receptor 5	β-cell function
KCNQ1	rs231362	11	K voltage-gated channel, KQT-like subfamily, member 1	β-cell function
IRS1	rs2943641	2	Insulin receptor substrate 1	Insulin action
MTNR1B	rs10830963	11	Melatonin receptor 1B	β-cell function
PROX1	rs340874	1	Prospero homeobox 1	β-cell function
BCL11A	rs243021	2	B-cell lymphoma/leukemia 11A	Unknown
GCKR	rs780094	2	Glucokinase (hexokinase 4) regulator	Insulin action
RBMS1	rs7593730	2	RNA binding motif, single stranded interacting protein 1	Insulin action
ADCY5	rs11708067	3	Adenylate cyclase 5	Unknown
ZBED3	rs4457053	5	Zinc finger, BED-type containing 3	Unknown
GCK	rs4607517	7	Glucokinase (Hexokinase 4)	β-cell function
DGKB/TMEM195	rs2191349	7	Diacylglycerol kinase, β 90 kDa/ Transmembrane protein 195	β-cell function
KLF14	rs972283	7	Kruppel-like factor 14	Unknown
TP53INP1	rs896854	8	Tumor protein p53 inducible nuclear protein 1	Unknown
TLE4 (CHCHD9)	rs13292136	9	Transducin-like enhancer protein 4	Unknown
CENTD2 (ARAP1)	rs1552224	11	ArfGAP with RhoGAP domain, ankyrin repeat and PH domain 1	β-cell function
HMGA2	rs1531343	12	High mobility group AT-hook 2	Unknown
HNF1A	rs7957197	12	HNF1 homeobox A	Unknown
PRC1	rs8042680	15	Protein regulator of cytokinesis 1	Unknown
ZFAND6	rs11634397	15	Zinc finger, AN1-type domain 6	Unknown
DUSP9	rs5945326	X	Dual specificity phosphatase 9	Unknown

Table 1 Susceptibility genes for type 2 diabetes

Adapted from two papers, (Bonnefond *et al.*, 2010; Qi and Hu, 2012), showing type 2 diabetes susceptibility genes, most of which have been discovered in genome wide association studies in recent years. The majority of the susceptibility genes appear to have an association with β-cell function.

1.2 Peroxisomes

Derived from the endoplasmic reticulum, peroxisomes are single membrane bound organelles which play major parts in metabolic pathways such as the oxidation of lipids, as well as plasmalogen biosynthesis and hydrogen peroxide metabolism. These metabolic activities are essential for human development, as is apparent from the number of peroxisomal disorders, some of which are lethal, arising through the failure of peroxisomes to properly assemble or defects in peroxisomal enzymes (Li *et al.*, 2002a; Fagarasanu *et al.*, 2007; Wanders *et al.*, 2010).

1.2.1 Peroxisomal Biogenesis

It has recently come to light that peroxisomal biogenesis begins in the endoplasmic reticulum (ER) (Figure 5). Evidence suggests that peroxisome biogenesis begins with the sorting of group 1 peroxisomal membrane proteins (PMPs) in the ER. In mammals PEX16 (peroxin 16), a group 1 PMP, is incorporated cotranslationally into the ER membrane. It has been shown that PEX16 is able to recruit other PMPs which are sorted into specialised subdomains within the ER (Geuze *et al.*, 2003; Kim *et al.*, 2006; Fagarasanu *et al.*, 2007). Then, it appears that, these subdomains form lamellar structures containing the peroxisomal proteins PMP70 and PEX13 which extend from the ER before detaching to become pleomorphic tubular-saccular carriers. This separation from the ER leads to the formation of the peroxisomal reticulum which is able to recruit thiolase and catalase (peroxisomal matrix proteins) from the cytosol. The matrix proteins are sorted into areas of the peroxisomal reticulum which then bud off to produce mature globular peroxisomes (Geuze *et al.*, 2003).

There is also evidence to suggest that a number of peroxisomes arise though division of pre-existing peroxisomes (Figure 5). Some studies in yeast and mammals have pointed to the independent division of peroxisomes without any input from the ER (Hoepfner *et al.*, 2001; Koch *et al.*, 2003). Studies showing that *PEX11* expression is associated with peroxisome proliferation support these findings (Schrader *et al.*, 1998; Li and Gould, 2002). This suggests that the biogenesis of peroxisomes can occur via two pathways, firstly through the peroxisomal endomembrane system derived from the ER, and secondly by the division and proliferation of pre-existing peroxisomes.

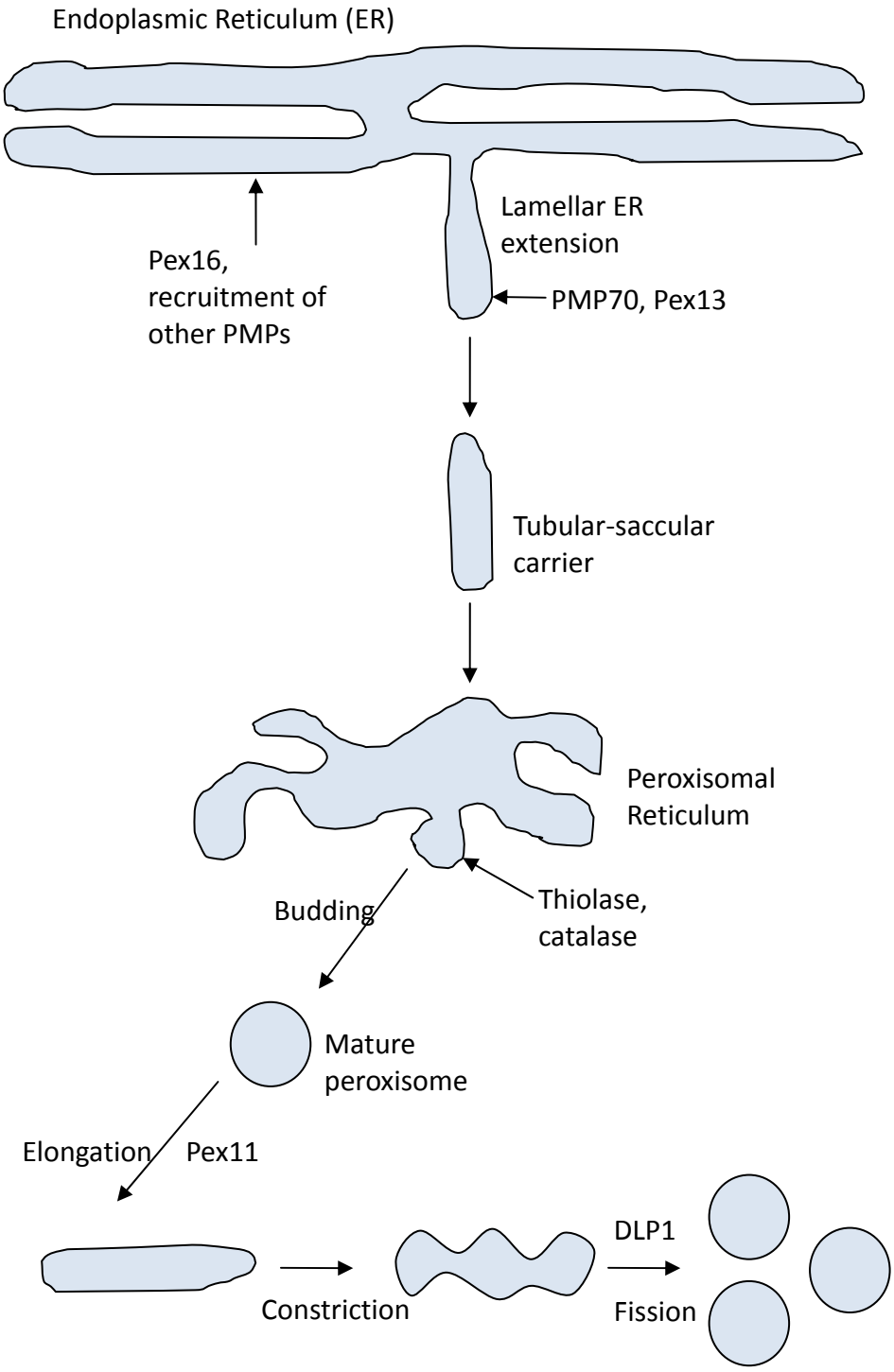

Figure 5 Peroxisome Biogenesis and Proliferation in Mammalian Cells

Diagram adapted from 2 papers (Titorenko and Mullen, 2006; Fagarasanu *et al.*, 2007). Peroxisome biogenesis begins at the ER where PMP's are recruited. A lamellar extension eventually buds from the ER to join the peroxisomal reticulum. Thiolase and catalase are recruited before a mature peroxisome buds off. Mature peroxisomes can also elongate with the involvement of PEX11 proteins. The elongated peroxisome constricts and DLP1 is involved in the fission to produce several peroxisomes.

1.2.2 Peroxisomal Proliferation

It has been shown that peroxisomes can divide independently of peroxisomal metabolism and extracellular stimuli (Schrader *et al.*, 1998; Li and Gould, 2002). In one study it was shown that over expression of the *PEX11*β gene, one of the human *PEX11* isoforms, was able to mediate peroxisomal proliferation without an extracellular stimulus. In the same study, it was also shown that over expression of *PEX11*α, another human isoform, was able to produce a similar result, but to a lesser extent. Human cells were transfected with plasmids for either expression of *PEX11*α or *PEX11*β. Cells transfected with the plasmid for *PEX11*β efficiently produced an increase in peroxisome proliferation. In the cells transfected with plasmids for *PEX11*α expression, less than 5% of the cells were showing increases in the abundance of peroxisomes. Although the percentage of cells showing the increases was small the increase in peroxisome abundance in these cells was similar to that seen in the cells induced by increases in *PEX11*β expression. When looking at mRNA levels, it was reported that *PEX11*β mRNA levels were fairly consistent throughout tissues, whereas *PEX11*α mRNA levels were very variable, with some tissues having a dramatic change when induced with peroxisome-proliferating agents. This suggested that *PEX11*β is likely to be involved in essential regulation of background peroxisomal abundance, and *PEX11*α, in the control of peroxisome number in response to extracellular stimuli (Schrader *et al.*, 1998).

Division of peroxisomes appears to have three main stages and begins with the elongation of the circular peroxisomes into tubules where PEX11 proteins are involved. This is then followed by constriction of the peroxisomal membrane, and finally fission of the peroxisomes, both which are catalysed by dynamins, and dynamin-related proteins (DRP).

1.2.2.1 Elongation of Peroxisomes: PEX11 Proteins

PEX11 (or peroxin 11) proteins are peroxisomal membrane proteins (PMPs). In addition to *PEX11*, several other PEX genes have been identified, and mutations within these genes are often the cause of many severe peroxisomal disorders. *PEX11* has been shown to play an essential role in peroxisomal division in both mammals and yeast (Marshall *et al.*, 1995; Abe and Fujiki, 1998; Schrader *et al.*, 1998; van Roermund *et al.*, 2000).

The first PEX11 protein found to be involved in peroxisome division was PEX11p (once called PMP-27) in the yeast *Saccharomyces cerevisiae.* It was shown that over-production of PEX11p led to elongated peroxisomal structures and an increase in the number of peroxisomes. Also, in the absence of PEX11p it was noted that large peroxisomes are present as fission does not occur easily, leading to few peroxisomes within the cell (Erdmann and Blobel, 1995; Marshall *et al.*, 1995).

There are 3 forms of PEX11 identified in mammals; PEX11α, PEX11β and PEX11γ. All three PEX11 protein isoforms are integral peroxisomal membrane proteins (PMP) with their carboxyl (COOH) termini and their amino (NH_2) termini exposed to the cytosol, and are anchored in place by two membrane spanning domains (Schrader *et al.*, 1998; Tanaka *et al.*, 2003).

Further indicating a role for *PEX11* in peroxisome proliferation, *PEX11*β knockout mice have a reduction in peroxisome abundance which led to about a 40% increase in liver very long chain fatty acids (VLCFA). In cultured cells the *PEX11*β deficiency led to about a 40% decrease in VLCFA metabolism. It was also noted that the loss of *PEX11*β led to a 1.5 fold increase in hepatic *PEX11*α expression. The *PEX11*β knockout mice were also shown to have several symptoms seen in the lethal disease Zellweger syndrome, however, these mice did not have any defects in the import of proteins to the peroxisomes and only mild defects in the metabolic function of the peroxisome were seen (Li *et al.*, 2002b).

Although the mechanism of action of PEX11 proteins is unknown, it is likely that they exert their effects through binding of phospholipids and the modification of the peroxisomal membrane (Fagarasanu *et al.*, 2007). Evidence suggests that PEX11 proteins are likely to promote peroxisome proliferation through membrane elongation but are unable to constrict or divide the peroxisomes themselves. When cells are deficient in functional DRP, which are responsible for fission of the elongated peroxisome, peroxisome number decreases and peroxisomes are seen as large tubular structures (Koch *et al.*, 2003; Schrader, 2006).

1.2.2.2 Constriction of the Peroxisomal Membrane

Little is known of the mechanisms leading to constriction of the peroxisomal membrane. Koch et al. (2004) found that in the absence of DLP1 (dynamin like protein

1) in COS-7 cells, elongated peroxisomes were seen to display segmented characteristics, giving them the appearance of beads on a string. These segmented peroxisomes were unable to divide into circular peroxisomes showing that constriction, but not division, occurs independently of dyanmins and DRPs. To confirm that DLP1 was not involved in constriction anti-DLP1 antibodies were used to detect the presence of the protein in the cells. In cells where DLP1 had been knocked down with siRNA very little of the protein was detected, and what was there was not associated with the elongated peroxisomes constriction sites. It is likely that the peroxisomal membrane has to thin down for DRPs to work efficiently to cause fission of the elongated peroxisome (Koch *et al.*, 2004).

In the same study it was also found that over expression of *PEX11*β, with the absence of DLP1, led to considerably more elongation of the peroxisomes than with the absence of DLP1 alone. It was also found that under these conditions, the segmented appearance of the peroxisomes appeared to be lost, and it was seen that tubulorecticular networks of the peroxisomes formed. This showed that although PEX11 proteins are important in the division of peroxisomes, PEX11β, and possibly the other mammalian PEX11 proteins are important in expansion and growth of the peroxisomal compartment rather than constriction and fission (Koch *et al.*, 2004). It is thought that *PEX11*β expression may have an influence in the assembly of constriction factors, and the modification of the peroxisomal membrane which may lead, through an indirect mechanism, to the recruitment of DLP1 to the peroxisomal membrane (Li and Gould, 2003; Koch *et al.*, 2004).

Further investigation is needed into the mechanism peroxisomal constriction. It is possible that it is mediated by PEX11β and Fis1 (the membrane adapter of DLP1), in combination with other unknown factors but this remains to be established (Delille *et al.*, 2010).

1.2.2.3 Fission of Elongated Peroxisomes: Dynamins and Dynamin Related Proteins

Dynamins and Dynamin related proteins (DRPs) are members of the dynamin family of large GTPases. All proteins in this family have a highly conserved N-terminal GTPase domain. They are involved in many essential cellular events from fission of membranes to anti-viral activity. DRPs are involved in the fission of the peroxisomal membrane,

leading to the formation of new peroxisomes (Danino and Hinshaw, 2001; Hoepfner *et al.*, 2001; Koch *et al.*, 2004; Thoms and Erdmann, 2005).

Hoefner et al (2001) were the first to report involvement of DRPs in the division of peroxisomes. Vps1p, a DRP in the yeast *Saccharomyces cerevisiae*, when deleted from the yeast genome, caused a reduction in the number of peroxisomes. Only a single large peroxisome was seen in most cells (Hoepfner *et al.*, 2001).

Dynamin like protein 1 (DLP1) is a mammalian DRP similar to Vps1p in yeast. It has been found to have a major role in peroxisomal division in mammalian cells (Koch *et al.*, 2003; Li and Gould, 2003). It has been shown that expression of a dominant negative DLP1 mutant deficient in GTP hydrolysis, or siRNA silencing of DLP1 led to a complete inhibition of peroxisomal division. Peroxisomes accumulated in elongated form and peroxisomal networks were seen. These results show that DLP1 has a direct effect in peroxisomal fission (Koch *et al.*, 2003). Consistent with these finding, another study also showed that loss of a functional DLP1 led to the inhibition of peroxisomal fission, but not inhibition of elongation (Li and Gould, 2003). Both of these studies found that DLP1 localised to the elongated peroxisomes, which was easier to detect when *PEX11*β was over expressed due to its ability to increase peroxisomal division and therefore increase the number of elongated tubular peroxisomes available to view within the cell (Koch *et al.*, 2003; Li and Gould, 2003). DLP1 was found in spots along the elongated peroxisome prior to fission (Koch *et al.*, 2003).

Dynamins contain a pleckstrin homology domain which is involved in membrane binding. DRPs don't contain this domain, meaning that other factors are needed to recruit DRPs to the membrane (Koch *et al.*, 2003; Koch *et al.*, 2005; Fagarasanu *et al.*, 2007). It was already known that Fis1 interacts with DLP1 in mammalian cells in the regulation of mitochondrial fission, which prompted investigation into whether Fis1 had a role in peroxisomal fission as one of these recruitment factors. Compared with *PEX11*β studies, similar results were seen for knockdown and increased expression of Fis1. The over expression of Fis1 causes an increase in peroxisomal fission as well as mitochondrial fission, whereas the loss of Fis1 leads to the presence of elongated peroxisomes (Koch *et al.*, 2005). Fis1 is a limiting factor in the fission of the peroxisomal membrane, as shown by these results since a functional DLP1 is required

for peroxisomal fission. As Fis1 interacts with DLP1, it is therefore a likely candidate that leads to the localisation of DLP1 to the peroxisomal membrane (Fagarasanu *et al.*, 2007).

1.3 Fatty Acid Oxidation

1.3.1 β-Oxidation of Fatty Acids

Fatty Acid (FA) β-oxidation is a process conserved in peroxisomes throughout a variety of species including yeast, plants and animals. Unlike yeast and plants where peroxisomes are the only site of β-oxidation, in other eukaryotes, β-oxidation can be carried out in both peroxisomes and mitochondria (Wanders and Waterham, 2006; Fidaleo, 2009). Although peroxisomes contain all the enzymes required to complete the β-oxidation process, intermediates are transported out of peroxisomes to the mitochondria before completion, and are then fully oxidised within the mitochondria (Wanders *et al.*, 2010). This has been well established in the oxidation of pristanic acid which undergoes three cycles of β-oxidation within the peroxisome, and then it seems that it is converted to the carnitine ester and exported from the peroxisome (Figure 6). It is then imported into the mitochondria where oxidation is completed to eventually produce carbon dioxide (CO_2) water (H_2O) (Verhoeven *et al.*, 1998; Wanders *et al.*, 2010).

Mitochondria are responsible for the oxidation of short chain with <6 carbon atoms, medium chain with 6-12 carbon atoms, and the majority of long chain fatty acids (LCFAs) with carbon chain lengths of >12. Although peroxisomes oxidise some LCFAs, they are primarily responsible for the oxidation of very long chain fatty acids (VLCFAs), with ≥ 22 carbons in the fatty acid chain, and branched chain fatty acids. In both mitochondria and peroxisomes there are several stages to β-oxidation which include dehydrogenation, hydration, dehydrogenation again, and thiolytic cleavage (Wanders and Waterham, 2006; Fidaleo, 2009; Wanders *et al.*, 2010; Kihara, 2012; Hara *et al.*, 2014).

Dehydrogenation: The first step in peroxisomal β-oxidation is catalysed by acyl-CoA oxidases (ACOX). These enzymes catalyse the formation of double bonds and hydrogen peroxide (H_2O_2) is formed which can then be split into oxygen and water. Human peroxisomes contain two ACOX enzymes. ACOX1 is responsible for the dehydrogenation of straight VLCFAs, and ACOX2, for the dehydrogenation of 2-methyl branched chain fatty acids such as pristanoyl-CoA (Wanders, 2004; Wanders and Waterham, 2006; Fidaleo, 2009; Wanders *et al.*, 2010).

Hydration and dehydrogenation: The following two steps in this oxidation pathway are catalysed by a bifunctional enzyme. It appears that two proteins, L-bifunctional protein (LBP) and D-bifunctional protein (DBP) have been found to have both enoyl-CoA hydratase activity, and 3-hydroxy-acyl-CoA dehydrogenase activity. DBP is known to be the main enzyme involved in these steps, whereas little is known of LBP (Wanders and Waterham, 2006; Wanders *et al.*, 2010).

Thiolytic cleavage: The final step in peroxisomal β-oxidation requires the presence of peroxisomal thiolases. Human peroxisomes contain two thiolases whereas mouse and rat liver peroxisomes have three thiolases. In this step the fatty acid molecule is cleaved into an acetyl-CoA molecule, and an acyl-CoA molecule. Each cycle of β-oxidation shortens the fatty acid molecule by two carbon atoms (Wanders and Waterham, 2006; Fidaleo, 2009; Wanders *et al.*, 2010).

Once enough cycles have been carried out the intermediate product goes to the mitochondria to complete the process and produce CO_2 and H_2O (Wanders, 2004).

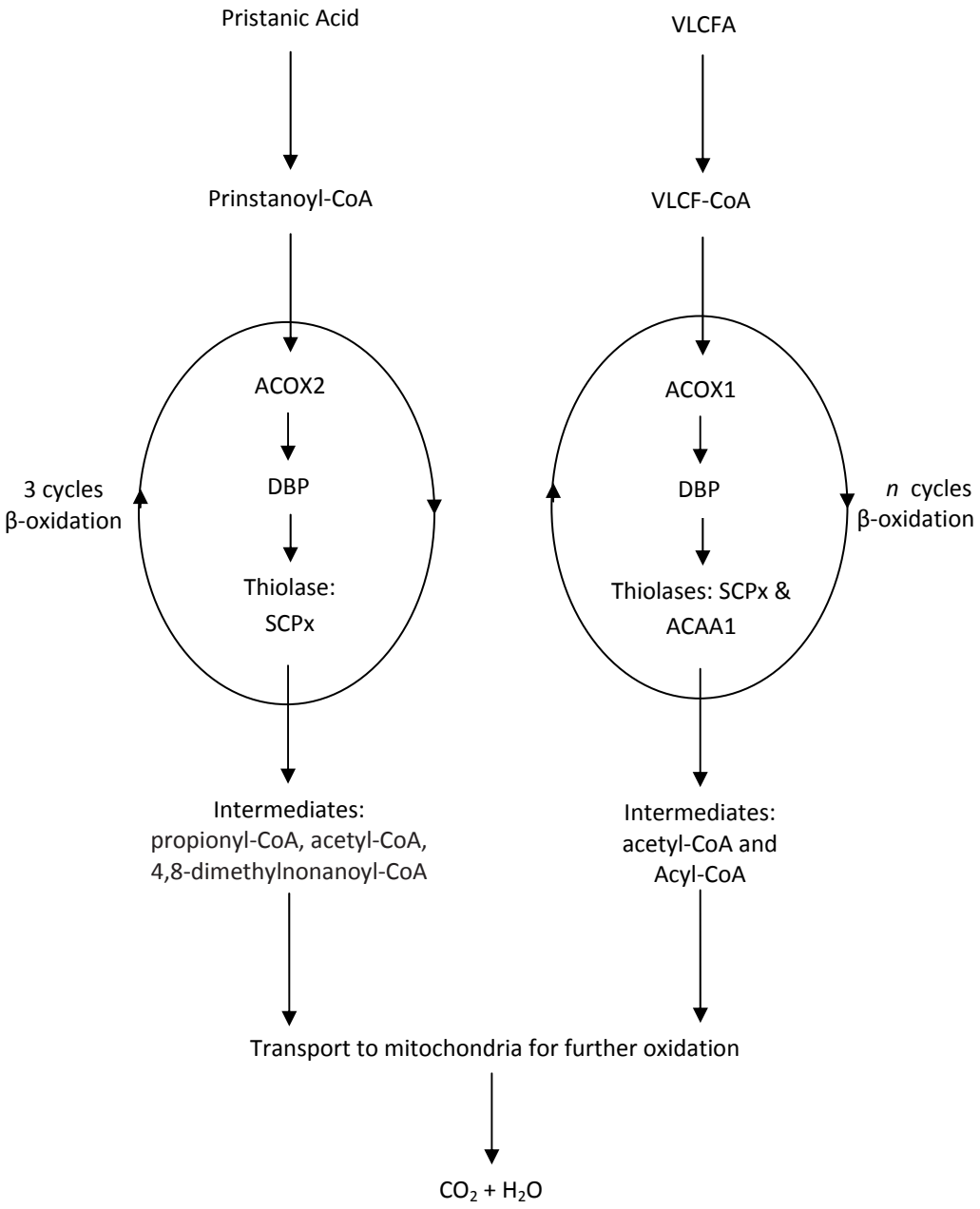

Figure 6 Peroxisomal Fatty Acid β-oxidation

The β-oxidation pathway for the 2-methyl branched chain fatty acid Pristanic acid, and any straight VLCFA within the peroxisome adapted from Wanders et al., 2010. Once activated to their CoA esters the fatty acids enter the peroxisomes and undergo several rounds of β-oxidation before they are transported to the mitochondria to complete oxidation and form CO_2 and H_2O

1.3.2 α-Oxidation of Fatty Acids

Branched chain fatty acids that contain a methyl group at the C3 position must first be oxidised by α-oxidation as β-oxidation is blocked by the 3-methyl group. It is now well established that peroxisomes are the only site of α-oxidation after the first evidence presented by Singh et al (1992) that oxidation of phytanic acid, a 3-methyl branched chain fatty acid undergoes α-oxidation (Figure 7) within the peroxisome rather than the mitochondria or ER as was once suspected (Singh *et al.*, 1992; Fidaleo, 2009; Wanders *et al.*, 2010).

The purpose of α-oxidation is to remove the carboxyl carbon to produce a 2-methyl fatty acid which is able to undergo β-oxidation. Phytanic acid, which is known to accumulate in a number of peroxisomal biogenesis disorders, has been used over the years as the fatty acid to study for α-oxidation. The process starts with production of the CoA-ester, which in the case of phytanic acid is phytanoyl-CoA, catalysed by the enzyme very-long-chain acyl-CoA synthetase (also called FATP4) (Steinberg *et al.*, 1999; Wanders and Waterham, 2006; Wanders *et al.*, 2010). From here, phytanoyl-CoA 2-hydroxylase hydroxylates phytanoyl-CoA to 2-hydroxyphytanoyl-CoA, which is then followed by cleavage of the molecule by 2-hydroxyphytanoyl-CoA ligase to yield pristanal and formyl-CoA. Pristanal is oxidised by a peroxisomal aldehyde dehdrogenase to pristanic acid which can then be activated and undergo β-oxidation. Formic acid and CO_2 are formed from the spontaneous separation of formyl-CoA as it is not stable at a neutral pH (Verhoeven *et al.*, 1997; Jansen and Wanders, 2006; Wanders and Waterham, 2006; Wanders *et al.*, 2010).

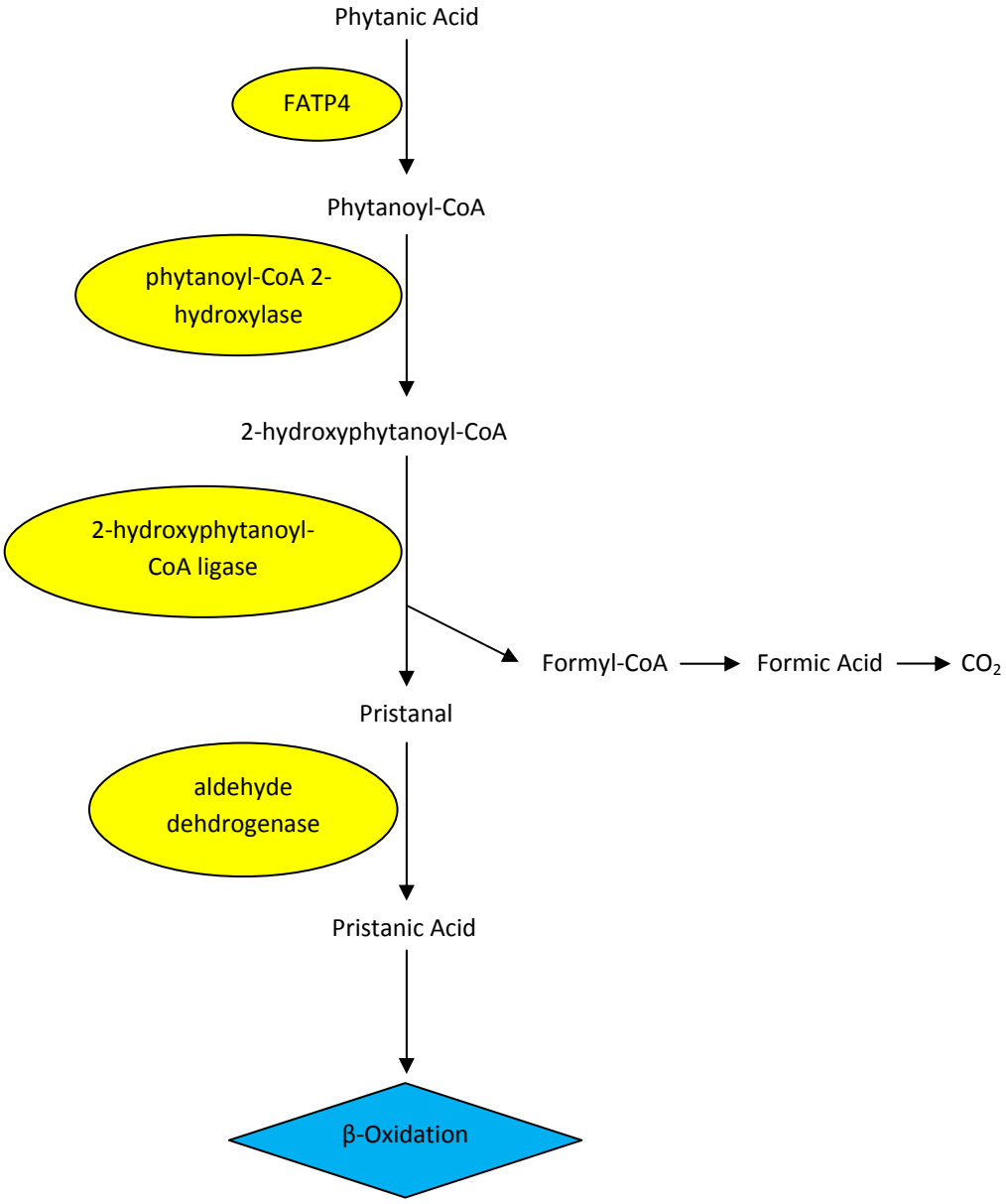

Figure 7 Peroxisomal fatty acid α-oxidation

The α-oxidation pathway of phytanic Acid within the peroxisome adapted from Jansen and Wanders, 2006. Once it has been activated to phytanoyl-CoA by FATP4 phytanic acid undergoes α-oxidation to remove the 3-methyl branched chain and yield pristanic acid. Pristanic Acid is then further oxidised by peroxisomal β-oxidation before being transported to the mitochondria.

1.4 Lipotoxicity

Obesity is a major risk factor in type 2 diabetes and can lead to the excessive deposition of lipids in the heart, skeletal muscle, the liver and the pancreas. Accumulation of lipids within these organs occurs when adipose tissue cannot cope with the excessive amounts of fat through either, the reduced oxidation or clearance of fatty acids, the increase in fatty acid uptake or an increase in de novo lipogenesis (fatty acid synthesis) (Figure 8). Lipotoxicity is the term given to the cell dysfunction and/or cell death caused by this accumulation of lipids within ectopic organs (van Herpen and Schrauwen-Hinderling, 2008; Kusminski *et al.*, 2009).

1.4.1 Skeletal Muscle

The majority of insulin resistance seen in type 2 diabetes is found in skeletal muscle. Several ways in which lipotoxicity may contribute to insulin resistance in skeletal muscle have been suggested. In 1963 Randle and colleagues proposed that insulin resistance was caused alone by elevated fatty acids which resulted in an increase in fat oxidation and therefore a reduction in glucose oxidation. Since then it has been found that a decrease in glycogen synthesised by the muscle may also have a major role in the progression of insulin resistance. This is thought to occur through the inhibition of insulin-stimulated glucose transport by elevated plasma fatty acids. It has also been suggested that fatty acids may lead to insulin resistance through the activation of JNK, possibly by the production of lysophosphatidylcholine (LPC). In addition, as previously described in section 1.1.4, the production of ceramide and DAG through the incomplete oxidation of lipids interferes with the insulin signalling cascade and impairs the effects of the hormone. (Randle *et al.*, 1963; Boden and Shulman, 2002; Yu *et al.*, 2002; Holland *et al.*, 2007; Wilding, 2007; Koves *et al.*, 2008; Han *et al.*, 2011a).

Although in type 2 diabetes elevated levels of fat do seem to contribute to insulin resistance, endurance athletes, who are highly sensitive to insulin, have also been found to have high levels of fat within the muscle cells (intramyocellular lipids). However, these athletes are able to use the fat as an energy source as exercise enhances their ability to fully oxidise the fats. It is therefore likely that it is not the presence of elevated fatty acids with the muscle, but rather the capacity of the muscle to fully oxidise fats which contributes to insulin resistance (Goodpaster *et al.*, 2001; Snel *et al.*, 2012).

1.4.2 The Heart

Myocardium has a limited compensatory fatty acid oxidation capacity so is prone to the accumulation of fat which can eventually result in heart failure. This can result from insulin resistance caused by the accumulation of fatty acids. A reduction in glucose oxidation due to the insulin resistance may lead to heart failure by "energy starvation" of the heart. Another mechanism in which lipotoxicity can result in myocardial dysfunction and heart failure is through the production of lipid metabolites. An increase in ceramide, an initiator of apoptosis, has been seen in lipid laden hearts of Zucker Diabetic Fatty (ZDF) rats which led to severe cardiac lipoapoptosis (van Herpen and Schrauwen-Hinderling, 2008; Kusminski *et al.*, 2009).

1.4.3 The Liver

The liver is one of the major organs for fatty acid metabolism. As well as synthesising triglycerides and cholesterol, it is also responsible for the production and uptake of lipoproteins. Although it has such a large role in these processes the storage of fats within the liver tends to be quite low, and liver steatosis (fatty liver) can result from the excess of hepatic fat content. The accumulation of fat within the liver can result in a number of problems associated with the metabolic syndrome including an increase in insulin resistance. It is thought that this excess of fat can come from a variety of sources including de novo lipogenesis, fat from the diet, and the release of fatty acids from adipose tissue. Defects in any of the processes of fatty acid metabolism that the liver is responsible for can contribute to the accumulation of fats within the liver which in turn can lead to insulin resistance, but the mechanism for this at present is poorly understood. It is thought, that in a similar way to muscle insulin resistance, the increase in liver fatty acids results in increases in ceramide production, DAG and other toxic intermediates which interfere with the insulin signalling cascade, causing hepatic insulin resistance (van Herpen and Schrauwen-Hinderling, 2008; Cusi, 2010).

1.4.4 The Pancreas

β-cells, like the myocardium have been suggested to have little capacity for compensatory fatty acid metabolism. Reduced fatty acid oxidation has been reported in the islets of *fa/fa* ZDF rats (Shimabukuro *et al.*, 1998b; Kusminski *et al.*, 2009). Whether or not this is the case, several mechanisms by which lipotoxicity can lead to pancreatic β-cell dysfunction and death in type 2 diabetes have been proposed. These

include changes in gene expression of proteins involved in insulin secretion and production as well as the cytotoxic effects of reactive oxygen species (ROS) and ceramide (Kusminski *et al.*, 2009).

A decrease in insulin biosynthesis in isolated rat islets has been witnessed after exposure to palmitate through disruption of expression of the preproinsulin gene. It is possible that one of the ways in which pancreatic β-cell dysfunction occurs is by reduction in the expression of this gene (Ritz-Laser *et al.*, 1999).

Ceramide formation is thought to be a major contributor of apoptosis in β-cells. It has been shown that in obese ZDF rats β-cell apoptosis resulted from an overproduction of ceramide. It was observed that induction of de novo synthesis of ceramide in response to fatty acids caused this increase rather than it being a product of sphingomyelin hydrolysis (Shimabukuro *et al.*, 1998a; Kusminski *et al.*, 2009).

The production of reactive oxygen species (ROS) has also been shown to contribute to β-cell dysfunction and failure. ROS production seems to be increased in the islets of type 2 diabetic patients compared with healthy controls (Sakuraba *et al.*, 2002; Marchetti *et al.*, 2004). Although ROS, which includes hydrogen peroxide (H_2O_2), superoxide anion ($O_2\bullet^-$) and the hydroxyl radical (HO•) can be generated by several sources such as NADPH oxidase and cytochrome P450 enzymes, mitochondria are a major source of ROS generated in pancreatic β-cells when under metabolic stress (Chen *et al.*, 2003; Schrauwen and Hesselink, 2004; Ježek and Hlavatá, 2005; Ma *et al.*, 2012). The metabolism of glucose and fatty acids within the mitochondria is through the tricarboxylic acid cycle which leads to the transfer of electrons to the electron transport chain (ETC). Small amounts of superoxide anion radicals are continually produced by the ETC. Under normal conditions these radicals are removed by Mn^{2+}-superoxide dismutase leading to the production of H_2O_2. H_2O_2 is then broken down by catalase into water and oxygen (Chen *et al.*, 2003; Gehrmann *et al.*, 2010; Ma *et al.*, 2012). However, in periods of metabolic stress, increased rates of fatty acid metabolism can result in the accumulation of H_2O_2 which, if not broken down as quickly as it is produced, in the presence of Fe^{2+}, can result the production of highly reactive hydroxyl radicals which can lead to mitochondrial dysfunction (Robertson *et al.*, 2004; Thomas *et al.*, 2009; Ma *et al.*, 2012).

Lipid peroxidation of the mitochondrial membrane phospholipids can result from the production of ROS. ROS appear to have a direct action on the oxidation of the mitochondrial membrane phospholipid cardiolipin. Oxidation of cardiolipin leads to the release of cytochrome *c* to which it is bound. Cytochrome *c* is involved in the initiation of apoptosis, which when released, can result in the destruction of the pancreatic β-cells (Ma *et al.*, 2012).

UCP2 is part of the uncoupling protein (UCP) family which act as proton channels and are located within the inner membrane of the mitochondria. They are involved in the uncoupling of the electrochemical gradient leading to a decrease in ATP synthesis (Lameloise *et al.*, 2001; Rousset *et al.*, 2004). Changes in UCP2 (uncoupling protein-2) expression in response to elevated levels of fatty acids may lead to pancreatic β-cell dysfunction. It was shown that INS-1 cells chronically exposed to fatty acids resulted in an increase in UCP2 gene expression, in addition to the inhibition of the increase in ATP/ADP ratio normally seen in response to glucose. This resulted in a decrease in GSIS which is controlled by the ATP/ADP ratio. It is likely that the increased UCP2 gene expression resulted in a decrease in ATP synthesis, and therefore the decrease in the ATP/ADP ratio seen, leading to the reduction in GSIS. It was also suggested that these deleterious effects can occur without the metabolism of fatty acids, but in the presence of elevated fatty acids alone (Lameloise *et al.*, 2001). In addition, UCP2 expression levels have also been shown to increase in response to superoxide production (Echtay *et al.*, 2002). As superoxide production is associated with increased oxidation of fatty acids (Gehrmann *et al.*, 2010), it is possible that increased fatty acid oxidation could further increase the levels of UCP2 expression. It is thought that the increase in UCP2 in response to elevated fatty acid levels could be a reason for the decrease in insulin secretion seen in obese patients with type 2 diabetes (Zhang *et al.*, 2001).

It is possible that endoplasmic reticulum (ER) stress may also contribute to β-cell dysfunction through lipotoxicity. ER calcium (Ca^{2+}) signalling is very important with β-cells. Fluctuations within the ER Ca^{2+} levels can cause problems in several functions of the ER including the synthesis and processing of proteins. ER stress occurs when there is an accumulation of misfolded proteins, or the demands for protein folding are too high. High Ca^{2+} levels in the ER are important for the folding of proinsulin, the

precursor for insulin. It is thought that elevated levels of FA can lead to the depletion of ER Ca^{2+} which prompts the ER stress response. Although there is evidence for the role of ER stress in the involvement of pancreatic β-cell dysfunction, human islets and MIN6 cells (insulin secreting mouse cell line) have been shown to be more resistant to palmitate induced ER stress compared with INS-1 (insulin secreting rat cell line). It is therefore possible that this is not one of the main mechanisms of β-cell dysfunction through lipotoxicity (Cnop *et al.*, 2005; Lai *et al.*, 2008; Karunakaran *et al.*, 2012).

Nitric oxide (NO) formation in response to long-chain fatty acids has been shown to have cytotoxic effects in the islets of rats predisposed to type 2 diabetes mellitus. A decrease in insulin secretion at both basal and stimulating glucose levels was seen with more than a 20-fold increase in fatty acid induced NO. Protection from this decrease was gained by the addition of an inhibitor against iNOS (inducible nitric oxide synthase) along with a decrease in NO production (Shimabukuro *et al.*, 1997). However, the role of nitric oxide in lipotoxicity is debated. While it has been reported that long term exposure of rats to fatty acids increased NO production in islets by inducing iNOS expression, and may act through caspases to induce β-cell dysfuction and apoptosis (Abaraviciene *et al.*, 2008), it has been suggested that NO regulates fatty acid metabolism. It has been shown that inhibition of NO production in mice during gestation can result in reduced fatty acid metabolism and hyperlipidemia (Ma *et al.*, 2011). While it seems that high NO concentrations contribute to β-cell dysfunction, the implications of its cytotoxic effects remain unclear and may be worthy of further investigation (Drews *et al.*, 2010).

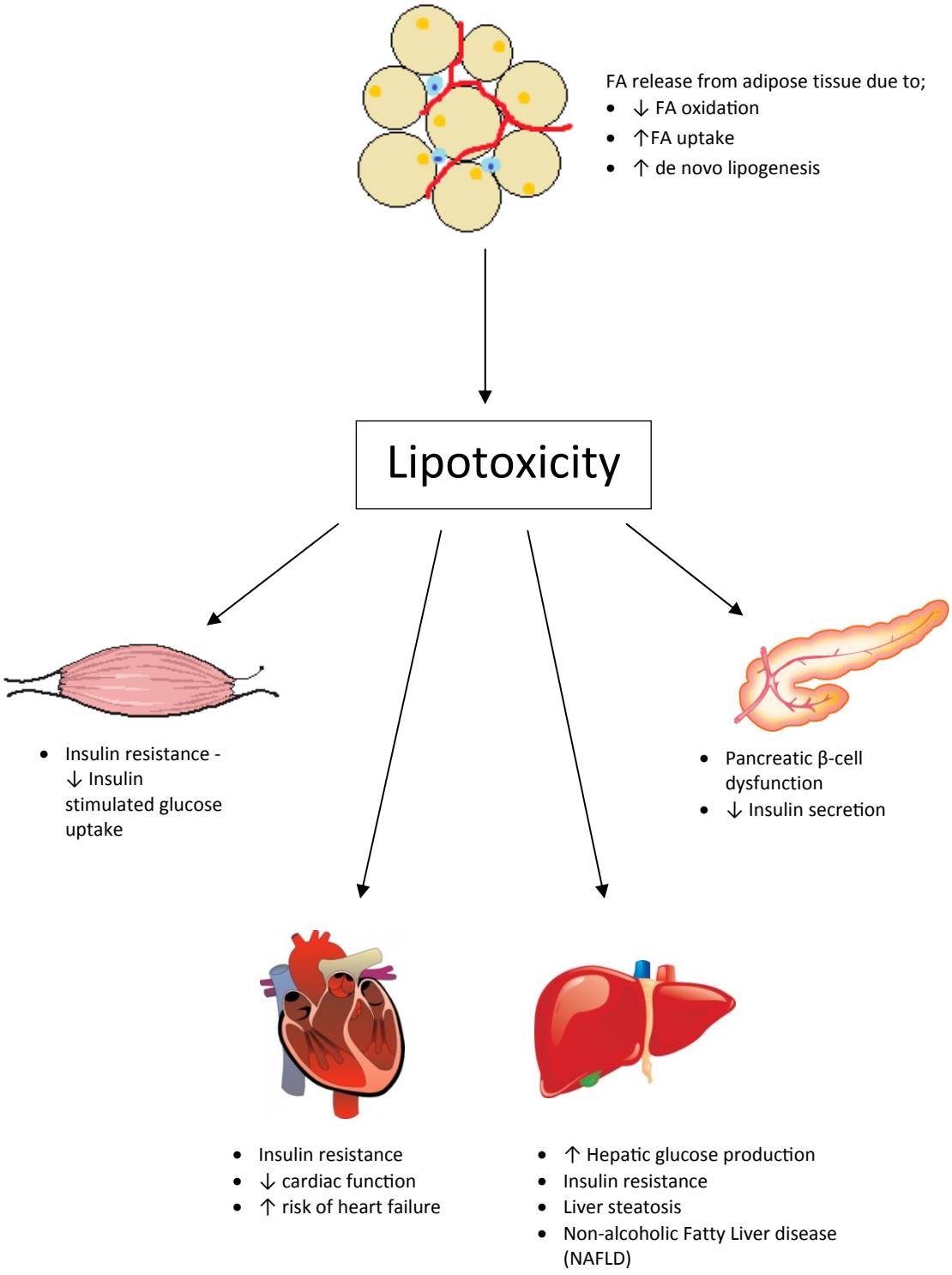

Figure 8 The effects of lipotoxicity in the muscle, the heart, the liver and the pancreas.

When fat spills from the adipose tissue it can be deposited in each of these organs and interfere with their normal function. This can lead to problems such as insulin resistance, pancreatic β-cell dysfunction, and the onset of type 2 diabetes.

1.4.5 The Role of Peroxisomes in Lipotoxicity

Recently, evidence has come to light that one of the major causes of lipotoxicity in pancreatic β-cells may be through ROS produced by β-oxidation of fatty acids by peroxisomes. β-oxidation carried out by peroxisomes leads to the formation of hydrogen peroxide (H_2O_2) whereas in the mitochondria reducing equivalents are produced. In most cells oxidoreductase catalase is expressed in peroxisomes and catabolises the toxic H_2O_2, however, this enzyme is lacking in the peroxisomes of insulin producing cells which leaves the pancreatic β-cells vulnerable to lipotoxicity by ROS. A 40% increase in ROS production was seen after treatment with palmitate in insulin producing RINm5F cells. Over expression of catalase in peroxisomes, but not mitochondria significantly reduced palmitate induced ROS generation. The study also found that peroxisomes are a major source of H_2O_2 production but mitochondria produced minimal amounts. (Elsner *et al.*, 2011)

Although increased levels of peroxisomes which may lead to an increase in the rate of fatty acid metabolism may seem like an advantageous trait, it is possible that this could lead to an increased risk of type 2 diabetes. Fat spillage from adipose tissue that arrives in the pancreatic β-cells may lead to an increased rate of H_2O_2 generation as more fat is likely to be metabolised by the peroxisomes. ROS-mediated lipotoxicity could give rise to pancreatic β-cell dysfunction and destruction leading to diabetes.

1.4.6 Glucolipotoxicity

It has been a greatly debated matter as to whether the combination of both chronic hyperglycaemia (glucotoxicity) and chronic dyslipidaemia (lipotoxicity), termed glucolipotoxicity, is essential for the detrimental effects of lipotoxicity seen on β-cell function and survival. There is evidence to suggest that palmitate inhibits insulin gene expression in rat islets, but only under hyperglycaemic conditions (Jacqueminet *et al.*, 2000) and glucotoxicity alone appears to lead to apoptosis in both rodent and human β-cells (Cnop *et al.*, 2005; Park *et al.*, 2007). However, a more recent study found that glucose was needed for lipotoxicity in INS-1E cells, an insulin secreting cell line derived from rat, but was dispensable for human islets and MIN6 cells. Although fatty acid induced apoptosis was shown to occur in all cell types at low glucose conditions, it was shown to be increased in only the INS-1E cells under high glucose conditions (Sargsyan and Bergsten, 2011). It seems that although glucolipotoxicity can result in pancreatic β-

cell dysfunction and cell death there is not always necessity for both hyperglycaemia and hyperlipidaemia to occur simultaneously for these detrimental effects to occur.

1.5 Peroxisomal Disorders

Peroxisomes are essential organelles for normal growth and development of mammalian cells, as is evident from disorders of peroxisomal function. There are two main groups of peroxisomal disorders with varying degrees of severity; peroxisomal biogenesis disorders (PBDs) and the single peroxisomal enzyme deficiencies (Wanders, 2004; Wanders and Waterham, 2006).

1.5.1 Peroxisomal Biogenesis Disorders (PBDs)

Evidence that peroxisomes play a very important part in human physiology has come from the studies of PBDs in conditions such as Zellweger syndrome. Other PBDs include neonatal adrenoleukodystrophy (NALD), infantile Refsum disease (IRD) and rhizomelic chondrodysplasia punctata Type 1 (RCDP1). These diseases (including Zellweger syndrome) are known collectively as the Zellweger spectrum disorders (Shimozawa *et al.*, 2004; Wanders, 2004; Fidaleo, 2009).

Most of these disorders are due to mutations in PEX genes (encoding peroxins) which are involved in the biogenesis of peroxisomes. Mutations in many PEX genes have been found including PEX1, PEX2, PEX3 and PEX14 to name just a few. Without the proper expression of these genes, peroxisomal function is not able to occur, which leads to an accumulation of VLCFA, branched chain fatty acids such as phytanic acid, and 3α,7α-dihydroxy-5β-cholestanoic acid (DHCA) from bile acid synthesis within tissues. Plasmalogens, a class of etherphospholipids, are also lacking in people with Zellweger syndrome, which shows the importance of peroxisomes in the synthesis of etherphospholipids (Shimozawa *et al.*, 2004; Wanders, 2004; Wanders and Waterham, 2006; Fidaleo, 2009).

The accumulation of fatty acids within these patients can lead to symptoms such as liver disease, retinopathy, and variable neurodevelopment delay. Zellweger syndrome itself often leads to death before the age of one as patients are very debilitated with severe brain dysfunction (Fidaleo, 2009).

It has been shown that *PEX11*β deficient mice present with features similar to Zellweger syndrome such as neonatal lethality, intrauterine growth retardation, and hypotonia. These mice, however, did not have such large increases in VLCFA accumulation, or huge decreases in plasmalogens as compared with Zellweger syndrome mouse models. The authors suggested that *PEX11*β deficiency is a novel peroxisomal disorder that appears to replicate some of the serious neurological and developmental characteristics of Zellweger syndrome, however, the mechanism by which this occurs is not yet fully understood. Pathological features of Zellweger syndrome are thought to occur due to the defects in β-oxidation of fatty acids, and VLCFA toxicity. This mechanism, however, seems unlikely for *PEX11*β deficiency as the accumulation of VLCFA is to a much lesser extent (Li *et al.*, 2002b).

1.5.2 Single peroxisomal enzyme deficiencies

Single peroxisomal enzyme deficiencies or peroxisomal enzyme/transporter deficiencies (PEDs) occur where there is a mutation leading to a defect in one enzyme leaving an intact peroxisome, but nevertheless, a potentially severe disease. Many of these diseases, even though only a single function of the peroxisome may have been lost, often these diseases show similar symptoms to PBDs (Fidaleo, 2009).

Disorders of peroxisomal β-oxidation include: X-linked adrenoleukodystrophy (X-ALD) where mutations in ABCD1 gene lead to a reduction in the transport of fatty acid-CoA-esters across the membrane of the peroxisome and the accumulation of VLCFA within the tissues ((Wanders, 2004; Fidaleo, 2009; Wanders *et al.*, 2010), D-bifunctional protein (DBP) deficiency where the most severe form can resemble Zellweger syndrome and can lead to early death, and peroxisomal acyl-CoA oxidase (ACOX) deficiency showing elevated levels of VLCFA but normal levels of e.g. pristanic acid which also undergoes β-oxidation. Other peroxisomal β-oxidation disorders that have been found are 2-methylacyl-CoA racemase (AMACR) deficiency and SCPx deficiency (Wanders, 2004; Wanders *et al.*, 2010).

The only known disorder of fatty acid α-oxidation is Refsum disorder, which is caused by a problem with the enzyme phytanoyl-CoA hydroxylase leading to the accumulation of phytanic acid. Features include retinitis pigmentosa leading to blindness, cerebellar ataxia and anosmia (Wanders, 2004; Wanders *et al.*, 2010).

1.6 Peroxisomal Proliferating Agents

1.6.1 PPAR-α agonists

Fibrates have been used in the treatment of dyslipidaemia for many years. They have been shown to induce peroxisome proliferation in rodents, mediated through peroxisome proliferator activated receptors (PPARs). There are three main types of PPARs; PPAR-α, PPAR-δ/β, and PPAR-γ. Fibrates, which are PPAR-α agonists, exert their effects by activating PPAR-α, which leads to the formation of a heterodimer with the retinoid X receptor (RXR). This heterodimer subsequently binds the peroxisome proliferator response element (PPRE), and along with the recruitment of cofactors, induces the transcription of genes involved in peroxisome proliferation and peroxisomal β-oxidation (Kota *et al.*, 2005; Katsiki *et al.*, 2013).

Bezafibrate, a fibric acid derivative, may have a preventative role in the development of type 2 diabetes. A study carried out over several years has concluded that bezafibrate leads to a delayed onset, and a decrease in incidence of type 2 diabetes in obese people (Tenenbaum *et al.*, 2005). In addition, a study carried out in 2012 found that patieints with diabetes when treated with bezafibrate resulted in reduced HbA1c (glycated haemoglobin used as an indicator of diabetes) levels. An improvement in blood glucose levels and lipid levels was also reported (Teramoto *et al.*, 2012). It is possible that these beneficial outcomes occurred through the increased oxidation of fatty acids as the drug is able to activate the genes for β-oxidation. This would in turn reduce the amount of fatty acids being spilled into ectopic tissues and lead to a reduction in lipotoxicity.

1.6.2 The effect of PPARα agonists on PEX11

*PEX11*α has been shown to be regulated by PPARα through a PPRE shared with perelipin. The study was able to confirm that *PEX11*α is a target of PPARα through the use of hepatic mRNA from wild type and PPARα knockout mice. PPARα knockout mice showed no signs of induction of *PEX11*α in the presence of the peroxisome proliferator Wy14,643 unlike the wild type mice in which *PEX11*α expression was induced (Shimizu *et al.*, 2004). This study reinforced the results from previous studies in which another PPARα agonist, clofibrate, was shown to induce *PEX11*α expression (Abe *et al.*, 1998; Schrader *et al.*, 1998).

In one of these studies it was found that rats fed with a diet of clofibrate for 10 days produced a 10 fold increase in *PEX11*α expression compared with control animals. *PEX11*β expression was not affected in these animals. As previously stated, the study found that expression levels of *PEX11*α were variable across a variety of tested tissues whereas *PEX11*β expression was seen at similar levels, so it is possible that constitutive peroxisome division is controlled by *PEX11*β, and *PEX11*α controls peroxisome abundance in response to a stimulus (Schrader *et al.*, 1998).

*PEX11*α knockout mouse have been generated, which were found to have normal peroxisome abundance. Although it has been previously shown that PPARα induces the expression of *PEX11*α, the group found that the mice had a normal peroxisome proliferation response after treatment with PPARα agonists. This implies that although PPARα does increase the expression of *PEX11*α it is not essential for the peroxisome proliferation response (Li *et al.*, 2002a).

The same study went on to show that although *PEX11*α is not needed for the PPARα activation response it is essential for the response to 4-Phenylbutyrate (4-PBA). In humans and mice 4-PBA leads to a 2 fold increase in peroxisome abundance, with similar increases seen in *PEX11*α mRNA levels. Peroxisomal fatty acid β-oxidation is also increased. In the *PEX11*α knockout mice this response to 4-PBA was lost (Li *et al.*, 2002a).

Another study has shown that the combination of clofibrate and 9-*cis* retinoic acid (RA) led to an increase in *PEX11*α expression in primary rat β-cells. The addition of palmitate to the clofibrate and RA led to an even more marked increase in expression of *PEX11*α, further strengthening the conclusion that Pex11α is induced in response to stimuli. However, in this study, palmitate alone was unable to induce a similar response in *PEX11*α expression. In addition, palmitate alone was found to be toxic to the β-cells (Hellemans *et al.*, 2007).

1.6.3 Protection of pancreatic β-cells

PPARα-RXR agonists have been shown to provide β-cells protection against palmitate toxicity. The highest level of protection was found using a combination of clofibrate and 9-cis RA. Most experiments in this study used 250μM clofibrate with 2μM 9-*cis* RA which resulted in a reduction of cytotoxicity in the β-cells by 90% (Hellemans *et al.*,

2007). PPARα-RXR agonists increased the expression levels of both mitochondrial β-oxidation and peroxisome (β-oxidation and membrane protein) genes. It is therefore unclear as to what extent the peroxisomes play in the protective effects of the β-cells. In the same study it was shown that abolishing the mitochondrial β-oxidation by the inhibition of CPT1 (Carnitine palmitoyl transferase 1) led to the loss of the protective effects of clofibrate and 9-*cis* RA in the β-cells and the cytotoxicity of palmitate increased 4 fold. This points to a key role for mitochondrial fatty acid metabolism in the protection of pancreatic β-cells from palmitate (Hellemans *et al.*, 2007).

In addition to this, isolated rat islets and INS-1 cells chronically exposed to 0.2mM palmitate have been shown to have a 30% and 40% reduction in GSIS respectively. The inclusion of fenofibrate, another PPARα agonist, in the palmitate culture medium resulted in a normal GSIS in both cell types. This suggests that fenofibrate has a protective role in the deleterious effects in GSIS caused by the chronic exposure of pancreatic β-cells to palmitate (Sun *et al.*, 2008).

1.7 Peroxisomes and Diabetes

It is known that one of the mechanisms of insulin resistance and β-cell dysfunction is through lipotoxicity; the accumulation of free fatty acids (FFAs) within non-adipose tissues (Unger, 1997; Unger and Zhou, 2001). A lack of peroxisomes can lead to the accumulation of FFAs (Wanders and Waterham, 2005) so it is possible that mutations within genes involved in peroxisomal function, biogenesis and/or division may be a cause of the increases in fat seen in ectopic tissues. However, it has also been proposed that peroxisomal β-oxidation could contribute to lipotoxicity in pancreatic β-cells due to the production of H_2O_2 (Elsner *et al.*, 2011). Although it is unsure what role peroxisomes play in the onset of type 2 diabetes, it is possible that defects in their proteins could lead to decreased insulin secretion and insulin resistance seen in the disease.

Candidate gene studies have been carried out within the Perilipin gene region to identify single nucleotide polymorphisms (SNPs) involved in the alteration of an individual's β-cell function or sensitivity to insulin. An association was found in *PEX11*α, which encodes a protein involved in peroxisomal division in response to extracellular stimuli and also shares a promoter with perilipin. The SNP, rs1972435, which is located

within intron 2 of *PEX11*α, was found to be associated with a significant decrease in insulin, measured through a 30 minute oral glucose tolerance test, indicating a decrease in β-cell function (Shimizu *et al.*, 2004; Shimizu *et al.*, 2006; Pascoe, 2009).

1.8 Cell line models of β-cell function

Establishing β-cell lines was a fundamental advance in the field of diabetes research. The ability of these cells to replicate through multiple passages has made them an invaluable tool for research into β-cell function. Many attempts were made to establish these cell lines, which would respond to glucose with the secretion of insulin, but only a few were successful. Some of the more commonly used are RINm5F, HIT, MIN6, INS-1 and βTC (Skelin *et al.*, 2010).

RINm5F cells are derived from a rat insulinoma which was induced by irradiation with high-dose x-rays. Despite it containing insulin, and being one of the most widely used β-cell lines, it would have been unsuitable for the work carried out in this thesis due to its inability to respond to glucose with the secretion of insulin (Halban *et al.*, 1983; Skelin *et al.*, 2010). Another cell line derived from rat insulinoma cells produced by irradiation to X-rays are INS-1 cells. Like the RINm5F cells, INS-1 cells contain insulin, but they also have a dose-related response to glucose with the secretion of insulin similar to that of rat islets. However, the stability of the insulin secretion over increasing passage numbers is minimal, which led to the production of the more stable clone, INS-1E which was able to maintain the insulin secretion between passages 40 and 100 (Merglen *et al.*, 2004; Skelin *et al.*, 2010).

HIT (Hamster β-cell line), produced by transformation of hamster pancreatic β-cell using the simian virus 40 (SV40), is another insulin-secreting cell line. However, insulin content and secretion upon glucose stimulation is vastly reduced compared with that of normal hamster islets (Santerre *et al.*, 1981).

MIN6 cells (a mouse insulinoma cell line), which are derived from a transgenic mouse expressing the large T-antigen of SV40, have been shown to have similar characteristics to isolated islet cells. A 7 fold insulin response has been seen from basal to stimulating levels of insulin, which is larger than the 2.2 fold response reported for INS-1 cells (Miyazaki *et al.*, 1990b; Asfari *et al.*, 1992; Ishihara *et al.*, 1993). However, it has been reported that higher passage number MIN6 cells (greater that passage 40)

have impaired insulin secretion (Cheng *et al.*, 2012). The βTC (beta tumour cells) cell line was also derived from a transgenic mouse expressing the large T-antigen of SV40. There are many different clones of this cell line, with the original βTC giving abnormally high insulin secretion in response to lower glucose levels. The βTC7 cell line was eventually developed which showed the same insulin responses to glucose to that of normal islets (Efrat *et al.*, 1993). Some of the βTC clones develop high hexokinase activity with high passage numbers which can result in abnormal insulin secretion (Skelin *et al.*, 2010).

Recently, the creation of the EndoC-βH1 cells has added a human β-cell line to the animal β-cell lines available. Human fetal pancreatic buds were grafted into SCID mice after transduction with a lentiviral vector expressing the large T-antigen of SV40. The resulting cell line was shown to secrete insulin in response to varying levels of glucose (Ravassard *et al.*, 2011). However, since this cell line has only recently been established and is not widely used, more testing may be required to assess its role in the future of research into diabetes and β-cell function.

As described above there is a choice of cell lines available for use into research of β-cell function; MIN6 cells were chosen for this project. MIN6 cells express GLUT2 glucose transporters and glucokinase allowing them to produce insulin in response to stimulating glucose levels within normal physiological ranges (Ishihara *et al.*, 1993). This was crucial for the planned experiments that specifically explored the impact of altered target gene expression on glucose stimulated insulin secretion. Lower passage cells were preferentially used for functional work, negating the potential impact of high passage on insulin secretion as mentioned earlier. A further contribution to the decision to use MIN6 cells for this project was the existing expertise within the lab in using this cell especially with the established method of transfection.

1.9 Aims

The overall aim of this project is to explore the hypothesis that altered expression of *PEX11*α or *PEX11*β changes peroxisome abundance, and contributes to lipotoxicity in cultured pancreatic β-cells, using MIN6 cells as the β-cell model.

To address this hypothesis, we aimed to carry out the following objectives:

- To produce a reliable system for the knockdown of *PEX11*α in MIN6 cells and assess the effects of *PEX11*α knockdown on peroxisome number.
- To determine whether *PEX11*α is an inducible gene in MIN6 cells, through the incubation with either fatty acids or peroxisome proliferating agents.
- To use the model of *PEX11*α knockdown to assess the effects on GSIS in the presence and absence of palmitate.
- To use the knockdown system to reduce *PEX11*β expression in MIN6 cells and further to investigate the effect of this knockdown on peroxisome abundance.
- To assess the effects that a reduction in peroxisome number has on GSIS in the presence and absence of palmitate.

Chapter 2

Materials and Methods

2 Materials and Methods

2.1 MIN6 Cell Culture

MIN6 cells, or mouse insulinoma cells, are a pancreatic β-cell line derived from a transgenic mouse expressing the insulin promoter-SV40 T antigen hybrid gene. They have many characteristics consistent with differentiated β-cells, most importantly, they can alter the amount of insulin they secrete in response to changes in extracellular glucose concentrations (Miyazaki *et al.*, 1990a). MIN6 cells at various passages were kindly donated by Dr Donna Hine and Dr Catherine Arden at Newcastle University. Experiments were carried out using MIN6 cells passages 22-31.

2.1.1 Media

MIN6 cells were cultured in Dulbecco's Modified Eagle's Medium (DMEM) containing 4500mg/L glucose, L-glutamine and sodium bicarbonate (Sigma), and supplemented with 15% Foetal Bovine Serum (FBS) (Invitrogen), 1% Penicillin/Streptomycin (PAA), 0.0005% β-mercaptoethanol. The supplements were filter sterilised upon addition to the DMEM using a 0.2µm filtropur syringe filter (Sarstedt).

2.1.2 Recovery of cells

A frozen vial of cells was quickly thawed in a 37°C water bath and then added to 9ml of growth medium in a centrifuge tube. The cells were centrifuged at 1750rpm for 3 minutes, and supernatant discarded. The cell pellet was then re-suspended in 12ml growth medium and either transferred to one or two 75cm^2 flasks. Where the suspension was split between two flasks another 6ml of growth medium was added. The cells were incubated at 37°C, 5% CO_2.

2.1.3 Sub-culture (Passaging)

Once flasks reached about 80% confluence MIN6 cells were passaged. Growth medium was removed and cells were rapidly washed with 5ml of PBS (without calcium and magnesium, Sigma). 2ml of trypsin was then added and the cells were incubated at 37°C for 3 to 5 minutes until the cells showed evidence of slipping away from the surface (by tapping the flask firmly). The cells were then re-suspended in 8ml of growth medium and transferred to a centrifuge tube. Cells were centrifuged at 1750rpm for 3 minutes to form a pellet and the supernatant was discarded. The pellet was then re-suspended in growth medium (usually 10ml), and the cell suspension

divided between the new T75 flasks (usually 5 for a 1:5 split). 10ml of growth medium was also added to the flasks and the cells were incubated at 37°C, 5% CO_2. Growth medium was changed every 2 to 3 days.

2.1.4 Storage

Cell pellets were re-suspended in 1ml of FBS containing 10% DMSO (Dimethyl sulphoxide) (Sigma). The cell suspension was transferred to a cryovial and put into a 5100 Cryo 1°C Freezing Container, "Mr. Frosty", in a -80°C freezer overnight. The vials could then be transferred to liquid nitrogen for long-term storage.

2.2 Transfection of MIN6 cells to knock down *PEX11* genes

Small interfering RNAs (siRNA) leads to gene silencing by using double-stranded RNA (dsRNA) to target complementary mRNA for degradation. This RNA interference can be used to reduce expression of genes, often by large percentages, which allows investigation into the effects of specific genes on cellular function.

2.2.1 Transfection with Lipofectamine

3 Ambion siRNA probes for *PEX11*α (s71494, s71495, s71496) were purchased from Life Technologies. siRNA information is detailed in

Table 2. 100µl nuclease free water was added to each tube to make a 50µM solution after the tubes were centrifuged to make sure the powder was at the bottom. The 100µl was then split into 20µl aliquots to avoid repeated freeze-thaw cycles.

The day before transfection, one T75 flask of MIN6 cells was split into 3 6-well plates at a density of $1x10^6$ cells/well to make sure the cells were only 30-50% confluent for transfection. For every treated sample (each well of the 6-well plate), siRNA-Lipofectamine™ 2000 mixtures were made up.

The siRNA was diluted in Opti-MEM® I Reduced Serum Medium without serum to attain the following concentrations:

Concentration	10nM	50nM	100nM
siRNA	0.4µl	2.0 µl	4.0 µl
Media	249.6 µl	240.0 µl	246.0 µl
Total	250 µl	250 µl	250 µl

These concentrations were made up for each *PEX11*α siRNA, and for a scrambled (Scr) control (Silencer® Select Negative Control #1 siRNA, Life Technologies). For each tube containing the siRNA, another tube was made up containing Lipofectamine™ 2000. 3µl of Lipofectamine™ 2000 was added to 247µl Opti-MEM® I Reduced Serum Medium and incubated for 5 minutes at room temperature. The Lipofectamine™ 2000 mixture was then added to the siRNA mixtures and incubated at room temperature for 20 minutes. Then the 500µl mixture was added to each well along with 1.5ml of Opti-MEM® I Reduced Serum Medium. 6 wells were left untreated (no siRNA was used) to ensure that transfection with the scrambled control was not affecting the PEX11α mRNA expression levels. The cells were incubated at 37°C, 5% CO_2. After about 5 hours the Opti-MEM® I Reduced Serum Medium was removed and DMEM (4500mg/L glucose, L-glutamine and sodium bicarbonate) containing FBS and β-mercaptoethanol, but no Penicillin/Streptomycin (antibiotic free) was added to the wells. The cells were then incubated at 37°C, 5% CO_2 for either 24 or 48 hours before carrying out RNA extractions and real-time PCR to assay for the knockdown of the gene.

2.2.2 Neon Transfection System (Invitrogen)

Transfections were carried out using the Neon Transfection System optimised for a 24 well plate using 2 of the 3 Ambion siRNA's, s71494 and s71495, for *PEX11*α. Following successful optimisation of the Neon System for knockdown of *PEX11*α, 3 Ambion siRNA's for *PEX11*β (s71497, s71498, s71499) were purchased from Applied Biosystems, and transfection were also carried out for the knockdown of *PEX11*β.

A 24 well plate was set up with 500µl antibiotic free media per well and left in the incubator at 37°C until needed. MIN6 cells of about 70% confluency were trypsinised, pelleted and resuspended in 10ml media and a 10µl aliquot was taken for counting using a haemocytometer. The volume of cell suspension for the desired number of cells needed ($5x10^5$ per well) was then removed, centrifuged and washed with 5ml Dulbecco's PBS. Cells were then centrifuged again to remove the PBS and resuspended in an appropriate volume (10µl per well) of resuspension buffer R (Neon 10µl kit).

The pipette station was set up with a Neon tube containing 3ml electrolytic buffer. Appropriate volumes of siRNA were put into sterile tubes to achieve concentrations of

50µM and 100µM. The correct volume of the buffer R cell suspension was then added to each tube containing the siRNAs.

A Neon tip was inserted into the Neon pipette and 10µl of siRNA-cell mixture was taken into the tip. The pipette was inserted into the Neon tube and 2 electrical pulses, each of 1200V, with a 20ms interval, were delivered. The mixture was then pipetted into the ready prepared 24 well plate. In addition to the 2 siRNA probes, scrambled controls and untransfected controls (buffer R, no siRNA) were also set up.

The transfected cells were incubated for up to 96hrs at 37°C, 5% CO_2. 24hrs after transfection the cells underwent a media change, using the antibiotic free media.

siRNA ID	Target Gene	Species	Product	Supplier	Sequence	Length
s71494	Pex11a	Mus musculus	*Silencer®* Select siRNA (Ambion)	Life Technologies	Sense: AAGAGGCCGUGGUACUGAAtt Antisense: UUCAGUACCACGGCCUCUUaa	21bp
s71495	Pex11a	Mus musculus	*Silencer®* Select siRNA (Ambion)	Life Technologies	Sense: GCACGUGACAGAGCAAAGAtt Antisense: UCUUUGCUCUGUCACGUGCaa	21bp
s71496	Pex11a	Mus musculus	*Silencer®* Select siRNA (Ambion)	Life Technologies	Sense: CUCCUAUUCCAGUCUCUAAtt Antisense: UUAGAGACUGGAAUAGGAGga	21bp
s71497	Pex11b	Mus musculus	*Silencer®* Select siRNA (Ambion)	Life Technologies	Sense: UCAUGAAUCUGAGCCGUGAtt Antisense: UCACGGCUCAGAUUCAUGAtg	21bp
s71498	Pex11b	Mus musculus	*Silencer®* Select siRNA (Ambion)	Life Technologies	Sense: AGAAAUGCAUGUAACCUUUtt Antisense: AAAGGUUACAUGCAUUUCUga	21bp
s71499	Pex11b	Mus musculus	*Silencer®* Select siRNA (Ambion)	Life Technologies	Sense: CAACCGAGCCUUGUACUUUtt Antisense: AAAGUACAAGGCUCGGUUGag	21bp
Silencer® Select Negative Control #1	N/A	N/A	*Silencer®* Select siRNA (Ambion)	Life Technologies	Sequence: N/A Catalogue number: 4390844	N/A

Table 2 Details of siRNA probes used for transfection

siRNA information for all siRNA probes purchased from Life Technologies and used for transfection of MIN6 cells.

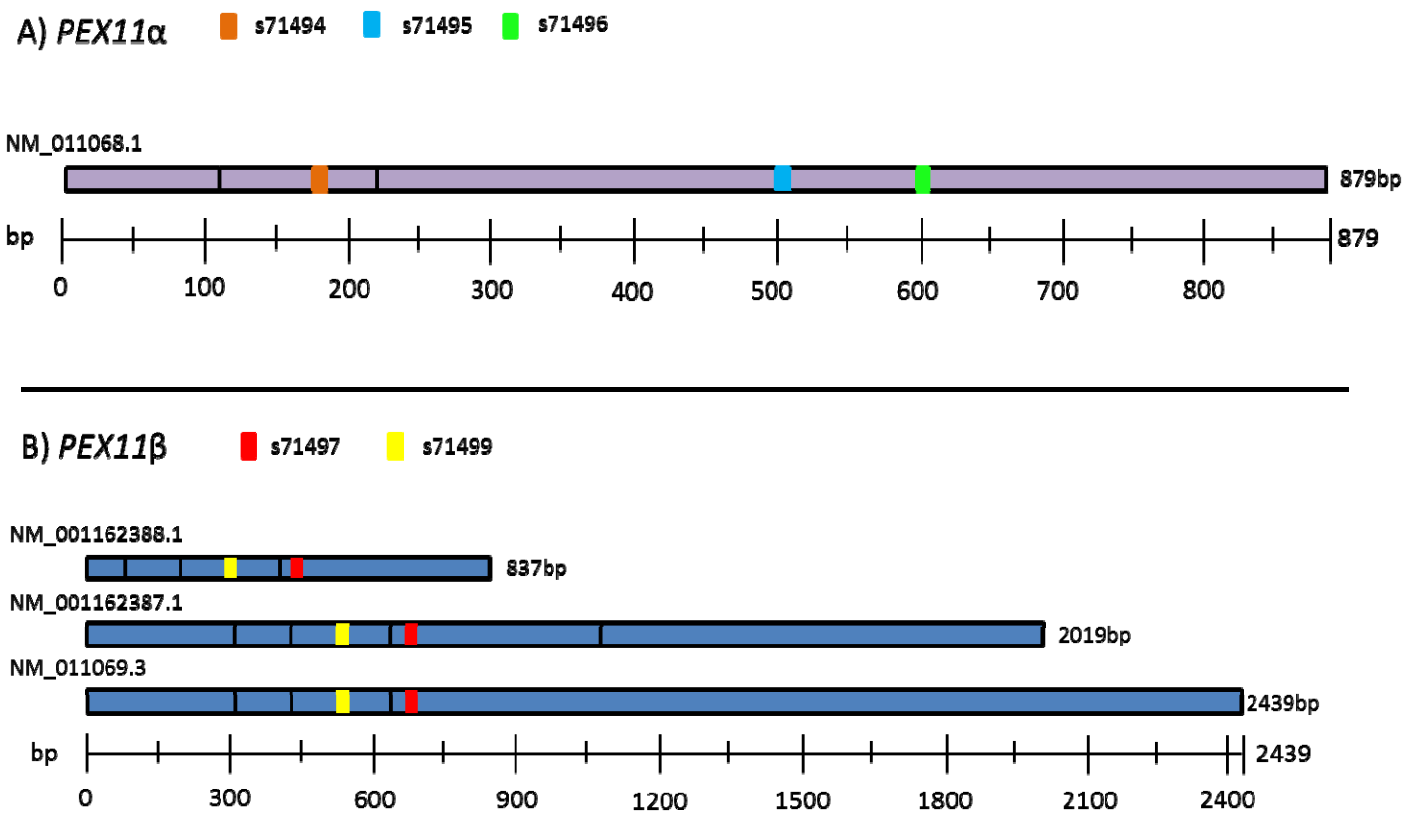

Figure 9 Mus Musculus *PEX*11α and *PEX11*β mRNA transcripts and siRNA targets

The position on the mRNA transcripts for the two genes, **A)** *PEX*11α, and **B)** *PEX11*β where the siRNA probes target. **A)** *PEX11*α transcript is 879bp. **B)** *PEX11*β has 3 coding transcripts of 837bp, 2019bp and 2439bp. For *PEX11*β, only 2 siRNA probes are shown as a nucleotide BLAST of the sequence for s71498 did not have any matches with the above transcripts.

2.3 Treatment of MIN6 cells to assess peroxisome abundance and toxicity

2.3.1 Palmitate and Oleate Media

9.2g of essentially fatty acid free Bovine Serum Albumin (BSA) was weighed out and added to 35ml complete high glucose DMEM in a 50ml centrifuge tube. Three falcon tubes were made up to make palmitate, oleate and BSA only media. The three tubes were sealed and left on roller for 3 hours to dissolve the BSA. Once the BSA had dissolved the solutions were made up to 50ml with DMEM.

Sodium palmitate was dissolved in 1ml 150mM NaCl at 70°C. Palmitate and oleate were then added to their respective tubes to give a concentration of 8mM. 1ml NaCl was added to the oleate and BSA control to ensure consistency throughout the solutions. The samples were incubated at 37°C overnight on a shaker.

Solutions were sterile filtered before dilutions were performed to achieve concentrations of 0.2, 0.25, 0.4 and 0.6mM palmitate or oleate for MIN6 cell incubation.

Final fat concentrations were kindly verified by Marie Appleton at Newcastle University.

2.3.1.1 Treatment of cells with Palmitate and Oleate

MIN6 cells of about 70% confluency were trypsinised, pelleted and resuspended in 10ml media. Cells were plated into 6 well plates at a density of $1x10^6$ cells/well and given 24hrs to settle and proliferate at 37°C, 5% CO_2. After 24hrs cells were treated in triplicate with different concentrations of palmitate or oleate. A BSA control was also set up in triplicate. The cells were then put back into the incubator at 37°C, 5% CO_2 for 4hrs, 12hrs, 24hrs or 48hrs.

2.3.2 PPARα agonist and Retinoic Acid Media

Clofibrate (liquid, Sigma) was diluted in 100% ethanol before being added to complete DMEM to make a stock solution of 10mM clofibrate (13.33% ethanol). Control medium containing 100% ethanol in complete DMEM was also made up.

Fenofibrate (Sigma) was weighed out and dissolved in DMSO to a concentration of 250mM. 1.84g essentially fatty acid free BSA was dissolved in 7ml of complete high glucose DMEM. 10µl of 250mM fenofibrate stock was added to the BSA solution and

made up to 10ml with DMEM to give a final concentration of 250µM fenofibrate containing 0.1% DMSO. BSA control was also made up containing 0.1% DMSO.

9-cis-Retinoic Acid (Sigma) was suspended in 1ml 100% sterile filtered ethanol to give a concentration of 3.33mM. This stock solution was diluted in 100% ethanol to make stocks of 200µM and 2µM which could be added directly to medium to acquire concentrations of 2000nM, 200nM, 20nM and 2nM with which to incubate the MIN6 cells. 9-*cis* retinoic acid (RA) was used in combination with fenofibrate, so 9-*cis* RA was added directly to the diluted stock of fenofibrate which the cells were to be incubated with, and 100% ethanol was added to the diluted BSA control.

2.3.2.1 Treatment of cells with Clofibrate

Cells were cultured in 6 well plates at a density of $1x10^6$ cells/well for 24 hours before being incubated with various concentrations (100µM, 250µM and 500µM) of clofibrate. Final percentage of ethanol in the above clofibrate concentrations were 0.13%, 0.33% and 0.67% respectively). Controls containing the equivalent amount of ethanol found in the 500µM clofibrate were also set up. Each experiment was carried out in triplicate. Compared with cells cultured in DMEM alone, the ethanol concentration in the control did not appear to cause any alterations in cell morphology (visualised with a microscope following treatment).

2.3.2.2 Treatment of cells with Fenofibrate

Cells were cultured in 6 well plates at a density of $1x10^6$ cells/well for 24 hours and then incubated with either: 2.5µM, 5µM, 10µM or 20µM of fenofibrate which contained 0.001%,0.002%, 0.004% and 0.008% DMSO repectively . Controls containing the equivalent amount of DMSO found in the 20µM fenofibrate (0.008% DMSO) were also set up and each experiment was carried out in triplicate. Again, cells were examined with a light microscope following treatment to ensure no obvious changes in cell morphology or the amount of debris were present.

2.3.2.3 Treatment of cells with Fenofibrate and Retinoic Acid

Again, cells were cultured in 6 well plates at a density of $1x10^6$ cells/well for 24 hours before treatment. Treatments containing 5µM of fenofibrate, 0.002% DMSO with varying concentrations of 9-*cis* RA (2000nM, 200nM, 20nM and 2nM) were set up. 2000nM and 20nM 9-*cis* RA contained 0.1% ethanol whereas 200nM and 2nM 9-*cis* RA

contained 0.01% ethanol. Controls containing the equivalent amount of DMSO (0.002%) and ethanol (0.1%) found in the 5µM fenofibrate with 2000nM 9-*cis* RA were also set up. Cells were incubated for 24 and 48hrs and each experiment was carried out in triplicate. Any experiments that were carried out using only the 2000nM 9-*cis* RA concentration with 5µM fenofibrate where made up using the 3.33mM stock of 9-*cis* RA and 250µM fenofibrate, and therefore contained 0.06% ethanol and 0.02% DMSO. The BSA control was set up to contain the same amounts of ethanol and DMSO. Following treatment images were taken of the cells to show whether any changes in morphology, or the amount of cell debris were present.

2.4 Real-time PCR

2.4.1 RNA extraction with on column DNase digest treatment

RNA was extracted using GenElute™ Mammalian Total RNA Miniprep Kit (Sigma) according to the manufacturer's instructions. RNA lysis solution was prepared by adding 10µl of β-mercaptoethanol to each 1ml of lysis solution needed. Medium was removed from the plates, cells were washed with PBS then lysis solution was added to each well (250µl per well in a 24 well plate). The lysis solution in the wells was then gently pipetted over the surface of the well several times to ensure all cells were lysed before the lysates either immediately underwent RNA extraction, or were collected in tubes, snap frozen in liquid nitrogen and stored at -80°C until needed.

For RNA extraction the cell lysates were transferred to filtration columns to remove cellular debris and shear DNA. An equal volume of 70% ethanol was then added to the filtered lysate before it was transferred to a binding column. The column was washed with wash solution 1 before carrying out a DNase digest.

The DNase digest was carried out using RNase-Free DNase Set (Qiagen). DNase I stock solution was prepared by dissolving solid DNase I in the RNase-free water provided. An appropriate volume of DNase incubation mix was made up (10µl DNase 1 stock solution added to 30µl of the supplied Buffer RDD per RNA binding column). 40µl of the mix was added directly onto the filter of each RNA binding column and incubated at room temperature for 15 minutes.

DNase treatment was followed by a series of washes which included an extra wash with 100% sterile filtered ethanol. The tubes were spun dry and RNA was eluted using the elution solution provided.

2.4.2 Agarose Gel Electrophoresis

1% agarose gel electrophoresis was used to check for the presence of the RNA and to make sure there was no DNA contamination. 1g agarose (Melford) was added to 100ml of 1x TBE buffer (89mM Tris-base, 89mM Boric acid, 2mM EDTA), and heated until dissolved. 2µl ethidium bromide solution (10mg/ml), (Sigma) was added to the solution. 5µl of RNA solution was added to 5µl water and 2µl loading dye (H_2O containing 15% Ficoll 900, 0.25% Bromophenol Blue). 10µl of this solution was loaded into wells and the gel was run in the presence of 1x TBE buffer at 100 volts for 45 minutes. Either BioLabs 1kb Quick-Load® DNA Ladder or Bioline HyperLadder™ IV was also loaded into a well.

2.4.3 NanoDrop

To measure the concentration of RNA in each sample so that equal concentrations of cDNA could be produced across samples, RNA was measured on a Thermo Scientific NanoDrop 1000 Spectrophotometer. 1µl of each sample was loaded onto the receiving fibre (end of the fibre optic cable) and RNA concentrations and purity (260/280 and 260/230 ratios) recorded. The volume of each sample added to the cDNA synthesis mixture could then be adjusted to account for differing concentrations of RNA.

2.4.4 cDNA Synthesis

cDNA synthesis was carried out using the High Capacity cDNA Reverse Transcription Kit (Applied Biosystems) according to the manufacturer's instructions. Briefly, an appropriate volume of master mix was made up so that each reaction contained:

Reaction component	Volume per reaction
10x RT Buffer	2.0µl
25x dNTP Mix	0.8µl
10x RT Random primers	2.0µl
MultiScribe™ Reverse Transcriptase	1.0µl
Nuclease-free H_2O	4.2µl
Total	10µl

The same concentration of RNA per sample was pipetted into a tube and topped up to 10µl with Nuclease-free H_2O if needed. 10µl of the RT master mix was then added to each tube and pipetted gently to mix. The tubes were briefly centrifuged to ensure that all contents of the tube were at the bottom. The tubes were then put in a thermal cycler and the reverse transcription was carried out under the following conditions:

Step	Temperature	Time
1	25°C	10 minutes
2	37°C	120 minutes
3	85°C	5 minutes
4	4°C	∞

cDNA was then stored at -20°C until needed.

2.4.5 Real-time PCR

Real-time PCR was carried out on LightCycler®480 (Roche). The SNARE gene Ykt6 was used as a reference gene as in a previous study it was found to be consistently expressed in a variety of different tissues (Pascoe, 2009). Primers (Figure 10 and Figure 11) detailed below are all 10x QuantiTect® Primer Assays (Qiagen) which were delivered as lyophilized powder and were reconstituted by adding 1.1ml Tris-EDTA (TE) buffer solution (Sigma), before being aliquoted to avoid repeated freeze-thaw cycles.

Probe	Assay Name	Catalogue Number	Transcript detected	Species	Amplicon Length	Amplified exons
Ykt6	Mm_Ykt6_1_SG	QT00165403	NM_019661	Mouse	81bp	6/7
Pex11α	Mm_Pex11a_1_SG	QT00110418	NM_011068	Mouse	70bp	2/3
Pex11β	Mm_Pex11b_2_SG	QT01052058	NM_011069	Mouse	111bp	2/3

Each reaction was performed in triplicate, with the reaction mixtures loaded into a LightCycler®480 Multiwell Plate 96, and sealed with LightCycler®480 Sealing Foil.

Several dilutions were tested, but for the *PEX11α* gene a 1 in 4 dilution was seen to be the best for the standard curve.

The following reagents were made up as a master mix:

Component	Amount per Reaction	Supplier
Water, PCR grade	7µl	Roche
LightCycler®480 SYBR Green I Master	10µl	Roche
10x QuantiTech Primer	1µl	Qiagen
Total	18µl	

18µl of master mix and 2µl of sample was added to each well to give a total volume of 20µl in each well before being sealed. The plate was then briefly centrifuged and loaded onto the LightCycler®480.

The conditions for PCR were as follows:

	Number of cycles	Temperature	Hold (time)
Pre-incubation	1 cycle	95.0°C	5 minutes
Amplification	45 cycles	95.0°C	10 seconds
		60.0°C	30 seconds
Melting Curve	1 cycle	95.0°C	5 seconds
		65.0°C	1 minute
	Increase to 97.0°C at a rate of 0.11°C/s		
Cooling	1 cycle	40.0°C	Continuous

Selected real time PCR products for each primer were run on a 1% agarose gel (section 2.4.2) to ensure they were of the correct amplicon size.

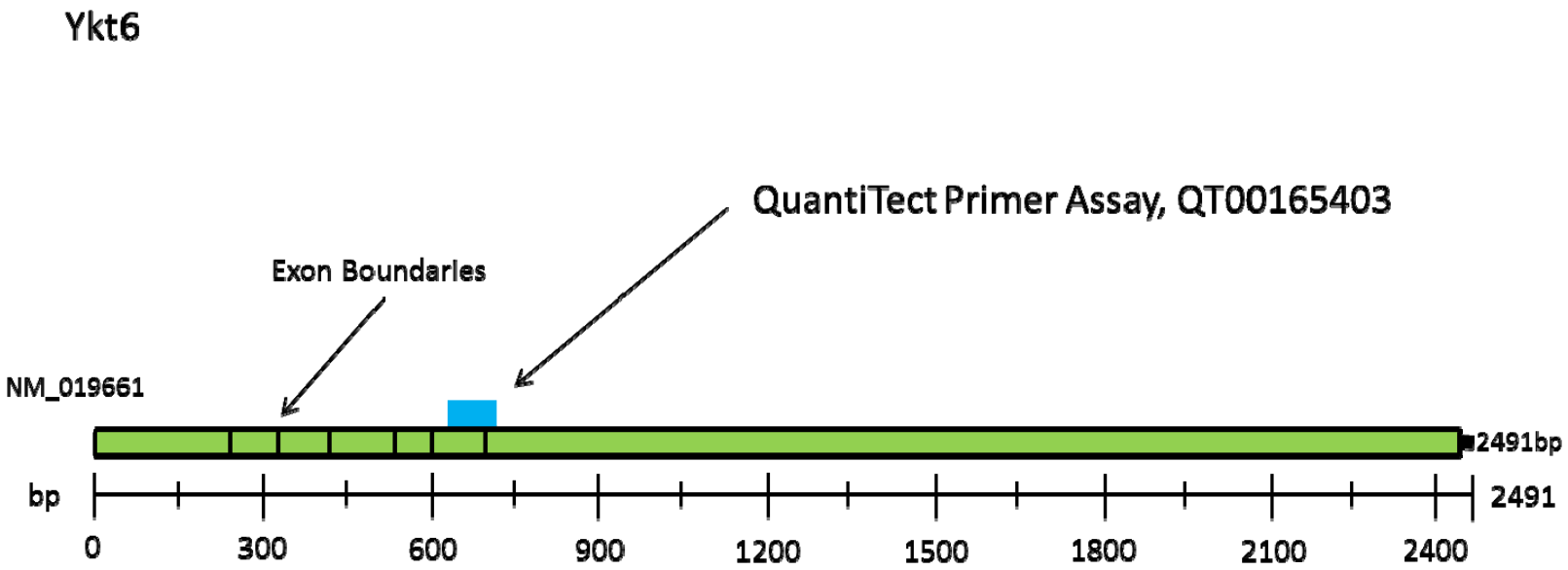

Figure 10 Ykt6 mRNA transcript and primer assay target

The reference gene Ykt6 is amplified by the QuantiTect Primer assay between exons 6 and 7 to produce an 81bp amplicon.

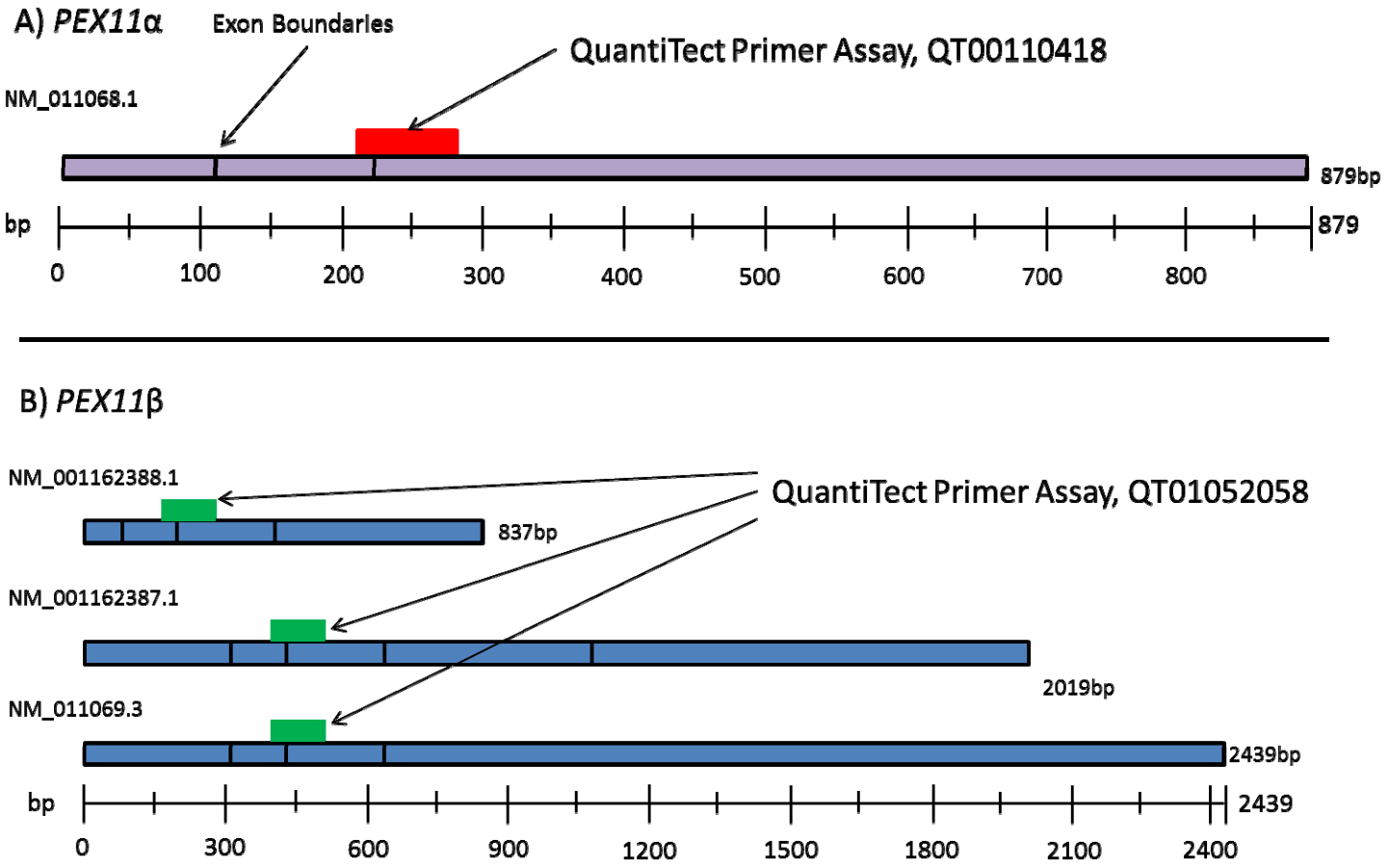

Figure 11 *PEX11*α and *PEX11*β mRNA transcripts and primer assay targets

A) *PEX11*α is amplified by the QuantiTect Primer assay between exons 2 and 3 to produce a 70bp amplicon. **B)** *PEX11*β is amplified by the QuantiTect Primer assay between exons 2 and 3 in all coding transcripts to produce a 111bp amplicon.

2.4.6 Comparative C_T Method ($\Delta\Delta C_T$ Method)

The $\Delta\Delta C_T$ Method was employed for the quantification of gene expression following the SYBR-Green real time PCR assays (Schmittgen and Livak, 2008). Providing the reaction efficiencies between the targets and the control are comparable, relative quantification can be calculated using a series of formula rather than a standard curve method. Briefly, following calculation of the mean C_T and standard deviation for the replicated samples, the ΔC_T is first calculated using the following:

$$\Delta C_T = C_{T\ target} - C_{T\ reference}$$

Once the ΔC_T for every sample had been calculated the $\Delta\Delta C_T$ was calculated by subtracting the ΔC_T of the control/untreated sample from the ΔC_T of the treated samples:

$$\Delta\Delta C_T = \Delta C_{T\ treated} - \Delta C_{T\ control}$$

Finally the fold change was determined by incorporating the reaction efficiency (which is 2) into the calculation:

$$\text{Fold change} = 2^{-\Delta\Delta Ct}$$

Once all experiments were repeated standard deviation was calculated and standard error of the mean (SEM) was determined to represent the error of the experiments in the plotted graphs.

2.5 Immunofluorescence

An antibody against peroxisomal membrane protein-70 (PMP-70, a peroxisomal membrane marker) was used for the detection of peroxisomes by immunofluorescence. An antibody against C-peptide was used to validate the ability of MIN6 cells to produce insulin. All primary and secondary antibodies used are included in Table 3.

Cells were grown directly onto sterile cover slips at a density of $2x10^5$ cells/cover slip in 6 well plates. Medium was removed and the cells were washed 3 times with PBS then fixed with 4% paraformaldehyde for 20 minutes at room temperature. Cells were then permeabilised with 0.2% t-octylphenoxy-polyethoxyethanol (Triton x-100, Sigma) for 45 minutes. Slides were treated with blocking buffer (20% FBS in PBS) for 1 hour at room temperature to block non-specific binding before the primary antibody was added. Cover slips were incubated in 1 in 600 dilution of primary antibody in 0.05% FBS in PBS at room temperature for 1 hour. Before secondary antibody incubation the cover slips were washed 3 times for 5 minutes in PBS. 1 in 300 dilution of secondary antibody in 0.05% FBS in PBS was applied for one hour at room temperature in the dark. The cover slips were then washed again 3 times for 5 minutes in PBS before mounting them on slides with DAPI (Vectashield Mounting Medium with DAPI, Vector). Varnish was used to seal the coverslip in place and prevent any mounting medium from leaking. Slides were visualised on a Zeiss LSM 780 confocal microscope.

A)

Protein	Primary Antibody	Reactivity	Supplier	Catalogue number	Dilution
Peroxisomal membrane protein-70 (PMP-70)	Rabbit polyclonal Anti-PMP70 antibody	Mouse, Rat, Hamster, Human, Non-Human Primates	Abcam	ab3421	1:600
C-peptide	Rabbit polyclonal antibody against C-peptide	Human, Mouse, Rat	Cell Signaling Technology	#4593	1:600

B)

Secondary Antibody	Conjugation	Supplier	Catalogue number	Dilution
AffiniPure Donkey Anti-Rabbit IgG	Cy3	Jackson ImmunoResearch Laboratories	711-165-152	1:300
AffiniPure Donkey Anti-Rabbit IgG	FITC	Jackson ImmunoResearch Laboratories	711-095-152	1:300
Goat Anti-Rabbit IgG	Alexa Fluor® 546	Life Technologies	A-11010	1:300

Table 3 Antibodies used for immunofluorescence

A) The Primary antibodies used for immunofluorescence and, **B)** the secondary antibodies used to allow detection of the bound primary antibody.

2.6 Oil Red O staining

To ensure that lipids were entering the cells after incubation with palmitate and oleate Oil Red O staining was carried out. For this staining, a Steatosis Colorimetric Assay Kit (Cayman Chemical Company) was used according to the manufacturer's instructions. Briefly, cells were grown in palmitate and oleate culture medium in 24 well plates at 37°C, 5% CO_2. 48hrs after treatment, medium was removed and fixative (diluted 1:10 in PBS) was added to each well and incubated for 15 minutes. Cells were washed 2 times for 5 minutes with Lipid Droplets Assay Wash Solution and then left to dry completely in the tissue culture hood. A working solution of Lipid Droplets Assay Oil Red O Solution was prepared by diluting the stock to 60% in dH_2O before filtering with a 0.45µm syringe filter. This working stock was then added to every well and incubated for 20 minutes. The Oil Red O solution was then removed and the wells washed several times with dH_2O until all the water no longer showed signs of red. The wells were then washed 2 times for 5 minutes with Lipid Droplets Assay Wash Solution before being visualised with a light microscope.

2.7 Analysis by Western Blot

2.7.1 Protein extraction

Cells were washed 3 times with PBS before an appropriate volume of protein extraction buffer (100mM Tris-Cl, pH 7.4, 100mM KCl, 1mM EDTA , 25mM KF, 0.1% Triton X-100, 0.5mM sodium orthovanadate, 1x protease inhibitor cocktail (Thermo Scientific) was added to each well (70µl per well for a 24 well plate, 150µl per well for a 6 well plate). To ensure all cells detached from the wells, cells were scraped using the end of a pipette tip or a cell scraper, and lysates were collected in screw-cap microcentrifuge tubes. Each sample was briefly sonicated for approximately 10 seconds at 5µm amplitude to ensure cell lysis. Samples were then snap frozen in liquid nitrogen and stored at -80°C until required.

2.7.2 Protein determination

Samples were defrosted on ice and then centrifuged at maximum speed for 5 minutes at 4°C before use to ensure any cell debris did not interfere with the determination process.

2mg/ml BSA (Thermo Scientific) was used to construct a standard curve. The BSA was diluted to a working concentration of 400µg/ml with protein extraction buffer. 1µl to 10µl of the diluted BSA was pipetted into a 96 well plate in duplicate and the final volume was made up to 10µl with protein extraction buffer to construct the standard curve. 10µl of each sample was also pipetted into the 96 well plate in duplicate. 200µl of Coomassie blue stain (Thermo Scientific) was then added to each well before being read on a plate reader at 595nm.

2.7.3 SDS-PAGE

For separation of the proteins on the gel, 10% resolving gels were made up with a 4% stacking gel. To make the gels, the following recipes were used:

	10%	4%
dH_2O	11.8ml	9.4ml
acrylamide (40% solution)	6.4ml	1.5ml
Buffer B (1.5M Tris, pH 8.8)	6.3ml	-
Buffer D (0.5M Tris, pH 6.8)	-	3.8ml
10% SDS	50µl	150µl
10% APS	250µl	150µl
TEMED	12.5µl	7.5µl

The 10% gel mixture was poured between the plates used to make the gel leaving a gap at the top for the stacking gel. A layer of dH_2O was applied on top and the gel was left to set. Once set, the 4% stacking gel was poured in the gap at top and a comb inserted.

4x sample buffer (0.25M Tris-HCl pH 6.8, 8% SDS, 40% Glycerol, 0.008% Bromo-phenol blue, 20% β-mercaptoethanol) was made up as a stock solution. Protein samples were made up to contain 10µg of protein and 1x sample buffer. Protein extraction buffer was used to ensure each sample had the same volume before adding the sample buffer. The samples were boiled for 3 minutes to denature the proteins before loading them, along with a prestained protein ladder (Broad Range (7-175 kDa), New England Biolabs, catalogue number P7708S) onto the gel. The gel was immersed in 1x electrode buffer (25mM Tris, 192mM glycine, 0.1% SDS) and run at 40mA (or 80mA for 2 gels) for 1hr to separate the proteins.

2.7.4 Western Blot

After SDS-PAGE the separated proteins were transferred to nitrocellulose membranes. The membranes were first soaked in dH_2O for 5 minutes before being placed in a cassette with filter paper. The cassette was then inserted into a tank containing transfer buffer (10mM CAPS, 10% methanol) and soaked for 10-15 minutes. The cassettes were then taken out and the gels put in. The membrane was laid gently on top of the gel inside the cassette ensuring there were no air bubbles before being inserted back inside the tank. The apparatus was run at 250mA for 2hrs to allow the transfer of the proteins onto the membrane.

Once transfer was complete the membrane was stained with Ponceau S solution (Sigma) for 5 minutes to check whether transfer was successful. The solution binds reversibly to the protein to show definite red bands. The membrane was washed several times with TBS-Tween (10mM Tris-HCl, pH 7.4, 150mM NaCl, 0.1% Tween) until all protein bands had disappeared.

The membranes were blocked in TBS-Tween containing 5% milk for 1 hour on a shaker at room temperature. Primary antibody (Table 4) was diluted in TBS-Tween containing 1% milk and the membranes were incubated in this overnight on a shaker at 4°C.

Following primary antibody incubation, cells were washed 3 times for 5 minutes on a shaker with TBS-Tween then incubated with secondary antibody (Table 5) conjugated to horse-radish peroxidase (HRP) diluted in TBS-Tween containing 1% milk for 2 hours on a shaker at room temperature. After secondary antibody incubation the membranes underwent another 3 5 minute washes before the addition of enhanced chemiluminescent (ECL) solution. ECL contains a substrate which is oxidised by the HRP on the secondary antibody in combination with hydrogen peroxide. It is a light emitting reaction which can be enhanced, and thus detected. Membranes were incubated on a shaker with 2.5ml SuperSignal West Pico Luminol Enhancer solution (Thermo Fisher Scientific) and 2.5ml SuperSignal West Pico Stable Peroxide solution (Thermo Fisher Scientific) for 5 minutes before they were wrapped in Saran wrap and secured with tape in a cassette for autoradiography.

Protein	Primary Antibody	Raised In	Reactivity	Supplier	Catalogue number	Dilution	Expected Protein Size
Peroxisomal membrane protein-70 (PMP-70)	Polyclonal Anti-PMP70 antibody	Rabbit	Mouse, Rat, Hamster, Human, Non-Human Primates	Abcam	ab3421	1:1000	70kDa
Peroxisomal biogenesis factor 11 alpha (PEX11α)	Polyclonal Peroxin 11α Antibody (Q-12)	Goat	Mouse, Rat	Santa Cruz Biotechnology	sc-104604	1:200	28kDa
Peroxisomal biogenesis factor 11 alpha (PEX11α)	Polyclonal Anti-PEX11A antibody	Rabbit	Human **Predicted to work with:** Mouse, Rat, Horse, Guinea pig, Cow, Cat, Dog	Abcam	ab104959	1:500	28kDa
Peroxisomal biogenesis factor 11 β (PEX11β)	Polyclonal Anti-PEX11B antibody	Rabbit	**Reacts with:** Human **Predicted to work with:** Mouse, Rat	Abcam	ab74507	1:1000	28kDa
β-Actin	Monoclonal Anti-β-Actin antibody	Mouse	Canine, Guinea pig, *Hirudo medicinalis*, Feline, Pig, Mouse, Carp, Chicken, Sheep, Rabbit, Rat, Human, Bovine	Sigma-Aldrich	A5441	1:10,000	42kDa

Table 4 Details of the primary antibodies used for Western blotting.

Secondary Antibody	Raised in	Conjugate	Supplier	Catalogue number	Dilution
Anti-Rabbit IgG (whole molecule) antibody	Goat	Peroxidase	Sigma-Aldrich	A0545	1:1000
Anti-Mouse IgG (whole molecule) antibody	Rabbit	Peroxidase	Sigma-Aldrich	A9044	1:10,000
Anti-Goat IgG (whole molecule) antibody	Rabbit	Peroxidase	Sigma-Aldrich	A5420	1:1000

Table 5 Details of the secondary antibodies used for western blotting.

2.7.5 Chemiluminscence detection

As the addition of ECL solution causes a light emitting reaction, it is able to be detected on a light sensitive autoradiography film. When the film is placed on top of the membrane, the light that is emitted exposes the film. Once developed, dark bands show the protein of interest, to which the HRP was bound. The entire process must be carried out in a dark room using red lights as other light could over-expose the film.

X-Ray film (CL-XPosure™ Film, Thermo Scientific, catalogue number #34089) was placed on top of the nitrocellulose membrane and the cassette lid closed. The film was exposed to the membrane for a certain time before being put into developing solution (Carestream® Kodak® autoradiography GBX developer/replenisher, Sigma-Aldrich, catalogue number P7042) for 1 minute. The film was washed briefly in water, and then placed in fixer solution (Carestream® Kodak® autoradiography GBX fixer/replenisher, Sigma-Aldrich, catalogue number P7167) for 1 minute. The film was washed again with water and left to dry. Before use, both the developer and fixer were diluted 1:10 in water. The protein bands on the film could then be quantified using densitometry.

2.7.6 Stripping of the nitrocellulose membrane

When more than one primary antibody was used, following development of the first protein of interest the nitrocellulose membranes were removed from the saran wrap and washed with TBS-Tween. Following this, they were incubated in Restore PLUS Western Blot Stripping Buffer (Thermo Fisher Scientific) for 10 minutes to remove both primary and secondary antibodies from the membrane. This allows successful reprobing of the membrane. Following incubation with the stripping buffer membranes were washed with TBS-Tween then re-blocked with 5% milk before primary antibody incubation.

2.7.7 Densitometry

Quantification of the protein bands was carried out using a GS-800 Calibrated Densitometer (BioRad) and the BioRad software Quantity One 4.2.3. All proteins were normalised to β-actin which was used as a loading control in each western blot.

2.8 Glucose Stimulated Insulin Secretion (GSIS) Assay

The method for glucose stimulated insulin secretion was adapted from (Ishihara *et al.*, 1994).

2.8.1 Krebs-Hepes buffer

Krebs-Hepes buffer was made up in dH_2O containing; 119mM NaCl, 4.74mM KCl, 2.54mM $CaCl_2$, 1.19mM $MgCl_2$, 1.19mM KH_2PO_4, 25mM $NaHCO_3$, 10mM Hepes and 0.5% BSA. The pH was adjusted to 7.4 using HCl before the addition of the BSA. The solution was sterile filtered using a 0.2µm filtropur syringe filter (Sarstedt) and preheated to 37°C before use.

2.8.2 GSIS

Cultured MIN6 cells were washed twice with Krebs-Hepes Buffer to wash away any media then the cells were pre-incubated with Krebs-Hepes (glucose free) for 30min at 37°C, 5% CO_2. Cells were then washed once with Krebs-Hepes before incubation with either 3mM glucose (basal levels) or 25mM glucose (stimulating levels) for 1 hour at 37°C, 5% CO_2. Following incubation, the Krebs-Hepes buffer containing the secreted insulin was collected in ice cold tubes and centrifuged at 1000g at 4°C for 5 minutes to remove any cellular debris. The supernatant was stored at -20°C until use with Insulin ELISA kit to determine insulin secretion. Cells were washed in PBS and harvested using protein extraction buffer as described in section 2.7.1.

2.8.3 Insulin Enzyme Linked Immunosorbent Assay (ELISA)

A high range rat insulin ELISA kit (Mercodia AB) was used, according to the manufacturer's instructions, to determine the amount of insulin that was secreted. The assay uses a sandwich ELISA technique whereby two different monoclonal antibodies, one of which is bound to the titration well, against insulin are able to bind to two separate antigenic determinants on the insulin molecules within the sample. A wash step removes any unbound antibody and the formation of the insulin-enzyme conjugate can be detected.

The ELISA was carried out in duplicate. A standard curve was constructed using the calibrators provided (3, 7.5, 30, 75 and 150µg/L). The samples were diluted in Krebs-Hepes before use to ensure the samples would fall within the standard curve. 10µl of the samples and calibrators were added to the pre-coated wells along with 50µl

enzyme conjugate solution and incubated on a plate shaker at room temperature for 2 hours. The ELISA plate was washed 6 times to remove any unbound labelled enzyme. Substrate TMB was then added to the wells and incubated at room temperature for 15 minutes.

Finally stop solution was added to stop the reaction, and the absorbance measured at 450nm. Insulin concentrations of the unknown samples were calculated using the reading from the calibrators at a known concentration and constructing a standard curve.

2.9 Lactate Dehydrogenase (LDH) assay

Lactate dehydrogenase (LDH) is an enzyme found throughout all cell types. When the plasma membrane is damaged it is released into the culture medium making it a good marker of cytotoxicity. The assay was carried out according to the manufacturer's instructions. Briefly, culture medium was collected in Eppendorf tubes at the end of an experiment, and centrifuged at 600g for 10 minutes to pellet any cells. WST Substrate Mix was reconstituted in dH_2O, and an aliquot was added to LDH Assay Buffer to make a working LDH Reaction Mix. Medium samples were pipetted into a clear flat-bottomed 96 well plate, LDH Reaction mix was added to each well and incubated for 30 minutes at room temperature. Positive controls using the control provided were set up to ensure all reagents were working correctly. After incubation, the absorbance was read at 450nm.

2.10 Caspase 3/7 assay

Apoptosis (programmed cell death) can be assessed by measuring the activities of caspases (cysteine aspartic acid-specific proteases) 3 and 7, effector caspases which mediate apoptosis.

Caspase 3/7 activity was measured using the luminescent Caspase-Glo® 3/7 Assay (Promega), which was carried out according to the manufacturer's instructions with a slight adaptation so the assay could be used with a 24 well plate. Briefly, to prepare the reagent, once at room temperature the entire contents of the Caspase-Glo® 3/7 buffer was added to the Caspase-Glo® 3/7 substrate and inverted several times until the substrate dissolved. Medium was removed from cells grown in 24 well plates and 100µl serum free DMEM was added to each well. 100µl Caspase-Glo® 3/7 reagent was

then added to each well and left for about 2 hours allowing all cells to lyse. The mixture was then transferred into white-walled 96 well plates and was left at room temperature for a further 30 minutes before the luminescence was read on a plate reader. Cells were treated with Staurosporine to use to as a positive control, and blank wells were also set up containing serum free medium and reagent without any cells.

2.11 Statistical Analysis

All statistical analysis was carried out using Graphpad Prism. Data are presented as mean ± SEM (standard error of the mean) for several experiments. One way ANOVA followed by Bonferroni's *post hoc* test (multiple comparisons) or an unpaired paired t-test was used to test for statistical significance. A p-value of <0.05 was considered significant.

Chapter 3

Model for Reducing Expression of *PEX11α* in MIN6 cells

3 Model for Reducing Expression of *PEX11α* in MIN6 cells

3.1 Introduction

In recent years, cases of type 2 diabetes mellitus have been rapidly rising towards pandemic levels (Hossain *et al.*, 2007; Ma, 2012). The characteristic insulin resistance and pancreatic β-cell dysfunction seen in the disease can be influenced by both genetic and environmental factors. The use of GWAS and candidate gene studies has greatly increased our knowledge of the genes which may have a role in an individual's susceptibility to the disease (McCarthy and Zeggini, 2009; Kato, 2013; Brunetti *et al.*, 2014).

Work carried out by Laura Pascoe during completion of her thesis in 2009 used the candidate gene approach, using data from the RISC (Relationship between Insulin Sensitivity and Cardiovascular Disease) cohort, to look within the perilipin gene region and identify SNPs associated with the alteration of an individual's β-cell function. β-cell function was assessed by means of a 30 minute oral glucose tolerance test. Susceptibility alleles were identified in two SNPs within the perilipin gene region, rs4578621 located within intron 1 of perilipin and rs1972435 located within intron 2 of *PEX11*α, a gene which shares a promotor region with perilipin. For both SNPs, the G allele, which also happens to be the major allele, was associated with a significant decrease in insulin in the 30 minute oral glucose tolerance test (Figure 12). Further studies led to the discovery that *PEX11*α, but not Perilipin is expressed in human islets and MIN6 cells (Pascoe, 2009).

PEX11α is a protein involved in the division of peroxisomes in response to extracellular stimuli. PEX11β, another isoform of PEX11, is thought to control constitutive peroxisome division. This was shown in a study carried out in 1998 where rats fed a diet of clofibrate, a peroxisomal proliferating agent, produced a 10-fold increase in *PEX11*α expression showing its inducible property to a stimulus. Although over-expression of *PEX11*β does lead to increases in peroxisome abundance, the expression levels did not appear to change with a stimulus. In addition expression of *PEX11*β was found to be consistent over a variety of tissues (Schrader *et al.*, 1998).

A)

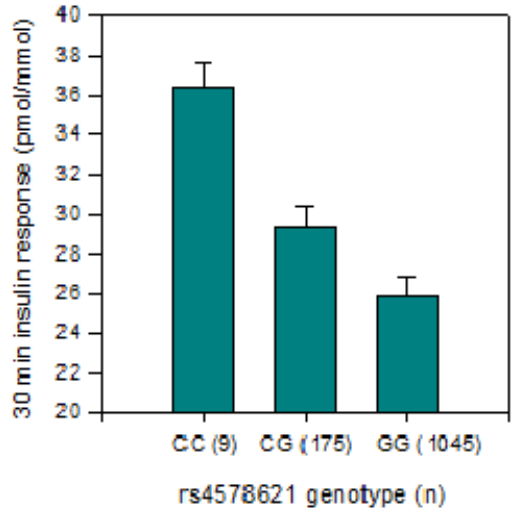

B)

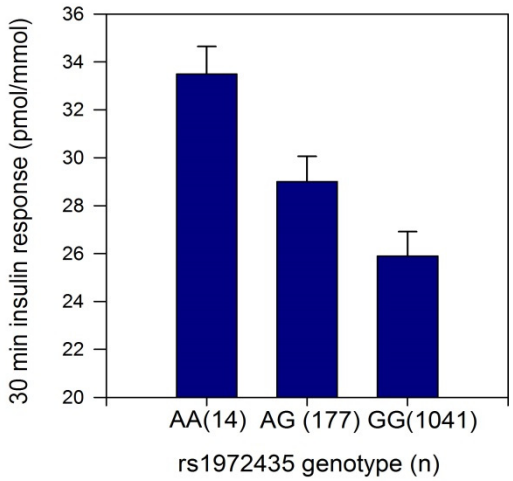

Figure 12 The 30 minute insulin response after an oral glucose tolerance test

Taken from (Pascoe, 2009), these graphs show the insulin response for subjects 30 minutes after taking glucose. The two graphs show the different SNPs found to be associated with a decreased insulin response. **A)** shows the SNP located on perilipin, rs4578621, and **B)** the SNP located on PEX11α, rs1972435. Both SNPs are separated by genotype.

3.2 Aim

The main aim of this chapter was to produce a reliable method for the reduction of *PEX11*α expression in MIN6 cells. We began by:

- Validating the use the MIN6 cells as an insulin producing cell line by staining for C-peptide.
- Confirming the presence of peroxisomes within MIN6 cells by staining for a known peroxisomal membrane protein.
- Ensuring the QuantiTect primer assays for *PEX11*α, *PEX11*β and the reference gene Ykt6 worked efficiently by producing real time PCR standard curves.
- Finding a method of transfection which gave consistent knockdown of *PEX11*α.
- Assessing the effect of *PEX11*α knockdown on the expression of *PEX11*β.

3.3 Methods

3.3.1 Immunofluorescence of MIN6 cells for the detection of C-peptide and peroxisomes

Immunofluorescence is a technique which allows visualisation of the relative abundance and location of the protein of interest. It uses antibodies conjugated to a fluorescently labelled dye which can bind the protein. There are two main methods of immunofluorescence. Less commonly used is the direct method which uses a fluorescent dye conjugated directly to the antibody against the protein of interest. The indirect method, used in this work, utilises a 2 antibody technique. An unlabelled primary antibody against the protein of interest which binds first, then a labelled secondary antibody against the primary antibody that has been raised in another species, and thus leads to the detection of the protein of interest.

An antibody against C-peptide was used to visualise whether MIN6 cells were producing insulin. C-peptide is cleaved from proinsulin to yield insulin at the last stage of insulin synthesis. For every molecule of insulin produced, there is one molecule of C-peptide, making it a good marker of insulin production (Bruemmer, 2006). An antibody against PMP-70 was used to visualise peroxisomes within the cells. PMP-70 is an ATP-binding cassette (ABC) transporter, and a major component of the peroxisomal membrane making it a good protein to use to detect the presence of peroxisomes in MIN6 cells (Imanaka *et al.*, 1999; Imanaka *et al.*, 2000). DAPI (4'.6-diamidino-2-

phenylindole), which can bind the A-T rich areas of DNA and form a fluorescent complex, was used to counterstain the nucleus (Kapuscinski, 1995).

Once antibody was bound to the cells (protocol detailed in section 2.5) coverslips were mounted onto slides with Vectashield mounting medium containing DAPI. To visualise the cells, light at different wavelengths, depending on the secondary antibody bound, was used to excite the electrons within the fluorescent dye. As the electrons drops from an excited state back down to a more stable energy level, it gives off light at a different wavelength to the one at which excitation occurred. For example, DAPI has an excitation wavelength of 360nm, and an emission wavelength of 460nm. Secondary antibodies used were able to be visualised using the TRITC (red) or FITC (green) filters. DAPI was visualised using the UV filter (blue).

3.3.2 Relative Real-Time PCR for the quantification of PEX11α and PEX11β Gene Expression

For the quantification of the expression of the genes *PEX11*α and *PEX11*β, relative real-time PCR using a SYBR green dye was carried out. SYBR green is a dye which specifically binds double-stranded DNA. As the DNA is amplified the fluorescence increases as more SYBR green dye binds, meaning that it can be detected. A slight disadvantage in its specificity is that it will bind all double stranded DNA, including non-specific reaction products. It is therefore important to ensure the reaction has a method in place in order to determine whether the fluorescence generated is a measure of the target gene amplification only, and not any genomic DNA contamination or primer dimer. A melt/dissociation curve can be carried out at the end of each PCR reaction. The melt curve shows a change in fluorescence at the point at which the double-stranded DNA becomes single stranded as the temperature is slowly raised. This change in fluorescence occurs as the SYBR green dye is released as it can no longer bind the denatured DNA. The temperature at which the DNA becomes denatured depends on several factors including the length of the amplicon and the GC content. This means that the amplicon produced by each primer can have a different melting point (T_m), and therefore the presence of contamination can be determined. Amplification curves, melting curves and melting peaks are shown in Figure 13 (*PEX11*α), Figure 14 (*PEX11*β) and Figure 15 (Ykt6).

For some PCR runs, rather than carrying out a melt curve the PCR products were separated on a 1% agarose gel (protocol detailed in section 2.4.2). Samples for each target gene as well as negative controls were loaded onto the gel and run at 100 volts for 45 minutes to separate the products. The gel was then visualised using UV light to determine the amplicon size generated by the primers.

There are two different methods of analysis for the quantification of the relative real-time PCR, the relative standard curve method, and the comparative C_T method ($\Delta\Delta C_T$). For the relative standard curve method a set of standards, made from a calibrator, are used to quantify the unknown samples. A calibrator would be the untreated sample where quantification was dependent on comparing treated to untreated. The $\Delta\Delta C_T$ method does not require the use of a standard curve for the actual calculations, however, standard curves are required to start with to ensure reaction efficiencies of the target and reference primers are approximately equal to validate the method. If the reaction efficiencies are not similar then $\Delta\Delta C_T$ may not be the correct method to use.

The quantification is achieved by utilising a series of mathematical formulas (detailed in section 2.4.6). For this work the $\Delta\Delta C_T$ method was used to quantify the results, however, standard curves were set up originally, using a 1:4 dilution, to check the reaction efficiencies for the primers.

MIN6 cells were seeded into 6 well plates and incubated at 37°C at 5% CO_2 until cells were confluent. RNA was then extracted, and cDNA synthesised before real-time PCR could be carried out.

A) Amplification Curve

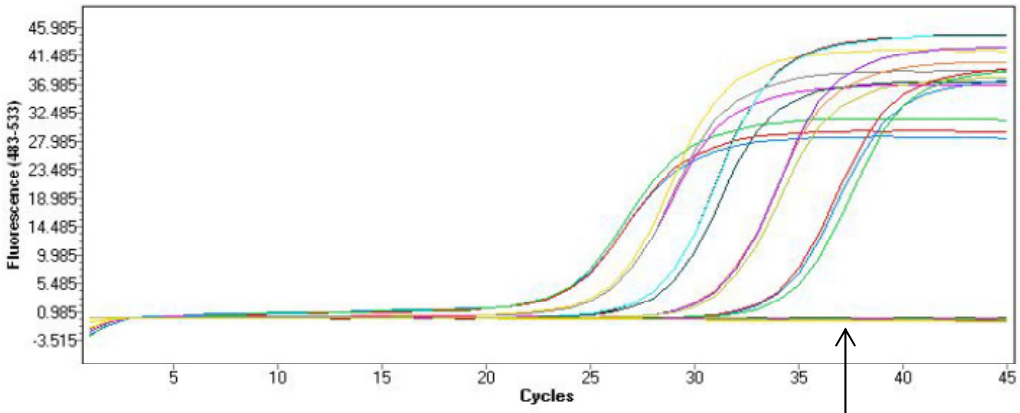

B) Melting Curves

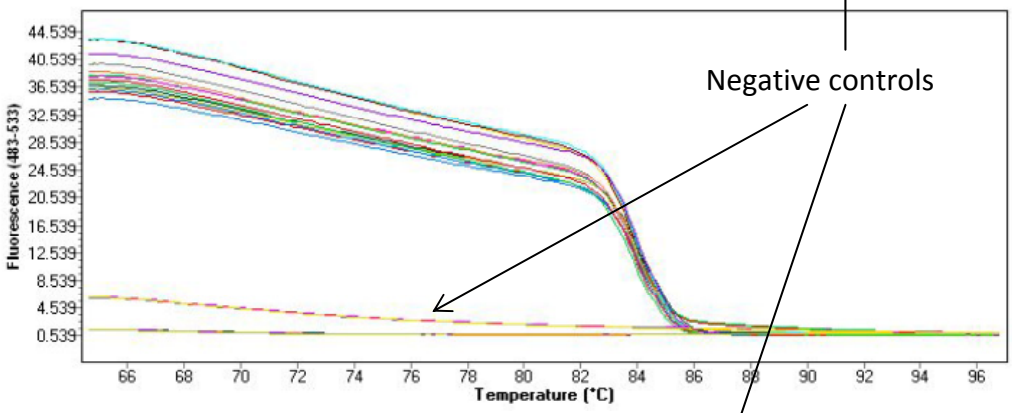

C) Melting Peaks

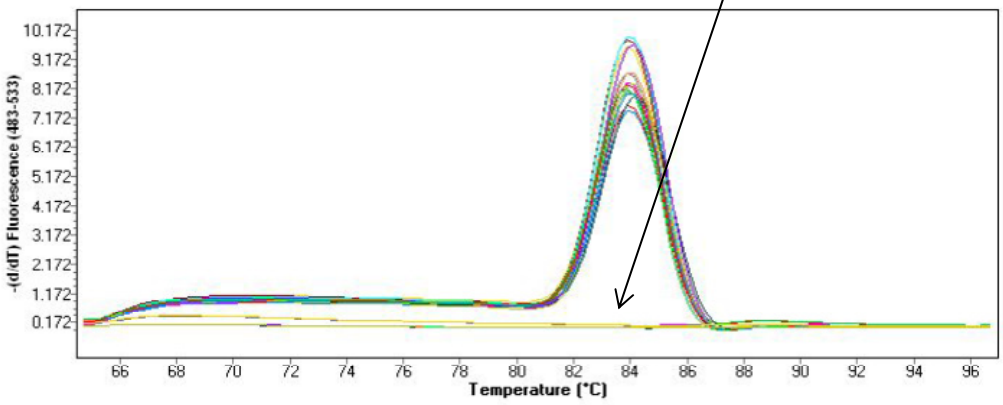

Figure 13 Typical amplification curves, melting curves, and melting peaks for *PEX11α*

Typical amplification curves for *PEX11*α produced through SYBR-green real-time PCR. A) An amplification curve is produced as the fluorescence increases though each cycle. A 1:4 dilution for the *PEX11*α primers is shown with no amplification present in the negative controls which contained PCR H_2O rather than cDNA. B) For each run a melting curve was produced showing the dissociation of the double stranded DNA as the temperature was increased. C) From the melting curves melting peaks were able to be generated. Each PCR amplicon has an individual melting peak (about 84°C for *PEX11*α) making it apparent whether target cDNA is amplified, or whether genomic DNA has been amplified or primer dimers produced.

A) Amplification Curves

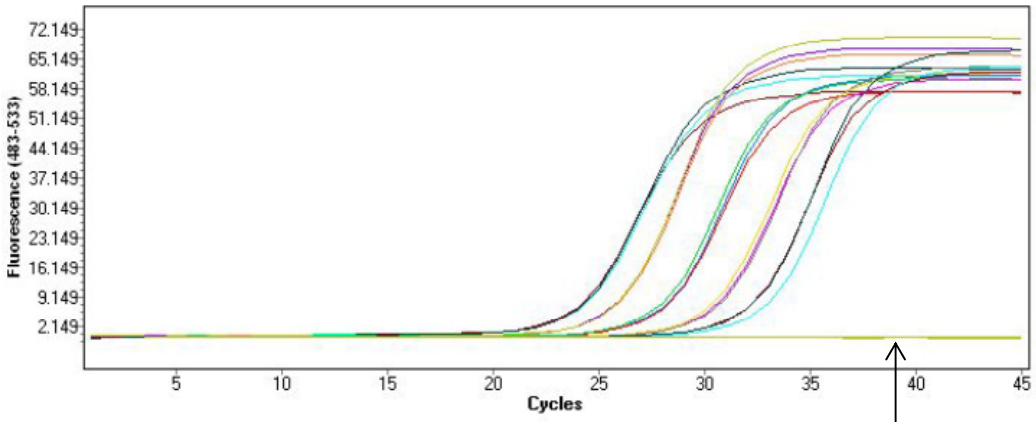

B) Melting Curves

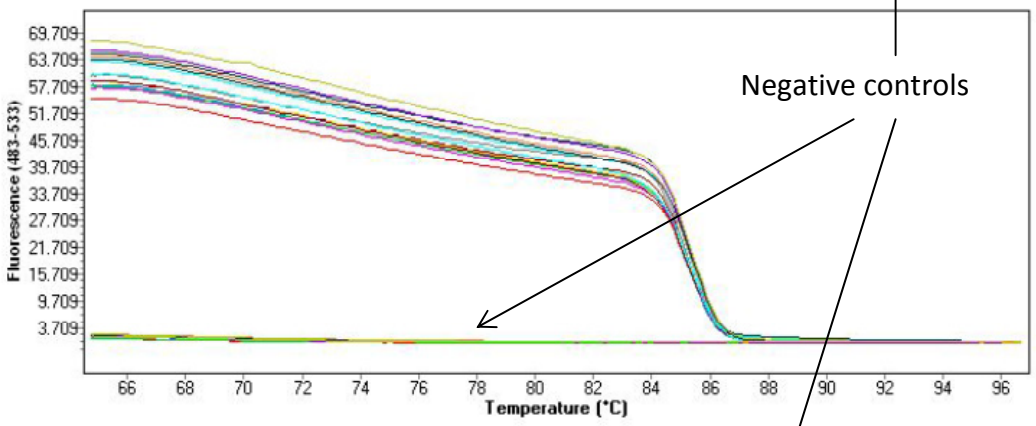

Negative controls

C) Melting Peaks

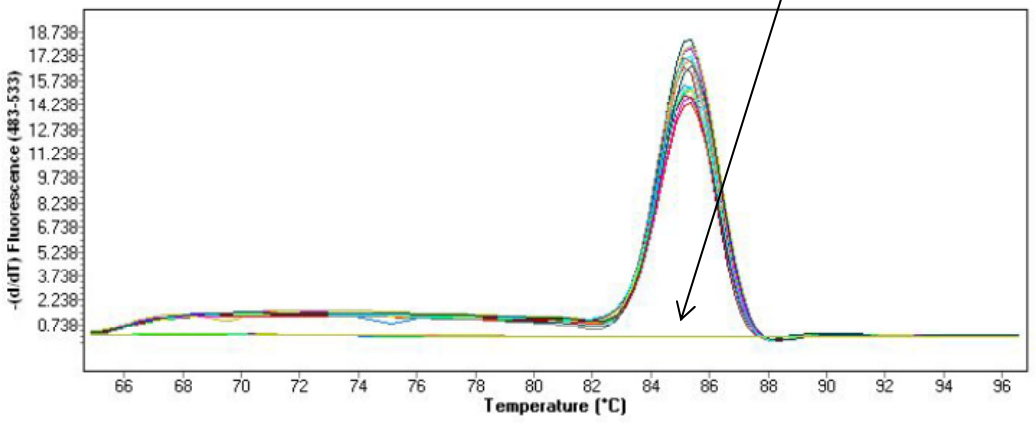

Figure 14 Typical amplification curves, melting curves, and melting peaks for *PEX11*β

Typical amplification curves for *PEX11*β produced through SYBR-green real-time PCR. **A)** An amplification curve showing a 1:4 dilution for the *PEX11*β primers. **B)** Melting curve and **C)** melting peaks again showing no amplification in the negative controls. *PEX11*β has a melting peak at about 85°C.

A) Amplification Curves

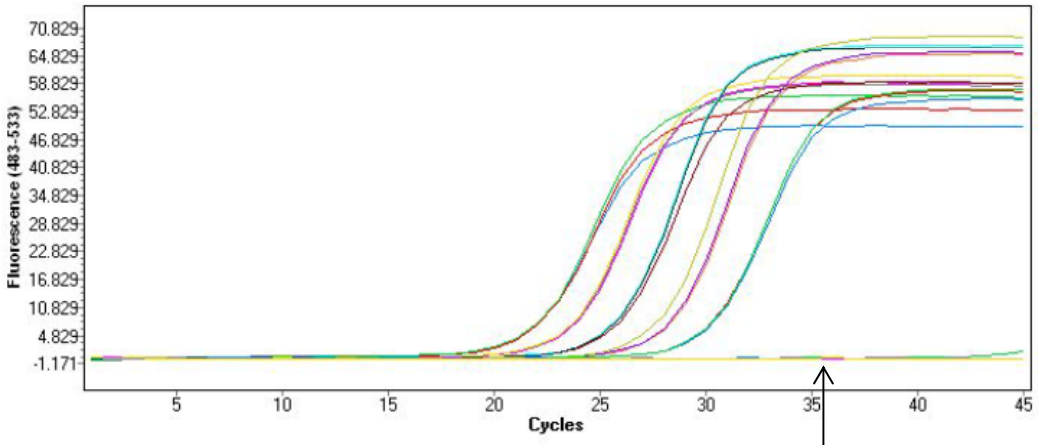

B) Melting Curves

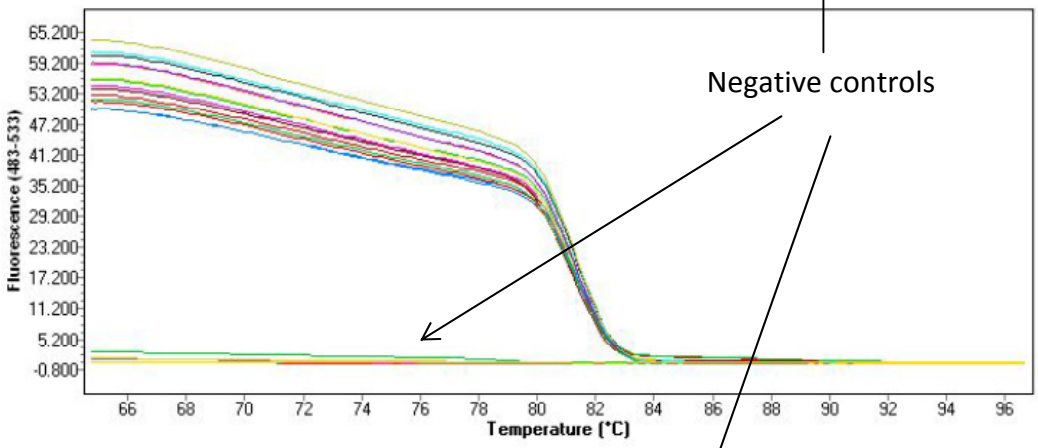

Negative controls

C) Melting Peaks

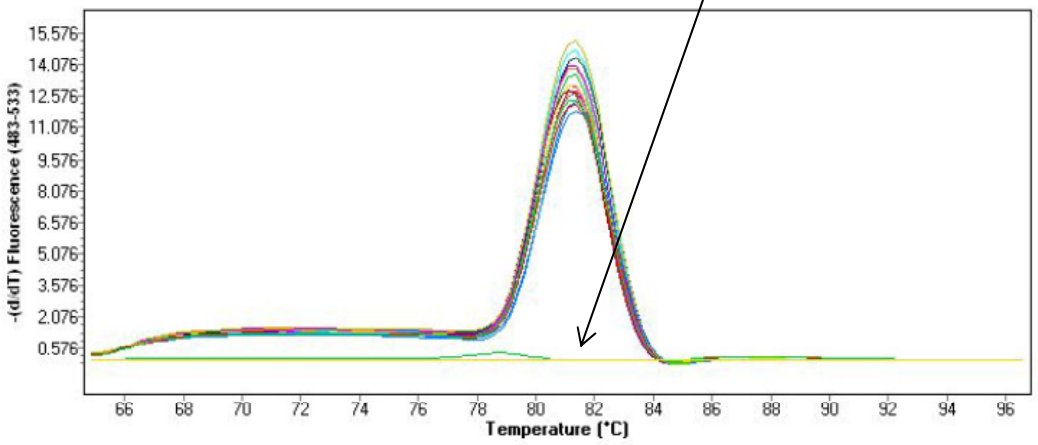

Figure 15 Typical amplification curves, melting curves, and melting peaks for Ykt6

Typical amplification curves for Ykt6 produced through SYBR-green real-time PCR. **A)** An amplification curve showing a 1:4 dilution for the Ykt6 reference primers. **B)** Melting curve and **C)** melting peaks again showing no amplification in the negative controls. Ykt6 has a melting peak at about 81°C.

3.3.3 Knockdown of PEX11α in MIN6 cells

Two methods were employed for the transfection of MIN6 cells with siRNA probes for *PEX11*α. Firstly, Lipofectamine® 2000 was tested as a means of transfecting the MIN6 cells with the siRNA probes for *PEX11*α. Lipofectamine uses a lipid mediated technique of facilitating the passage of siRNA into cells. The siRNA becomes complexed with liposomes, and is able to enter the cells through endocytosis. Unfortunately, transfection using Lipofectamine 2000 proved unsuccessful (results shown in section 3.4.4.1), so an alternative method of transfection was found.

Following advice from Unilever (our industrial collaborator), who had been working with Invitrogen to find a transfection system capable of yielding efficient knockdowns in MIN6 cells, we moved onto using the Neon System. The Neon Transfection System uses electroporation to disrupt the phospholipid bilayer of the cell membrane, causing temporary pores, and allowing the passage of siRNA into the cell. The system was fully optimised by Invitrogen for the knockdown of TFAM in MIN6 cells for Donna Hine during completion of her PhD. The same parameters were put in place for the knockdown of *PEX11*α in the MIN6 cells. MIN6 cells were shocked with 2 pulses for 2ms at a voltage of 1200V (Hine, 2012).

Following transfection using the Neon system, samples were also taken for protein determination. Western blots were performed in order to determine PMP-70 protein levels as a marker of peroxisome abundance, compared with β-actin which was used as a reference protein.

3.4 Results

3.4.1 Validation of MIN6 cells as an insulin producing cell line: C-peptide staining

MIN6 cells are an insulin secreting cell line which are able to respond to glucose within the normal physiological range. It is known that at higher passage numbers, the insulin response to glucose can be lost (Ishihara *et al.*, 1993; Cheng *et al.*, 2012). It was thought wise to begin by validating that the MIN6 cells to be used did indeed produce insulin.

An antibody against C-Peptide was used for this validation experiment. Cells were washed, then a secondary antibody conjugated to FITC (fluorescein isothiocyanate) was bound so the cells could be visualised. Using the FITC filter, the FITC conjugate absorbs the most light at a wavelength of 492nm, and emits light at 520nm making the fluorescence green. Nuclear counterstaining was also carried out with DAPI, with excitation at 360 nm and emission at 460 nm, which can be visualised with the UV filter. Negative controls, where cells were incubated with antibody incubation buffer without the primary antibody, were also carried out with DAPI staining to ensure the fluorescence seen was specific to the primary antibody and not because of any auto-fluorescence from the cells. Negative controls should only fluoresce under the UV filter with the DAPI dye and show the distribution of the nuclei.

Later passage (P28 and P31) MIN6 cells were grown on cover slips at 37°C, 5% CO_2 for 48hrs before being fixed with 4% paraformaldehyde. The cells were then stained using the antibody against C-peptide. Later passage MIN6 cells were used as these have a tendency to lose their glucose responsiveness. C-peptide was present in the MIN6 cells tested (Figure 16) indicating that the cells to be used were still producing insulin at the higher passage. From this stage, experiments were carried out in MIN6 cells no higher than passage 28.

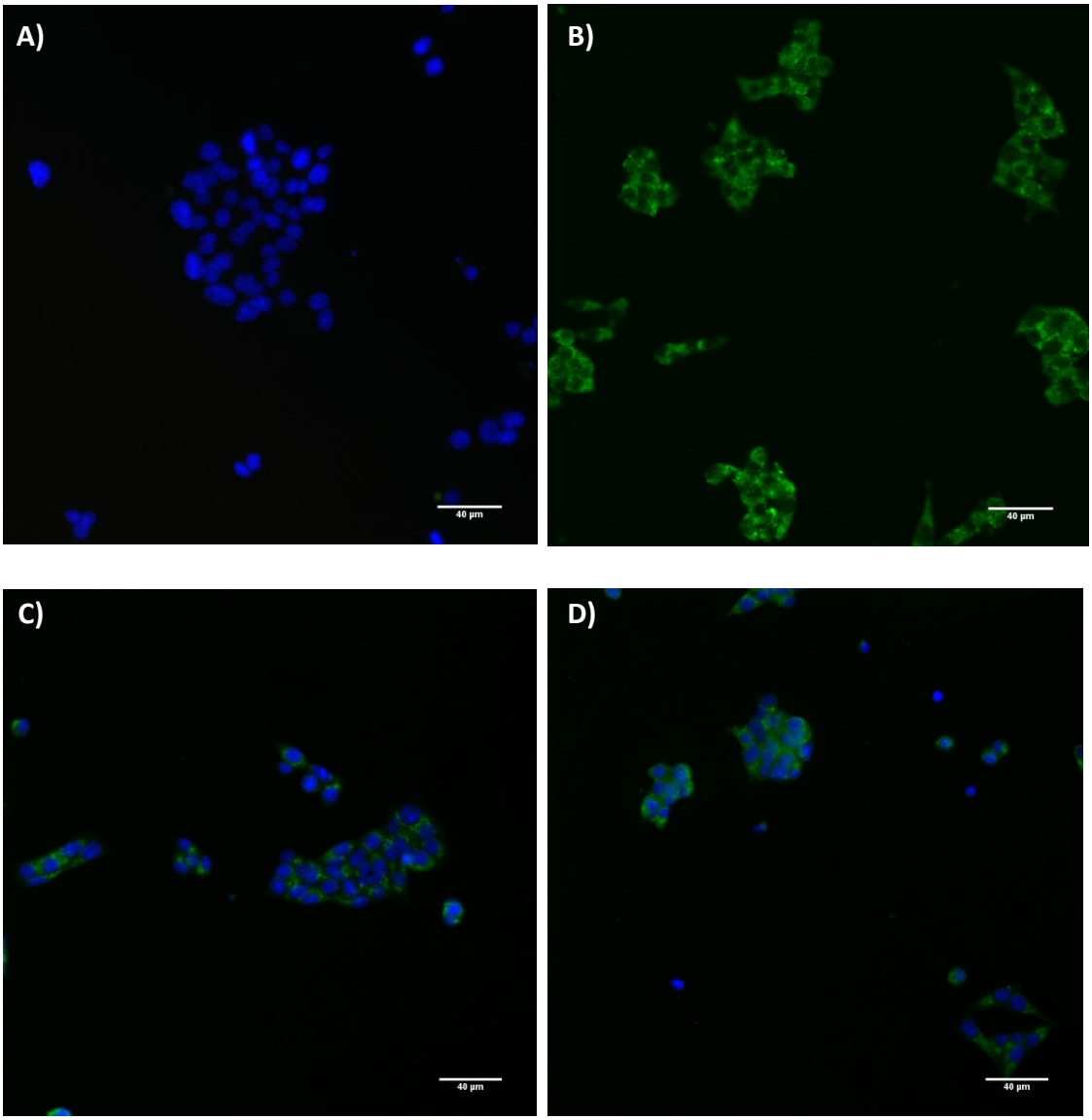

Figure 16 C-peptide (green) staining in late passage MIN6 cells with DAPI (blue) nuclear counterstaining

MIN6 cells were seeded onto cover slips at a density of $2x10^5$ cells/cover slip in 6 well plates. Following incubation at 37°C, 5% CO_2 cells were fixed with 4% paraformaldehyde, and permeabilised with 0.2% triton. Following blocking in 20% FBS cells were stained using a primary antibody against C-Peptide (Cell Signaling Technology), then a secondary antibody with a FITC tag (Jackson ImmunoResearch Laboratories) making the C-peptide stain green using the FITC filter on the fluorescent microscope. Cells were counterstained with DAPI which is visible as blue light using the UV filter. All images were taken at x20 magnification. **A)** P31 cells showing C-peptide staining with DAPI. **B)** P28 cells showing C-peptide staining without the DAPI counterstain. **C)** P28 cells showing C-peptide staining with DAPI. **D)** P31 composite negative control with no primary antibody indicating that the fluorescence seen in the other samples is because of the binding of the C-peptide antibody.

3.4.2 Peroxisome staining in MIN6 cells

Peroxisomes have previously been visualised in another mammalian pancreatic β-cell line, RINm5F cells, using an antibody against PMP-70 (Elsner *et al.*, 2011). PMP-70 is a protein found within the membrane of the peroxisome, and is often used to detect the presence of peroxisomes within cells. MIN6 cells were stained for PMP-70, using a secondary antibody conjugated to Cy3 (Cyanine dye) which fluoresces red. Cy3 has an excitation peak at 550nm, and an emission peak at 570nm, meaning it can be visualised using the TRITC filter. The cells were once again counterstained with DAPI so the nuclei could be visualised, and negative controls without primary antibody were also included.

As for C-peptide staining, MIN6 cells were seeded onto cover slips and incubated at 37°C and 5% CO_2 for 48hrs, then fixed with 4% paraformaldehyde before staining was carried out. The images show that MIN6 cells do express peroxisomes (Figure 17). The presence of the peroxisomes indicates that MIN6 cells should be a suitable cell line to use for the investigation into the role of *PEX11*α in lipotoxicity of pancreatic β-cells.

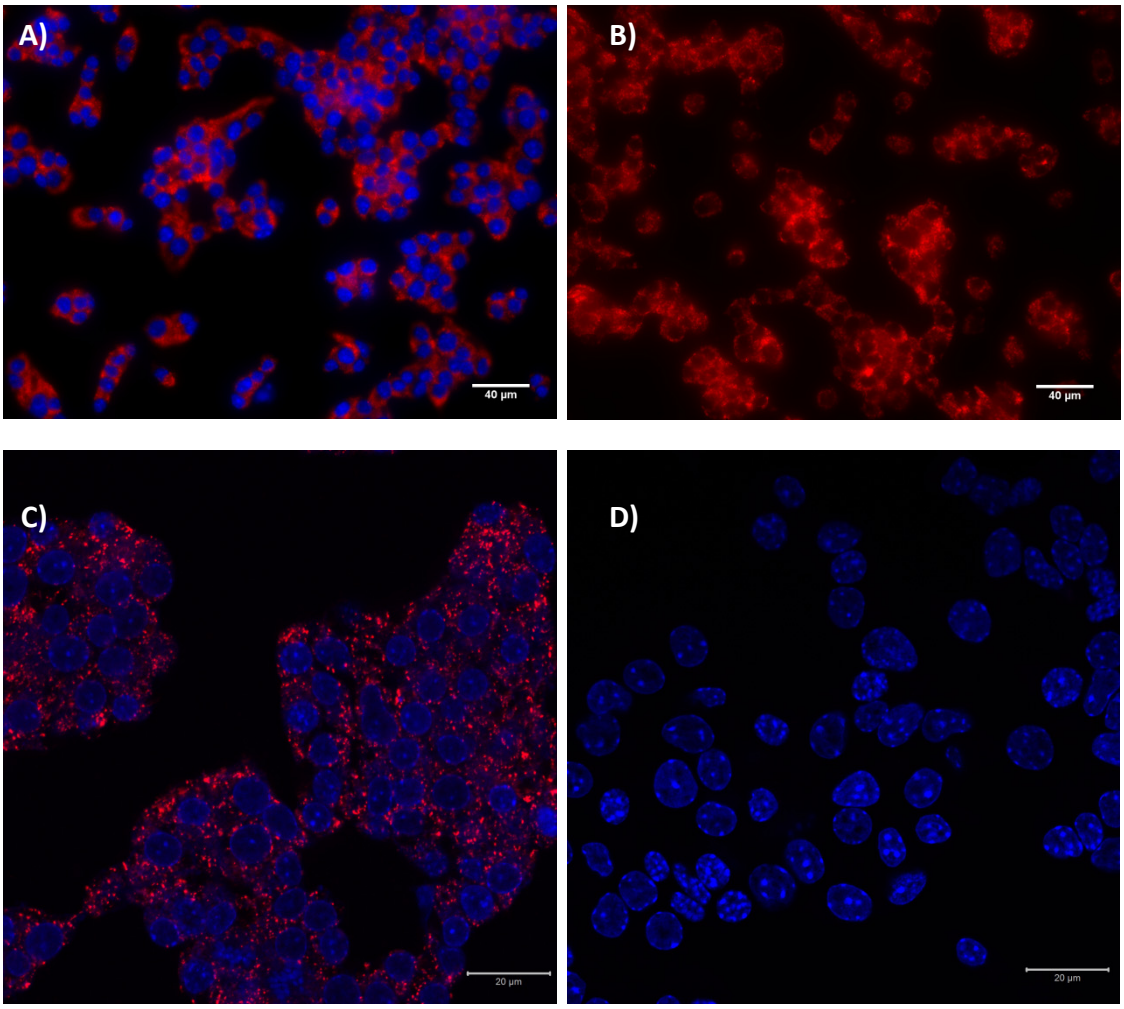

Figure 17 Peroxisome (red) staining in MIN6 cells with DAPI (blue) nuclear counterstain

As for C-peptide staining, MIN6 cells were seeded onto cover slips at a density of $2x10^5$ cells/cover slip in 6 well plates. Cells were fixed, permeabilised and blocked before they were stained using a primary antibody against PMP-70 (Abcam), a good marker of peroxisomes. A secondary antibody was then used to make the peroxisomes visible in the red light spectrum. In these images 2 different secondary antibodies were used. For **A)** and **B)** Cy3 AffiniPure Donkey Anti-Rabbit IgG (Jackson ImmunoResearch Laboratories) was used for fluorescent microscopy, and for **C)** and **D)** Alexa Fluor® 546 Goat Anti-Rabbit IgG (Life Technologies) was used for fluorescent confocal microscopy. Cells were counterstained with DAPI. **A)** Cells at x40 magnification showing PMP-70 staining with DAPI. **B)** Cells at x40 magnification showing PMP-70 staining without DAPI. **C)** Cells imaged on a confocal microscope, x63 magnification showing PMP-70 staining with DAPI. **D)** Composite negative no primary antibody control visualised at x63 magnification on a confocal microscope.

3.4.3 Production of Real Time Standard Curves to ensure primer efficiencies

For the quantification of gene expression of *PEX11*α and *PEX11*β SYBR-Green real time PCR was carried out using Quantitect Primer Assays from Qiagen. Although the Quantitect assays are ready optimised by the company, standard curves were carried out to ensure the reaction efficiencies were high, and approximately equal between the target and reference primers to validate the use of the $\Delta\Delta C_T$ method.

Following cDNA synthesis, real-time PCR plates were set up with 1:4 dilutions to produce standard curves using the protocol detailed in section 2.4.5. Larger dilutions were originally looked at but due to the slightly lower expression levels of the target genes, it was determined that 1:4 dilutions would be best.

The primers produced reaction efficiencies of 92.94% for *PEX11*α, 93.32% for *PEX11*β, and 93.93% for Ykt6 (Figure 18) indicating that the primers should give reliable relative quantification of gene expression for the future experiments to be performed.

For some PCR runs, the melt curve was omitted so that the PCR product could be run on a 1% agarose gel to ensure the amplicons generated were of the size expected. *PEX11*α is 70bp, *PEX11*β is 111bp, and Ykt6 is 81bp. These can be seen on the agarose gel image (Figure 19) which shows 3 samples for each primer and 2 negative controls which contained PCR H_2O rather than cDNA. The amplicons generated for each primer are of the expected size showing that the primers were specific for the target genes, and have not amplified any genomic DNA rather than cDNA. The negatives show no sign of any amplification indicating that no contamination was present.

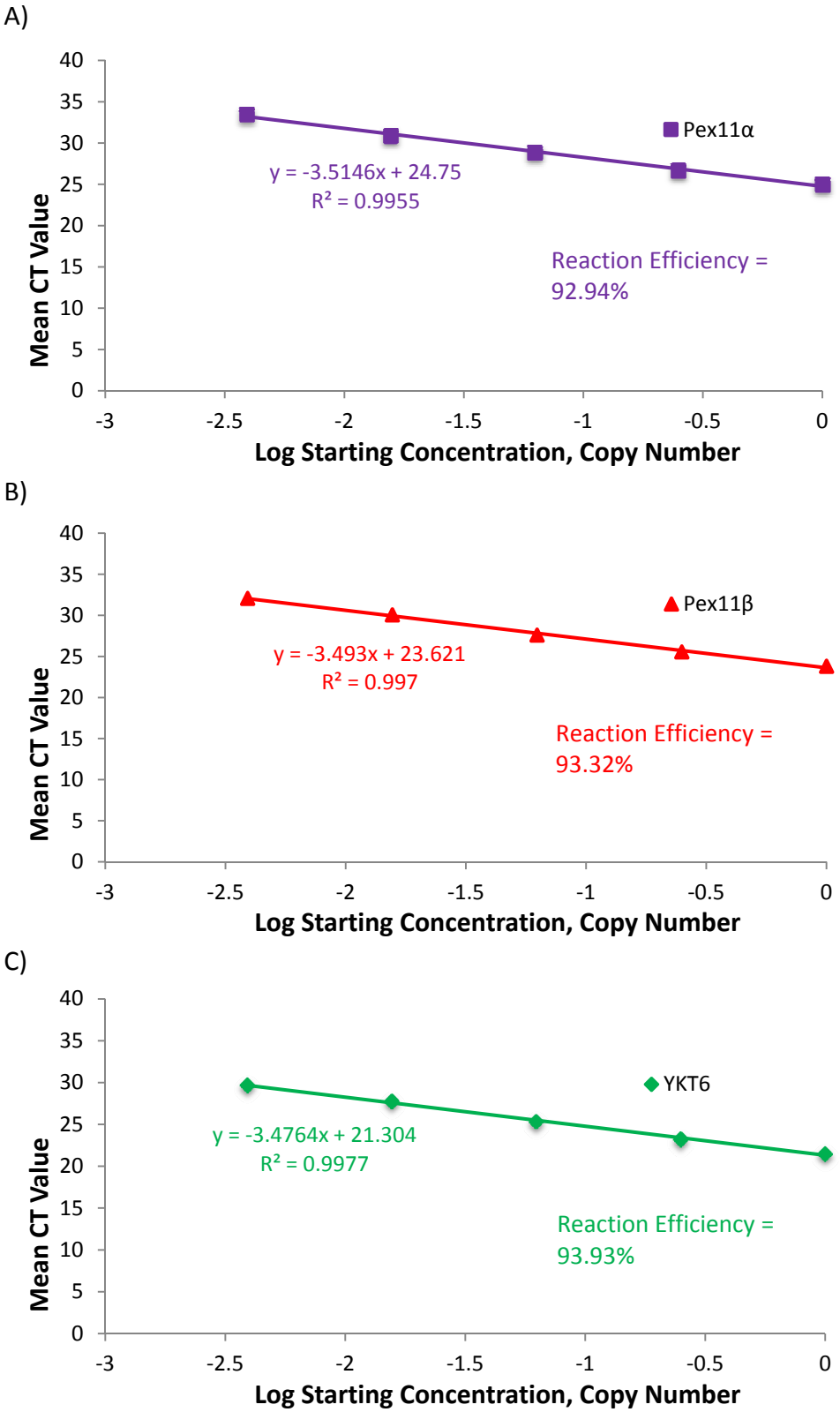

Figure 18 Real time PCR standard curves for *PEX11α*, *PEX11β* and Ykt6 primers

RNA was extracted from MIN6 cell samples and cDNA samples synthesised. Following this real-time PCR was carried out using 1:4 serial dilutions to produce standard curves for each primer and check reaction efficiencies. **A)** *PEX11α* standard curve, **B)** *PEX11β* standard curve, and **C)** Ykt6 standard curve.

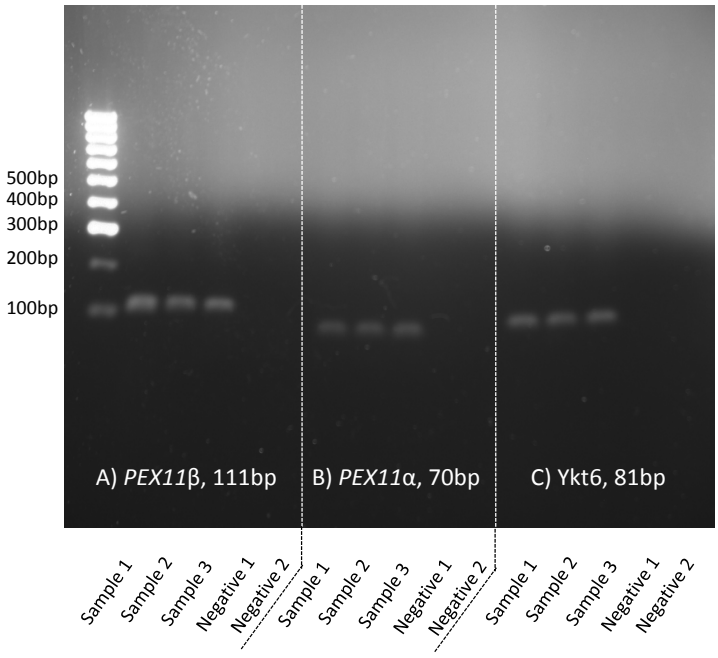

Figure 19 Agarose gel electrophoresis showing real-time PCR products

Following real time PCR where melt curve analysis was omitted, amplified samples were run on a 1% agarose gel to ensure amplicons were of the expected sizes. 3 positive samples were run for each primer along with 2 negative (PCR H_2O rather than cDNA) samples. All amplicons were of the size expected. **A)** *PEX11*β amplicons, with an expected sixe of 111bp, can be seen just above the 100bp marker. **B**) *PEX11*α amplicons, with an expected size of 70bp are below the 100bp marker. **C)** Ykt6 amplicons, with an expected size of 81bp are visible just below the 100bp marker, but above the *PEX11*α amplicons.

3.4.4 Model for the reduction of PEX11α expression in MIN6 cells

3.4.4.1 Knockdown of PEX11α using Lipofectamine 2000

Following successful real time PCR to produce standard curves with good efficiencies, the next step was to develop a method for the reduction of *PEX11*α expression in MIN6 cells.

MIN6 cells have previously been successfully transfected using both Lipofectamine RNAiMAX and Lipofectamine 2000 (Akimoto *et al.*, 2007; Lai *et al.*, 2008; Han *et al.*, 2011b; Huising *et al.*, 2011; Liu *et al.*, 2012). *PEX11*α has previously been knocked down using Lipofectamine RNAiMAX in MIN6 cells. Although the knockdown achieved was consistent, the fold change was not large enough to consider any functional changes it may have (Pascoe, 2009). Lipofectamine 2000 was chosen instead as the transfection reagent to test in the hope that a greater knockdown could be achieved.

MIN6 cells were seeded into 6 well plates and incubated at 37°C, 5% CO_2. 24hrs later transfection was carried out using 3 siRNA probes specific for *PEX11*α and Lipofectamine 2000 as the transfection reagent, and cells were once again incubated at 37°C, 5% CO_2. 48hrs after transfection, cells were harvested in RNA lysis buffer, cDNA was synthesised and *PEX11*α expression was determined using real-time PCR using *PEX11*α primers for the target gene, and Ykt6 as the reference gene.

The results (Figure 20) show that although the probes do appear to be reducing the expression of *PEX11*α it is only by about 30% which may not be enough to produce any functional changes. It was therefore decided that an alternative method of knockdown should be investigated. Following advice from our industrial collaborator, Unilever, the Neon Transfection System (Invitrogen) was suggested, and further transfections were carried out using this system.

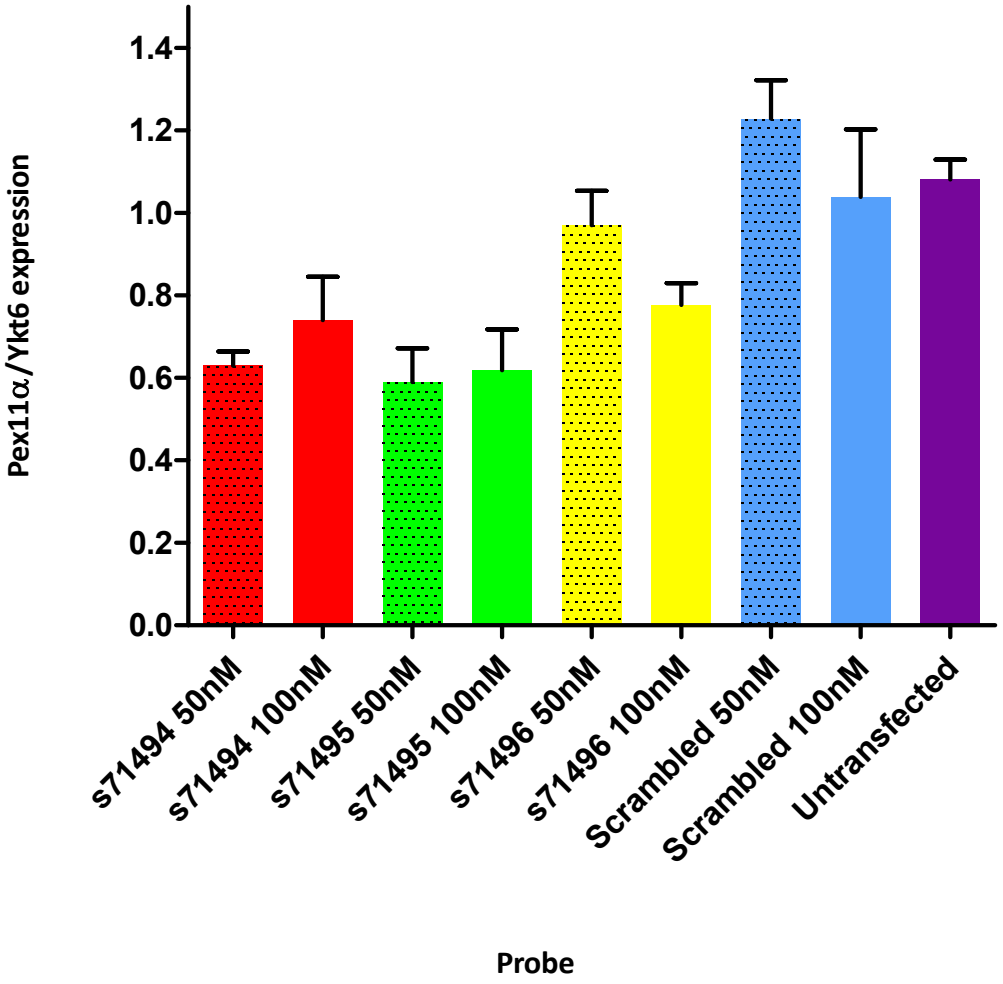

Figure 20 Transfection of MIN6 cells using Lipofectamine 2000 for the knockdown of *PEX11*α expression

MIN6 cells were seeded into 6 well plates at a density of $1x10^6$ cells/well and incubated at 37°C, 5% CO_2 for 24hrs before transfection. Cells were then transfected with either 1 of 3 siRNA probes for *PEX11*α or a scrambled control siRNA probe using Lipofectamine 2000 and incubated in Opti-MEM medium. 6 hours after transfection Opti-MEM medium was removed and replaced with antibiotic free DMEM. 48hrs post transfection cells were harvested, RNA was extracted and cDNA was synthesised. *PEX11*α gene expression was determined using real-time PCR. Experiments were carried out 5 times. Results are normalised to 100nM scrambled control, and are mean±SEM.

3.4.4.2 Knockdown of PEX11α using the Neon Transfection System

The Neon Transfection System utilises electroporation in order to create temporary pores within the cell membrane to allow the transfer of siRNA.

Following from transfection using Lipofectamine 2000, it was decided that only 2 siRNA's for *PEX11*α would be carried through and used with the Neon System. Although the knockdown was not great for any of the probes, s71494 and s71495 appeared to give the better reductions in *PEX11*α expression levels, so these were chosen to use with the Neon system. A preliminary experiment was carried out using both concentrations, 50nM and 100nM, of siRNA probe previously used. However, after seeing that a slightly larger decrease in *PEX11*α expression was attained with 100nM (Figure 21), further experiments were carried out using the two siRNAs at a concentration of 100nM only.

Using the method detailed in section 2.2.2, MIN6 cells were resuspended in Buffer R along with siRNA. Cells were electroporated using the Neon system then seeded into 24 well plates. They were incubated in antibiotic free medium for either 24hrs or 48hrs at 37°C, 5% CO_2 before being harvested in RNA extraction buffer. cDNA was synthesised and gene expression was determined using real-time PCR. Ykt6 was used as the reference gene.

*PEX11*α expression was knocked down by more than 70% (Figure 22) with the s71495 probe at both 24hr and 48hr ($P<0.001$). Over time the level of knock down appeared to decrease slightly. This was more evident with the s71494 probe which decreased from 70% knockdown at 24hrs to 54% knockdown at 48hrs, although the decrease in *PEX11*α expression was still significant. It is also evident that the scrambled control siRNA does not have an effect on *PEX11*α expression compared with the shocked control in which no siRNA was present.

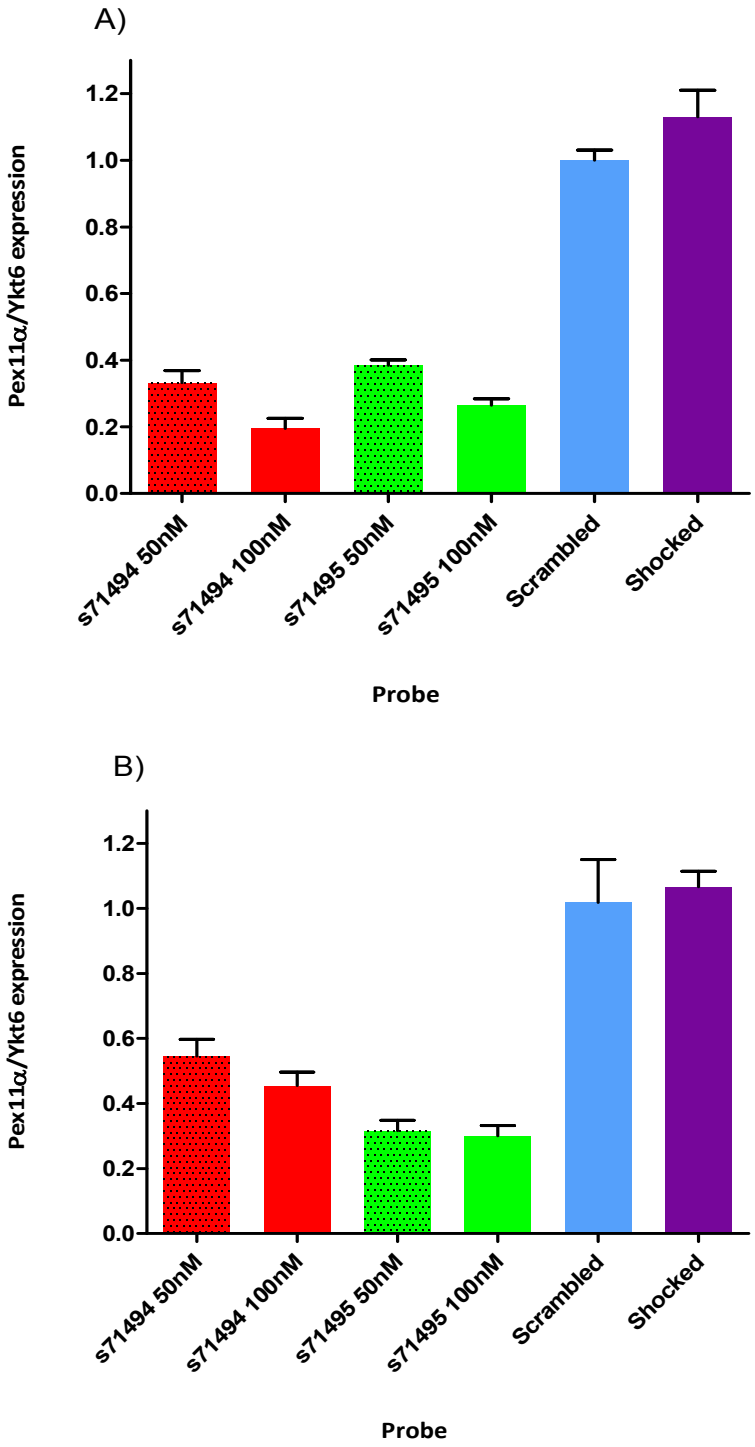

Figure 21 Transfection of MIN6 cells using the Neon System for the knockdown of *PEX11α*

MIN6 cells were transfected in suspension using either 50nM or 100nM of *PEX11*α siRNA probes s71494 or s71495, 100nM scrambled siRNA or no siRNA (shocked). Cells were incubated in a 24 well plate at a density of $5x10^5$ cells/well for either **A)** 24hrs or **B)** 48hrs in antibiotic free DMEM at 37°C, 5% CO_2 before RNA was extracted, and cDNA synthesised. *PEX11*α gene expression was quantified using real-time PCR. These are the mean results from 1 experiment carried out in triplicate. Results are normalised to scrambled control, and are mean±SEM.

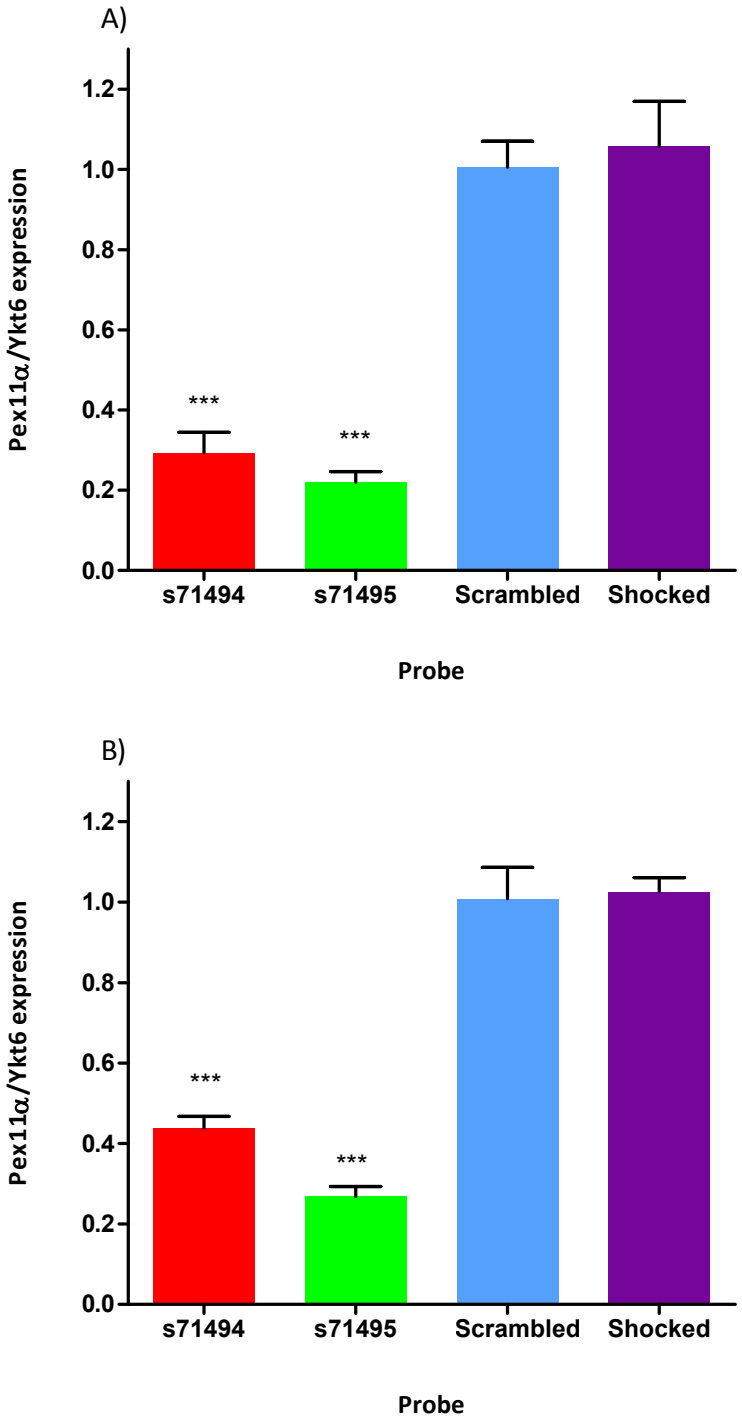

Figure 22 Average *PEX11*α knockdown using the Neon transfection system

MIN6 cells were transfected in suspension using 100nM of *PEX11*α siRNA probes s71494 or s71495, scrambled siRNA or no siRNA (shocked). Cells were incubated in a 24 well plate at a density of $5x10^5$ cells/well for either A) 24hrs or B) 48hrs in antibiotic free DMEM at 37°C, 5% CO_2 before RNA was extracted, and cDNA synthesised. *PEX11*α gene expression was quantified using real-time PCR. Results are normalised to scrambled control, and are mean±SEM (n=3) of three independent experiments. ***P<0.001 compared to scrambled control; one-way ANOVA and Bonferroni's *post hoc* test.

3.4.5 The effect of PEX11α knockdown on peroxisome abundance

Following successful transfection of MIN6 cells with the Neon system it was decided to look at PMP-70 protein levels following *PEX11*α knockdown. PEX11α is responsible for the division of peroxisomes in response to an extracellular stimulus, and although previous studies have shown that an increase in *PEX11*α can lead to an increase in peroxisome abundance, it has also been demonstrated that a loss of *PEX11*α in mice does not affect peroxisome abundance (Schrader *et al.*, 1998; Li *et al.*, 2002a).

We wanted to see if this was the case with our model of *PEX11*α knockdown in MIN6 cells. We chose the 48hr time point following transfection to give time for protein levels to change. Unfortunately we were unable to find an antibody against mouse PEX11α which would help us determine whether PEX11α protein levels were being decreased following a reduction in *PEX11*α gene expression. Two human PEX11α antibodies, one from Santa Cruz Biotechnology (sc-104604) and one from Abcam (ab104959) were tested with MIN6 samples as they shared a large percentage of homology with the mouse *PEX11*α gene. Neither antibody showed any sign of binding so we moved on to working with the PMP-70 antibody to determine peroxisome abundance.

48hr post transfection MIN6 cells were harvested in protein extraction buffer. Protein quantities were determined before the samples were run on a western. Samples were adjusted with protein extraction buffer to attempt to load equal quantities of protein into each well. Following transfer, membranes were probed with antibodies before developing using chemiluminescence. β-actin was used as a loading control.

The results (Figure 23) show that there is no difference between the cells transfected with siRNA probes s71494 and s71495 compared with the scrambled control. *PEX11*α knockdown has no effect on PMP-70 protein expression 48hrs post transfection.

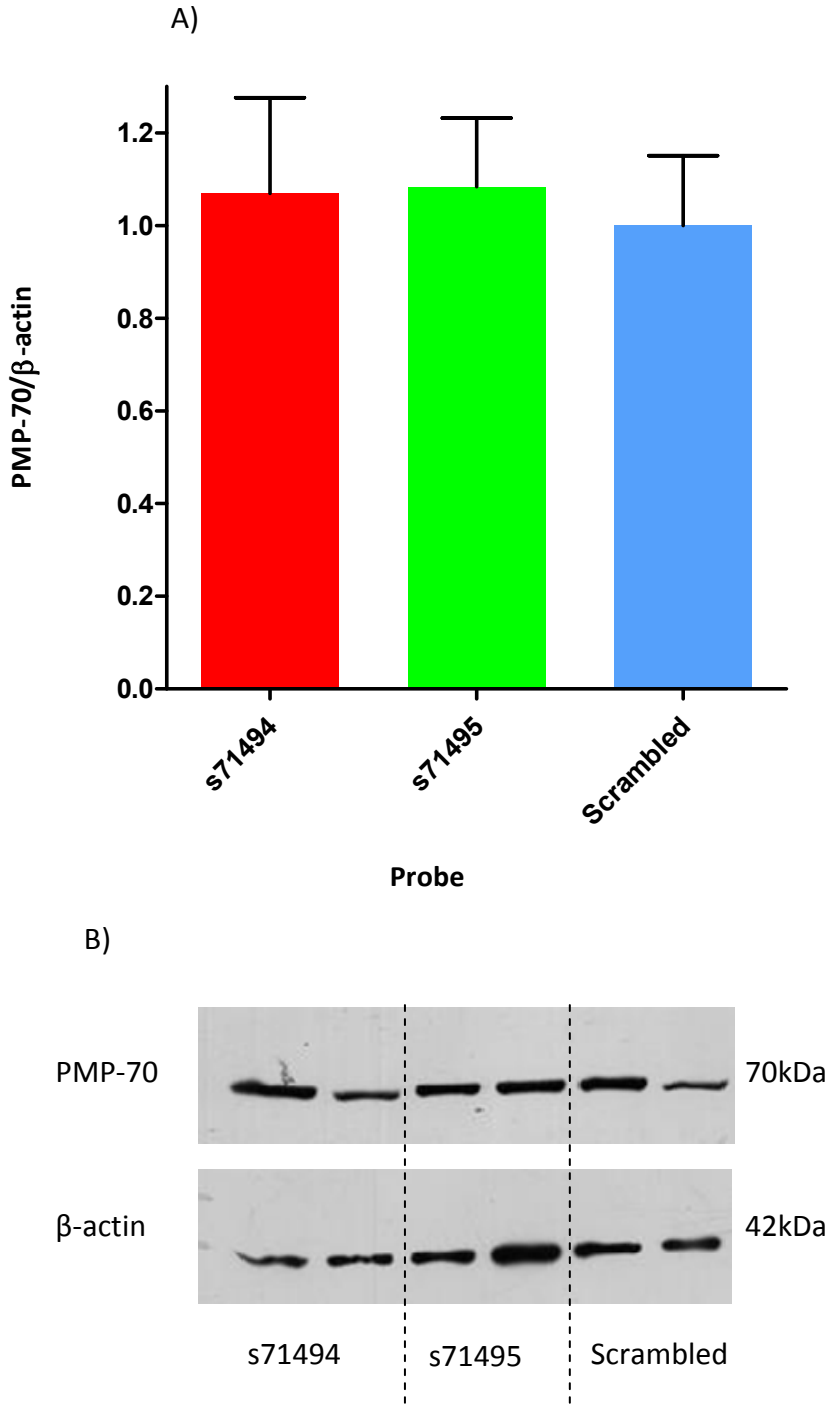

Figure 23 PMP-70 protein expression following *PEX11*α knockdown

MIN6 cells were transfected in suspension using 100nM of *PEX11*α siRNA probes s71494 or s71495 or scrambled siRNA. Cells were incubated in a 24 well plate at a density of $5x10^5$ cells/well for 48hrs in antibiotic free DMEM at 37°C, 5% CO_2 before protein was extracted and quantified. **A)** PMP-70 protein expression, in a ratio of PMP-70 to β-actin, was quantified using western blotting. Experiments were carried out twice in duplicate. Results are normalised to scrambled control. Error bars are representative of SEM. **B)** A western blot from one of the experiments.

3.4.6 The effect of PEX11α knockdown on PEX11β expression

As PEX11α is not the only PEX11 protein involved in peroxisome division it was appropriate to determine whether *PEX11*β may have some compensatory effects when *PEX11*α expression is reduced. Compensatory increases in *PEX11*β could mean that any functional changes that might have occurred due to a reduction in *PEX11*α could be cancelled out.

The cDNA samples used for determination of *PEX11*α expression were then used again for real-time PCR using primers for *PEX11*β to detect the expression of *PEX11*β after *PEX11*α knockdown. Ykt6 was again used as the reference gene.

The results (Figure 24) show that reduction of *PEX11*α did not lead to any compensatory increases in *PEX11*β. There was however, a significant decrease in *PEX11*β expression with the s71495 probe of 40% at 24hrs, and 30% at 48hrs ($P<0.05$). As the siRNA against *PEX11*α did not share any homology with *PEX11*β this is unlikely to be a direct effect of the siRNA against *PEX11*α silencing the *PEX11*β gene expression. It is unsure as to why this has happened, however, although significant, the decreases seen may not be large enough to cause many functional changes, especially after 48hrs as the levels of *PEX11*β begin to increase back to normal cellular levels. In addition, as it is a decrease in *PEX11*β expression rather than an increase, it is unlikely that any functional changes within the cells due to a decrease in *PEX11*α expression will be compensated for.

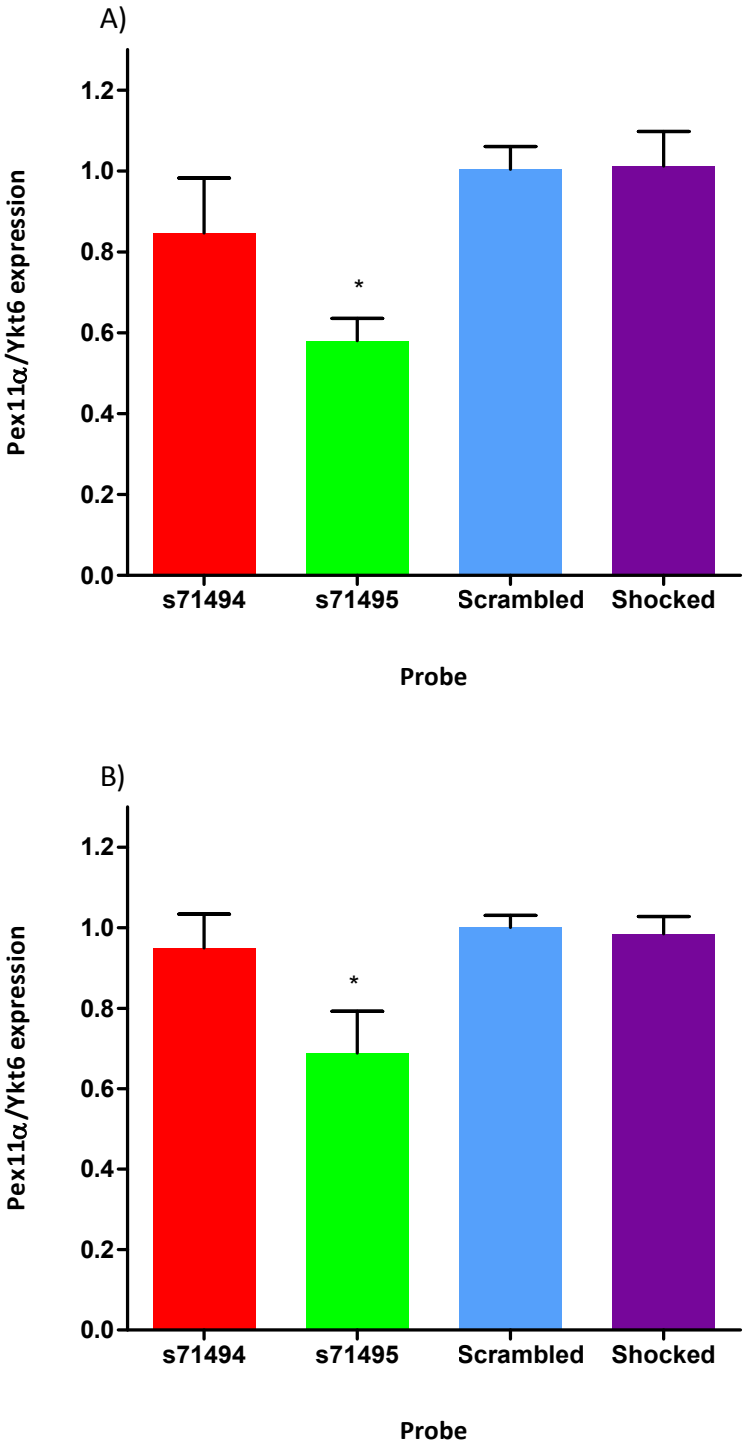

Figure 24 *PEX11*β mRNA levels after *PEX11*α knockdown.

*PEX11*β gene expression was quantified using real-time PCR and the cDNA samples originally used to quantify *PEX11*α expression in the transfected cells. A) 24hrs post transfection, B) 48hrs post transfection. Results are normalised to scrambled control , and are mean±SEM (n=3) of three independent experiments. *P < 0.05 compared to scrambled control; one-way ANOVA and Bonferroni's *post hoc* test.

3.5 Discussion

The main aim of this chapter was to develop a method for the reduction of *PEX11*α expression in MIN6 cells, a mouse pancreatic β-cell line. MIN6 cells were chosen as the insulin secretion is glucose responsive (Ishihara *et al.*, 1993). In addition, when this work first began there was no established human pancreatic β-cell line. This, however, has changed in recent years with the development of the EndoC-βH1 human β-cell line which, like MIN6 cells, is able to respond to increasing glucose concentrations with the secretion of insulin (Ravassard *et al.*, 2011). As this human cell line is a recent development further testing may be required before the cells can be used confidently, and commonly to facilitate pancreatic β-cell research and diabetes.

Although many groups use MIN6 cells when investigating insulin secretion (Watson *et al.*, 2011; Cheng *et al.*, 2012), we wanted to ensure our MIN6 cells were producing insulin. We stained MIN6 cells for C-peptide, a product produced in addition to insulin through the cleavage of proinsulin, confirming the ability of the MIN6 cells to produce insulin (Figure 16), as we expected.

It has previously been shown that the gene *PEX11*α is present in MIN6 cells (Pascoe, 2009). PEX11α is responsible for the division of peroxisomes in response to extracellular stimuli, which in turn are partially responsible for fatty acid metabolism (Schrader *et al.*, 1998; Wanders *et al.*, 2010). As the main aim of the project is to look at the effect of altered *PEX11*α expression on the lipotoxicity of MIN6 cells it was important to check for the presence of peroxisomes. Peroxisomes have previously been visualised in the rat pancreatic β-cell line RINm5F using PMP-70 as a marker of peroxisomes (Elsner *et al.*, 2011). We were also able to detect peroxisomes in MIN6 cells using this marker (Figure 17) strengthening the decision to use MIN6 cells for this project.

As we established that peroxisomes were present within the MIN6 cells, the next step was to find a method for reducing the expression of *PEX11*α. Although previous studies have use Lipofectamine 2000 successfully as a means of transfection in MIN6 cells (Garcia-Haro *et al.*, 2010; Huising *et al.*, 2011), in this study the use of the reagent was unsuccessful at producing the desired knockdown (Figure 20). Although a decrease in *PEX11*α was seen, it was small and unlikely to yield any functional effects. This

accompanies evidence from a previous study which used Lipofectamine RNAiMAX as a transfection reagent in an attempt to reduce expression of *PEX11*α (Pascoe, 2009). It seems that the lipid based transfection techniques aren't the most efficient method for the knockdown of gene expression in MIN6 cells.

As we were still wanting to achieve a successful knockdown of *PEX11*α of >70% we looked to Unilever, our industrial collaborator, for advice. Since the Neon transfection system had just been optimised for the knockdown of TFAM in MIN6 cells (Hine, 2012), it was suggested as an alternative to Lipofectamine 2000. The Neon transfection system has been used in other cells types and was been found to be a reliable and efficient method of transfection (Moore *et al.*, 2010; Covello *et al.*, 2014). In MIN6 cells, the Neon transfection system was shown to lead to a >80% reduction in TFAM when transfected with siRNA to target the gene (Hine, 2012). We were able to consistently reduce *PEX11*α expression by >70% (Figure 22) using the Neon transfection system, further validating its reliability and efficiency as a means of transfection.

PMP-70 protein expression did not change with *PEX11*α knockdown at 48hrs (Figure 23). This is in accordance with a previous study which produced *PEX11*α knockout (*PEX11*$\alpha^{-/-}$) mice. The livers and cultured mouse embryonic fibroblasts (MEF's) from these mice were examined, and it was found that there were no differences in the abundance of peroxisomes in the *PEX11*$\alpha^{-/-}$ mice compared with normal control mice in either the liver or the MEF's. It was also noted that there was no striking effects on morphology of the peroxisomes, although they had a habit of clustering when *PEX11*α was absent (Li *et al.*, 2002a). *PEX11*α expression has been shown to increase in response to extracellular stimuli (Schrader *et al.*, 1998; Li *et al.*, 2002a). Indeed, rats fed a 2 week diet of clofibrate, a peroxisome proliferator, produced a 10 fold increase in *PEX11*α expression (Schrader *et al.*, 1998). It is therefore possible that changes in peroxisome abundance may not been seen under normal cellular conditions, and differences in peroxisome abundance may only be seen following the response of *PEX11*α to its stimuli after knockdown.

PEX11β is a protein involved in the constitutive regulation of peroxisome abundance (Schrader *et al.*, 1998). It has been reported that loss of *PEX11*β expression led to a 1.5

fold increase in hepatic *PEX11*α expression (Li *et al.*, 2002b). We wanted to see whether knockdown in *PEX11*α resulted in a compensatory increase in *PEX11*β expression. As it was, a reduction in *PEX11*α expression did not lead to any increases in *PEX11*β expression (Figure 24). There was, however, an unexpected decrease in *PEX11*β expression with one of the *PEX11*α probes. Although significant, this decrease was small and is unlikely to lead to any functional effects.

In conclusion, we were able to produce a model for the efficient knockdown of *PEX11*α expression in MIN6 cells. Knockdown of *PEX11*α expression alone does not affect peroxisome abundance in MIN6 cells. Next we wanted to move onto to look at the inducible properties of *PEX11*α, and whether this can be achieved through fatty acid incubation.

Chapter 4

Induction of *PEX11α* expression in MIN6 cells

4 Induction of *PEX11α* expression in MIN6 cells

4.1 Introduction

Following the development of a successful model for *PEX11α* mRNA knockdown we wanted to find a way of increasing expression of the gene. As *PEX11α* has already been shown to be an inducible gene in rat (Schrader *et al.*, 1998), we wanted to confirm that *PEX11α* was an inducible gene in MIN6 cells.

PEX11α is regulated through a PPRE, which is activated when PPARα forms a heterodimer with RXR and binds the PPRE (Li *et al.*, 2002a; Shimizu *et al.*, 2004). It has previously been shown that rats fed a diet of clofibrate, a PPARα agonist, produce a 10-fold increase in hepatic *PEX11α* expression (Schrader *et al.*, 1998). In line with this, mice fed a chow diet supplemented with ciprofibrate for two weeks showed a significant increase in *PEX11α* gene expression compared with mice fed on a standard chow diet (Li *et al.*, 2002a). *PEX11α* was shown to be a target of PPARα when PPARα null mice were fed a diet supplemented with Wy14,643 (a known peroxisome proliferator). Wy14,643 failed to produce an increase in *PEX11α* expression in the PPARα null mice compared with the wild type controls (Shimizu *et al.*, 2004).

As peroxisomes are responsible for the metabolism of fatty acids we anticipated that fatty acid exposure might also induce the expression of *PEX11α*. It has previously been reported that some fatty acids are capable of inducing peroxisome proliferation in mammalian cells and yeast (Berge *et al.*, 1989; van Roermund *et al.*, 2000; Camões *et al.*, 2009). In addition, it has been shown that fatty acids activate PPAR's, which in turn are thought responsible for the activation of *PEX11α* gene expression (Dreyer *et al.*, 1993; Shimizu *et al.*, 2004). In preliminary experiments conducted by Laura Pascoe during completion of her PhD, it was shown that 400μM palmitate incubation, but not 400μM oleate incubation was able to lead to an increase in *PEX11α* expression at 24hrs, 48hrs and 72hrs (Pascoe, 2009). We hoped to replicate these results, and use different concentrations of the fats to examine whether there was a dose dependent response to palmitate.

4.2 Aims

The main aim of this chapter was to explore whether *PEX11*α expression was inducible in MIN6 cells. To do this, we aimed to:

- Incubate MIN6 cells with the saturated fatty acid palmitate and the unsaturated fatty acid oleate to see if these fats could increase the expression of *PEX11*α.
- Incubate MIN6 cells with peroxisomal proliferating agents to increase expression of *PEX11*α.
- See if an increase in *PEX11*α expression coincided with an increase in peroxisome abundance.

4.3 Methods

4.3.1 Incubation of MIN6 cells with fatty acids

With the aim of increasing *PEX11*α expression MIN6 cells were seeded into 6 well plates and given 24hrs to proliferate before being exposed to various concentrations of either palmitate or oleate for different time periods, following the protocol detailed in section 2.3.1. Following incubation, RNA was extracted, cDNA synthesised, and real time PCR was carried out to determine gene expression (as previously described).

In addition, following exposure to either 250µM palmitate, or oleate, cells were stained with Oil Red O dye. Oil Red O is a fat soluble diazo dye often used to stain lipids in tissue sections, but can be used in cell culture. Following the protocol detailed in section 2.6, cells were stained with the dye, then visualised on a light microscope. Images were taken of the stained fat droplets within the cells. This technique was used to determine whether the fat was being taken up into the cells following incubation.

4.3.2 Incubation of MIN6 cells with Peroxisomal Proliferating agents

As well as incubating MIN6 cells with fats to attempt to increase *PEX11*α expression, peroxisomal proliferating agents Clofibrate and Fenofibrate, were also used (protocols methods section 2.3.2). Both of these fibric acid derivatives are potent PPARα agonistswhich have been used in the treatment of high cholesterol and dyslipidaemia, but clofibrate is no longer used clinically. Since *PEX11*α expression is controlled through the activation of the PPARα/RXR heterodimer (ref), it was thought that

incubation with these PPARα agonists would upregulate *PEX11*α. The RXR agonist *9-cis* retinoic acid (RA) was also added in combination with Fenofibrate. Briefly, MIN6 cells were seeded into 6 well plates and allowed to proliferate for 24hrs before being exposed to various concentrations of the different treatments, for different time periods. Following incubation, RNA was extracted, cDNA synthesised, and real time PCR was carried out to determine gene expression (as previously described).

Following treatment with either a combination of 5μM fenofibrate and 2000nM *9-cis* RA, BSA vehicle control, or no treatment (incubated with MIN6 DMEM), protein was extracted for determination. Western blotting was then performed to determine PMP-70 protein levels as a marker of peroxisome abundance.

4.4 Results

4.4.1 The effect of fatty acids on PEX11α expression in MIN6 cells

Palmitate, a saturated fatty acid, and oleate, an unsaturated fatty acid are the two most common circulating fatty acids (Biden *et al.*, 2004). As we were interested in investigating response of *PEX11*α to saturated fatty acids compared with unsaturated fatty acids, these two were chosen for the experiments.

MIN6 cells were seeded into 6 well plates and given 24hrs to proliferate at 37°C, 5% CO_2. In order to determine a time period and concentration of fatty acid to use, MIN6 cells were then incubated for 4hrs, 12hrs, 24hrs or 48hrs with either 200µM, 400µM, or 600µM palmitate conjugated to BSA, or 200µM, 400µM, or 600µM oleate conjugated to BSA. A BSA control and an antibiotic free DMEM control were also included at every time period. Following incubation, cells were harvested and RNA was extracted. Following this, cDNA was synthesised, and *PEX11*α expression was analysed using real time PCR. Ykt6 was used as the reference gene, and results were normalised to the BSA control.

The results (Figure 25) show that incubation with either palmitate or oleate did not result in changes in *PEX11*α expression compared with the BSA control at any time period tested. There was a trend for an increase in *PEX11*α expression with increasing palmitate concentrations after 48hrs exposure (Figure 25 D), but the changes were not significant. The use of BSA as a vehicle did not affect *PEX11*α expression compared with the DMEM control as expected. As the failure to increase *PEX11*α expression was unexpected we checked to see whether the fatty acids were entering the MIN6 cells by using oil red O staining.

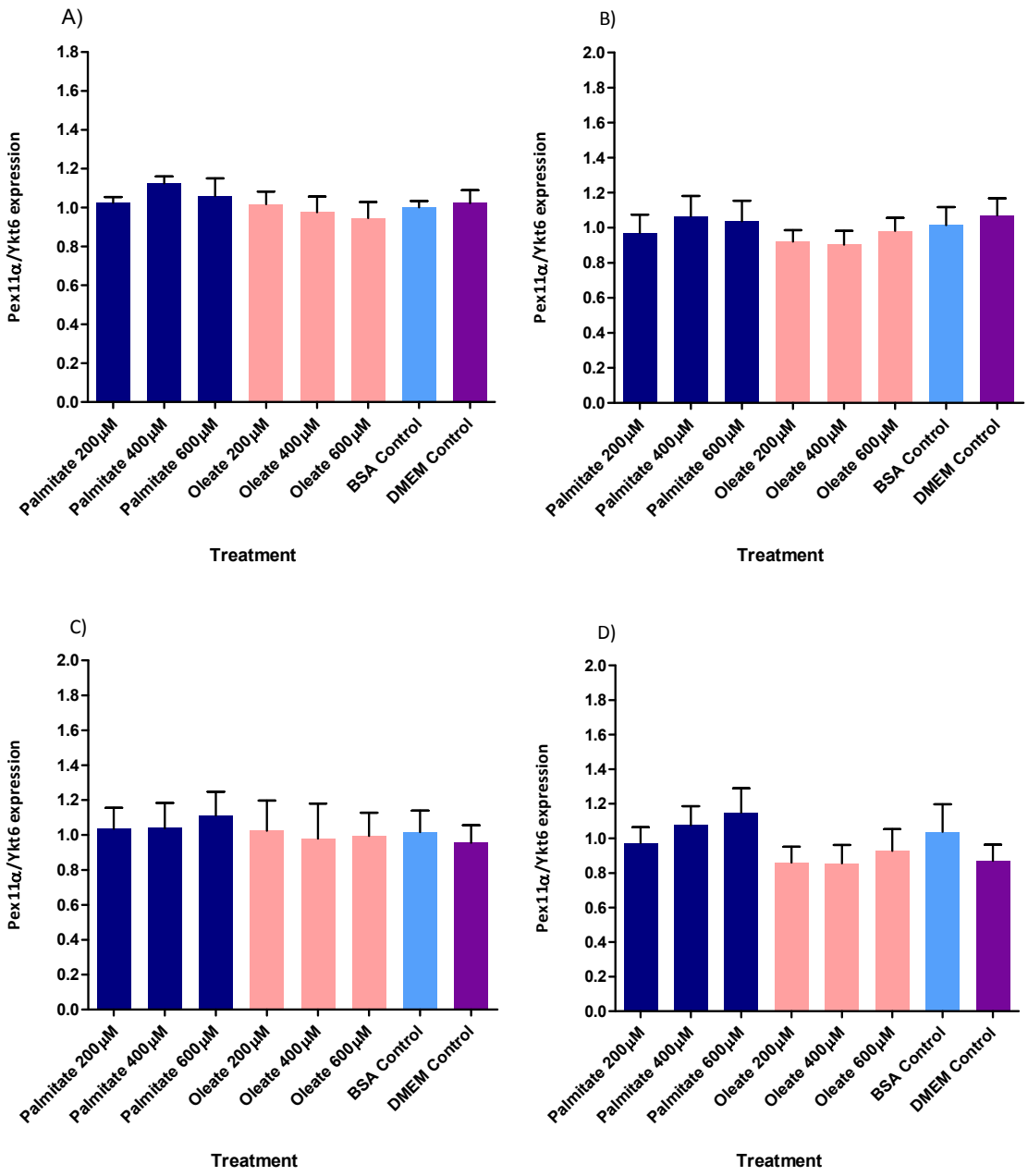

Figure 25 *PEX11*α mRNA expression following incubation with fatty acids

MIN6 cells were seeded into 6 well plates at a density of $1x10^6$ cells/well and given 24hrs to proliferate in antibiotic free DMEM at 37°C, 5% CO_2. Cells were then incubated for **A)** 4hrs, **B)** 6hrs, **C)** 24hrs or **D)** 48hrs with either 200µM, 400µM or 600µM of saturated fatty acid palmitate or 200µM, 400µM or 600µM of unsaturated fatty acid oleate, or a BSA vehicle control, or antibiotic free DMEM control. Following incubation with the treatments for the various time periods at 37°C, 5% CO_2, RNA was extracted, and cDNA synthesised. Pex11α gene expression was quantified using real-time PCR. Ykt6 was used as the reference gene. Results are normalised to BSA control, and are **A)** mean±SEM (n=3) representative of two independent experiments and **B,C,D)** mean±SEM (n=3) of three independent experiments.

4.4.2 Oil Red O staining to determine the uptake of fatty acids into the MIN6 cells

Oil red o staining uses a fat soluble sudan dye to stain lipid droplets within tissues. Once stained, the cells can be visualised under a light microscope to view the red oil droplets.

MIN6 cells were incubated in 24 well plates for 24hrs at 37°C, 5% CO_2 before they were treated with either palmitate, oleate, a BSA control or DMEM control for a further 48hrs. Fat droplets have previously been shown to be visible in INS-1E cells treated with either 1.0mM palmitate, or 1.0mM oleate (Li *et al.*, 2010). Fat droplets have been visualised with Oil Red O staining in U937 (Human leukemic monocyte lymphoma) cells treated with 0.2mM palmitate, and in HepG2 (human hepatoma) cells treated with 0.2mM to 0.4mM palmitate (Joshi-Barve *et al.*, 2007; Luo *et al.*, 2012; Iio *et al.*, 2013; Zeng *et al.*, 2013). Although these are human cell lines, we hoped that a concentration similar to the ones used in these studies would be sufficient to be able to visualise fat droplets within the MIN6 cells. We therefore decided to use 250µM of palmitate or oleate with which to treat the MIN6 cells as this concentration was within the range we had previously used for the *PEX11*α expression studies.

Following 48hr treatment, MIN6 cells were stained using a steatosis colorimetric assay which uses the Oil Red O dye (protocol detailed in section 2.6). Following the staining, cells were visualised using a light microscope and images taken.

The images (Figure 26) show that red fat droplets can be visualised in both the cells treated with palmitate and the cells treated with oleate. As expected, we were not able to see any fat droplets present in the BSA vehicle control or the DMEM control. The results show an increase in staining following palmitate and oleate exposure and would suggest therefore that these lipids are entering into the MIN6 cells. It would appear, therefore, that the failure of *PEX11*α expression to change following fatty acid incubation was not due to a lack of fatty acid uptake by the cells.

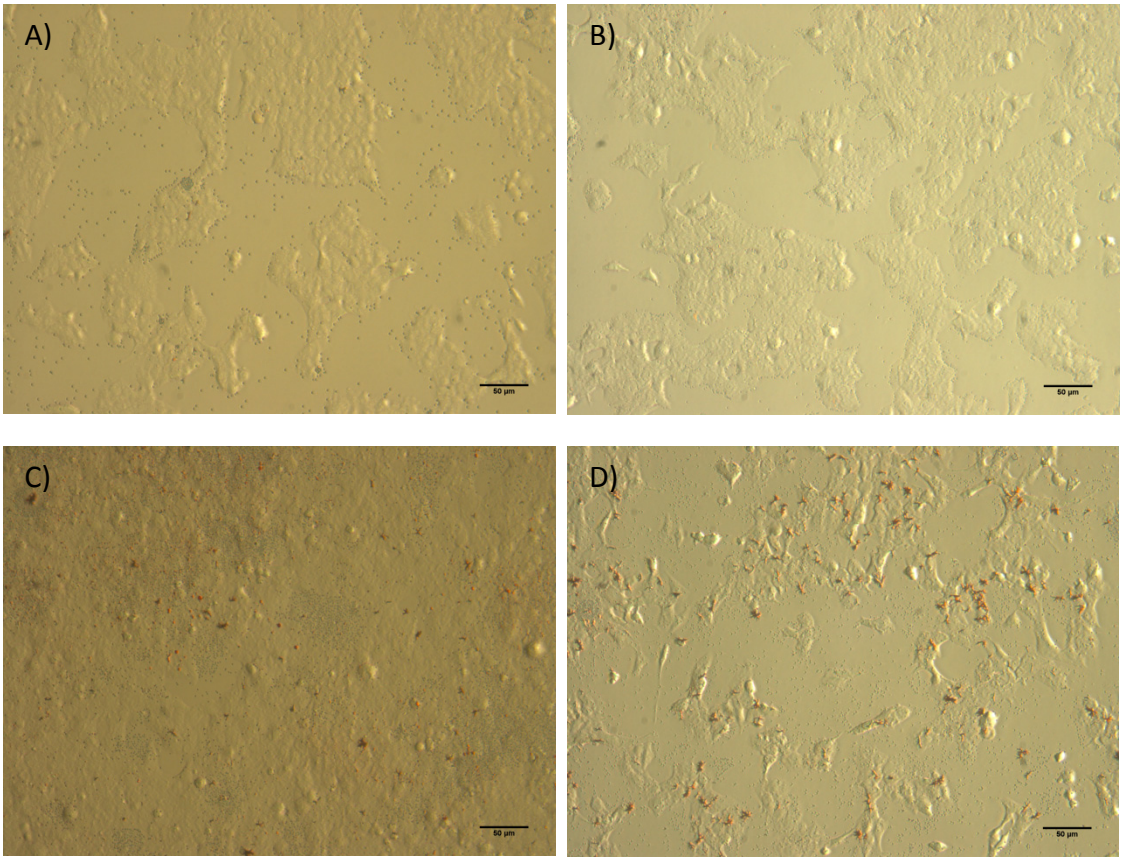

Figure 26 Oil Red O staining of cells following fat incubation

MIN6 cells were seeded into 24 well plates at a density of $2x10^5$ cells/well and given 24hrs to proliferate in antibiotic free DMEM at 37°C, 5% CO_2. Cells were then incubated for 48hrs with either **A)** antibiotic free DMEM control, **B)** BSA vehicle control, **C)** 250µM oleate or **D)** 250µM palmitate. Following treatment Oil Red O staining was carried out, and cells were visualised with a light microscope.

4.5 The effect of peroxisomal proliferating agents on *PEX11*α expression in MIN6 cells

Although we were not able to increase *PEX11*α expression in MIN6 cells through fatty acid incubation, we still wanted to show the inducible property of *PEX11*α in MIN6 cells. We therefore decided to explore the response to peroxisomal proliferating agents.

4.5.1 Incubation of MIN6 cells with Clofibrate

As it has been previously shown that the PPARα agonist clofibrate is able to increase *PEX11*α expression in human cells (Schrader *et al.*, 1998), we started by incubating MIN6 cells with clofibrate. Clofibrate is a fibric acid derivative previously used in the treatment of dyslipidemia. Due to toxicity seen with the drug, other fibric acid derivatives tend to be used instead. However, it is still a potent PPARα agonist which regulates gene expression by activating PPARα. As described previously, this leads to the formation of a heterodimer with RXR, which then binds a PPRE and leads to transcription (Barter and Rye, 2008).

MIN6 cells were seeded into 6 well plates and given 24hrs to proliferate at 37°C, 5% CO_2 before they were incubated with either 250µM or 500µM clofibrate, or an antibiotic free DMEM control. Following treatment with clofibrate for either 24hrs, 48hrs or 72hrs, cells were harvested and RNA was extracted. A 100µM clofibrate concentration was also included for the 24hr incubations. Concentrations of clofibrate were chosen by using previous studies with the drug as a guide. 250µM has previously been used with primary rat β-cells (Hellemans *et al.*, 2007), and 300µM with human adipocytes (Guo *et al.*, 2005). As we were not sure what would be tolerated by the MIN6 cells we chose a range of concentrations to work with.

*PEX11*α gene expression was quantified as previously described using Ykt6 as a reference gene. The 24hr incubation was carried out once in triplicate, and the 48hr and 72hr incubations were carried out twice in triplicate. Results are normalised to the (antibiotic free DMEM) control.

The results (Figure 27) show that *PEX11*α expression did not change with clofibrate incubation compared with the control. The 24hr incubation was only carried out once

as we did not show an increase in expression, however, later time points with the 2 higher concentrations of clofibrate showed the same pattern. Although this was unexpected as previous studies indicated that we should get an increase in *PEX11*α expression (Schrader *et al.*, 1998), we had some problems with the clofibrate in the media. We were not able to get results from all experiments carried out with the clofibrate as it sometimes came out of solution, so we moved on to try another fibric acid derivative, fenofibrate.

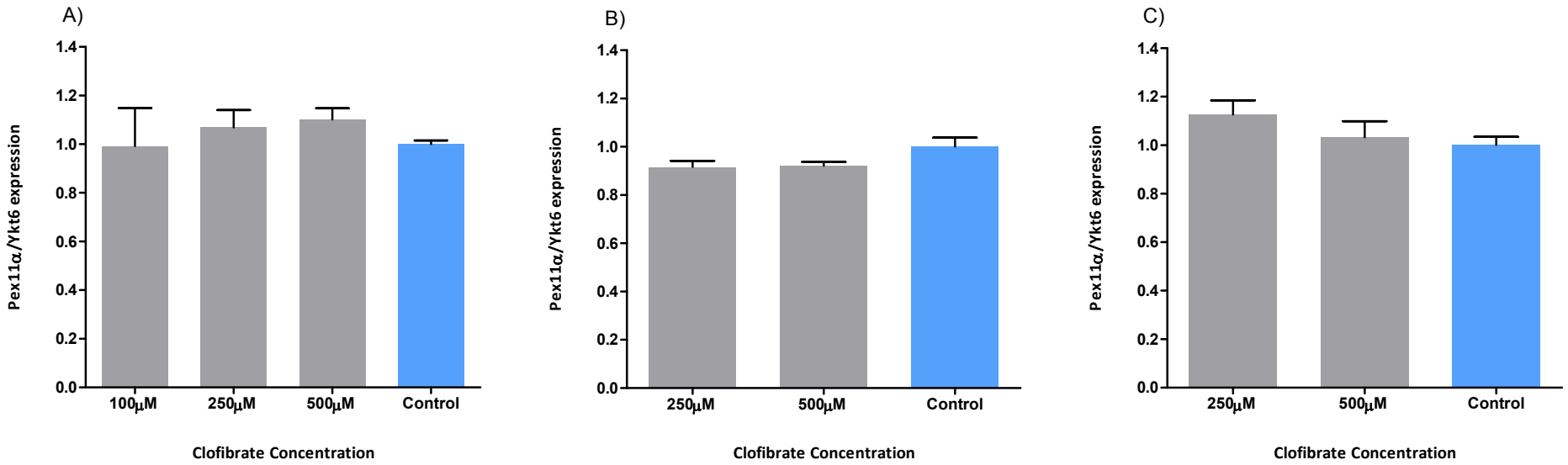

Figure 27 *PEX11*α expression following clofibrate incubation

MIN6 cells were seeded into 6 well plates at a density of $1x10^6$ cells/well, and given 24hrs to proliferate in antibiotic free DMEM at 37°C, 5% CO_2. Cells were then incubated for **A)** 24hrs, **B)** 48hrs, or **C)** 72hrs with either different concentrations of clofibrate or an antibiotic free DMEM control. For **A)** 24hrs, cells were incubated with 100μM, 250μM or 500μM clofibrate, for **B)** 48hrs and **C)** 72hrs, cells were incubated with 250μM or 500μM clofibrate. Following incubation with the treatments for the various time periods at 37°C, 5% CO_2, RNA was extracted, and cDNA synthesised. Pex11α gene expression was quantified using real-time PCR. Ykt6 was used as the reference gene. Results are normalised to BSA control, and are mean±SEM (n=3), representative of **A)** one, and **B,C)** two independent experiments.

4.5.2 PEX11α expression following incubation with Fenofibrate

Fenofibrate, like clofibrate, is a PPARα agonist and it too is used in the treatment of dyslipidaemia. It has also been shown that treatment with fenofibrate is beneficial to pancreatic β-cells, as was shown in a study using INS-1 cells. Impaired GSIS following 48hr 0.2mM palmitate incubation in these cells was restored with the addition of 5µM fenofibrate into the culture medium (Koh *et al.*, 2003; Sun *et al.*, 2008).

MIN6 cells were seeded into 6 well plates and given 24hrs to proliferate at 37°C, 5% CO_2 before they were incubated with either 2.5µM, 5µM, 10µM or 20µM fenofibrate or a BSA vehicle control. After either 24hrs or 48hrs with the various treatments, cells were harvested and *PEX11*α gene expression measured. Ykt6 was used as a reference gene. The 24hr incubation was carried out once in triplicate, and the 48hr incubation was carried out twice in triplicate. Results are normalised to the BSA control.

We decided to use a range of different concentrations around 5µM to see if there was a dose dependent response in *PEX11*α expression, and again, as we were unsure what concentration would be tolerated by the MIN6 cells.

The results (Figure 28) show that fenofibrate alone did not increase *PEX11*α expression at either 24hr or 48hr. Although this was unexpected, the higher concentrations of fenofibrate (10 and 20 µM) seemed to suggest a small increase in *PEX11*α expression, although this was not significant. As a recent paper used 9-*cis*-Retinoic Acid (RA) in addition to clofibrate in primary rat cells, and were able to show a significant increase in *PEX11*α expression with the combination, we moved on to using fenofibrate in combination with 9-*cis*-RA (Hellemans *et al.*, 2007).

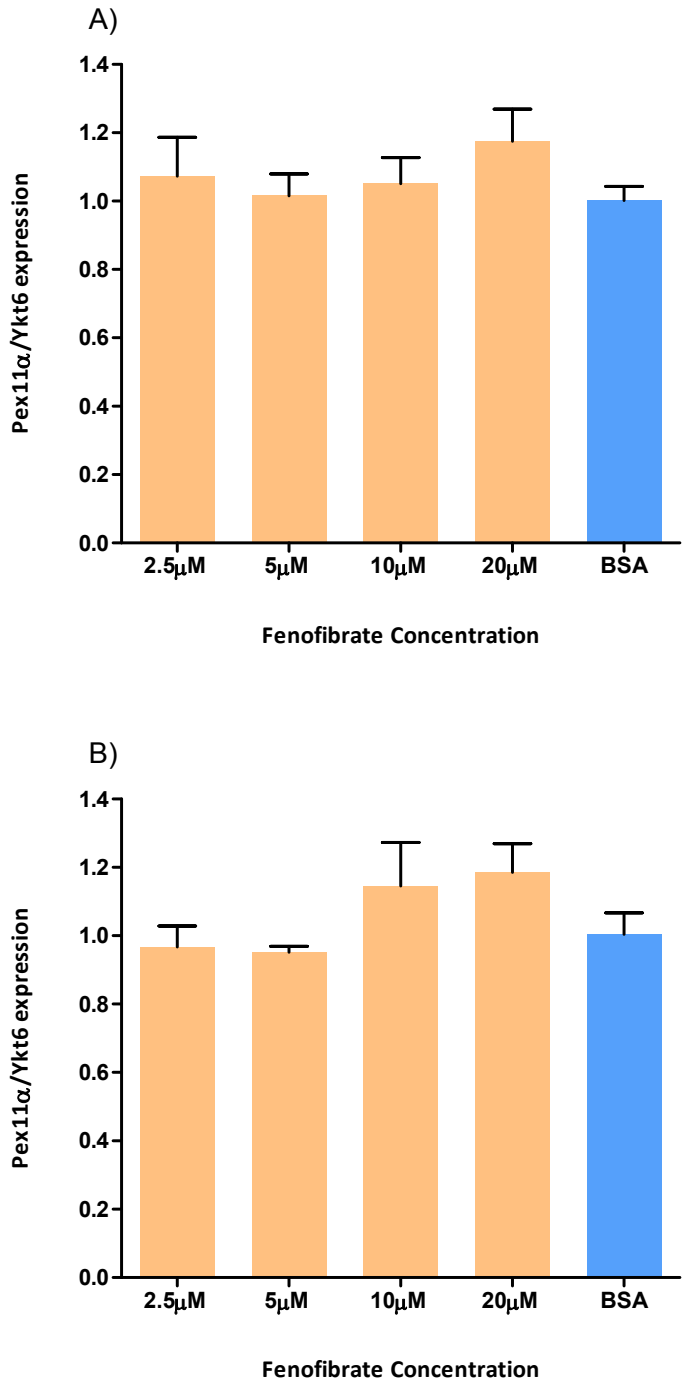

Figure 28 *PEX11*α expression following incubation with Fenofibrate

MIN6 cells were seeded into 6 well plates at a density of $1x10^6$ cells/well and given 24hrs to proliferate in antibiotic free DMEM at 37°C, 5% CO_2. Cells were then incubated for **A)** 24hrs, or **B)** 48hrs with either 2.5μM, 5μM, 10μM or 20μM of fenofibrate or a BSA vehicle control. Following incubation with the treatments for the various time periods at 37°C, 5% CO_2, RNA was extracted, and cDNA synthesised. Pex11α gene expression was quantified using real-time PCR. Ykt6 was used as the reference gene. **A)** was carried out once in triplicate, and **B)** was carried out twice in triplicate. Results are normalised to BSA control, and are mean±SEM (n=3), representative of **A)** one, and **B)** two independent experiments.

4.5.3 The effect of Fenofibrate in combination with 9-cis-Retinoic acid on PEX11α expression in MIN6 cells

In a previous study it was shown that primary rat β-cells incubated with 250µM clofibrate in combination with 2µM 9-*cis*-RA led to significant increases in several genes encoding proteins involved in fatty acid metabolism including *PEX11*α. A 1.3 fold increase was seen in *PEX11*α in response to this treatment (Hellemans *et al.*, 2007). We explored whether a similar response was seen in MIN6 cells using 9-*cis*-RA with fenofibrate rather than clofibrate.

MIN6 cells were seeded into 6 well plates and incubated for 24hrs at 37°C, 5% CO_2 to proliferate before treatment. Cells were then treated with 5µM fenofibrate and a range of 9-*cis*-RA concentrations (either 2nM, 20nM, 200nM or 2000nM) for 48hrs. A BSA vehicle control and, in order to ensure once again that the BSA was not having any effects on *PEX11*α expression, an antibiotic free DMEM control were also included. Following these treatments images were taken to ensure the combination of the treatments did not have a deleterious effect on cell growth and morphology (Figure 29).

MIN6 cells were seeded into 6 well plates and were incubated at 37°C, 5% CO_2 for 24hrs before treatment with 5µM fenofibrate in combination with either 2nM, 20nM, 200nM or 2000nM 9-*cis*-RA concentrations for 24hr or 48hrs. Again, both a BSA control and an antibiotic free DMEM control were included at both time points. *PEX11*α expression was determined as before using real time PCR, with Ykt6 as a reference gene. 24hr experiments were carried out three times in triplicate. 48hr experiments were carried out three times in triplicate and once in duplicate. Results are normalised to the BSA control.

The results (Figure 30) show that a trend towards an increase in *PEX11*α expression was seen with 5µM fenofibrate in combination with each of the 9-*cis*-RA concentrations tested, compared with the BSA control. However, the 5µM fenofibrate in combination with 2000nM 9-*cis*-RA gave the largest, and only significant fold increase of 1.5 ($P<0.01$) at 48hr. As has been shown previously (Figure 25) there was again no difference between the BSA vehicle control and the antibiotic free DMEM control indicating that the BSA is not having any effect on *PEX11*α expression.

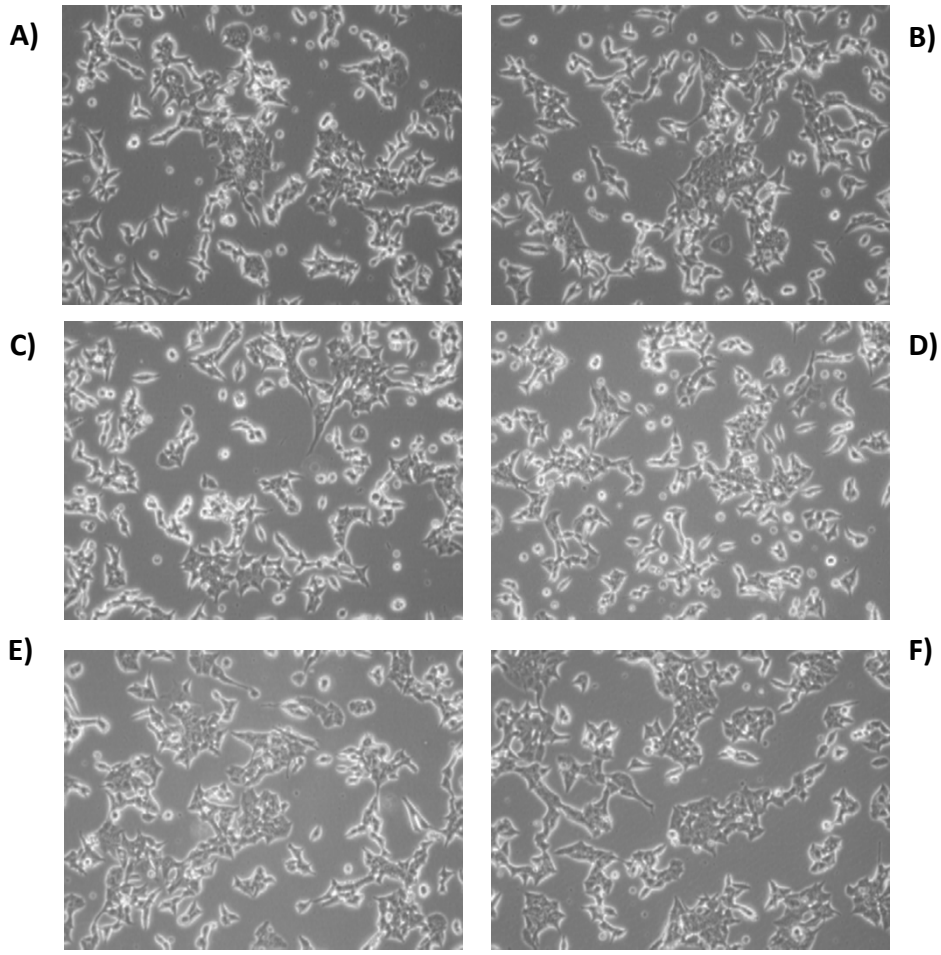

Figure 29 Images showing MIN6 cells following 48hr treatment with Fenofibrate and 9-*cis*-Retinoic Acid

MIN6 cells were seeded into 6 well plates at a density of $1x10^6$ cells/well and given 24hrs to proliferate in antibiotic free DMEM at 37°C, 5% CO_2. Cells were then incubated for 48hrs with **A)** 5µM fenofibrate, 2nM 9-*cis*-RA, **B)** 5µM fenofibrate, 20nM 9-*cis*-RA, **C)** 5µM fenofibrate, 200nM 9-*cis*-RA, **D)** 5µM fenofibrate, 2000nM 9-*cis*-RA, **E)** BSA vehicle control, or **F)** an antibiotic free DMEM control.

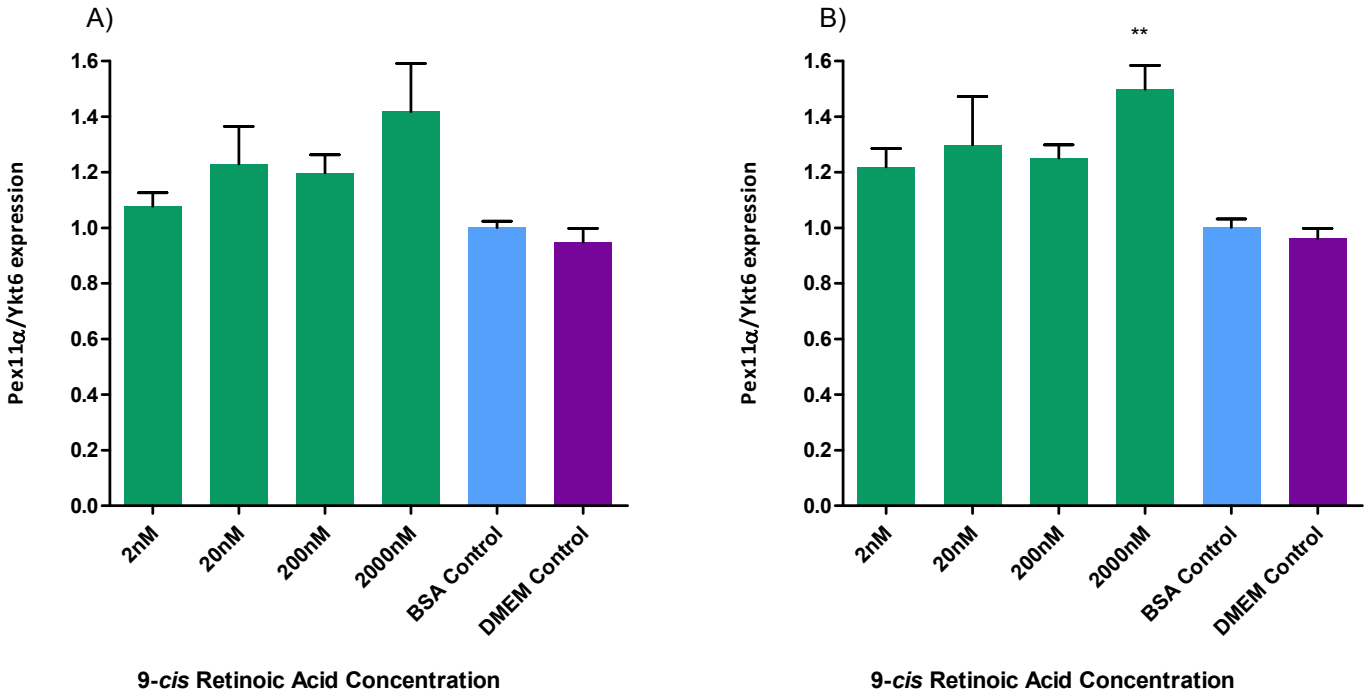

Figure 30 *PEX11*α expression following treatment with a combination of 5µM Fenofibrate with varying concentrations of 9-*cis*-Retinoic Acid

MIN6 cells were seeded into 6 well plates at a density of $1x10^6$ cells/well and given 24hrs to proliferate in antibiotic free DMEM at 37°C, 5% CO_2. Cells were then incubated for **A)** 24hrs, or **B)** 48hrs with either a combination of 5µM fenofibrate and a varying concentration of 9-*cis*-RA (2nM, 20nM, 200nM or 2000nM), or a BSA vehicle control, or an antibiotic free DMEM control. Following incubation with the treatments at 37°C, 5% CO_2, RNA was extracted, and cDNA synthesised. Pex11α gene expression was quantified using real-time PCR. Ykt6 was used as the reference gene. Results are normalised to BSA control, and are mean±SEM (n=3) of **A)** three and **B)** four independent experiments. **P<0.01 compared to BSA control; one-way ANOVA and Bonferroni's *post hoc* test.

4.6 The effect of Fenofibrate and 9-*cis*-Retinoic Acid incubation on peroxisome abundance

Following the successful increase in *PEX11*α expression following treatment with fenofibrate and 9-*cis*-RA we decided to look at the effect of the treatment on PMP-70 protein expression as a marker of peroxisome abundance.

MIN6 cells were seeded into 6 well plates and given 24hrs to proliferate at 37°C, 5% CO_2. Cells were then incubated with either 5μM fenofibrate in combination with 2000nM 9-*cis*-RA (the combination which gave the largest increase in *PEX11*α expression), or a BSA control for 24hr or 48hr. To ensure the BSA was not having any effect on PMP-70 protein levels, an antibiotic free DMEM control was also included. Following the treatments, cells were harvested in protein extraction buffer. Protein quantities were determined and western blots were run to quantify the expression of PMP-70 protein. β-actin was used as a loading control. Results are expressed as a ratio of PMP-70 to β-actin, and are normalised to BSA control.

The results (Figure 31) show that PMP-70 protein expression was not changed after incubation with fenofibrate and 9-*cis*-RA compared with the BSA control. Although we were able to produce a 1.5 fold increase in *PEX11*α gene expression with a combination of 5μM fenofibrate and 2000nM 9-*cis*-RA with 48hr treatment (Figure 30), this did not result in a significant increase in peroxisome abundance at either 24hr or 48hr. There was no significant difference between the BSA control and the DMEM control indicating that the BSA did not cause any changes in PMP-70 protein levels as expected.

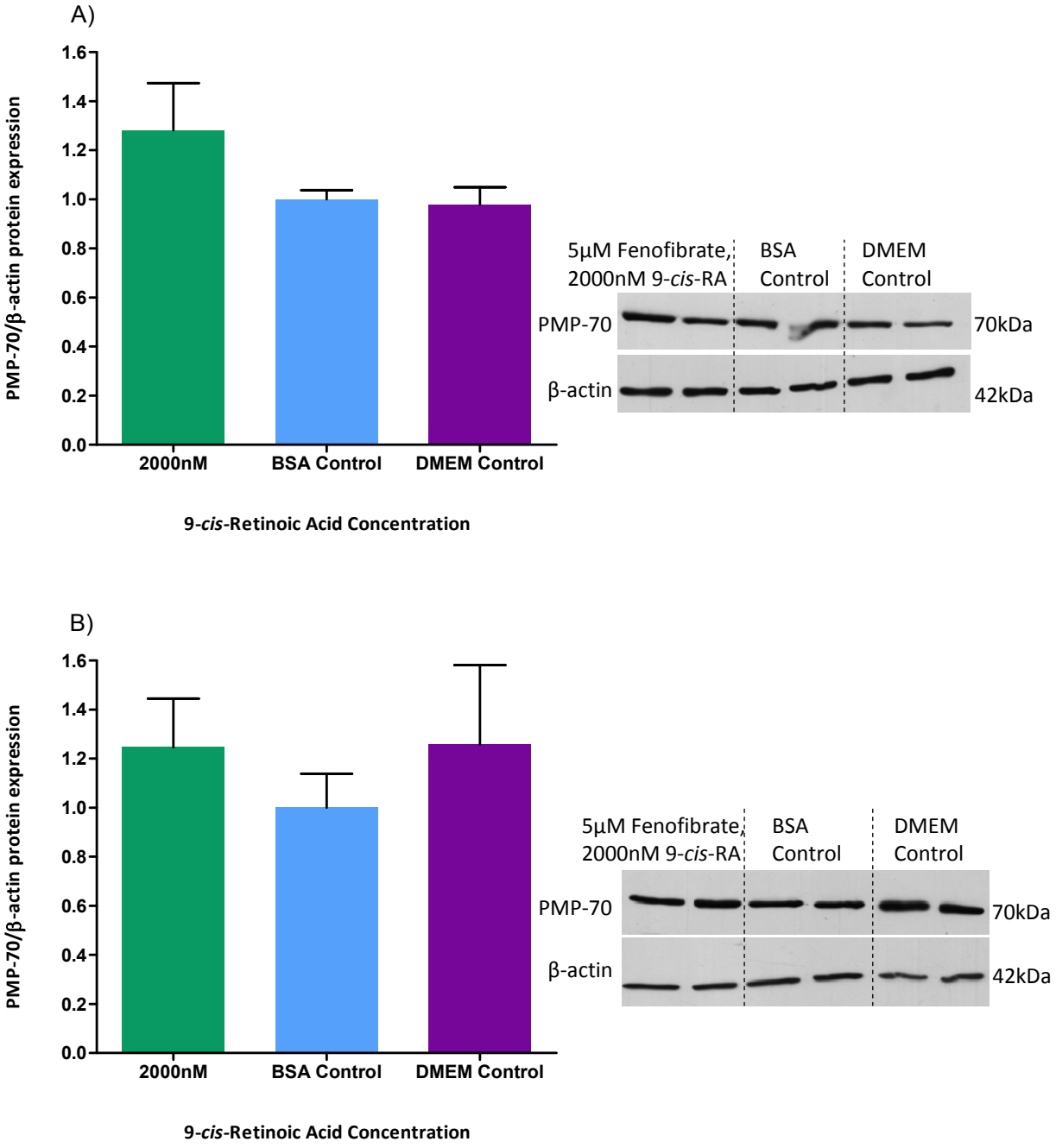

Figure 31 PMP-70 protein expression following treatment with 5µM Fenofibrate and 2000nM 9-*cis*-Retinoic Acid

MIN6 cells were seeded into 6 well plates at a density of $1x10^6$ cells/well and given 24hrs to proliferate in antibiotic free DMEM at 37°C, 5% CO_2. Cells were then incubated for **A)** 24hrs, or **B)** 48hrs with either a combination of 5µM fenofibrate and 2000nM 9-*cis*-RA, a BSA vehicle control, or an antibiotic free DMEM control. Following incubation with the treatments at 37°C, 5% CO_2, protein was extracted. PMP-70 protein expression was quantified using western blotting. β-actin was used as a loading control. Results are normalised to the BSA control. Experiments were carried out three times in duplicate. Error bars are representative of SEM. Next to each graph is one of the western blots given as an example.

4.7 Discussion

The overall aim of the studies described in this chapter was to explore whether *PEX11*α expression was inducible in MIN6 cells. We first examined the effect of palmitate and oleate, but it was evident that neither altered *PEX11*α expression under our study conditions (Figure 25). Our work corresponds with another paper which showed that incubation with palmitate alone was unable to result in an increase in *PEX11*α expression in primary rat β-cells. Although palmitate treatment resulted in a significant increase in some other peroxisomal membrane protein genes, it was unable to lead to similar increases in *PEX11*α expression (Hellemans *et al.*, 2007). It has been reported that peroxisome abundance might be under metabolic control. It was shown that human peroxisomal biogenesis disorder (PBD) cell lines with defects in either of 2 enzymes involved in peroxisomal metabolism (acyl-CoA oxidase or 2-enoyl-CoA hydratase/D-3-hydroxyacyl-CoA dehydrogenase) have a fivefold reduction in peroxisome abundance (Chang *et al.*, 1999). It is therefore possible that incubation with fatty acids may have led to an increase in peroxisome abundance, however, if this was so, it is unlikely to have been through an increase in *PEX11*α expression. Although in yeast it has been reported that PEX11 proteins are required for peroxisomal proliferation in response to oleate (Erdmann and Blobel, 1995), it appears that this may not the case for MIN6 cells.

We next explored the impact of peroxisomal proliferators on *PEX11*α expression. We tried by using either clofibrate, or fenofibrate which are both PPARα agonists capable of causing the proliferation of peroxisomes (Aoyama *et al.*, 1998). Clofibrate is known to increase *PEX11*α expression in the rat (Abe *et al.*, 1998; Schrader *et al.*, 1998).

We were unable to increase the expression of *PEX11*α by incubation with either of the peroxisomal proliferating agents, fibric acid derivatives, fenofibrate or clofibrate (Figures 27 and 28), which was unexpected. As the previous studies mentioned had used the fibric acid derivative alone to induce an increase in *PEX11*α expression we expected a similar effect for the MIN6 cells. Although there seemed to be a trend towards an increase in *PEX11*α expression with fenofibrate alone (Figure 28) which may have reached significance with further experiments, the results were inconsistent. It is possible that low endogenous levels of RA within the MIN6 cells may be a possibility for this. *PEX11*α expression is controlled through the binding of the PPARα-

RXR heterodimer to the PPRE located downstream of *PEX11*α (Shimizu *et al.*, 2004). Previous experiments have been carried out to examine the induction of a peroxisomal enzyme, acyl-CoA oxidase, which like *PEX11*α is also activated through the binding of a PPARα-RXR heterodimer to a PPRE. Whilst it was shown that the promoter for rat acyl-CoA oxidase could be induced by either the PPARα agonist clofibrate alone by the activation of PPARα, or by 9-*cis*-RA alone though the activation of RXR, it was noted that the combination of the two agonists resulted in a synergistic increase in the activity of the acyl-CoA oxidase promoter (Kliewer *et al.*, 1992).

It was shown in one study that increasing concentrations of RA resulted in increasing activity of peroxisomal acyl-CoA oxidase in cultured rat hepatocytes (Hertz and Bar-Tana, 1992), while another group were able to show, again in rat hepatocytes, that the addition of RA with fenofibrate resulted in a longer and enhanced induction of peroxisomal acyl-CoA oxidase compared with RA treatment alone. It was thought that this was likely through the activation of PPARα by fenofibrate, and the activation of RXR by RA leading to formation of the PPARα-RXR heterodimer which was then able to bind the PPRE located within the acyl-CoA oxidase gene promoter (Berthou *et al.*, 1995). This mechanism was demonstrated previously by a group in 1993, which were able to show through a series of transfection experiments, that the two receptors worked co-operatively to activate the PPRE within the acyl-CoA oxidase gene promoter (Keller *et al.*, 1993). It is therefore possible that we were unable to see a clear and consistent increase in *PEX11*α expression with fenofibrate alone if RA levels were relatively low in the MIN6 cells. We were able to build on this as the combination of fenofibrate and 9-*cis*-RA resulted in a 1.5 fold increase in *PEX11*α expression in the MIN6 cells (Figure 30). This is in line with a study from 2007 which reported a 1.3 fold increase in *PEX11*α expression with the combination of clofibrate and 9-*cis*-RA in primary rat β-cells (Hellemans *et al.*, 2007). It is therefore likely that the 1.5 fold increase we saw in *PEX11*α expression with the combination of fenofibrate and 9-*cis*-RA, and not with fenofibrate alone, was through the mechanism described for acyl-CoA oxidase by Keller et al., 1993, since (as previously mentioned) *PEX11*α expression is also regulated through the binding of a PPARα-RXR heterodimer to a PPRE (Shimizu *et al.*, 2004). Our results also support the idea that endogenous RA levels were a limiting factor under these study conditions.

Since fatty acids are also activators of PPARα (Rakhshandehroo *et al.*, 2009), it is possible that another reason we were unable to achieve any increases in *PEX11*α expression through the incubation of palmitate and oleate was also because of possible low levels of RA within the MIN6 cells. The addition of RA with the fatty acids may have led to formation of the PPARα-RXR heterodimer to lead to the initiation of *PEX11*α transcription as seen in the MIN6 cells when incubated with a combination of fenofibrate and RA (Figure 30).

Studies showing increases in peroxisome proliferation and peroxisomal oxidation in response to fatty acids, or fibric acid derivatives have often been carried out in the mammalian liver (Berge *et al.*, 1989; Lee *et al.*, 1995). Since natural 9-*cis*-RA has been shown to be present in the mouse liver (Heyman *et al.*, 1992), it is likely that incubation with fatty acids or fibric acid derivatives in the liver can result in the formation of the PPARα-RXR heterodimer without the addition of further 9-*cis*-RA. However, it has also been shown that mouse kidneys express 9-*cis*-RA in larger amounts than the liver (Heyman *et al.*, 1992) which shows a tissue specific production of the RXR agonist. Although our results point to possible low levels of endogenous RA levels within the MIN6 cells, a study carried out in 2010 found that mouse pancreas, including the β-cells, and the 832/13 (INS-1) β-cell line produce 9-*cis* RA. This retinoid was found to attenuate the sensitivity of the pancreas to glucose. The study also found that GSIS in the 832/13 β-cell line was reduced at 60 minutes in cells treated with 9-*cis*-RA compared with the control, however, this reduction did not appear to be present following 120 minutes incubation (Kane *et al.*, 2010). Although it seems that β-cells may produce their own 9-*cis*-RA, it is possible that MIN6 cells are deficient in natural 9-*cis*-RA rendering them incapable of producing the PPARα-RXR heterodimer in response to a PPARα agonist alone. Studies into the naturally occurring levels of RA in MIN6 cells, and other commonly used β-cell lines may be worth pursuing in the future.

Incubation with fenofibrate and 9-*cis*-RA did not lead to an increase in PMP-70 expression as marker of peroxisome abundance. Although this was unexpected, we were unsure how long it would take for peroxisome abundance to increase following treatment with the drugs. It is thought that the half-life of peroxisomes is about 2 days (Huybrechts *et al.*, 2009; Nordgren *et al.*, 2013), and it was found that the daily turnover rate for peroxisomes was about 30% (Huybrechts *et al.*, 2009). In addition, we

show in chapter 6 that it requires 96hrs following *PEX11*β knockdown to result in a decrease in peroxisome abundance indicating the turnover rate may be longer than 2 days in MIN6 cells, and it therefore could take up to 96hrs to witness an increase in peroxisome number following treatment with fenofibrate and 9-*cis*-RA.

Fibrate treatment has been shown to increase peroxisome abundance in rodents, however, this has been looked at in rats 7 to 10 days following treatment. The effect of the peroxisome proliferators on peroxisome abundance following less than 7 days incubation does not appear to have been investigated. (Lazarow and De Duve, 1976; Colton *et al.*, 2004; Islinger *et al.*, 2007). It has also been shown that cynomolgus monkeys treated with ciprofibrate produce an increase in hepatic peroxisome abundance in response to a 15 day treatment (Colton *et al.*, 2004). Increases in gene expression of peroxisomal membrane proteins and enzymes involved in peroxisomal fatty acid oxidations have been witnessed following 48hrs treatment with fibrates, but the effects on the proteins were not investigated in this study (Hellemans *et al.*, 2007). We tried to investigate whether an increase in *PEX11*α expression resulted in an increase in PEX11α protein expression, however, the antibody against PEX11α was unspecific and we were unable to determine this. However, compared with the BSA control (Figure 31), although not significant, there does appear to be a trend towards an increase in the expression of PMP-70 in response to fenofibrate and 9-*cis*-RA treatment. It is therefore possible that we were not able to produce a significant increase in peroxisome abundance following 24hr or 48hr treatment with fenofibrate and 9-*cis*-RA as more time is required for the increased transcription of *PEX11*α to result in an increase in peroxisome abundance.

Chapter 5

The role of *PEX11α* in lipotoxicity

5 The role of *PEX11α* in lipotoxicity

5.1 Introduction

Lipotoxicity is thought to be one of the ways in which β-cell dysfunction occurs in type 2 diabetes (Unger and Zhou, 2001; Hellemans *et al.*, 2007). It has been shown that there is an increase in the levels of intracellular fatty acids in the pancreas of Zucker Diabetic Fatty (ZDF) rats (Shimabukuro *et al.*, 1998b). One of the consequences of this increase in fatty acids within the pancreas appears to be a decrease in GSIS, indicating pancreatic β-cell dysfunction (Watson *et al.*, 2011).

In isolated islets from humans and mouse, exposure to 500µM palmitate for 72hrs reduced GSIS by about 60% (Hoppa *et al.*, 2009). It has also been shown that in MIN6 cells, exposure to 400µM to 500µM palmitate for 48hrs resulted in a 50% to 75% decrease in GSIS (Thörn and Bergsten, 2010; Watson *et al.*, 2011; Kristinsson *et al.*, 2013). These results indicate that chronic exposure to palmitate is toxic to the β-cell.

As a SNP located in the *PEX11*α gene region was found to have an association with a decreased β-cell function (Pascoe, 2009) we decided to look at the effect of changing *PEX11*α gene expression on GSIS. As *PEX11*α is involved in the division of peroxisomes (Schrader *et al.*, 1998), which in turn are partially responsible for the metabolism of fatty acids (Wanders, 2004) we wanted to do this in the presence and absence of palmitate.

5.2 Aims

The main aim of this chapter was to investigate the role of *PEX11*α in lipotoxicity in MIN6 cells. We did this by:

- Examining the effect of *PEX11*α knockdown alone on GSIS.
- Assessing the effect of palmitate incubation on GSIS and cytotoxicity.
- Measuring GSIS following a combination of *PEX11*α knockdown and palmitate incubation.

5.3 Methods

5.3.1 Glucose Stimulated Insulin Secretion (GSIS) Assay

The GSIS assay (protocol section 2.8) is used to determine the amount of insulin secreted by cells in one hour when challenged with either basal (3mM), or stimulating (25mM) glucose levels. As described in section 1.1.2, when cells are exposed to glucose eventual rises in intracellular Ca^{2+} levels result in the exocytosis of insulin granules. Under cell culture conditions, this insulin is secreted into the culture medium (Krebs-Hepes buffer in this assay). The culture medium can then be collected and analysed using an insulin ELISA. The insulin ELISA is based on a direct sandwich assay technique which uses two different monoclonal antibodies against insulin. The insulin in the sample can react with both the anti-insulin antibodies which are bound to the microtitration well, and the anti-insulin antibodies conjugated to peroxidase with which the sample is incubated. Following incubation, the unbound peroxidase-conjugated antibody is removed by washing, and the reaction is detected with the addition of 3,3',5,5'-tetramethylbenzidine (TMB). TMB detects the peroxidase bound to the anti-insulin antibody, yielding a colour change. The reaction is halted by the addition of sulphuric acid (H_2SO_4) producing a yellow colour which can be read on a plate reader at a wavelength of 450nm. The intensity of the yellow relates to the amount of insulin in the sample.

5.3.2 Caspase 3/7 Assay

Apoptosis, or programmed cell death is a regulated process responsible for the safe removal of damaged cells, or cells which are no longer needed. Following the initiation of apoptosis by apoptotic factors, cells eventually shrink. They are then removed by phagocytosis, often by macrophages which engulf the dead cells. The cells can also be recognised by neighbouring cells which also clear the dead cells by the process of phagocytosis. This process leads to an avoidance of the inflammatory response in surrounding tissue (Afford and Randhawa, 2000; Jin and El-Deiry, 2005).

Caspases are proteins involved in the initiation and execution of apoptosis. There are three main groups of caspases which have been identified: inflammatory caspases which are involved in inflammation rather than apoptosis, apoptotic initiator caspases which are responsible for the activation of apoptosis, and apoptotic effector caspases

which are involved in the execution of apoptosis. Caspases 3 and 7 are both effector caspases, so once activated they serve as a good marker of apoptosis (Jin and El-Deiry, 2005).

The Caspase-Glo® 3/7 Assay (Promega) which has been used for this work is a luminescent assay that measures the activities of caspases 3 and 7. The substrate provided in the assay, when added to the cells, results in cell lysis, and the substrate is cleaved by the caspases. This cleavage results in a luminescent signal produced by luciferase. The amount of luminescence produced, and therefore the amount of substrate which undergoes cleavage, is proportional to the caspase activity.

5.3.3 LDH assay

In addition to assessing cell cytotoxicity through the use of the caspase 3/7 assay, lactate dehydrogenase (LDH) was also assessed. LDH catalyses the conversion of lactate to pyruvate and the reverse reaction, and is present in many organisms. It is a fairly stable enzyme released following cell injury, and therefore is released into the medium during cell culture making it a good molecule to detect cell viability. When LDH oxidises lactate, it generates NADH. This NADH can then react with the WST (Water soluble Tetrazolium salts) included in the assay kit, and produce a colour change which can be read on a plate reader at a wavelength of 450nm. The intensity of the colour relates to the amount of LDH released into the culture medium. Medium was retained from various experiments and analysed using this assay.

5.3.4 The role of PEX11α in lipotoxicity

MIN6 cells were either transfected with siRNA against *PEX11*α or a scr control. For each experiment, cells were seeded at a density of $2.5x10^5$ cells/well. Following transfection, a GSIS assay was carried out. Protein was harvested and quantified using a Bradford assay (section 2.7.2) in order to normalise total insulin secreted in one hour to total protein.

Following incubation with 250µM palmitate in untransfeced cells, either GSIS was carried out, and insulin secretion was normalised to protein, or a caspase 3/7 assay was carried out to assess apoptosis following treatment. Media was retained from the latter experiments for analysis with an LDH assay.

For transfection of MIN6 cells in combination with palmitate, a GSIS assay was carried out 72hrs after transfection. It was therefore necessary to ensure that *PEX11*α expression was deceased at 72hrs. 72hrs after transfection, RNA was extracted from MIN6 cells, cDNA was synthesised, and *PEX11*α expression was determined using real time PCR. For the transfected cells incubated with 250µM palmitate, media was retained for analysis with an LDH assay before carrying out GSIS.

5.4 Results

5.4.1 The effect of PEX11α knockdown on GSIS

We wanted to find out what role *PEX11*α might play in lipotoxicity of pancreatic β-cells. Having established a reliable method for the knockdown of *PEX11*α in MIN6 cells, we moved on to examine *PEX11*α knockdown on GSIS.

MIN6 cells were transfected in suspension using the Neon system with either 100nM of the *PEX11*α siRNA probes s71494 or s71495, or a scrambled control. In addition, controls without siRNA were also shocked with the neon system to ensure the scrambled control was not having any effect on insulin secretion. Cells were plated into 24 well plates and given either 24hr or 48hr to proliferate at 37°C, 5% CO_2 before GSIS was carried out. Following the protocol detailed in materials and methods section 2.8, cells were pre-incubated in Krebs-Hepes buffer for 30mins before being challenged with either basal (3mM) or stimulating (25mM) glucose levels for 1hr. Following GSIS, cell supernatants were collected and the cells were harvested in protein extraction buffer. The amount of insulin secreted into the incubation buffer was determined using an insulin ELISA. Insulin secreted was normalised to protein content. Separate wells were set up with each probe for every transfection experiment so RNA could be extracted. This allowed further analysis by real time PCR to ensure that *PEX11*α expression was knocked down.

The results (Figure 32) show that there is a significant insulin response from the basal 3mM glucose concentration to the stimulating 25mM glucose concentration for cells transfected with the s71494 probe ($P<0.01$), the s71494 probe ($P<0.001$), the scrambled control ($P<0.01$) and for the shocked control ($P<0.05$) at 24hr.This response was also seen at 48hr for the s71494 probe ($P<0.001$), the s71494 probe ($P<0.001$), the scrambled control ($P<0.01$) and the shocked control ($P<0.01$). There was however, no difference between the *PEX11*α knockdowns and the scrambled controls at either 3mM glucose or 25mM glucose, indicating that *PEX11*α knockdown alone does not have any effect on GSIS.

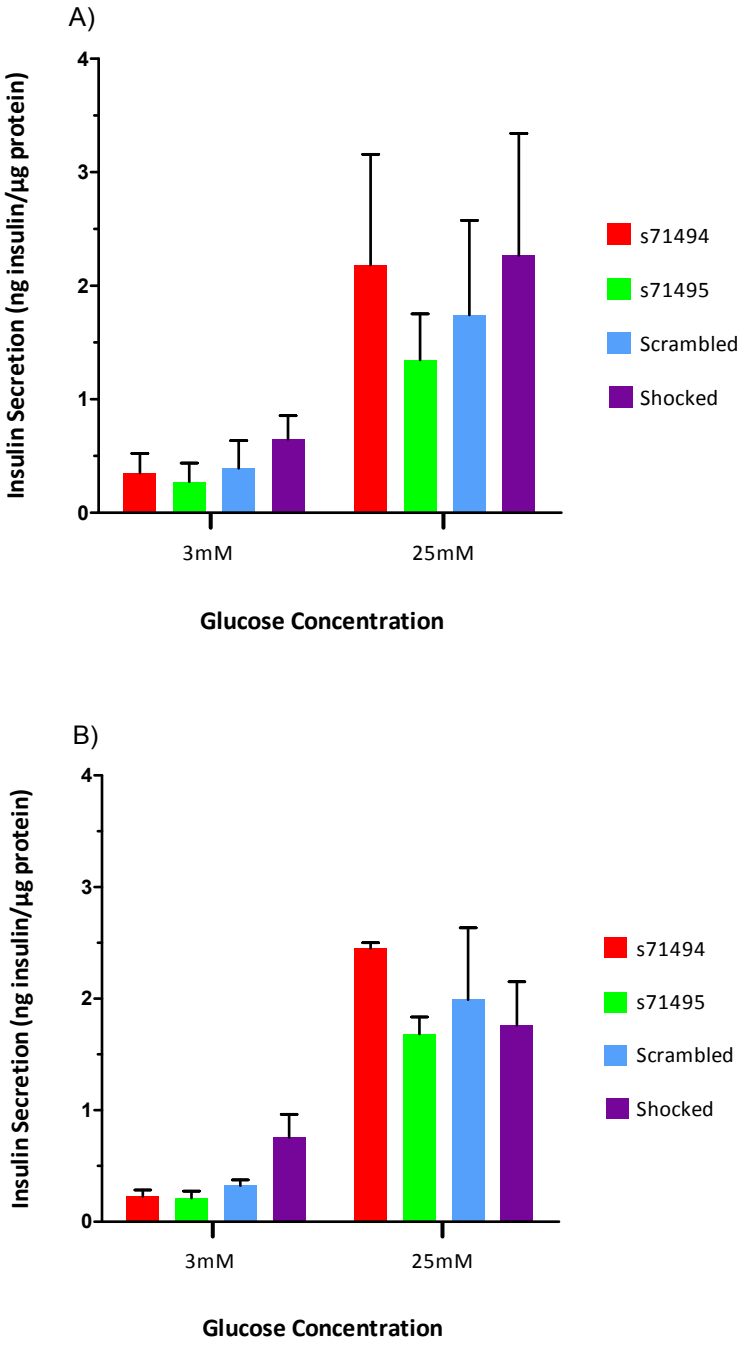

Figure 32 The effect of *PEX11*α knockdown on glucose stimulated insulin secretion

MIN6 cells were transfected in suspension using 100nM of Pex11α siRNA probes s71494 or s71495, scrambled siRNA or no siRNA (shocked). Cells were incubated in a 24 well plate for either A) 24hrs or B) 48hrs in antibiotic free DMEM at 37°C, 5% CO2 before cells were challenged with either basal (3mM) or stimulating (25mM) glucose concentrations for 1 hour. Cell supernatants were collected and insulin secretion was determined by insulin ELISA. Protein was extracted from the cells and used to normalise the insulin secretion. Results are normalised to 3mM scrambled control. Protein was extracted from the cells and used to normalise the insulin secretion. Results are mean±SEM (n=3) of three independent experiments.

5.4.2 Palmitate incubation causes a diminished response to stimulating glucose concentrations in MIN6 cells

To ensure that our MIN6 cells were behaving as previously described, with a reduction in GSIS following palmitate incubation (Watson *et al.*, 2011), we next incubated MIN6 cells with 250μM palmitate.

MIN6 cells were seeded into 24 well plates and given 24hrs to proliferate at 37°C, 5% CO_2. Cells were then incubated with either 250μM palmitate conjugated to BSA, a BSA vehicle control, or an antibiotic free DMEM control for 48hrs at 37°C, 5% CO_2. Following this incubation, as previously described, GSIS was carried out and insulin secretion was determined using an insulin ELISA. Insulin secretion was normalised to protein content. All results were further normalised to the 3mM glucose BSA control. Experiments were carried out 3 times in triplicate.

The results (Figure 33) show that a significant insulin response can be seen from 3mM basal glucose concentrations to 25mM stimulating glucose concentrations for all treatment groups ($P<0.001$). Incubation with 250μM palmitate, however, resulted in a 50% decrease in insulin secretion at 25mM glucose ($P<0.05$) compared with the scrambled control demonstrating that palmitate incubation decreases GSIS in MIN6 cells. Although it appears that palmitate is inhibiting the insulin secretion at 3mM glucose, there was no significant difference. In addition, there was no difference between the BSA control and the DMEM control at either 3mM glucose, or 25mM glucose, indicating that BSA does not affect GSIS.

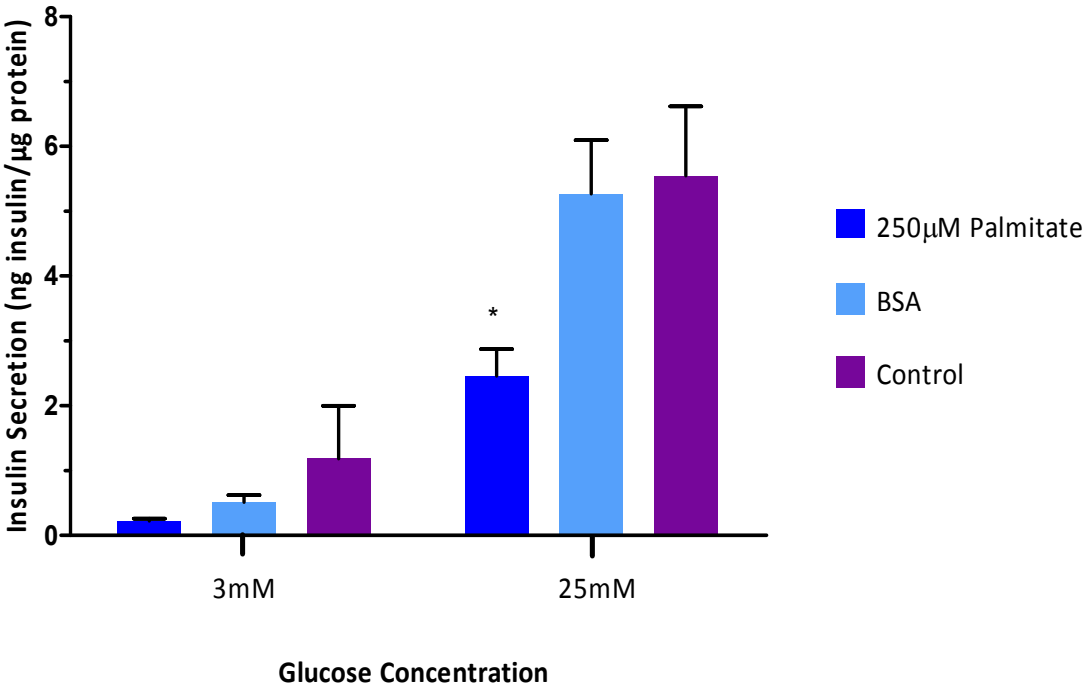

Figure 33 The effect of palmitate incubation on glucose-stimulated insulin secretion from MIN6 cells

MIN6 cells were given 24hrs to proliferate in antibiotic free DMEM before being incubated with either 250µM palmitate, a BSA control, or an antibiotic free DMEM control for 48hrs at 37°C, 5% CO_2. Cells were then challenged with either basal (3mM) or stimulating (25mM) glucose concentrations for 1 hour. Cell supernatants were collected and insulin secretion was determined by insulin ELISA. Protein was extracted from the cells and used to normalise the insulin secretion. Results are mean±SEM (n=3), of three independent experiments. *P<0.05 compared to 25mM glucose BSA control; one-way ANOVA and Bonferroni's *post hoc* test.

5.4.3 The cytotoxic effects of palmitate incubation on MIN6 cells

In order to determine whether the decreases in insulin secretion witnessed in response to palmitate incubation were due to cell death in the palmitate treated cells we carried out some cytotoxicity assays. Both Caspase-Glo® 3/7 assays and LDH assays were used for this. The protocols are detailed in methods sections 2.9 and 2.10.

MIN6 cells were seeded into 24 well plates and given 24hrs to proliferate at 37°C, 5% CO_2. Cells were then incubated with either staurosporine as a positive control, 250µM palmitate conjugated to BSA, a BSA vehicle control, or DMEM control for 48hrs at 37°C, 5% CO_2. Following this, medium was removed and stored in microcentrifuge tubes. 100µl serum free DMEM was then added to each well before adding 100µl Caspase-Glo® 3/7 reagent. Cells were incubated at room temperature for 2hrs with the reagent before being transferred into a white 96 well plate. Luminescence was read on a plate reader. Experiments were carried out 6 times in triplicate.

Medium from 3 of the experiments carried out in triplicate, collected prior to carrying out the apoptosis caspase assay, was analysed using an LDH assay. Briefly, samples were added to LDH reaction mix in clear 96 well plates and incubated for 30 minutes at room temperature. An LDH assay positive control was included to ensure the assay was working correctly. Optical densities were then read on a plate reader at 450nm.

The results (Figure 34) show that there is no significant difference in either caspase 3/7 activity or LDH release following palmitate treatment compared with the BSA control. This indicates that 250µM palmitate incubation for 48hr does not cause cell death by either apoptosis or necrosis in the MIN6 cells. This would indicate that these mechanisms are not resulting in the decrease in GSIS seen in the MIN6 cells following 250µM palmitate incubation. Demonstrating that the assays worked correctly, the results show a significant increase ($P<0.01$) in caspase 3/7 following treatment with staurosporine. Also, the addition of the LDH positive control within the LDH assay shows a significant increase ($P<0.001$) compared with the BSA control, indicating that the LDH assay reagents are working correctly.

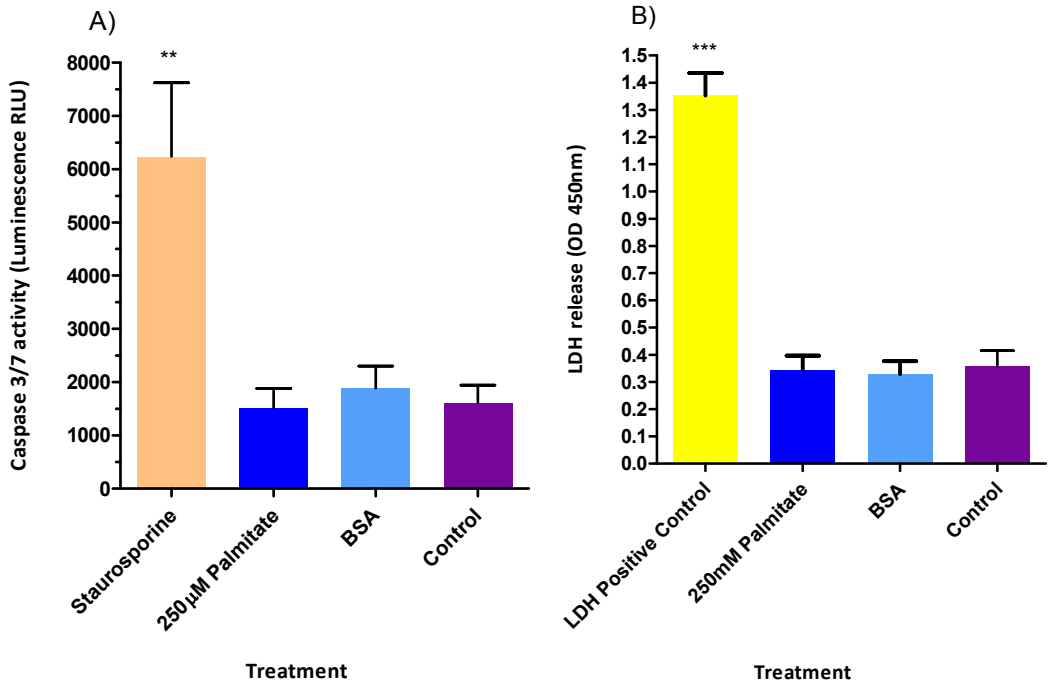

Figure 34 Cytotoxicity in MIN6 cells caused by 250µM palmitate incubation

MIN6 cells were seeded into 24 well plates at a density of $2x10^5$ cells/well and given 24hrs to proliferate in antibiotic free DMEM before being incubated with either 250µM palmitate, a BSA control, or an antibiotic free DMEM control for 48hrs at 37°C, 5% CO_2. **A)** Caspase 3/7 activity was then measured using the luminescent Caspase-Glo® 3/7 assay. Staurosporine was used as a positive control. Results are mean±SEM (n=6), of six independent experiments. Data is shown as a measure of luminescence, RLU (relative luminescence units). **B)** LDH release into the medium was measured using an LDH assay, and optical density was read at 450nm. An LDH assay positive control (included in the kit) was also measured. Results are mean±SEM (n=3), of three independent experiments. **P<0.01, ***P<0.001 compared to BSA control; one-way ANOVA and Bonferroni's *post hoc* test.

5.4.4 The effect of palmitate incubation on GSIS from MIN6 cells following PEX11α knockdown

We were interested in whether *PEX11*α knockdown changed the insulin response in MIN6 cells following palmitate incubation. As the previous experiments looked at GSIS following 48hr palmitate incubation with 24hrs for cells to proliferate before incubation, we decided to check whether *PEX11*α was knocked down 72hrs post transfection. We chose to use the s71495 probe as it gave the greatest knockdown of *PEX11*α gene expression at both 24hrs and 48hrs post transfection (Figure 22). As previously described, MIN6 cells were transfected using the Neon system with either 100nM siRNA *PEX11*α s71495 probe, scrambled siRNA control, or a no siRNA shocked control. Following 72hrs, cells were harvested and *PEX11*α gene expression was determined using real time PCR. Experiments were carried out 3 times in triplicate.

Figure 35A shows that 72hr post transfection *PEX11*α expression is significantly knocked down by 70% ($P<0.001$). As shown previously for 24hr and 48hr, there was no difference between the scrambled control and the shocked control. These results were encouraging and meant we were able to allow cells a 24hrs recovery period in which to proliferate following transfection before they were incubated with palmitate for 48hrs, while *PEX11*α expression was still knocked down.

To determine the effect of *PEX11*α knockdown on the insulin response following palmitate treatment, cells were either transfected with 100nM of siRNA probe s71495 to reduce *PEX11*α expression, or the scrambled siRNA control. 24hrs following transfection, cells were incubated with 250µM palmitate for 48hrs. As previously described, GSIS was carried out and insulin secretion was determined using an insulin ELISA. Protein was extracted, and protein content was used to normalise insulin secretion. Results are normalised to 3mM glucose scrambled BSA control. Experiments were carried out twice in triplicate. For each experiment separate wells were set up with each probe for RNA extraction and further analysis by real time PCR to ensure that *PEX11*α expression was knocked down.

Figure 35B shows that there is a significant increase in insulin secreted from basal (3mM) glucose concentrations to stimulating (25mM) glucose concentrations for all treatment groups ($P<0.01$). In addition, palmitate treatment led to a significant 50% decrease in insulin secretion at 25mM glucose for both *PEX11*α knockdowns, and scrambled controls ($P<0.001$), compared with their respective BSA controls. As shown for 24hr and 48hr post transfection (Figure 32), there was also no difference between *PEX11*α knockdown BSA controls compared with the scrambled BSA controls indicating that at 72hrs post transfection, a decrease in *PEX11*α alone does not affect GSIS. Unexpectedly, there was also no difference in GSIS between the *PEX11*α knockdown cells treated with palmitate compared with the scrambled control treated with palmitate. In other words, the inhibitory effect of palmitate on GSIS was not amplified by *PEX11*α knockdown.

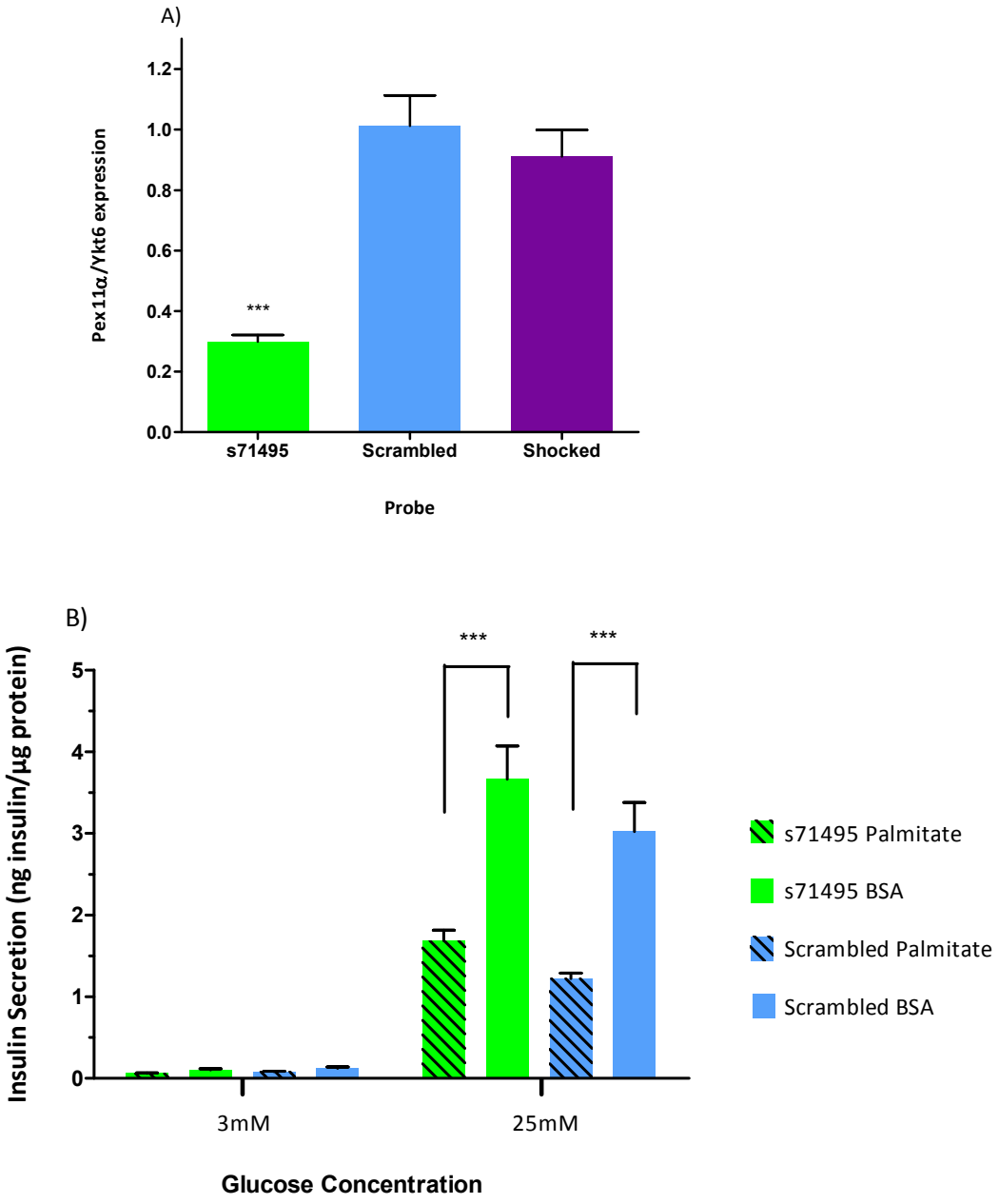

Figure 35 The effect of *PEX11α* knockdown on insulin secretion in the presence of palmitate

MIN6 cells were transfected with siRNA probe s71495, or a scrambled control were seeded at a density of $5x10^5$ cells/well in 24 well plates. Cells were incubated in antibiotic free DMEM at 37°C, 5% CO_2. A shocked control was also included. **A)** 72hrs post transfection RNA was extracted, cDNA transcribed, and *PEX11*α gene expression determined using real time PCR. Experiments were carried out 3 times in triplicate. Results are mean±SEM (n=3), from three independent experiments. **B)** 24hrs post transfection, MIN6 cells were incubated with 250µM palmitate for 48hrs before being challenged with either basal (3mM) or stimulating (25mM) glucose concentrations for 1 hour. Cell supernatants were collected and insulin secretion was determined by insulin ELISA. Protein was extracted from the cells and used to normalise the insulin secretion. Results are mean±SEM (n=3), representative of three independent experiments. ***P<0.001 compared to **A)** scrambled control, **B)** 25mM BSA control; one-way ANOVA and Bonferroni's *post hoc* test.

5.4.5 The effect of palmitate incubation on MIN6 cell cytotoxicity following PEX11α knockdown

Although incubation with palmitate alone did not lead to any changes in cell death compared with the control (Figure 34), we thought it worth investigating whether there were any changes in cell death following *PEX11*α knockdown in combination with palmitate incubation. It was decided that LDH assay would be carried out for this as it is a good marker of overall cell death, rather than the caspase 3/7 assay which just focuses on apoptosis.

Following transfection of MIN6 cells with the Neon system using 100nM of siRNA probe s71495 and the scrambled control, cells were given 24hrs to proliferate at 37°C, 5% CO_2. This was followed with 48hr incubation with 250µM palmitate before medium was collected. Samples were added to LDH reaction mix in a clear 96 well plate and incubated for 30 minutes at room temperature. Optical densities were then read on a plate reader at 450nm to determine LDH release. Results are from experiments carried out 4 times in triplicate.

Figure 36 shows there is no difference in LDH release between any of the treatment groups compared with the scrambled BSA control. This indicates that *PEX11*α knockdown in combination with palmitate incubation is no more toxic to the cells than the control conditions.

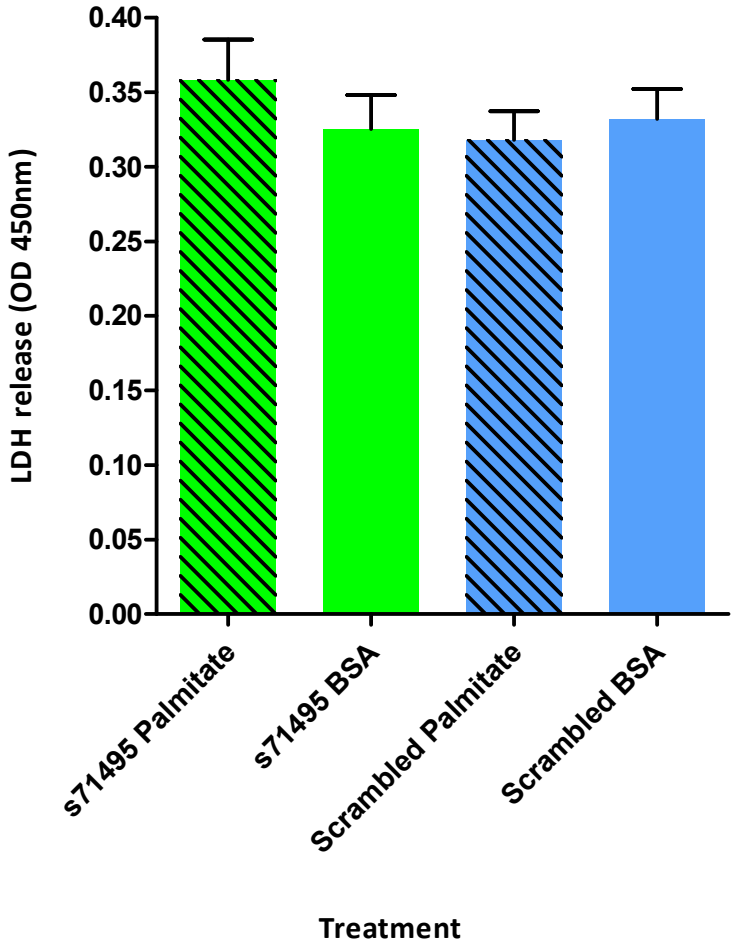

Figure 36 The effect of *PEX11α* mRNA knockdown on cell cytotoxicity in the presence of palmitate

MIN6 cells were transfected with siRNA probe s71495, or a scrambled control, were seeded at a density of $5x10^5$ cells/well in 24 well plates. Cells were incubated in antibiotic free DMEM at 37°C, 5% CO_2. 24hrs post transfection, transfected MIN6 cells were incubated with either 250µM palmitate, or a BSA control at 37°C, 5% CO_2 for 48hrs before medium was collected and analysed using LDH cytoxicity assay. Optical density was read on a plate reader at 450nm to determine LDH release. Results are mean±SEM (n=4), from four independent experiments.

5.5 Discussion

Although it is known that *PEX11*α is involved in the division of peroxisomes in response to extracellular stimuli (Schrader *et al.*, 1998), little is known of how it exerts its effects. It is thought that PEX11 proteins initiate the first steps in the pathway of growth and division of pre-existing peroxisomes before fission which is carried out by dynamin-like proteins (Schrader *et al.*, 2012). Despite this lack of knowledge of how *PEX11*α works, it has recently come to light that *PEX11*α might have a role in type 2 diabetes. A SNP found through candidate gene studies, shown to be associated with a decrease in the insulin response following an oral glucose tolerance test, was located within the *PEX11*α gene region (Pascoe, 2009). Following this work, a model for the knockdown of *PEX11*α gene expression was developed (chapter 3), and it was decided that the direct influence of *PEX11*α knockdown on GSIS was to be investigated.

MIN6 cells were used for this work as they are known to respond to changes in glucose concentration through the secretion of insulin (Miyazaki *et al.*, 1990a; Ishihara *et al.*, 1993). We were encouraged to find that the MIN6 cells we were using responded to an increase in glucose by increasing the amount of insulin they secreted (Figure 32). However, the transfected cells in which *PEX11*α gene expression was knocked down showed no differences in the insulin secreted compared with the control cells. Although this indicated that *PEX11*α gene knockdown alone had no effect on GSIS it was not entirely surprising. As previously mentioned *PEX11*α is involved in peroxisome division in response to an extracellular stimulus (Schrader *et al.*, 1998), so we thought it was therefore more likely that changes might be seen in GSIS following the addition of a stimulus.

As we were interested in the role of *PEX11*α in lipotoxicity of pancreatic β-cells, we next moved onto looking at the effect of palmitate incubation on MIN6 cells. Palmitate, a long-chain saturated fatty acid, has previously been shown to diminish the insulin response in a variety of primary pancreatic β-cells, and pancreatic β-cell lines. Human islet cells exposed to 125μM palmitate for 48hrs were shown to decrease their insulin response by 40% (Zhou and Grill, 1995), with 72hr exposure to 500μM resulting in 60% decrease in GSIS (Hoppa *et al.*, 2009), and further, exposure to 500μM for 7 days caused a 70% decrease in GSIS (Kristinsson *et al.*, 2013). In line with this, primary rat islets exposed to 125μM palmitate for 48hrs resulted in about a 50% decrease in

insulin secreted at stimulating glucose levels (Zhou and Grill, 1995). In addition, palmitate incubation in the insulin producing cell lines INS-1 and MIN6 have been shown to result in a decrease in GSIS. Incubation for 48hr with 200μM palmitate in INS-1 cells led to a 40% reduction in insulin secreted under stimulating glucose conditions (Sun *et al.*, 2008), and in MIN6 cells it has been shown that a 48hr incubation with 400μM palmitate resulted in about a 75% decrease in GSIS (Watson *et al.*, 2011). Contributing to this evidence of palmitate leading to a diminished response in stimulated insulin secretion, we were able to show that incubation with 250μM palmitate resulted in a 50% decrease in GSIS in the MIN6 cells. It was important that incubation with palmitate alone did not result in a complete inhibition of the insulin response as we wanted to assess the effect of *PEX11*α knockdown on GSIS in the presence of palmitate. Had insulin secretion been almost completely inhibited, we would have limited availability to assess whether *PEX11*α knockdown was having an additional inhibitory effect on GSIS.

In addition to reducing the insulin response from pancreatic β-cells, palmitate incubation has also been shown to lead to an increase in apoptosis. Incubation with 500μM palmitate has been shown to significantly increase apoptosis in human islet cells, primary rat β-cells and the cell line INS-1E after 72hrs (Cunha *et al.*, 2008). In addition, another study found that toxic effects were found after 2 days, leading to a 38% increase in cell death following an 8 day incubation with 250μM palmitate in primary rat β-cells (Hellemans *et al.*, 2007). Although we showed that palmitate incubation resulted in a decrease in GSIS in the MIN6 cells, we found this not to be through cell death. While this was slightly unexpected, it has previously been shown that MIN6 cells and human islets are more resistant to palmitate induced cell death than INS-1 cells. Although palmitate did induce apoptosis in both the MIN6 cells and the human islets, it was found to be remarkably less than the apoptosis seen in the INS-1 cells (Lai *et al.*, 2008). It would appear that the concentrations of palmitate we used for this work were enough to impair GSIS, but insufficient to cause significant apoptosis. It is possible that a longer time period with the lower concentration or a higher concentration for the same time period may have led to apoptosis in the MIN6 cells. This is perhaps an enquiry worth investigating in the use of mammalian β-cell lines as a model for human islets. As we were interested in the role of *PEX11*α and

whether knockdown of the gene was associated with a change in insulin secretion we moved on.

We found that a decrease in *PEX11*α expression was not associated with any changes in insulin secreted with and without the presence of palmitate. This was unexpected, but there are likely a few reasons for this. Firstly, we chose to carry out GSIS following 72hrs transfection. Although we were able to show a 70% decrease in *PEX11*α expression following this (Figure 35), as mentioned in previous chapters, we were unable to find an antibody for *PEX11*α, so we can't be certain that the protein in addition to the gene was knocked down. It is therefore not possible to know whether our time point was long enough to lead to any functional effects.

In addition, upon starting the project we were aware that a SNP associated with a decreased insulin response was found in the *PEX11*α gene region (Pascoe, 2009). However, we were unclear as to whether this SNP caused a change in *PEX11*α expression or whether indeed the SNP was in linkage disequilibrium (LD) with a functional variant in another nearby gene. *PEX11*α knockout (*PEX11*$\alpha^{-/-}$) mice have been shown to have a normal peroxisome abundance (Li *et al.*, 2002a), so it is unlikely that through the knockdown of *PEX11*α in the MIN6 cells we were able to change background peroxisome abundance. As peroxisomes are partially responsible for the metabolism of fatty acids (Wanders and Waterham, 2006), we thought that a reduction in *PEX11*α expression may lead to a reduction in fatty acid oxidation. However, it is possible we were unable to see any changes in GSIS following *PEX11*α knockdown as the peroxisome abundance was responding appropriately, with fat metabolism being normal.

Although *PEX11*α knockdown did not affect the inhibitory effect of palmitate incubation on GSIS we did not test other fatty acids. While it is unlikely that other LCFA would have had any additional effects, it is possible that VLCFA or branched chain FA such as pristanic acid may have done, as these FA are exclusively metabolised by the peroxisomes (Wanders and Waterham, 2006; Van Veldhoven, 2010). In addition, as palmitate is a LCFA, it is metabolised by both the mitochondria and the peroxisomes (Wanders and Waterham, 2006). It is possible that during situations which lead to a reduced mitochondrial function, there may be a greater reliance of peroxisomal

oxidation of fatty acids which may reveal an effect on GSIS when *PEX11*α expression is reduced.

Over-expression of *PEX11*α is sufficient to induce peroxisome proliferation (Schrader *et al.*, 1998). We have not explored the effect of increasing *PEX11*α expression in the MIN6 cells. It is possible that the SNP associated with a decrease in the insulin response (Pascoe, 2009) is actually due to an increase in *PEX11*α expression rather than a decrease. Recent evidence suggests that H_2O_2 produced during peroxisomal fatty acid oxidation is one of the causes of lipotoxicity in pancreatic β-cells (Elsner *et al.*, 2011). This is probably due to the low expression levels of oxidoreductase catalase, which inactivates the H_2O_2, found in pancreatic islets (Lenzen *et al.*, 1996). It is therefore possible that an increase in *PEX11*α expression may lead to an increase in peroxisome abundance in MIN6 cells. Once incubated with fats, it is possible that peroxisomal fatty acid metabolism would be increased, and therefore a larger amount of H_2O_2 could be produced. This excess of H_2O_2 could cause an even greater diminished insulin response from the β-cells, and could possibly explain why a SNP found in the *PEX11*α gene region is associated with a reduced β-cell function. It seems that the production of a system for the over-expression of *PEX11*α in β-cells would be a worthwhile project so that further investigation can be carried out into the role of *PEX11*α in lipotoxicity, β-cell dysfunction, and type 2 diabetes.

Chapter 6

The effect of *PEX11*β knockdown on peroxisome abundance and insulin secretion

6 The effect of *PEX11*β knockdown on peroxisome abundance and insulin secretion

6.1 Introduction

So far, *PEX11*α has been the focus of this work, as this was the gene in which a SNP was identified in candidate gene studies as being associated with a reduced insulin response in an oral glucose tolerance test (Pascoe, 2009). The data so far have led to the conclusion that a reduction in *PEX11*α expression does not have any influence over insulin secretion in response to glucose in the presence or absence of palmitate. Recent evidence, however, has come to light that peroxisomes may play a role in the path to lipotoxicity in pancreatic β-cells (Elsner *et al.*, 2011).

During the metabolism of fatty acids through peroxisomal β-oxidation, hydrogen peroxide (H_2O_2) is produced. In the majority of cells, this by-product is catabolised by an enzyme, oxidoreductase catalase, which is expressed in the peroxisomes (Gehrmann *et al.*, 2010). Pancreatic β-cells are essentially deficient in this enzyme (Lenzen *et al.*, 1996; Tiedge *et al.*, 1997) leaving the β-cells at potential risk to lipotoxicity from ROS. The group who investigated the role of peroxisomes in lipotoxicity found a 40% increase in ROS production in insulin producing cells following palmitate treatment, which was significantly reduced when peroxisomal catalase, but not mitochondrial catalase, was over-expressed. The study also found peroxisomes to be a major site of H_2O_2 production compared with the mitochondria, further strengthening the evidence that peroxisomal β-oxidation, and not mitochondrial β-oxidation of fats, may contribute to the lipotoxicity (Elsner *et al.*, 2011).

As previous studies have reported that over-expression of *PEX11*α can lead to an increase in peroxisomal abundance (Schrader *et al.*, 1998) it would have been interesting to see what effect *PEX11*α over-expression had on insulin secretion from pancreatic β-cells. However, due to time constraints it was not possible to optimise an over-expression system. We therefore decided to use a slightly different approach to look at the effect of peroxisome abundance on insulin secretion. It has previously been shown that reductions in *PEX11*β can lead to decreases in steady state peroxisomal abundance (Li *et al.*, 2002b; Li and Gould, 2002). We wondered if we could replicate this decrease in peroxisome abundance in MIN6 cells through the reduction in *PEX11*β

expression. Further, we hoped to assess the effect of a decrease in peroxisome abundance on insulin secretion.

6.2 Methods

MIN6 cells were transfected with siRNA against *PEX11*β using the Neon System, as previously described. MIN6 cells were seeded at a density of $2.5x10^5$ cells/well. Following various time periods after transfection, either: RNA was extracted, cDNA synthesised, and both *PEX11*β and *PEX11*α mRNA expression quantified using real time PCR; or, protein was extracted and western blotting was carried out to determine PMP-70 protein expression.

Immunofluorescence was also used to investigate peroxisome abundance within the MIN6 cells following transfection. MIN6 cells were transfected with siRNA against *PEX11*β and seeded onto glass cover slips at a density of $2.5x10^5$ cells/well. 96hrs after transfection cells were fixed and stained using an antibody against PMP-70. Following staining, cells were visualised using a confocal microscope. The images were then analysed by Michael-Van Ginkel from Unilever R&D to perform quantification.

At 2 time points following transfection, MIN6 cells were also incubated with 250μM palmitate for 48hrs. Insulin secretion was then quantified using the GSIS assay with an insulin ELISA as previously described.

6.3 Aims

The main aim of this chapter was to explore the effect of *PEX11*β knockdown on peroxisome abundance and lipotoxicity of pancreatic β-cells. We did this by:

- Using the already optimised Neon transfection system to reduce *PEX11*β expression in MIN6 cells.
- Carrying out immunofluorescence and western blotting to look at the effect of *PEX11*β knockdown on peroxisome abundance.
- Investigating the effects of this knockdown on insulin secretion from MIN6 cells in the presence and absence of palmitate.

6.4 Results

6.4.1 Knockdown of PEX11β expression in MIN6 cells using the Neon Transfection System

As the Neon transfection system had proved a reliable method for the knock-down of *PEX11*α expression in MIN6 cells (Chapter 3), it was employed once again for the transfection of MIN6 cells in an attempt to knockdown *PEX11*β expression.

3 Ambion siRNA's (s71497, s71498 and s71499) against *PEX11*β were used at a concentration of 100nM to transfect MIN6 cells. Following the first transfection however, it became clear that only 2 of the siRNA's would reduce *PEX11*β expression (results not shown for siRNA probe s71498). For all future experiments the probes s71497 and s71499 were used for the knockdown of *PEX11*β.

Following transfection, MIN6 cells were incubated for 48hrs, 72hrs or 96hrs at 37°C at 5% CO_2. RNA was then extracted and cDNA synthesised. Gene expression was quantified using real time PCR as previously described. Quantitect primer assays (Chapter 3) were used to target *PEX11*β, and Ykt6 was again used as the reference gene.

The results show a more than an 80% decrease in *PEX11*β expression for 48hrs ($P<0.001$), 72hrs ($P<0.001$) and 96hrs ($P<0.001$) post transfection (Figure 37). For 48hrs and 72hrs a shocked control was carried out to compare against the scrambled. This showed that the scrambled siRNA was not having any effect on *PEX11*β expression. For this reason, a shocked control was not carried out for the 96hr transfection. All transfection results were normalised to the scrambled control. The 96hr time point for gene expression was added following western blotting results for PMP-70 protein levels for cells 72hrs post transfection (Figure 38).

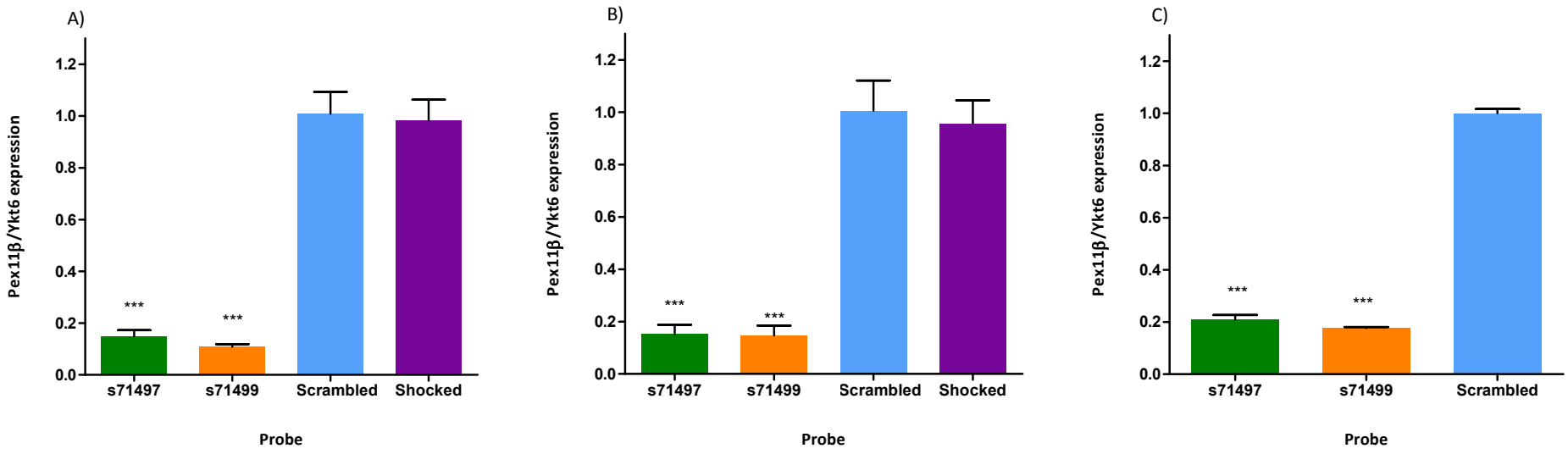

Figure 37 Transfection of MIN6 cells using the Neon System for the knockdown of *PEX11*β

MIN6 cells were transfected in suspension using 100nM of *PEX11*β siRNA probes s71497 or s71499, scrambled siRNA or no siRNA (shocked (for 48hr and 72hr only)). Cells were incubated in a 24 well plate, at a density of $5x10^5$ cells/well, for either A) 48hrs, B) 72hrs or C) 96hrs in antibiotic free DMEM at 37°C, 5% CO_2 before RNA was extracted, and cDNA synthesised. *PEX11*β gene expression was quantified using real-time PCR. Results are normalised to scrambled control and show mean±SEM (n=3), from three independent experiments. ***p<0.001 compared to scrambled control; one-way ANOVA and Bonferroni's *post hoc* test.

6.4.2 PEX11β knockdown reduces peroxisome abundance in MIN6 cells

It has been shown that the embryonic fibroblasts from *PEX11*β knockout mice have a 50% decrease in peroxisomes compared with the cells from wild type mice (Li and Gould, 2002). We anticipated that knocking down *PEX11*β gene expression would also lead to a reduction in peroxisome abundance in MIN6 cells.

6.4.2.1 Analysis by western blot

Firstly, we wanted to quantify PMP-70 protein expression, a marker of peroxisomes, in MIN6 cells by western blotting following the knockdown of *PEX11*β expression. MIN6 cells were transfected with siRNA for *PEX11*β as was described in section 6.4.1. Several time periods were used as we were unsure how long it would take for a reduction in *PEX11*β to result in a decrease in peroxisome number. Following incubation periods of 48hr, 72hr and 96hr, protein was extracted, and western blotting was carried out to determine PMP-70 protein expression. β-actin was used as a reference loading control.

The results (Figure 38) show that 48hr post transfection, PMP-70 protein expression was no different to the scrambled control indicating that although *PEX11*β mRNA expression is reduced after 48hrs (Figure 37), this does not result in a decrease in PMP-70 protein expression. The results for 72hr post transfection seemed to suggest some slight reductions in PMP-70 protein levels, however, these results were not significant. 96hr post transfection, a 35% reduction in PMP-70 protein levels with the s71497 probe ($P<0.01$) was achieved. Although the s71499 probe resulted in a similar knockdown in *PEX11*β gene expression compared with the s71497 probe (Figure 37), it appears that it does not lead to a clear decrease in PMP-70 protein levels.

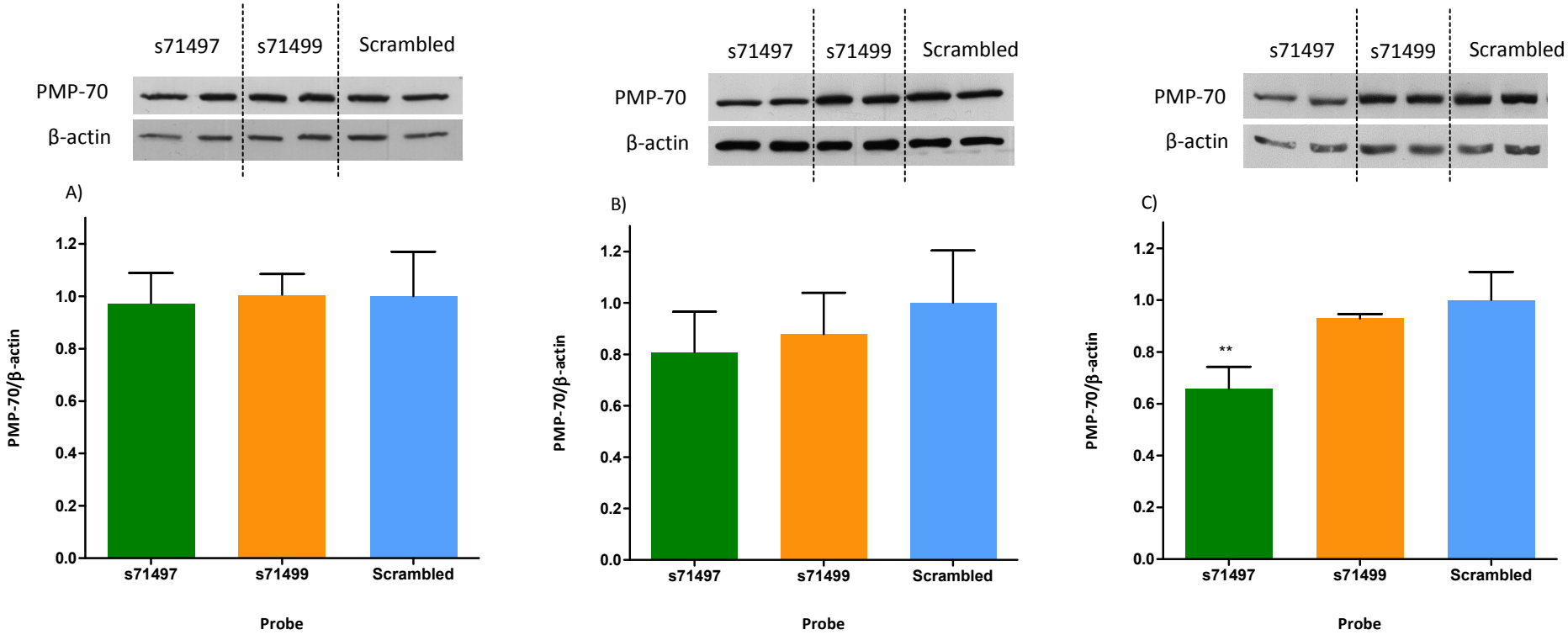

Figure 38 Analysis of PMP-70 protein expression by western blot following *PEX11*β knockdown

MIN6 cells were transfected in suspension using 100nM of *PEX11*β siRNA probes s71497 or s71499 or scrambled siRNA. Cells were incubated in a 24 well plate, at a density of $5x10^5$ cells/well, for **A)** 48hrs, **B)** 72hrs and **C)** 96hrs in antibiotic free DMEM at 37°C, 5% CO_2 before protein was extracted and quantified. PMP-70 protein expression is given as a ratio of PMP-70 to β-actin, and was quantified using western blotting. Above each graph is one of the blots used for quantification shown as an example. Experiments were carried out twice in duplicate for **A)** 48hr and **C)** 96hr, and three times in duplicate for **B)** 72hr. Results are normalised to scrambled control. Error bars are representative of SEM. **p<0.01

6.4.2.2 Analysis by immunofluorescence

Although western blotting data showed a significant decrease in PMP-70 protein levels 96hr hours post transfection, we thought it useful to visualise these decreases in peroxisomes within the cells. Immunofluorescence was carried out in cells 96hr post transfection only.

MIN6 cells were transfected with either s71497 and s71499 siRNA probes against *PEX11*β, or a scrambled control at a concentration of 100nM. Cells were seeded onto coverslips within 6 well plates and were incubated for 96hrs at 37°C at 5% CO_2 before being fixed using 4% paraformaldehyde. Following staining using the antibody against PMP-70, cells were visualised using a confocal microscope.

The images (Figure 39) show that the cells transfected for 96hrs with the s71497 probe have less PMP-70 staining compared with the scrambled control corroborating the western blotting results. In addition, we were fortunate enough to have Michael-Van Ginkel from Unilever R&D to analyse the images and perform quantification. The results were given as a count of peroxisomes per area of the image that was covered by the cells, and results were normalised to the scrambled control. 18 images for each probe were used for the quantification. These results (Figure 40) show a significant decrease in PMP-70 expression with both siRNA probes. Like the western blotting data, it was the s71497 probe which yielded the greatest decrease, of 23%, in PMP-70 expression ($P<0.001$) compared with the scrambled control. Although significant, knockdown with the s71499 probe only resulted in a 13% reduction ($P<0.05$) in PMP-70 expression.

Using the two techniques to quantify peroxisome abundance we can confirm that an 80% decrease in *PEX11*β gene expression at 96hr post transfection (Figure 37) results in a significant decrease in PMP-70 expression as a marker of peroxisome abundance.

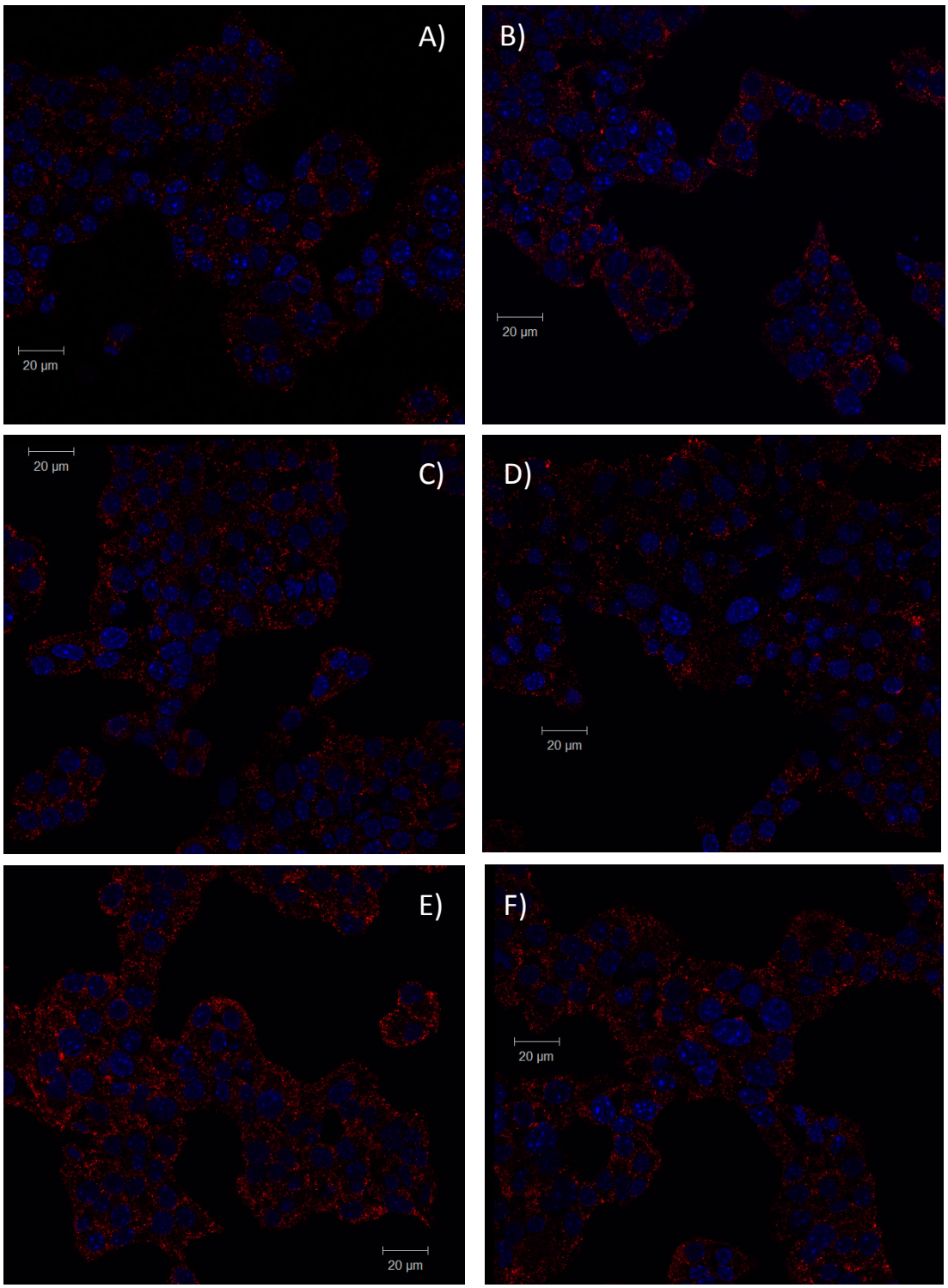

Figure 39 Peroxisome abundance in MIN6 cells following *PEX11*β knockdown

Following transfection with siRNA probes against *PEX11*β, or a scrambled control, MIN6 cells were seeded onto cover slips in 6 well plates at a density of $2x10^5$ cells/well and incubated for 96hrs. Cells were fixed, permeabilised and blocked before they were stained using a primary antibody against PMP-70 (Abcam), and secondary antibody Alexa Fluor® 546 Goat Anti-Rabbit IgG (Life Technologies). Nuclear counterstaining was carried out with DAPI. Cells were visualised at magnification x63 on a fluorescent confocal microscope. **A)** and **B)** s71497 probe, **C)** and **D)** s71499 probe, and **E)** and **F)** scrambled control.

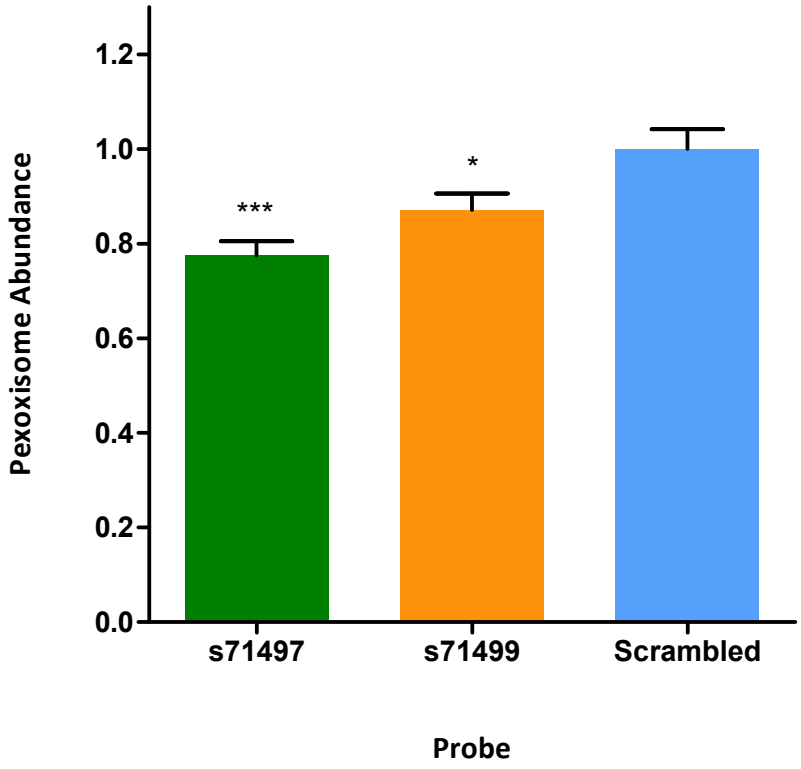

Figure 40 Analysis of PMP-70 protein expression by immunofluorescence following *PEX11*β knockdown

Following transfection with siRNA probes against *PEX11*β, or a scrambled control, MIN6 cells were seeded onto cover slips in 6 well plates and incubated for 96hrs. Cells were fixed, permeabilised and blocked before they were stained using a primary antibody against PMP-70 (Abcam), and secondary antibody Alexa Fluor® 546 Goat Anti-Rabbit IgG (Life Technologies). Nuclear counterstaining was carried out with DAPI. Cells were visualised at magnification x63 on a fluorescent confocal microscope. Michael-Van Ginkel from Unilever R&D carried out some analysis on the images taken and the peroxisome abundance was quantified. The results were given as a count of peroxisomes per area of the image that was covered by the cells. Results were normalised to the scrambled control. 18 images for each probe were used for the quantification. Error bars are representative of SEM. *p<0.05, ***p<0.001

6.4.3 The effect of PEX11β knockdown on PEX11α expression

As a previous study has reported a 1.5 fold increase in hepatic *PEX11*α expression in *PEX11*β knockout mice (Li *et al.*, 2002b) we decided to investigate the effects of reducing *PEX11*β expression in MIN6 cells on the expression of *PEX11*α. We thought it possible that reducing *PEX11*β expression in MIN6 cells may have a similar effect on *PEX11*α expression as was shown for the *PEX11*β knockout mice.

Real time PCR was carried out using samples collected following transfection of MIN6 cells in section 6.4.1. Primers for the target gene, *PEX11*α, and reference gene, Ykt6, were used for the quantification.

The results (Figure 41) show that *PEX11*α expression was not altered at any time point tested (48hrs, 72hrs and 96hrs post transfection). The levels of *PEX11*α are comparable for both siRNA probes which knocked down *PEX11*β, as well as the scrambled and shocked controls. This indicates that knockdown of *PEX11*β expression does not result in a compensatory change in *PEX11*α expression.

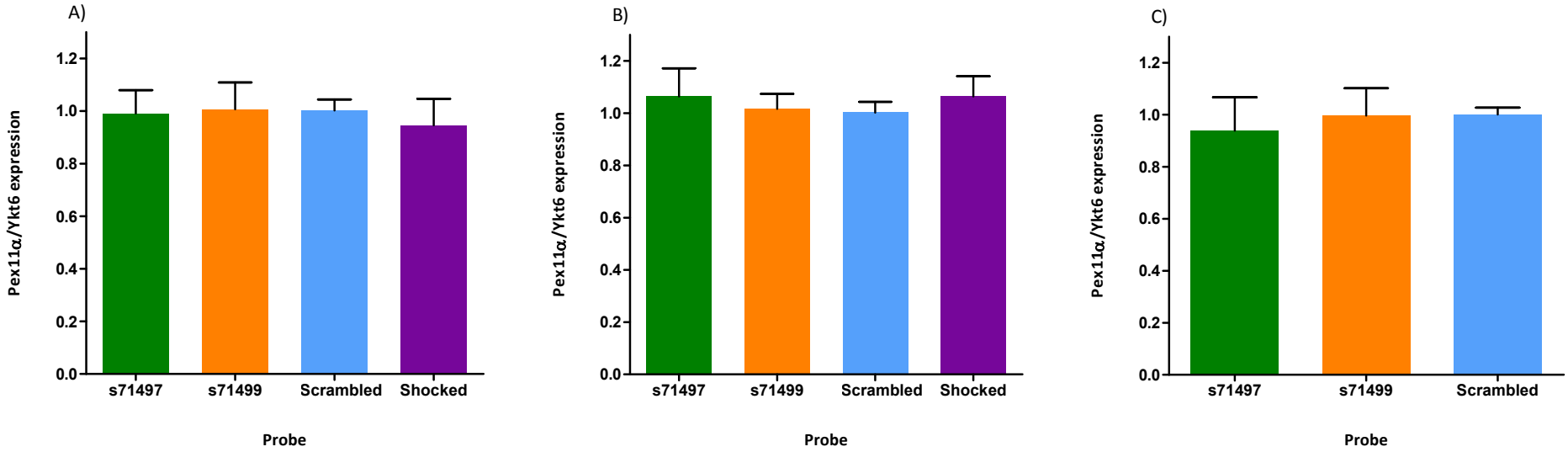

Figure 41 The effect of *PEX11*β knockdown on *PEX11*α expression

*PEX11*α gene expression was quantified using real-time PCR and the cDNA samples originally used to quantify *PEX11*β expression in the transfected cells. Samples were looked at for **A)** 48hrs, **B)** 72hrs, **C)** 96hrs post transfection. Experiments were carried out three times in triplicate. Results are normalised to scrambled control and show mean±SEM (n=3), from three independent experiments.

6.4.4 PEX11β knockdown in MIN6 cells partially recovers the diminished insulin response caused by the saturated fatty acid palmitate

Having established *PEX11*β knockdown and peroxisome depletion based on diminished PMP-70 expression, we wanted to explore whether this altered the detrimental effect of palmitate on glucose stimulated insulin secretion. It has been suggested that peroxisomes are a cause of lipotoxicity in pancreatic β-cells (Elsner *et al.*, 2011), so we were interested in what sort of effect reducing peroxisome number might have on this lipotoxicity.

MIN6 cells were transfected with the siRNA probe s71497, which gave the best reduction in peroxisome abundance. Although a significant reduction in peroxisomes was achieved 96hrs post transfection, there seemed to be a slight difference at 72hrs, so both time points were investigated. Following transfection MIN6 cells were incubated for either 24hrs (72hr transfections) or 48hrs (96hr transfections) before being treated with 250µM palmitate or a BSA control for a further 48hrs. Subsequently, GSIS was measured as previously described. GSIS results were normalised to protein content, and then to the 3mM scrambled BSA control. For each experiment, additional wells were set up for RNA extraction, and analysis by real-time PCR to ensure *PEX11*β gene expression was knocked down to the same degree as previously shown.

The results (Figure 42) show the effect of palmitate treatment compared with cells treated with a BSA control. These treatments were carried out for both cells transfected with the s71497 siRNA probe to knock-down *PEX11*β expression, and cells transfected with the scrambled control siRNA.

For both 72hrs and 96hrs post transfection, the *PEX11*β knockdowns treated with the BSA control show no difference compared with the scrambled control treated with BSA control indicating that *PEX11*β knockdown alone, and therefore a reduction in peroxisome abundance, does not have any effect on GSIS.

At 72hrs post transfection, both *PEX11*β knockdown cells and scrambled control cells treated with palmitate resulted in a comparable significant decrease in insulin

secretion (P<0.001). This suggests that 72hrs after transfection, *PEX11*β knockdown does not have any effect on GSIS in the presence or absence of palmitate.

At 96hrs post transfection, although palmitate treatment significantly decreased the GSIS at 25mM glucose stimulation for both the cells transfected with the siRNA probe s71497 (P<0.001) and the scrambled controls (P<0.001) compared with their respective BSA controls, the decreases were no longer comparable. There was a significant difference in insulin secretion in the *PEX11*β knockdown treated with palmitate compared with the scrambled control treated with palmitate (P<0.01). This evidence suggests that a reduction in peroxisome number leads to a partial recovery of the diminished insulin response seen with fatty acid incubation.

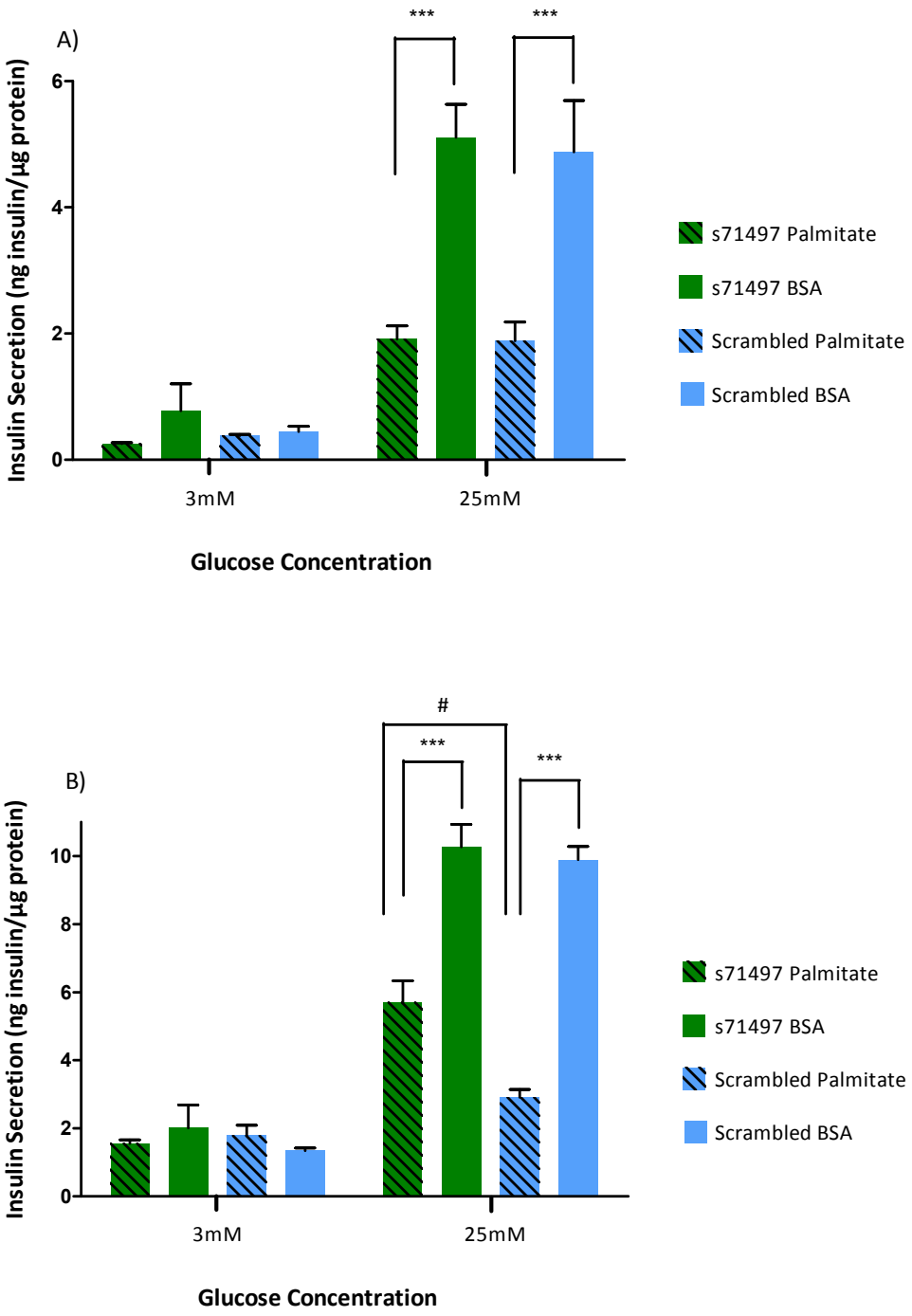

Figure 42 The effect of palmitate treatment on GSIS following *PEX11*β knockdown

MIN6 cells were transfected with siRNA probe s71497 against *PEX11*β, or with a scrambled control siRNA and seeded into 24 well plates at a density of $5x10^5$ cells/well. **A)** 72hrs transfection, or **B)** 96 hrs transfection, cells were incubated either with 250µM palmitate or BSA control for the final 48hrs. Following 48hr palmitate incubation, samples were stimulated with 3mM (basal) or 25mM (high) glucose for 1hr. Samples were analysed by ELISA and normalised to protein content. Results are mean±SEM (n=3), representative of three independent experiments. ***P<0.001 compared to 25mM glucose BSA control, #P<0.01 comparing palmitate treatments; one-way ANOVA and Bonferroni's *post hoc* test.

6.5 Discussion

Peroxisomes are important organelles which play a role in the metabolism of long chain, very long chain, and branched-chain fatty acids. Fatty acids imported into the peroxisome for metabolism, including 3-methyl branched chain fatty acids which have to undergo α-oxidation first, are metabolised by β-oxidation (Jansen and Wanders, 2006; Wanders *et al.*, 2010). One of the by-products of peroxisomal β-oxidation is H_2O_2 which can be toxic, but in most cells throughout the body it is broken down by catalase into H_2O and O_2. Pancreatic cells have very low expression levels of this enzyme making them susceptible to damage through lipotoxicity (Lenzen *et al.*, 1996; Wanders and Waterham, 2006; Gehrmann *et al.*, 2010; Elsner *et al.*, 2011).

PEX11 proteins are involved in the division of peroxisomes (Li and Gould, 2002; Koch *et al.*, 2010; Koch and Brocard, 2012). Although little is understood about how the PEX11 proteins exert their effects it is apparent that the over-expression and knockout of *PEX11*β can result in changes in peroxisome abundance. Over-expression of *PEX11*β in human cells through transfection with plasmids has been shown to increase peroxisome proliferation in the absence of extracellular stimuli, while *PEX11*β deficiency has been shown to result in reduced peroxisome abundance (Schrader *et al.*, 1998; Li *et al.*, 2002b; Li and Gould, 2002).

Peroxisomes are synthesised not only through the division of pre-existing peroxisomes where *PEX11*β is involved, but also by de novo synthesis from the endoplasmic reticulum in mammalian cells (Hoepfner *et al.*, 2005; Kim *et al.*, 2006; Hettema and Motley, 2009). Embryonic fibroblasts from *PEX11*β knockout mice were shown to have decreases in peroxisome abundance of about 50% (Li and Gould, 2002), which implies that the pathway for peroxisomal proliferation through the division of pre-existing peroxisomes contributes to 50% of total peroxisome abundance in mice. We were encouraged to find that our model of *PEX11*β gene expression knockdown resulted in a 35% decrease in PMP-70 protein levels (Figure 38), a peroxisomal membrane protein commonly used as a peroxisome marker. There has been some debate over the relative contribution of the different mechanisms of peroxisome proliferation (Li and Gould, 2002; Huybrechts *et al.*, 2009; Schrader *et al.*, 2012), however, the reduction in peroxisome abundance following *PEX11*β knockdown certainly suggests that the

pathway for peroxisome proliferation through the division of pre-existing peroxisomes is involved at maintaining peroxisome numbers in MIN6 cells.

*PEX11*β gene knockdown did not result in any changes in *PEX11*α gene expression. Although previously it has been reported that the loss of *PEX11*β led to about a 1.5 fold increase in hepatic *PEX11*α expression in *PEX11*β knockout mice (Li *et al.*, 2002b) we were unable to replicate this in our model of *PEX11*β knockdown. This could be due to the differences in the models. The livers from newborn *PEX11*β knockout mice were examined which means the *PEX11*β knockout had the whole gestation period in which to cause any effects (Li *et al.*, 2002b), compared with our model which looked at *PEX11*α expression 96hrs following *PEX11*β knockdown. In addition, peroxisomes are very highly expressed in the liver. The 1.5 fold increase in hepatic *PEX11*α expression reported in the *PEX11*β knockout mice may be a tissue selective response specific to the liver due to its need for high peroxisome abundance as it is a major organ for fatty acid metabolism (Li *et al.*, 2002b; Reddy and Sambasiva Rao, 2006; van Herpen and Schrauwen-Hinderling, 2008). Alternatively, our model was for the knock down of *PEX11*β, and did not completely eradicate expression of the gene. It is possible that any increases in *PEX11*α may only be seen when there is no expression of *PEX11*β.

Lipotoxicity is thought to be a major contributor to pancreatic β-cell dysfunction and death. The breakdown of fatty acids by both mitochondria and peroxisomes produce ROS in various forms. Recent evidence has come to light that the ROS H_2O_2, produced through the oxidation of fatty acids in the peroxisomes, may be a mediator of lipotoxicity in pancreatic β-cells (Unger and Zhou, 2001; Gehrmann *et al.*, 2010; Elsner *et al.*, 2011; Ivashchenko *et al.*, 2011). H_2O_2 production by the peroxisomes has been reported to account for as much as 35% of total cellular H_2O_2 in the rat liver indicating that peroxisomes are a major site for ROS production (Boveris *et al.*, 1972; Gehrmann *et al.*, 2010).

In the majority of cell types the H_2O_2 produced is catabolised by oxidoreductase catalase. Pancreatic β-cells have, however, been shown to be lacking in a variety of antioxidant enzymes including catalase (Lenzen *et al.*, 1996; Tiedge *et al.*, 1997). Rat pancreatic islets and the rat insulin producing cell line RINm5F have been shown to be unable to adapt to cellular stress by adjusting their levels of anti-oxidant enzymes. In

addition, over-expression of catalase in the RINm5f cells was shown to dramatically increase the resistance of the cells to H_2O_2 toxicity when the cells were exposed to increasing levels of H_2O_2 (Tiedge *et al.*, 1997). Studies into the presence of catalase in human islets showed that catalase activity in human islets was increased compared with rat islets, along with an increased resistance to oxidative stress (Welsh *et al.*, 1995). However, it has also been shown that catalase activity in the mouse liver is 50 times higher compared to mouse pancreatic islets (Johansson and Håkan Borg, 1988). Although human islets appear to have an increased catalase activity, it is unlikely to be at similar levels to that of the human liver. Further investigation is needed into this increased resistance of human islets compared with rat islets, however, as it has been shown that palmitate incubation decreases GSIS in human islet cells (Hoppa *et al.*, 2009), it is possible that this is also though an increase in H_2O_2 production.

Following the evidence that it may be peroxisomes contributing to lipotoxicity in pancreatic β-cells, we decided to look at the effect of *PEX11*β knockdown, and therefore a reduction in peroxisomes, on insulin secretion from the MIN6 cells following palmitate incubation. Pancreatic β-cell dysfunction can be shown through a loss in insulin secretion in response to glucose (GSIS). It has been reported that palmitate incubation decreases GSIS from pancreatic β-cells and β-cell lines including MIN6 cells (Biden *et al.*, 2004; Watson *et al.*, 2011). We were able to confirm this for MIN6 cells (Figure 33), and further, show that the inhibited response seen with the palmitate incubation can be partially recovered in the presence of *PEX11*β knockdown and reduced peroxisome number (Figure 42). This complements the work carried out by Elsner et al., 2011, where they were able to conclude that H_2O_2 produced through peroxisomal β-oxidation of fatty acids and not mitochondrial β-oxidation was a mediator of lipotoxicity in pancreatic β-cells. The group over-expressed catalase in either the peroxisomes or the mitochondria in RINm5f cells in the presence of palmitate. It was shown that toxicity of the palmitate, as well as H_2O_2 production was reduced in the cells over-expressing catalase in the peroxisomes and the cytosol rather than in the mitochondria. It was also noted that following palmitate incubation in cells expressing a H_2O_2 sensor in either the peroxisomes, or the mitochondria, there was a significant increase in H_2O_2 production in the peroxisomes but not in the mitochondria. This pointed to the peroxisomes being the major site of H_2O_2 production (Elsner *et al.*,

2011). It appears therefore that a reduction in peroxisome abundance is beneficial to pancreatic β-cells. It is likely that this is through a reduction in the amount of H_2O_2 produced when there are fewer peroxisomes.

There are several suggested mechanisms as to how long chain fatty acids such as palmitate contribute to lipotoxicity in β-cells (Cnop *et al.*, 2005), see introduction section 1.4.4. It certainly appears that one such explanation could be through this peroxisomal route suggested. The first step of β-oxidation within the peroxisome leads to the production of H_2O_2, which is usually broken down by catalase into O_2 and H_2O (Wanders and Waterham, 2006). Due to the low levels of catalase within pancreatic β-cells (Lenzen *et al.*, 1996), it is possible that oxidation of palmitate leads to a toxic build-up of H_2O_2. It has been reported that in rat pancreatic islets low levels of H_2O_2 can impair GSIS through the inhibition of glucose oxidation, in addition to a reduction in amplitude of intracellular calcium oscillations which may in turn trigger the ER stress response (Rebelato *et al.*, 2010; Karunakaran *et al.*, 2012). It would be worthy to pursue investigation into whether a reduction in *PEX11*β expression leads to a decrease in H_2O_2 production, and further to explore whether glucose oxidation and the amplitude of calcium oscillations are increased following this knockdown.

Chapter 7

General Discussion

7 General Discussion

7.1 General Discussion

Obesity is a major risk factor for type 2 diabetes mellitus (Hussain *et al.*, 2007; van Herpen and Schrauwen-Hinderling, 2008), with lipotoxicity being a major contributor to the β-cell dysfunction seen in the disease (Cnop *et al.*, 2005; van Herpen and Schrauwen-Hinderling, 2008). High levels of fat within the pancreas can lead to an increase in fatty acid metabolism, which can result in high levels of ROS production (Gehrmann *et al.*, 2010; Ma *et al.*, 2012). In addition, the incomplete oxidation of fats can lead to the formation of ceramide (Kusminski *et al.*, 2009). These toxic metabolites inhibit insulin secretion through a variety of mechanisms and can eventually result in pancreatic β-cell death (Kusminski *et al.*, 2009; Ma *et al.*, 2012).

Peroxisomes are responsible for the partial metabolism of some LCFA, including palmitate, as well as all VLCFA and branched-chain FA prior to completion within the mitochondria (Wanders and Waterham, 2006; Gehrmann *et al.*, 2010). Recently, through candidate gene studies, a SNP was found within the *PEX11*α gene region that was associated with reduced insulin response to an oral glucose tolerance test (Pascoe, 2009). *PEX11*α encodes a protein responsible for the division of peroxisomes in response to an extracellular stimulus (Schrader *et al.*, 1998). We therefore decided to explore the role of altered *PEX11*α expression in the lipotoxicity of pancreatic β-cells. In addition, as decreased expression of another *PEX11* gene, *PEX11*β, has been shown to result in a decrease in peroxisome abundance (Li *et al.*, 2002b; Li and Gould, 2002), we also explored the effect of decreased *PEX11*β expression in relation to the lipotoxicity of pancreatic β-cells.

We began by producing a model for the knockdown of *PEX11*α expression in MIN6 cells. Using siRNA against *PEX11*α we were able to produce a 70% knockdown in *PEX11*α expression that was sustained 24hr, 48hr and 72hr post-transfection. Unfortunately, we were unable to determine whether this knockdown resulted in a decrease in the PEX11α protein. Commercially available antibodies were for human proteins, and despite the homology shared between the species, the antibody did not bind to the mouse protein. This made it difficult to determine how long it took for a decrease in *PEX11*α gene expression to result in a decrease in the protein. We moved

on to assess PMP-70 protein expression as a marker of peroxisome abundance, to determine whether a decrease in *PEX11*α expression would result in a decrease in PMP-70 protein expression.

The reduction in *PEX11*α expression 24hr and 48hr post transfection did not result in a decrease in peroxisome abundance. This was not completely unexpected as, unlike *PEX11*β which is responsible for the constitutive control of peroxisome abundance, *PEX11*α responds by increasing peroxisome abundance in the presence of a stimulus (Schrader *et al.*, 1998). We therefore assumed that without the presence of a stimulus, a decrease in *PEX11*α expression would not affect background peroxisome abundance. This is in line with one study which reported that the livers and MEFs (mouse embryonic fibroblasts) from *PEX11*$\alpha^{-/-}$ mice have normal peroxisome abundance. Liver tissue for analysis was extracted from 6-8 week old mice fed a standard chow diet (Li *et al.*, 2002a). In contrast to this, another recent study which also used *PEX11*$\alpha^{-/-}$ mice found that *PEX11*α deficiency resulted in a significant decrease in peroxisome abundance in the livers of these mice which had been fed a normal chow diet. This study specified normal chow to contain 51.4% carbohydrate, 24.9% protein and 4.6% fat (Weng *et al.*, 2013). It is possible that the differences seen in these studies could have been due to the diet of the mice. Although they both suggest that standard chow was used Li et al., 2002a did not list ingredients. It is possible that 4.6% fat could have induced peroxisome proliferation through *PEX11*α resulting in a slightly higher abundance of peroxisomes in WT mice compared with the *PEX11*$\alpha^{-/-}$ mice. In addition, the two studies using the *PEX11*$\alpha^{-/-}$ mice used different methods for counting peroxisomes. Although both stained for the peroxisomal enzyme catalase, Li et al., 2002a used a light microscope to capture pictures and analysed 60 independent fields from four mice whereas Weng et al., 2013 used a confocal laser-scanning microscope and at least 20 independent fields were analysed. Also, these may have been carried out with mice of different ages. Although Li et al., 2002a states 6-8 week old mice were used, Weng at al., 2013 don't state the age at which the livers were extracted to determine peroxisome abundance (Li *et al.*, 2002a; Weng *et al.*, 2013). It is possible that the discrepancies between the two studies could have been caused by these different methods, and warrant further investigation.

It has previously been shown that *PEX11*α expression can be induced in rats and mice with the treatment of fibric acid derivatives (Abe *et al.*, 1998; Schrader *et al.*, 1998; Li *et al.*, 2002a). Fibric acid derivatives are agonists of PPARα, which are known to control the transcription of a variety of genes involved in the regulation of lipid metabolism (Katsiki *et al.*, 2013). It has also been shown that fatty acids are activators of PPARα (Dreyer *et al.*, 1993; Pawar and Jump, 2003). We therefore decided to start by incubating MIN6 cells with either a saturated fatty acid, palmitate, or an unsaturated fatty acid, oleate, to assess the effect they had on *PEX11*α expression. Although it has previously been shown that palmitate incubation resulted in an increase in *PEX11*α expression in MIN6 cells (Pascoe, 2009), we were unable to replicate these findings. We found that *PEX11*α expression did not increase with either fatty acid, however, we later found that this may have been due to the availability of endogenous RA within pancreatic β-cells (discussed below).

Incubation with the fibric acid derivative, fenofibrate, alone did not result in a significant increase in *PEX11*α expression, which was unexpected. As mentioned above, animals studies have shown that *PEX11*α is inducible in response to fibrate treatment (Schrader *et al.*, 1998; Li *et al.*, 2002a). However, it is possible that endogenous RA may have been a limiting factor. *PEX11*α expression is controlled through the binding of a PPARα/RXR heterodimer to a PPRE located downstream of *PEX11*α (Shimizu *et al.*, 2004). The incubation of MIN6 cells with a combination of fenofibrate and 9-*cis*-RA resulted in a significant increase in *PEX11*α expression. This is in line with another study which also reported a significant increase in *PEX11*α expression in primary rat β-cells with the combination of clofibrate and 9-*cis*-RA (Hellemans *et al.*, 2007). It is therefore possible that β-cells express low levels of endogenous RA, and the addition of exogenous RA is needed to accompany the PPARα agonist before the PPARα/RXR heterodimer can be activated and initiate transcription. This is also a possible reason for the lack of increased expression of *PEX11*α in response to fatty acids. As fatty acids are activators of PPARα (Pawar and Jump, 2003), it is possible that the addition of exogenous RA would have resulted in an increase in *PEX11*α expression.

Through the addition of exogenous RA in combination with fenofibrate we were able to show an increase in *PEX11*α expression in MIN6 cells. It had previously been

reported that human islet cells expressed *PEX11*α, but 20 fold lower than in the liver. Through the analysis of real time PCR fold change data using the human liver as a reference, it was revealed that the expression of *PEX11*α in MIN6 cells was found to be at similar levels to that found in human islets (Pascoe, 2009). Through the use of PPARα and RXR agonists we were able to confirm that *PEX11*α is an inducible gene in the MIN6 cell line in line with previous β-cell line studies (Schrader *et al.*, 1998). In addition, although we did not look at the expression of *PEX11*β following incubation with the agents responsible for increasing *PEX11*α expression, we were able to show that *PEX11*β was also expressed in the MIN6 cells. The inducible property of *PEX11*α in MIN6 cells along with the detection of *PEX11*β within the cells further strengthened our decision to use this cell line for the remainder of the project.

We were unable to observe an increase in peroxisome abundance in response to the peroxisome proliferators. Although this was unexpected, it is possible that the time periods investigated were not long enough for the induction of *PEX11*α expression to result in an increase in peroxisomes. We showed that it requires 96hrs in MIN6 cells following the decrease in *PEX11*β expression to result in a decrease in peroxisome number, so it is possible that a longer time period is needed for increases in peroxisome abundance to be witnessed following treatment. In addition, increases in peroxisome abundance have been reported in response to peroxisome proliferators, but have often been seen in rats and mice after exposure to fibrates for 7 – 10 days (Lazarow and De Duve, 1976; Colton *et al.*, 2004; Islinger *et al.*, 2007). It therefore may be valuable to investigate the effects of peroxisome proliferators in MIN6 cells on peroxisome abundance following 3 – 6 days incubation.

It has been shown that increases in PEX11 proteins, including PEX11α, result in an increase in peroxisome abundance after 24hrs. This was determined through the transfection of fusion proteins into human cells (Koch *et al.*, 2010). It is therefore probable that had we increased PEX11α protein expression, it would have resulted in an increase in PMP-70 expression as our marker of peroxisomes. As it is, due to the unavailability of suitable antibodies against PEX11α, we were unable to determine whether an increase in *PEX11*α gene expression resulted in an increase in PEX11α protein expression.

The role of *PEX11*α in the lipotoxicity of pancreatic β-cells was next investigated. As has been shown previously in pancreatic β-cells and β-cell lines (Zhou and Grill, 1995; Hoppa *et al.*, 2009), including MIN6 cells (Thörn and Bergsten, 2010; Watson *et al.*, 2011), we demonstrated that palmitate incubation resulted in a diminished insulin response in the presence of stimulating glucose levels. Although we were unable to show an increase *PEX11*α expression in untransfected MIN6 cells following palmitate treatment, we wanted to determine whether the inhibitory effect of palmitate on GSIS was amplified under conditions of *PEX11*α deficiency. However, there was no difference in the palmitate-affected insulin response in the controls compared with the *PEX11*α knockdown cells. These experiments were carried out with GSIS being investigated 72hrs post transfection. We chose 72hrs as a starting point as we wanted to incubate cells for 48hrs with palmitate as previous groups have done (Watson *et al.*, 2011), but we also wanted the transfected cells to have a recovery period of 24hrs before palmitate was added. *PEX11*α expression was still shown to be knocked down 72hrs post transfection, but data for PMP-70 protein expression as a marker of peroxisome abundance was not collected, although we hoped that an additional 24hrs may have resulted in a change at the peroxisome level which may have shown during the GSIS experiments.

When we originally carried out our experiments, it had been shown that *PEX11*$\alpha^{-/-}$ mice had normal peroxisome abundance (Li *et al.*, 2002a), so we thought the reason we were unable to show that *PEX11*α knockdown alone in MIN6 cells did not result in any changes in GSIS was due to not being able to produce a reduction in peroxisome abundance. We thought that the presence of palmitate may affect GSIS in the *PEX11*α knockdown cells compared with the controls. It may be that this change is limited again by a lack of expression of endogenous RA within the MIN6 cells, and perhaps exogenous RA should have been added to both controls and palmitate treated cells to mimic the effects of what might happen in vivo. Alternatively, when similar experiments were carried out with *PEX11*β knockdown cells, differences were only witnessed with an additional time point of 96hrs post-transfection. Perhaps additional time points to look at the effect of palmitate treatment on GSIS following *PEX11*α knockdown should be investigated in the future.

It is not known whether the SNP found in the *PEX11*α gene region which is associated with a reduced β-cell function led to a change in *PEX11*α expression, and whether this might be an increase or decrease (Pascoe, 2009). We have only looked at decreasing the expression of *PEX11*α in relation to lipotoxicity, however, it may be possible that an increase in the expression of *PEX11*α may be a culprit involved in the process of lipotoxicity in pancreatic β-cells. It has recently been suggested that peroxisomes could contribute to lipotoxicity in pancreatic β-cells due to the H_2O_2 that they produce during β-oxidation of fatty acids (Elsner *et al.*, 2011). The lack of peroxisomal catalase expression leaves them vulnerable to the toxic effects of H_2O_2 (Lenzen *et al.*, 1996; Tiedge *et al.*, 1997; Gehrmann *et al.*, 2010). In addition, the over-expression of *PEX11*α has been shown to result in an increase in peroxisome proliferation (Schrader *et al.*, 1998). In the pancreas, increases in peroxisome abundance could lead to more fatty acids being β-oxidised within the peroxisomes, leading to an increase in the H_2O_2 production. Although this hypothesis is worth pursuing in the future, it was thought that a decrease in the PEX11 proteins would be detrimental to pancreatic β-cell function, as it was assumed that this would lead to a decrease in peroxisome abundance, and therefore, a decrease in the fat clearance from the pancreatic cells. As it has been previously shown that *PEX11*β deficiency resulted in a decrease in peroxisome abundance (Li *et al.*, 2002b), we therefore went onto look at the effect of decreasing peroxisome abundance through the reduction of *PEX11*β expression.

Using siRNA against *PEX11*β we were able to reduce expression of the gene in MIN6 cells by 80% 48hr, 72hr and 96hr post-transfection. *PEX11*$\beta^{-/-}$ mice have been shown to have about a 50% reduction in peroxisome abundance compared with wild type mice (Li and Gould, 2002). We saw a decrease in PMP-70 expression as a marker of peroxisome abundance 72hrs following *PEX11*β knockdown but this wasn't significant. However, a 35% reduction in PMP-70 expression was identified following 96hrs PEX11β knockdown, which is in line with the *PEX11*$\beta^{-/-}$ mice study. As we had produced a model of decreased peroxisome abundance in MIN6 cells, we were then able to assess the effects of a reduction in peroxisome abundance on GSIS following palmitate incubation.

In the *PEX11*β knockdown cells treated with palmitate, there was a partial recovery in the decreased insulin response compared with the scrambled control treated with

palmitate. This would suggest that a reduction in the peroxisome number is protective to the MIN6 cells when incubated with palmitate. This complements work carried out by Elsner et al., 2011, in which they reported that peroxisomes were a major producer of toxic H_2O_2 in β-cells, which was a major cause of β-cell dysfunction through lipotoxicity. If this is indeed a mechanism of lipotoxicity, it is likely that a reduction in *PEX11*β expression achieved a reduction in H_2O_2. It is possible the reduction in peroxisomes may have led to more of the palmitate being oxidised through mitochondrial β-oxidation, leading to less toxic metabolites. However, the mechanism by which a reduction of peroxisomes leads to a partial recovery of the inhibited insulin response merits further investigation.

Although our evidence suggests that an increase in peroxisomes may be harmful to pancreatic β-cells, it has been reported that treatment with a peroxisome proliferator, fibric acid derivative bezafibrate, in obese patients delayed the onset of type 2 diabetes mellitus (Tenenbaum *et al.*, 2005). In addition, fenofibrate treatment was shown to improve GSIS in β-cells that were incubated with palmitate (Sun *et al.*, 2008). Despite these studies seemingly contradicting our work, there are some possible explanations for this. The combination of clofibrate and 9-*cis*-RA has been shown to be protective against palmitate toxicity in rat β-cells. In this study it was shown that the PPARα-RXR agonist combination was able to up-regulate a variety of genes including those involved in mitochondrial fatty acid oxidation (Hellemans *et al.*, 2007). It is possible that although peroxisomal β-oxidation may be increased with fibrate treatment, an increase in mitochondrial β-oxidation provides the protection. In addition, the reduced incidence of type 2 diabetes mellitus seen in the bezafibrate study carried out in obese patients (Tenenbaum *et al.*, 2005) may be due to the increased fatty acid oxidation throughout the whole body through an improvement in insulin resistance, rather than a direct effect on the pancreas. Increased peroxisomal oxidation may be beneficial in other body cells, and may lead to a reduction in the spillage of fat into the pancreas.

We have shown that a decrease in peroxisome number could be beneficial to pancreatic β-cells, but there is evidence suggesting that peroxisome proliferators, which increase peroxisome number, improve β-cell function. We must ask ourselves how these drugs work in patients with type 2 diabetes? Is it through an increase in

mitochondrial fatty acid oxidation, as Hellemans et al., 2007 showed that genes involved in mitochondrial fatty acid oxidation were increased in response to these drugs? If this is so, would these drugs work effectively in the ageing population, as a reduction in mitochondria function has been associated with ageing (Peterson *et al.*, 2012)?

It seems that if the SNP that was found in the *PEX11*α gene region, which led onto this work, is responsible for increasing peroxisome abundance in humans, future treatments for patients with type 2 diabetes who have this risk SNP could be tailored towards increasing mitochondrial fatty acid oxidation over peroxisomal oxidation. This would hopefully reduce the H_2O_2 production through peroxisomal fatty acid oxidation, and help recover the decreased insulin secretion seen in type 2 diabetes. Alternatively targeting a reduction in peroxisomal oxidation may also reduce the H_2O_2 production. However, if peroxisome abundance is reduced too far this could cause other problems. A reduction in total peroxisomal fatty acid oxidation could lead to less fat being oxidised throughout the whole body leading to an increase in fat spillage into the pancreas. Peroxisomes are needed for the oxidation of VLCFA and branched chain FA. A reduction in peroxisomes could lead to a build-up of VLCFA and branched chain FA, including 3-methyl branched chain FA which are exclusively oxidised through peroxisomal α-oxidation. The accumulation of these FA could result in symptoms characteristic of peroxisomal biogenesis disorders (PBD) such as Zellweger syndrome (Wanders, 2004). It is also possible that increases in LCFA could result in mitochondrial fatty acid oxidation becoming exhausted and may contribute to mitochondrial dysfunction.

Many genes have been identified as being risk factors for type 2 diabetes mellitus through GWAS and candidate gene studies (Bonnefond *et al.*, 2010; Qi and Hu, 2012). So far it seems that the SNP in *PEX11*α which was found to be a risk factor for the disease is the only one discovered to be involved in peroxisome proliferation. Although GWAS studies themselves don't appear to have found genes involved in fatty acid metabolism which have an increased risk in type 2 diabetes, one of the diabetes risk SNPs is located in FTO. This diabetes risk allele is associated with increased fat mass, increased triglyceride levels and cholesterol as well as increased risk of obesity. Other genes such as MC4R (melanocortin-4 receptor) which is associated with weight gain,

and Lipin, which is has roles in fatty acid metabolism with effects on PPARα, have been found through the use of mouse genetics (Kebede and Attie; Kato, 2013). Other genes with an associated risk in type 2 diabetes which have an involvement in fatty acid transport are FABP1 and FABP2 (fatty acid binding proteins 1 and 2) (Mansego *et al.*, 2012; Abbas *et al.*, 2013). Carriers of the risk allele in FABP2 are associated with an increased absorption of long chain fatty acids (Abbas *et al.*, 2013). These genes could have effects on peroxisomal fatty metabolism.

With the evidence that peroxisomes may have a role in mediating lipotoxicity in pancreatic β-cells, and with the role they have in fatty acid metabolism, further gene studies may reveal other peroxisomal, and fatty acid oxidation genes with a risk associated with type 2 diabetes mellitus.

7.2 Conclusion

The original aim of the project was to explore the hypothesis that altered expression of *PEX11*α and *PEX11*β individually would result in changes in peroxisome abundance, and contribute to lipotoxicity in cultured pancreatic β-cells. We found that decreases in *PEX11*β expression, but not *PEX11*α expression resulted in a decrease in peroxisome abundance. *PEX11*α was found to be an inducible gene in MIN6 cells, but the time periods investigated following incubation with peroxisome proliferators which induced expression of *PEX11*α did not result in an increase in peroxisome abundance. Investigation of GSIS from MIN6 cells following siRNA knockdown of either *PEX11*α or *PEX11*β revealed no differences compared with the controls. However, knockdown of *PEX11*β expression, but not *PEX11*α expression, in the presence of palmitate resulted in a partial recovery of the diminished insulin response seen with palmitate incubation. This suggests that a reduction in peroxisome abundance through the knockdown of *PEX11*β expression is protective against lipotoxicity in pancreatic β-cells. It is therefore possible that increases in either *PEX11*α or *PEX11*β expression may contribute to lipotoxicity in these cells, and further, may be one of the reasons for the development of type 2 diabetes.

7.3 Future work

We managed to produce a system for the knockdown of *PEX11*α expression and *PEX11*β expression in MIN6 cells. However, it was not possible to assess whether we had reduced expression of the corresponding proteins. Commercially available

antibodies for both PEX11α and PEX11β were against the human proteins, and despite the PEX11α antibody sharing >80% homology with the mouse protein, and the PEX11β antibody being predicted to react in mice, neither were successful at binding. Although through the knockdown of *PEX11*β gene expression we were able to show a decrease in peroxisome number, our conclusion would be strengthened with the evaluation of whether the PEX11β protein expression was also decreased. In addition, we were not able to decrease peroxisome number through a decrease in *PEX11*α gene expression. Although it is possible that a decrease in PEX11α does not lead to a decrease in peroxisome number in MIN6 cells, we cannot be certain as we were unable to assess PEX11α protein expression. Therefore, it would be worth producing antibodies that will bind mouse PEX11α and PEX11β to ensure a decrease in PEX11 proteins is attained following decreases in their gene expression.

As candidate gene studies pointed to a SNP downstream of *PEX11*α being associated with a reduced insulin response (Pascoe, 2009), it would have been better to thoroughly explore the altered expression of *PEX11*α. Although we did show that treatment with PPARα/RXR agonists led to an increase in the expression of *PEX11*α, we did not produce an over expression system for this work. We thought that a decrease in *PEX11* expression would be harmful to the β-cell, so we looked at the effects of decreasing *PEX11*β expression on GSIS following palmitate incubation. However, with evidence pointing to peroxisomes playing a role in lipotoxicity in pancreatic β-cells (Elsner *et al.*, 2011), and the suggestion that over-expression of *PEX11*α in human cells leads to an increase in peroxisome abundance (Schrader *et al.*, 1998), it would be worth investigating the over-expression of *PEX11*α in MIN6 cells in relation to peroxisome abundance, fatty acid metabolism and insulin secretion.

We were able to show that a decrease in *PEX11*β expression led to a decrease in peroxisome abundance which was protective to pancreatic β-cells, and surprisingly resulted in a partial recovery in the inhibited insulin secretion in response to palmitate. As it has been suggested that H_2O_2 produced during peroxisomal β-oxidation of fatty acids is a major mediator of lipotoxicity in pancreatic β-cells (Elsner *et al.*, 2011) it would be worth taking this work further to examine whether a decrease in *PEX11*β expression results in a decrease in fatty acid metabolism and/or a decrease in H_2O_2 production.

It might be worth pursuing how changes in peroxisome abundance and function influence mitochondrial function in the presence of fats. It may be possible that reductions in peroxisomes lead to a compensatory and beneficial increase in mitochondrial fatty acid metabolism. Furthermore, it would be interesting to see whether decreases in TFAM, which has previously been shown to decrease mitochondrial DNA copy and have deleterious effects on GSIS in MIN6 cells (Hine, 2012), might lead to an increase in peroxisome fatty acid metabolism.

Finally, since the work carried out in this thesis was using a mouse cell line, it would be worthy to take this work forwards into human cells. Although MIN6 cells are a good β-cell model (see section 1.8), the implications of these findings need to be assessed in human β-cells to determine whether this is representative of the case in humans. Taking this work further could lead to a better understanding of type 2 diabetes, and a possibility of tailored treatments in the future for people with differences in peroxisome abundance.

References

References

Abaraviciene, S.M., Lundquist, I. and Salehi, A. (2008) 'Rosiglitazone counteracts palmitate-induced β-cell dysfunction by suppression of MAP kinase, inducible nitric oxide synthase and caspase 3 activities', *Cellular and Molecular Life Sciences*, 65(14), pp. 2256-2265.

Abbas, S., Raza, S.T., Ahmed, F., Ahmad, A., Rizvi, S. and Mahdi, F. (2013) 'Association of genetic polymorphism of PPARgamma-2, ACE, MTHFR, FABP-2 and FTO genes in risk prediction of type 2 diabetes mellitus', *J Biomed Sci*, 20, p. 80.

Abe, I. and Fujiki, Y. (1998) 'cDNA Cloning and Characterization of a Constitutively Expressed Isoform of the Human Peroxin Pex11p', *Biochemical and Biophysical Research Communications*, 252(2), pp. 529-533.

Abe, I., Okumoto, K., Tamura, S. and Fujiki, Y. (1998) 'Clofibrate-inducible, 28-kDa peroxisomal integral membrane protein is encoded by PEX11', *FEBS Letters*, 431(3), pp. 468-472.

Afford, S. and Randhawa, S. (2000) 'Demystified …: Apoptosis', *Molecular Pathology*, 53(2), pp. 55-63.

Akimoto, Y., Hart, G.W., Wells, L., Vosseller, K., Yamamoto, K., Munetomo, E., Ohara-Imaizumi, M., Nishiwaki, C., Nagamatsu, S., Hirano, H. and Kawakami, H. (2007) 'Elevation of the post-translational modification of proteins by O-linked N-acetylglucosamine leads to deterioration of the glucose-stimulated insulin secretion in the pancreas of diabetic Goto-Kakizaki rats', *Glycobiology*, 17(2), pp. 127-140.

Aoyama, T., Peters, J.M., Iritani, N., Nakajima, T., Furihata, K., Hashimoto, T. and Gonzalez, F.J. (1998) 'Altered Constitutive Expression of Fatty Acid-metabolizing Enzymes in Mice Lacking the Peroxisome Proliferator-activated Receptor α (PPARα)', *Journal of Biological Chemistry*, 273(10), pp. 5678-5684.

Asfari, M., Janjic, D., Meda, P., Li, G., Halban, P.A. and Wollheim, C.B. (1992) 'Establishment of 2-mercaptoethanol-dependent differentiated insulin-secreting cell lines', *Endocrinology*, 130(1), pp. 167-78.

Barter, P.J. and Rye, K.-A. (2008) 'Is There a Role for Fibrates in the Management of Dyslipidemia in the Metabolic Syndrome?', *Arteriosclerosis, Thrombosis, and Vascular Biology*, 28(1), pp. 39-46.

Bell, G.I. and Polonsky, K.S. (2001) 'Diabetes mellitus and genetically programmed defects in [beta]-cell function', *Nature*, 414(6865), pp. 788-791.

Berge, R.K., Aarsland, A., Kryvi, H., Bremer, J. and Aarsaether, N. (1989) 'Alkylthioacetic acid (3-thia fatty acids) — a new group of non-β-oxidizable, peroxisome-inducing fatty acid analogues. I. A study on the structural requirements for proliferation of peroxisomes and mitochondria in rat liver', *Biochimica et Biophysica Acta (BBA) - Lipids and Lipid Metabolism*, 1004(3), pp. 345-356.

Berthou, L., Saladin, R., Yaqoob, P., Branellec, D., Calder, P., Fruchart, J.-C., Denèfle, P., Auwerx, J. and Staels, B. (1995) 'Regulation of Rat Liver Apolipoprotein A-I, Apolipoprotein A-II and Acyl-Coenzyme A Oxidase Gene Expression by Fibrates and Dietary Fatty Acids', *European Journal of Biochemistry*, 232(1), pp. 179-187.

Biden, T.J., Robinson, D., Cordery, D., Hughes, W.E. and Busch, A.K. (2004) 'Chronic Effects of Fatty Acids on Pancreatic β-Cell Function: New Insights From Functional Genomics', *Diabetes*, 53(suppl 1), pp. S159-S165.

Boden, G. and Shulman, G.I. (2002) 'Free fatty acids in obesity and type 2 diabetes: defining their role in the development of insulin resistance and β-cell dysfunction', *European Journal of Clinical Investigation*, 32, pp. 14-23.

Bonnefond, A., Froguel, P. and Vaxillaire, M. (2010) 'The emerging genetics of type 2 diabetes', *Trends in Molecular Medicine*, 16(9), pp. 407-416.

Boveris, A., Oshino, N. and Chance, B. (1972) 'The cellular production of hydrogen peroxide', *Biochem J*, 128(3), pp. 617-30.

Bruemmer, D. (2006) 'C-Peptide in Insulin Resistance and Vascular Complications: Teaching an Old Dog New Tricks', *Circulation Research*, 99(11), pp. 1149-1151.

Brunetti, A., Chiefari, E. and Foti, D. (2014) 'Recent advances in the molecular genetics of type 2 diabetes mellitus', *World J Diabetes*, 5(2), pp. 128-40.

Camões, F., Bonekamp, N.A., Delille, H.K. and Schrader, M. (2009) 'Organelle dynamics and dysfunction: A closer link between peroxisomes and mitochondria', *Journal of Inherited Metabolic Disease*, 32(2), pp. 163-180.

Chang, C.C., South, S., Warren, D., Jones, J., Moser, A.B., Moser, H.W. and Gould, S.J. (1999) 'Metabolic control of peroxisome abundance', *Journal of Cell Science*, 112(10), pp. 1579-1590.

Chen, Q., Vazquez, E.J., Moghaddas, S., Hoppel, C.L. and Lesnefsky, E.J. (2003) 'Production of Reactive Oxygen Species by Mitochondria: CENTRAL ROLE OF COMPLEX III', *Journal of Biological Chemistry*, 278(38), pp. 36027-36031.

Cheng, K., Delghingaro-Augusto, V., Nolan, C.J., Turner, N., Hallahan, N., Andrikopoulos, S. and Gunton, J.E. (2012) 'High Passage MIN6 Cells Have Impaired Insulin Secretion with Impaired Glucose and Lipid Oxidation', *PLoS ONE*, 7(7), p. e40868.

Cherrington, A.D. (2005) 'The role of hepatic insulin receptors in the regulation of glucose production', *The Journal of Clinical Investigation*, 115(5), pp. 1136-1139.

Chiasson, J.L. and Rabasa-Lhoret, R. (2004) 'Prevention of type 2 diabetes: insulin resistance and beta-cell function', *Diabetes*, 53 Suppl 3, pp. S34-8.

Cnop, M., Welsh, N., Jonas, J.-C., Jörns, A., Lenzen, S. and Eizirik, D.L. (2005) 'Mechanisms of Pancreatic β-Cell Death in Type 1 and Type 2 Diabetes: Many Differences, Few Similarities', *Diabetes*, 54(suppl 2), pp. S97-S107.

Colton, H.M., Falls, J.G., Ni, H., Kwanyuen, P., Creech, D., McNeil, E., Casey, W.M., Hamilton, G. and Cariello, N.F. (2004) 'Visualization and quantitation of peroxisomes using fluorescent nanocrystals: treatment of rats and monkeys with fibrates and detection in the liver', *Toxicol Sci*, 80(1), pp. 183-92.

Covello, G., Siva, K., Adami, V. and Denti, M.A. (2014) 'An electroporation protocol for efficient DNA transfection in PC12 cells', *Cytotechnology*, 66(4), pp. 543-53.

Cunha, D.A., Hekerman, P., Ladriere, L., Bazarra-Castro, A., Ortis, F., Wakeham, M.C., Moore, F., Rasschaert, J., Cardozo, A.K., Bellomo, E., Overbergh, L., Mathieu, C., Lupi, R., Hai, T., Herchuelz, A., Marchetti, P., Rutter, G.A., Eizirik, D.L. and Cnop, M. (2008) 'Initiation and execution of lipotoxic ER stress in pancreatic beta-cells', *J Cell Sci*, 121(Pt 14), pp. 2308-18.

Cusi, K. (2010) 'The Role of Adipose Tissue and Lipotoxicity in the Pathogenesis of Type 2 Diabetes', *Current Diabetes Reports*, 10(4), pp. 306-315.

Danino, D. and Hinshaw, J.E. (2001) 'Dynamin family of mechanoenzymes', *Current Opinion in Cell Biology*, 13(4), pp. 454-460.

Delille, H.K., Agricola, B., Guimaraes, S.C., Borta, H., Luers, G.H., Fransen, M. and Schrader, M. (2010) 'Pex11p{beta}-mediated growth and division of mammalian peroxisomes follows a maturation pathway', *J Cell Sci*, 123(16), pp. 2750-2762.

Diabetes Genetics Initiative of Broad Institute of, H., Mit, L.U., Novartis Institutes of BioMedical, R., Saxena, R., Voight, B.F., Lyssenko, V., Burtt, N.l.P., de Bakker, P.I.W., Chen, H., Roix, J.J., Kathiresan, S., Hirschhorn, J.N., Daly, M.J., Hughes, T.E., Groop, L., Altshuler, D., Almgren, P., Florez, J.C., Meyer, J., Ardlie, K., Bengtsson BostrÃ¶m, K., Isomaa, B., Lettre, G., Lindblad, U., Lyon, H.N., Melander, O., Newton-Cheh, C., Nilsson, P., Orho-Melander, M., RÃ¥stam, L., Speliotes, E.K., Taskinen, M.-R., Tuomi, T., Guiducci, C., Berglund, A., Carlson, J., Gianniny, L., Hackett, R., Hall, L., Holmkvist, J., Laurila, E., SjÃ¶gren, M., Sterner, M., Surti, A., Svensson, M., Svensson, M., Tewhey, R., Blumenstiel, B., Parkin, M., DeFelice, M., Barry, R., Brodeur, W., Camarata, J., Chia, N., Fava, M., Gibbons, J., Handsaker, B., Healy, C., Nguyen, K., Gates, C., Sougnez, C., Gage, D., Nizzari, M., Gabriel, S.B., Chirn, G.-W., Ma, Q., Parikh, H., Richardson, D., Ricke, D. and Purcell, S. (2007) 'Genome-Wide Association Analysis Identifies Loci for Type 2 Diabetes and Triglyceride Levels', *Science*, 316(5829), pp. 1331-1336.

Diabetes UK (2009) *Blood glucose target ranges*. Available at: http://www.diabetes.org.uk/MyLife-YoungAdults/Treatment-and-care/Testing-blood-glucose/Blood-glucose-target-ranges/ (Accessed: 13/01/14).

Diabetes UK (2012) *Diabetic Complications: Hypos & Hypers*. Available at: http://www.diabetes.org.uk/Guide-to-diabetes/Complications/Hypos-Hypers/ (Accessed: 13/01/2014).

Diabetes UK (2014a) *Diabetes UK: Better Futures, Our Annual Report 2013*.

Diabetes UK (2014b) *Diabetes: Facts and Stats (version 3)*.

Donath, M.Y., Ehses, J.A., Maedler, K., Schumann, D.M., Ellingsgaard, H., Eppler, E. and Reinecke, M. (2005) 'Mechanisms of beta-cell death in type 2 diabetes', *Diabetes*, 54 Suppl 2, pp. S108-13.

Drews, G., Krippeit-Drews, P. and Dufer, M. (2010) 'Oxidative stress and beta-cell dysfunction', *Pflügers Archiv - European Journal of Physiology*, 460(4), pp. 703-18.

Dreyer, C., Keller, H., Mahfoudi, A., Laudet, V., Krey, G. and Wahli, W. (1993) 'Positive regulation of the peroxisomal β-oxidation pathway by fatty acids through activation of peroxisome proliferator-activated receptors (PPAR)', *Biology of the Cell*, 77(0), pp. 67-76.

Dupuis, J., Langenberg, C., Prokopenko, I., Saxena, R., Soranzo, N., Jackson, A.U., Wheeler, E., Glazer, N.L., Bouatia-Naji, N., Gloyn, A.L., Lindgren, C.M., Magi, R., Morris, A.P., Randall, J., Johnson, T., Elliott, P., Rybin, D., Thorleifsson, G., Steinthorsdottir, V., Henneman, P., Grallert, H., Dehghan, A., Hottenga, J.J., Franklin, C.S., Navarro, P., Song, K., Goel, A., Perry, J.R., Egan, J.M., Lajunen, T., Grarup, N., Sparso, T., Doney, A., Voight, B.F., Stringham, H.M., Li, M., Kanoni, S., Shrader, P., Cavalcanti-Proenca, C., Kumari, M., Qi, L., Timpson, N.J., Gieger, C., Zabena, C., Rocheleau, G., Ingelsson, E., An, P., O'Connell, J., Luan, J., Elliott, A., McCarroll, S.A., Payne, F., Roccasecca, R.M., Pattou, F., Sethupathy, P., Ardlie, K., Ariyurek, Y., Balkau, B., Barter, P., Beilby, J.P., Ben-Shlomo, Y., Benediktsson, R., Bennett, A.J., Bergmann, S., Bochud, M., Boerwinkle, E., Bonnefond, A., Bonnycastle, L.L., Borch-Johnsen, K., Bottcher, Y., Brunner, E., Bumpstead, S.J., Charpentier, G., Chen, Y.D., Chines, P., Clarke, R., Coin, L.J., Cooper, M.N., Cornelis, M., Crawford, G., Crisponi, L., Day, I.N., de Geus, E.J., Delplanque, J., Dina, C., Erdos, M.R., Fedson, A.C., Fischer-Rosinsky, A., Forouhi, N.G., Fox, C.S., Frants, R., Franzosi, M.G., Galan, P., Goodarzi, M.O., Graessler, J., Groves, C.J., Grundy, S., Gwilliam, R., Gyllensten, U., Hadjadj, S., et al. (2010) 'New genetic loci implicated in fasting glucose homeostasis and their impact on type 2 diabetes risk', *Nat Genet*, 42(2), pp. 105-16.

Echtay, K.S., Roussel, D., St-Pierre, J., Jekabsons, M.B., Cadenas, S., Stuart, J.A., Harper, J.A., Roebuck, S.J., Morrison, A., Pickering, S., Clapham, J.C. and Brand, M.D. (2002) 'Superoxide activates mitochondrial uncoupling proteins', *Nature*, 415(6867), pp. 96-9.

Efrat, S., Leiser, M., Surana, M., Tal, M., Fusco-Demane, D. and Fleischer, N. (1993) 'Murine Insulinoma Cell Line With Normal Glucose-Regulated Insulin Secretion', *Diabetes*, 42(6), pp. 901-907.

Elsner, M., Gehrmann, W. and Lenzen, S. (2011) 'Peroxisome-Generated Hydrogen Peroxide as Important Mediator of Lipotoxicity in Insulin-Producing Cells', *Diabetes*, 60(1), pp. 200-208.

Erdmann, R. and Blobel, G. (1995) 'Giant peroxisomes in oleic acid-induced Saccharomyces cerevisiae lacking the peroxisomal membrane protein Pmp27p', *The Journal of Cell Biology*, 128(4), pp. 509-523.

Fagarasanu, A., Fagarasanu, M. and Rachubinski, R.A. (2007) 'Maintaining Peroxisome Populations: A Story of Division and Inheritance', *Annual Review of Cell and Developmental Biology*, 23(1), pp. 321-344.

Fidaleo, M. (2009) 'Peroxisomes and peroxisomal disorders: The main facts', *Experimental and Toxicologic Pathology*, 62(6), pp. 615-625.

Frayling, T.M. (2007) 'Genome-wide association studies provide new insights into type 2 diabetes aetiology', *Nat Rev Genet*, 8(9), pp. 657-662.

Frayling, T.M., Timpson, N.J., Weedon, M.N., Zeggini, E., Freathy, R.M., Lindgren, C.M., Perry, J.R.B., Elliott, K.S., Lango, H., Rayner, N.W., Shields, B., Harries, L.W., Barrett, J.C., Ellard, S., Groves, C.J., Knight, B., Patch, A.-M., Ness, A.R., Ebrahim, S., Lawlor, D.A., Ring, S.M., Ben-Shlomo, Y., Jarvelin, M.-R., Sovio, U., Bennett, A.J., Melzer, D., Ferrucci, L., Loos, R.J.F., Barroso, I.s., Wareham, N.J., Karpe, F., Owen, K.R., Cardon, L.R., Walker, M., Hitman, G.A., Palmer, C.N.A., Doney, A.S.F., Morris, A.D., Smith, G.D., The Wellcome Trust Case Control, C., Hattersley, A.T. and McCarthy, M.I. (2007) 'A Common Variant in the FTO Gene Is Associated with Body Mass Index and Predisposes to Childhood and Adult Obesity', *Science*, 316(5826), pp. 889-894.

Garcia-Haro, L., Garcia-Gimeno, M.A., Neumann, D., Beullens, M., Bollen, M. and Sanz, P. (2010) 'The PP1-R6 protein phosphatase holoenzyme is involved in the glucose-induced dephosphorylation and inactivation of AMP-activated protein kinase, a key regulator of insulin secretion, in MIN6 β cells', *The FASEB Journal*, 24(12), pp. 5080-5091.

Gehrmann, W., Elsner, M. and Lenzen, S. (2010) 'Role of metabolically generated reactive oxygen species for lipotoxicity in pancreatic β-cells', *Diabetes, Obesity and Metabolism*, 12, pp. 149-158.

Geuze, H.J., Murk, J.L., Stroobants, A.K., Griffith, J.M., Kleijmeer, M.J., Koster, A.J., Verkleij, A.J., Distel, B. and Tabak, H.F. (2003) 'Involvement of the Endoplasmic Reticulum in Peroxisome Formation', *Mol. Biol. Cell*, 14(7), pp. 2900-2907.

Goodpaster, B.H., He, J., Watkins, S. and Kelley, D.E. (2001) 'Skeletal Muscle Lipid Content and Insulin Resistance: Evidence for a Paradox in Endurance-Trained Athletes', *The Journal of Clinical Endocrinology & Metabolism*, 86(12), pp. 5755-5761.

Gribble, F.M. (2009) 'Intolerant of glucose and gasping for oxygen', *Nat Med*, 15(3), pp. 247-249.

Guo, W., Xie, W., Lei, T. and Hamilton, J. (2005) 'Eicosapentaenoic acid, but not oleic acid, stimulates β-oxidation in adipocytes', *Lipids*, 40(8), pp. 815-821.

Halban, P.A., Praz, G.A. and Wollheim, C.B. (1983) 'Abnormal glucose metabolism accompanies failure of glucose to stimulate insulin release from a rat pancreatic cell line (RINm5F)', *Biochem J*, 212(2), pp. 439-43.

Han, M.S., Lim, Y.-M., Quan, W., Kim, J.R., Chung, K.W., Kang, M., Kim, S., Park, S.Y., Han, J.-S., Park, S.-Y., Cheon, H.G., Dal Rhee, S., Park, T.-S. and Lee, M.-S. (2011a) 'Lysophosphatidylcholine as an effector of fatty acid-induced insulin resistance', *Journal of Lipid Research*, 52(6), pp. 1234-1246.

Han, S.-i., Yasuda, K. and Kataoka, K. (2011b) 'ATF2 interacts with β-cell-enriched transcription factors, MafA, Pdx1, and Beta2, and activates insulin gene transcription', *Journal of Biological Chemistry*.

Hara, T., Kashihara, D., Ichimura, A., Kimura, I., Tsujimoto, G. and Hirasawa, A. (2014) 'Role of free fatty acid receptors in the regulation of energy metabolism', *Biochimica et Biophysica Acta (BBA) - Molecular and Cell Biology of Lipids*, 1841(9), pp. 1292-1300.

Hellemans, K., Kerckhofs, K., Hannaert, J.-C., Martens, G., Van Veldhoven, P. and Pipeleers, D. (2007) 'Peroxisome proliferator-activated receptor α–retinoid X receptor agonists induce beta-cell protection against palmitate toxicity', *FEBS Journal*, 274(23), pp. 6094-6105.

Hernandez, C., Zapata, M.A., Losada, E., Villarroel, M., Garcia-Ramirez, M., Garcia-Arumi, J. and Simo, R. (2010) 'Effect of intensive insulin therapy on macular biometrics, plasma VEGF and its soluble receptor in newly diagnosed diabetic patients', *Diabetes Metab Res Rev*, 26(5), pp. 386-92.

Hertz, R. and Bar-Tana, J. (1992) 'Induction of peroxisomal beta-oxidation genes by retinoic acid in cultured rat hepatocytes', *Biochem J*, 281 (Pt 1), pp. 41-3.

Hettema, E.H. and Motley, A.M. (2009) 'How peroxisomes multiply', *Journal of Cell Science*, 122(14), pp. 2331-2336.

Heyman, R.A., Mangelsdorf, D.J., Dyck, J.A., Stein, R.B., Eichele, G., Evans, R.M. and Thaller, C. (1992) '9-cis retinoic acid is a high affinity ligand for the retinoid X receptor', *Cell*, 68(2), pp. 397-406.

Hine, D.L. (2012) *Mitochondrial DNA Depletion and Insulin Secretion*. Newcastle University.

Hoepfner, D., Berg, M.v.d., Philippsen, P., Tabak, H.F. and Hettema, E.H. (2001) 'A Role for Vps1p, Actin, and the Myo2p Motor in Peroxisome Abundance and Inheritance in Saccharomyces cerevisiae', *The Journal of Cell Biology*, 155(6), pp. 979-990.

Hoepfner, D., Schildknegt, D., Braakman, I., Philippsen, P. and Tabak, H.F. (2005) 'Contribution of the Endoplasmic Reticulum to Peroxisome Formation', *Cell*, 122(1), pp. 85-95.

Holland, W.L., Brozinick, J.T., Wang, L.-P., Hawkins, E.D., Sargent, K.M., Liu, Y., Narra, K., Hoehn, K.L., Knotts, T.A., Siesky, A., Nelson, D.H., Karathanasis, S.K., Fontenot, Greg K., Birnbaum, M.J. and Summers, S.A. (2007) 'Inhibition of Ceramide Synthesis Ameliorates Glucocorticoid-, Saturated-Fat-, and Obesity-Induced Insulin Resistance', *Cell Metabolism*, 5(3), pp. 167-179.

Hoppa, M.B., Collins, S., Ramracheya, R., Hodson, L., Amisten, S., Zhang, Q., Johnson, P., Ashcroft, F.M. and Rorsman, P. (2009) 'Chronic Palmitate Exposure Inhibits Insulin Secretion by Dissociation of Ca2+ Channels from Secretory Granules', *Cell Metabolism*, 10(6), pp. 455-465.

Hossain, P., Kawar, B. and El Nahas, M. (2007) 'Obesity and Diabetes in the Developing World — A Growing Challenge', *New England Journal of Medicine*, 356(3), pp. 213-215.

Hotamisligil, G.S., Murray, D.L., Choy, L.N. and Spiegelman, B.M. (1994) 'Tumor necrosis factor alpha inhibits signaling from the insulin receptor', *Proceedings of the National Academy of Sciences of the United States of America*, 91(11), pp. 4854-4858.

Huising, M.O., Pilbrow, A.P., Matsumoto, M., van der Meulen, T., Park, H., Vaughan, J.M., Lee, S. and Vale, W.W. (2011) 'Glucocorticoids differentially regulate the expression of CRFR1 and CRFR2alpha in MIN6 insulinoma cells and rodent islets', *Endocrinology*, 152(1), pp. 138-50.

Hussain, A., Claussen, B., Ramachandran, A. and Williams, R. (2007) 'Prevention of type 2 diabetes: A review', *Diabetes Research and Clinical Practice*, 76(3), pp. 317-326.

Huybrechts, S.J., Van Veldhoven, P.P., Brees, C., Mannaerts, G.P., Los, G.V. and Fransen, M. (2009) 'Peroxisome Dynamics in Cultured Mammalian Cells', *Traffic*, 10(11), pp. 1722-1733.

Iio, A., Ito, M., Itoh, T., Terazawa, R., Fujita, Y., Nozawa, Y., Ohsawa, I., Ohno, K. and Ito, M. (2013) 'Molecular hydrogen attenuates fatty acid uptake and lipid accumulation through downregulating CD36 expression in HepG2 cells', *Med Gas Res*, 3(1), p. 6.

Imanaka, T., Aihara, K., Suzuki, Y., Yokota, S. and Osumi, T. (2000) 'The 70-kDa peroxisomal membrane protein (PMP70) an ATP-binding cassette transporter', *Cell Biochemistry and Biophysics*, 32(1-3), pp. 131-138.

Imanaka, T., Aihara, K., Takano, T., Yamashita, A., Sato, R., Suzuki, Y., Yokota, S. and Osumi, T. (1999) 'Characterization of the 70-kDa peroxisomal membrane protein, an ATP binding cassette transporter', *J Biol Chem*, 274(17), pp. 11968-76.

International Diabetes Federation (2013) *IDF Diabetes Atlas, 6th edn*. Brussels, Belgium: International Diabetes Federation.

Ishihara, H., Asano, T., Tsukuda, K., Katagiri, H., Inukai, K., Anai, M., Kikuchi, M., Yazaki, Y., Miyazaki, J. and Oka, Y. (1994) 'Overexpression of hexokinase I but not GLUT1 glucose transporter alters concentration dependence of glucose-stimulated insulin secretion in pancreatic beta-cell line MIN6', *Journal of Biological Chemistry*, 269(4), pp. 3081-3087.

Ishihara, H., Asano, T., Tsukuda, K., Katagiri, H., Inukai, K., Anai, M., Kikuchi, M., Yazaki, Y., Miyazaki, J.I. and Oka, Y. (1993) 'Pancreatic beta cell line MIN6 exhibits characteristics of glucose metabolism and glucose-stimulated insulin secretion similar to those of normal islets', *Diabetologia*, 36(11), pp. 1139-1145.

Islinger, M., Lüers, G.H., Li, K.W., Loos, M. and Völkl, A. (2007) 'Rat Liver Peroxisomes after Fibrate Treatment: A SURVEY USING QUANTITATIVE MASS SPECTROMETRY', *Journal of Biological Chemistry*, 282(32), pp. 23055-23069.

Ivashchenko, O., Van Veldhoven, P.P., Brees, C., Ho, Y.-S., Terlecky, S.R. and Fransen, M. (2011) 'Intraperoxisomal redox balance in mammalian cells: oxidative stress and interorganellar cross-talk', *Molecular Biology of the Cell*, 22(9), pp. 1440-1451.

Jacqueminet, S., Briaud, I., Rouault, C., Reach, G. and Poitout, V. (2000) 'Inhibition of insulin gene expression by long-term exposure of pancreatic β cells to palmitate is dependent on the presence of a stimulatory glucose concentration', *Metabolism*, 49(4), pp. 532-536.

Jansen, G.A. and Wanders, R.J.A. (2006) 'Alpha-Oxidation', *Biochimica et Biophysica Acta (BBA) - Molecular Cell Research*, 1763(12), pp. 1403-1412.

Ježek, P. and Hlavatá, L. (2005) 'Mitochondria in homeostasis of reactive oxygen species in cell, tissues, and organism', *The International Journal of Biochemistry & Cell Biology*, 37(12), pp. 2478-2503.

Jin, Z. and El-Deiry, W.S. (2005) 'Overview of cell death signaling pathways', *Cancer Biology & Therapy*, 4(2), pp. 139-163.

Johansson, L.H. and Håkan Borg, L.A. (1988) 'A spectrophotometric method for determination of catalase activity in small tissue samples', *Analytical Biochemistry*, 174(1), pp. 331-336.

Joshi-Barve, S., Barve, S.S., Amancherla, K., Gobejishvili, L., Hill, D., Cave, M., Hote, P. and McClain, C.J. (2007) 'Palmitic acid induces production of proinflammatory cytokine interleukin-8 from hepatocytes', *Hepatology*, 46(3), pp. 823-30.

Kane, M.A., Folias, A.E., Pingitore, A., Perri, M., Obrochta, K.M., Krois, C.R., Cione, E., Ryu, J.Y. and Napoli, J.L. (2010) 'Identification of 9-cis-retinoic acid as a pancreas-specific autacoid that attenuates glucose-stimulated insulin secretion', *Proc Natl Acad Sci U S A*, 107(50), pp. 21884-9.

Kapuscinski, J. (1995) 'DAPI: a DNA-specific fluorescent probe', *Biotech Histochem*, 70(5), pp. 220-33.

Karunakaran, U., Kim, H.-J., Kim, J.-Y. and Lee, I.-K. (2012) 'Guards and Culprits in the Endoplasmic Reticulum: Glucolipotoxicity and β-Cell Failure in Type II Diabetes', *Experimental Diabetes Research*, 2012, p. 9.

Kato, N. (2013) 'Insights into the genetic basis of type 2 diabetes', *J Diabetes Investig*, 4(3), pp. 233-44.

Katsiki, N., Nikolic, D., Montalto, G., Banach, M., Mikhailidis, D.P. and Rizzo, M. (2013) 'The role of fibrate treatment in dyslipidemia: an overview', *Curr Pharm Des*, 19(17), pp. 3124-31.

Kebede, M.A. and Attie, A.D. 'Insights into obesity and diabetes at the intersection of mouse and human genetics', *Trends in Endocrinology & Metabolism*, 25(10), pp. 493-501.

Keller, H., Dreyer, C., Medin, J., Mahfoudi, A., Ozato, K. and Wahli, W. (1993) 'Fatty acids and retinoids control lipid metabolism through activation of peroxisome proliferator-activated receptor-retinoid X receptor heterodimers', *Proc Natl Acad Sci U S A*, 90(6), pp. 2160-4.

Kelley, D.E. and Mandarino, L.J. (2000) 'Fuel selection in human skeletal muscle in insulin resistance: a reexamination', *Diabetes*, 49(5), pp. 677-683.

Kihara, A. (2012) 'Very long-chain fatty acids: elongation, physiology and related disorders', *J Biochem*, 152(5), pp. 387-95.

Kim, P.K., Mullen, R.T., Schumann, U. and Lippincott-Schwartz, J. (2006) 'The origin and maintenance of mammalian peroxisomes involves a de novo PEX16-dependent pathway from the ER', *The Journal of Cell Biology*, 173(4), pp. 521-532.

King, M.W. (2014) *Introduction to Insulin Activities*. Available at: http://themedicalbiochemistrypage.org/insulin.php.

Kliewer, S.A., Umesono, K., Noonan, D.J., Heyman, R.A. and Evans, R.M. (1992) 'Convergence of 9-cis retinoic acid and peroxisome proliferator signalling pathways through heterodimer formation of their receptors', *Nature*, 358(6389), pp. 771-4.

Koch, A., Schneider, G., Luers, G.H. and Schrader, M. (2004) 'Peroxisome elongation and constriction but not fission can occur independently of dynamin-like protein 1', *J Cell Sci*, 117(17), pp. 3995-4006.

Koch, A., Thiemann, M., Grabenbauer, M., Yoon, Y., McNiven, M.A. and Schrader, M. (2003) 'Dynamin-like Protein 1 Is Involved in Peroxisomal Fission', *Journal of Biological Chemistry*, 278(10), pp. 8597-8605.

Koch, A., Yoon, Y., Bonekamp, N.A., McNiven, M.A. and Schrader, M. (2005) 'A Role for Fis1 in Both Mitochondrial and Peroxisomal Fission in Mammalian Cells', *Mol. Biol. Cell*, 16(11), pp. 5077-5086.

Koch, J. and Brocard, C. (2012) 'PEX11 proteins attract Mff and human Fis1 to coordinate peroxisomal fission', *Journal of Cell Science*, 125(16), pp. 3813-3826.

Koch, J., Pranjic, K., Huber, A., Ellinger, A., Hartig, A., Kragler, F. and Brocard, C. (2010) 'PEX11 family members are membrane elongation factors that coordinate peroxisome proliferation and maintenance', *J Cell Sci*, 123(19), pp. 3389-3400.

Koh, E.H., Kim, M.-S., Park, J.-Y., Kim, H.S., Youn, J.-Y., Park, H.-S., Youn, J.H. and Lee, K.-U. (2003) 'Peroxisome Proliferator-Activated Receptor (PPAR)-α Activation Prevents Diabetes in OLETF Rats: Comparison With PPAR-γ Activation', *Diabetes*, 52(9), pp. 2331-2337.

Komatsu, M., Takei, M., Ishii, H. and Sato, Y. (2013) 'Glucose-stimulated insulin secretion: A newer perspective', *J Diabetes Investig*, 4(6), pp. 511-6.

Kota, B.P., Huang, T.H.-W. and Roufogalis, B.D. (2005) 'An overview on biological mechanisms of PPARs', *Pharmacological Research*, 51(2), pp. 85-94.

Koves, T.R., Ussher, J.R., Noland, R.C., Slentz, D., Mosedale, M., Ilkayeva, O., Bain, J., Stevens, R., Dyck, J.R.B., Newgard, C.B., Lopaschuk, G.D. and Muoio, D.M. (2008) 'Mitochondrial Overload and Incomplete Fatty Acid Oxidation Contribute to Skeletal Muscle Insulin Resistance', *Cell Metabolism*, 7(1), pp. 45-56.

Krishnamurthy, J., Ramsey, M.R., Ligon, K.L., Torrice, C., Koh, A., Bonner-Weir, S. and Sharpless, N.E. (2006) 'p16INK4a induces an age-dependent decline in islet regenerative potential', *Nature*, 443(7110), pp. 453-457.

Kristinsson, H., Smith, D.M., Bergsten, P. and Sargsyan, E. (2013) 'FFAR1 is involved in both the acute and chronic effects of palmitate on insulin secretion', *Endocrinology*, 154(11), pp. 4078-88.

Kusminski, C., Shetty, S., Orci, L., Unger, R. and Scherer, P. (2009) 'Diabetes and apoptosis: lipotoxicity', *Apoptosis*, 14(12), pp. 1484-1495.

Lai, E., Bikopoulos, G., Wheeler, M.B., Rozakis-Adcock, M. and Volchuk, A. (2008) 'Differential activation of ER stress and apoptosis in response to chronically elevated free fatty acids in pancreatic β-cells', *American Journal of Physiology - Endocrinology And Metabolism*, 294(3), pp. E540-E550.

Lameloise, N., Muzzin, P., Prentki, M. and Assimacopoulos-Jeannet, F. (2001) 'Uncoupling Protein 2: A Possible Link Between Fatty Acid Excess and Impaired Glucose-Induced Insulin Secretion?', *Diabetes*, 50(4), pp. 803-809.

Lazarow, P.B. and De Duve, C. (1976) 'A fatty acyl-CoA oxidizing system in rat liver peroxisomes; enhancement by clofibrate, a hypolipidemic drug', *Proc Natl Acad Sci U S A*, 73(6), pp. 2043-6.

Lee, S.S., Pineau, T., Drago, J., Lee, E.J., Owens, J.W., Kroetz, D.L., Fernandez-Salguero, P.M., Westphal, H. and Gonzalez, F.J. (1995) 'Targeted disruption of the alpha isoform of the peroxisome proliferator-activated receptor gene in mice results in abolishment of the pleiotropic effects of peroxisome proliferators', *Mol Cell Biol*, 15(6), pp. 3012-22.

Lenzen, S., Drinkgern, J. and Tiedge, M. (1996) 'Low antioxidant enzyme gene expression in pancreatic islets compared with various other mouse tissues', *Free Radical Biology and Medicine*, 20(3), pp. 463-466.

Li, J., Liu, X., Ran, X., Chen, J., Li, X., Wu, W., Huang, H., Huang, H., Long, Y., Liang, J., Cheng, J. and Tian, H. (2010) 'Sterol regulatory element-binding protein-1c knockdown protected INS-1E cells from lipotoxicity', *Diabetes Obes Metab*, 12(1), pp. 35-46.

Li, X., Baumgart, E., Dong, G.-X., Morrell, J.C., Jimenez-Sanchez, G., Valle, D., Smith, K.D. and Gould, S.J. (2002a) 'PEX11{alpha} Is Required for Peroxisome Proliferation in Response to 4-Phenylbutyrate but Is Dispensable for Peroxisome Proliferator-Activated Receptor Alpha-Mediated Peroxisome Proliferation', *Mol. Cell. Biol.*, 22(23), pp. 8226-8240.

Li, X., Baumgart, E., Morrell, J.C., Jimenez-Sanchez, G., Valle, D. and Gould, S.J. (2002b) 'PEX11{beta} Deficiency Is Lethal and Impairs Neuronal Migration but Does Not Abrogate Peroxisome Function', *Mol. Cell. Biol.*, 22(12), pp. 4358-4365.

Li, X. and Gould, S.J. (2002) 'PEX11 Promotes Peroxisome Division Independently of Peroxisome Metabolism', *The Journal of Cell Biology*, 156(4), pp. 643-651.

Li, X. and Gould, S.J. (2003) 'The Dynamin-like GTPase DLP1 Is Essential for Peroxisome Division and Is Recruited to Peroxisomes in Part by PEX11', *Journal of Biological Chemistry*, 278(19), pp. 17012-17020.

Lim, G.E. and Brubaker, P.L. (2006) 'Glucagon-Like Peptide 1 Secretion by the L-Cell: The View From Within', *Diabetes*, 55(Supplement 2), pp. S70-S77.

Liu, B., Barbosa-Sampaio, H., Jones, P.M., Persaud, S.J. and Muller, D.S. (2012) 'The CaMK4/CREB/IRS-2 cascade stimulates proliferation and inhibits apoptosis of beta-cells', *PLoS ONE*, 7(9), p. e45711.

Luo, X., Yang, Y., Shen, T., Tang, X., Xiao, Y., Zou, T., Xia, M. and Ling, W. (2012) 'Docosahexaenoic acid ameliorates palmitate-induced lipid accumulation and inflammation through repressing NLRC4 inflammasome activation in HepG2 cells', *Nutr Metab (Lond)*, 9(1), p. 34.

Ma, R.Q., Sun, M.N. and Yang, Z. (2011) 'Inhibition of nitric oxide synthase lowers fatty acid oxidation in preeclampsia-like mice at early gestational stage', *Chin Med J (Engl)*, 124(19), pp. 3141-7.

Ma, Z.A. (2012) 'The role of peroxidation of mitochondrial membrane phospholipids in pancreatic beta -cell failure', *Curr Diabetes Rev*, 8(1), pp. 69-75.

Ma, Z.A., Zhao, Z. and Turk, J. (2012) 'Mitochondrial Dysfunction and β-Cell Failure in Type 2 Diabetes Mellitus', *Experimental Diabetes Research*, 2012, p. 11.

Maechler, P. and Wollheim, C.B. (2001) 'Mitochondrial function in normal and diabetic [beta]-cells', *Nature*, 414(6865), pp. 807-812.

Mahler, R.J. and Adler, M.L. (1999) 'Type 2 Diabetes Mellitus: Update on Diagnosis, Pathophysiology, and Treatment', *J Clin Endocrinol Metab*, 84(4), pp. 1165-1171.

Mansego, M.L., Martínez, F., Martínez-Larrad, M.T., Zabena, C., Rojo, G., Morcillo, S., Soriguer, F., Martín-Escudero, J.C., Serrano-Ríos, M., Redon, J. and Chaves, F.J. (2012) 'Common Variants of the Liver Fatty Acid Binding Protein Gene Influence the Risk of Type 2 Diabetes and Insulin Resistance in Spanish Population', *PLoS ONE*, 7(3), p. e31853.

Marchetti, P., Del Guerra, S., Marselli, L., Lupi, R., Masini, M., Pollera, M., Bugliani, M., Boggi, U., Vistoli, F., Mosca, F. and Del Prato, S. (2004) 'Pancreatic islets from type 2 diabetic patients have functional defects and increased apoptosis that are ameliorated by metformin', *J Clin Endocrinol Metab*, 89(11), pp. 5535-41.

Marshall, P.A., Krimkevich, Y.I., Lark, R.H., Dyer, J.M., Veenhuis, M. and Goodman, J.M. (1995) 'Pmp27 promotes peroxisomal proliferation', *The Journal of Cell Biology*, 129(2), pp. 345-355.

Mathis, D., Vence, L. and Benoist, C. (2001) '[beta]-Cell death during progression to diabetes', *Nature*, 414(6865), pp. 792-798.

Matschinsky, F.M. (2002) 'Regulation of pancreatic beta-cell glucokinase: from basics to therapeutics', *Diabetes*, 51 Suppl 3, pp. S394-404.

McCarthy, M.I. and Zeggini, E. (2009) 'Genome-wide association studies in type 2 diabetes', *Curr Diab Rep*, 9(2), pp. 164-71.

Merglen, A., Theander, S., Rubi, B., Chaffard, G., Wollheim, C.B. and Maechler, P. (2004) 'Glucose Sensitivity and Metabolism-Secretion Coupling Studied during Two-Year Continuous Culture in INS-1E Insulinoma Cells', *Endocrinology*, 145(2), pp. 667-678.

Miyazaki, J.-I., Araki, K., Yamato, E., Ikegami, H., Asano, T., Shibasaki, Y., Oka, Y. and Yamamura, K.-I. (1990a) 'Establishment of a Pancreatic β Cell Line That Retains Glucose-Inducible Insulin Secretion: Special Reference to Expression of Glucose Transporter Isoforms', *Endocrinology*, 127(1), pp. 126-132.

Miyazaki, J., Araki, K., Yamato, E., Ikegami, H., Asano, T., Shibasaki, Y., Oka, Y. and Yamamura, K. (1990b) 'Establishment of a pancreatic beta cell line that retains glucose-inducible insulin secretion: special reference to expression of glucose transporter isoforms', *Endocrinology*, 127(1), pp. 126-32.

Moore, J.C., Atze, K., Yeung, P.L., Toro-Ramos, A.J., Camarillo, C., Thompson, K., Ricupero, C.L., Brenneman, M.A., Cohen, R.I. and Hart, R.P. (2010) 'Efficient, high-throughput transfection of human embryonic stem cells', *Stem Cell Res Ther*, 1(3), p. 23.

National Collaborating Centre for Chronic Conditions (2008) *Type 2 Diabetes: National clinical guideline for management in primary and secondary care (update)*. London: Royal College of Physicians.

Nieto-Vazquez, I., FernÃ¡ndez-Veledo, S., KrÃ¤mer, D.K., Vila-Bedmar, R., Garcia-Guerra, L. and Lorenzo, M. (2008) 'Insulin resistance associated to obesity: the link TNF-alpha', *Archives Of Physiology And Biochemistry*, 114(3), pp. 183-194.

Nordgren, M., Wang, B., Apanasets, O. and Fransen, M. (2013) 'Peroxisome degradation in mammals: mechanisms of action, recent advances, and perspectives', *Frontiers in Physiology*, 4.

Nordlie, R.C., Foster, J.D. and Lange, A.J. (1999) 'Regulation Of Glucose Production By The Liver', *Annual Review of Nutrition*, 19(1), pp. 379-406.

Park, K.-G., Lee, K.-M., Seo, H.-Y., Suh, J.-H., Kim, H.-S., Wang, L., Won, K.-C., Lee, H.-W., Park, J.-Y., Lee, K.-U., Kim, J.-G., Kim, B.-W., Choi, H.-S. and Lee, I.-K. (2007) 'Glucotoxicity in the INS-1 Rat Insulinoma Cell Line Is Mediated by the Orphan Nuclear Receptor Small Heterodimer Partner', *Diabetes*, 56(2), pp. 431-437.

Pascoe, L. (2009) *Genetic Determinants of Type 2 Diabetes*. Newcastle University.

Pascoe, L., Tura, A., Patel, S.K., Ibrahim, I.M., Ferrannini, E., Zeggini, E., Weedon, M.N., Mari, A., Hattersley, A.T., McCarthy, M.I., Frayling, T.M. and Walker, M. (2007) 'Common Variants of the Novel Type 2 Diabetes Genes CDKAL1 and HHEX/IDE Are Associated With Decreased Pancreatic β-Cell Function', *Diabetes*, 56(12), pp. 3101-3104.

Pawar, A. and Jump, D.B. (2003) 'Unsaturated Fatty Acid Regulation of Peroxisome Proliferator-activated Receptor α Activity in Rat Primary Hepatoctes', *Journal of Biological Chemistry*, 278(38), pp. 35931-35939.

Peterson, C.M., Johannsen, D.L. and Ravussin, E. (2012) 'Skeletal Muscle Mitochondria and Aging: A Review', *Journal of Aging Research*, 2012, p. 20.

Qi, Q. and Hu, F.B. (2012) 'Genetics of type 2 diabetes in European populations', *J Diabetes*, 4(3), pp. 203-12.

Rakhshandehroo, M., Hooiveld, G., MÃ¼ller, M. and Kersten, S. (2009) 'Comparative Analysis of Gene Regulation by the Transcription Factor PPARÎ± between Mouse and Human', *PLoS ONE*, 4(8), p. e6796.

Randle, P.J., Garland, P.B., Hales, C.N. and Newsholme, E.A. (1963) 'THE GLUCOSE FATTY-ACID CYCLE ITS ROLE IN INSULIN SENSITIVITY AND THE METABOLIC DISTURBANCES OF DIABETES MELLITUS', *The Lancet*, 281(7285), pp. 785-789.

Ravassard, P., Hazhouz, Y., Pechberty, S., xE, verine, Bricout-Neveu, E., Armanet, M., Czernichow, P. and Scharfmann, R. (2011) 'A genetically engineered human pancreatic β cell line exhibiting glucose-inducible insulin secretion', *The Journal of Clinical Investigation*, 121(9), pp. 3589-3597.

Rebelato, E., Abdulkader, F., Curi, R. and Carpinelli, A.R. (2010) 'Low doses of hydrogen peroxide impair glucose-stimulated insulin secretion via inhibition of glucose metabolism and intracellular calcium oscillations', *Metabolism*, 59(3), pp. 409-413.

Reddy, J.K. and Sambasiva Rao, M. (2006) *Lipid Metabolism and Liver Inflammation. II. Fatty liver disease and fatty acid oxidation*.

Ritz-Laser, B., Meda, P., Constant, I., Klages, N., Charollais, A., Morales, A., Magnan, C., Ktorza, A. and Philippe, J. (1999) 'Glucose-Induced Preproinsulin Gene Expression Is Inhibited by the Free Fatty Acid Palmitate', *Endocrinology*, 140(9), pp. 4005-4014.

Robertson, R.P., Harmon, J., Tran, P.O.T. and Poitout, V. (2004) 'Beta-cell glucose toxicity, lipotoxicity, and chronic oxidative stress in type 2 diabetes', *Diabetes*, 53 Suppl 1, pp. S119-24.

Rorsman, P. and Braun, M. (2013) 'Regulation of Insulin Secretion in Human Pancreatic Islets', *Annual Review of Physiology*, 75(1), pp. 155-179.

Rousset, S., Alves-Guerra, M.-C., Mozo, J., Miroux, B., Cassard-Doulcier, A.-M., Bouillaud, F. and Ricquier, D. (2004) 'The Biology of Mitochondrial Uncoupling Proteins', *Diabetes*, 53(suppl 1), pp. S130-S135.

Sakuraba, H., Mizukami, H., Yagihashi, N., Wada, R., Hanyu, C. and Yagihashi, S. (2002) 'Reduced beta-cell mass and expression of oxidative stress-related DNA damage in the islet of Japanese Type II diabetic patients', *Diabetologia*, 45(1), pp. 85-96.

Saltiel, A.R. and Kahn, C.R. (2001) 'Insulin signalling and the regulation of glucose and lipid metabolism', *Nature*, 414(6865), pp. 799-806.

Santerre, R.F., Cook, R.A., Crisel, R.M., Sharp, J.D., Schmidt, R.J., Williams, D.C. and Wilson, C.P. (1981) 'Insulin synthesis in a clonal cell line of simian virus 40-transformed hamster pancreatic beta cells', *Proceedings of the National Academy of Sciences of the United States of America*, 78(7), pp. 4339-4343.

Sargsyan, E. and Bergsten, P. (2011) 'Lipotoxicity is glucose-dependent in INS-1E cells but not in human islets and MIN6 cells', *Lipids in Health and Disease*, 10(1), p. 115.

Schmittgen, T.D. and Livak, K.J. (2008) 'Analyzing real-time PCR data by the comparative CT method', *Nat. Protocols*, 3(6), pp. 1101-1108.

Schrader, M. (2006) 'Shared components of mitochondrial and peroxisomal division', *Biochimica et Biophysica Acta (BBA) - Molecular Cell Research*, 1763(5-6), pp. 531-541.

Schrader, M., Bonekamp, N.A. and Islinger, M. (2012) 'Fission and proliferation of peroxisomes', *Biochimica et Biophysica Acta (BBA) - Molecular Basis of Disease*, 1822(9), pp. 1343-1357.

Schrader, M., Reuber, B.E., Morrell, J.C., Jimenez-Sanchez, G., Obie, C., Stroh, T.A., Valle, D., Schroer, T.A. and Gould, S.J. (1998) 'Expression of PEX11{beta} Mediates Peroxisome Proliferation in the Absence of Extracellular Stimuli', *Journal of Biological Chemistry*, 273(45), pp. 29607-29614.

Schrauwen, P. and Hesselink, M.K.C. (2004) 'Oxidative Capacity, Lipotoxicity, and Mitochondrial Damage in Type 2 Diabetes', *Diabetes*, 53(6), pp. 1412-1417.

Scobie, I.N. and Samaras, K. (2009) *Fast Facts: Diabetes Mellitus* Third Edition edn. Health Press.

Scott, L.J., Mohlke, K.L., Bonnycastle, L.L., Willer, C.J., Li, Y., Duren, W.L., Erdos, M.R., Stringham, H.M., Chines, P.S., Jackson, A.U., Prokunina-Olsson, L., Ding, C.-J., Swift, A.J., Narisu, N., Hu, T., Pruim, R., Xiao, R., Li, X.-Y., Conneely, K.N., Riebow, N.L., Sprau, A.G., Tong, M., White, P.P., Hetrick, K.N., Barnhart, M.W., Bark, C.W., Goldstein, J.L., Watkins, L., Xiang, F., Saramies, J., Buchanan, T.A., Watanabe, R.M., Valle, T.T., Kinnunen, L., Abecasis, G.a.R., Pugh, E.W., Doheny, K.F., Bergman, R.N., Tuomilehto, J., Collins, F.S. and Boehnke, M. (2007) 'A Genome-Wide Association Study of Type 2 Diabetes in Finns Detects Multiple Susceptibility Variants', *Science*, 316(5829), pp. 1341-1345.

Shimabukuro, M., Higa, M., Zhou, Y.-T., Wang, M.-Y., Newgard, C.B. and Unger, R.H. (1998a) 'Lipoapoptosis in Beta-cells of Obese Prediabeticfa/fa Rats: ROLE OF SERINE PALMITOYLTRANSFERASE OVEREXPRESSION', *Journal of Biological Chemistry*, 273(49), pp. 32487-32490.

Shimabukuro, M., Ohneda, M., Lee, Y. and Unger, R.H. (1997) 'Role of nitric oxide in obesity-induced beta cell disease', *The Journal of Clinical Investigation*, 100(2), pp. 290-295.

Shimabukuro, M., Zhou, Y.T., Levi, M. and Unger, R.H. (1998b) 'Fatty acid-induced beta cell apoptosis: a link between obesity and diabetes', *Proc Natl Acad Sci U S A*, 95(5), pp. 2498-502.

Shimizu, M., Akter, M.H., Emi, Y., Sato, R., Yamaguchi, T., Hirose, F. and Osumi, T. (2006) 'Peroxisome Proliferator - Activated Receptor Subtypes Differentially Cooperate with Other Transcription Factors in Selective Transactivation of the Perilipin/PEX11α Gene Pair', *Journal of Biochemistry*, 139(3), pp. 563-573.

Shimizu, M., Takeshita, A., Tsukamoto, T., Gonzalez, F.J. and Osumi, T. (2004) 'Tissue-Selective, Bidirectional Regulation of PEX11{alpha} and Perilipin Genes through a Common Peroxisome Proliferator Response Element', *Mol. Cell. Biol.*, 24(3), pp. 1313-1323.

Shimozawa, N., Tsukamoto, T., Nagase, T., Takemoto, Y., Koyama, N., Suzuki, Y., Komori, M., Osumi, T., Jeannette, G., Wanders, R.J.A. and Kondo, N. (2004) 'Identification of a new complementation group of the peroxisome biogenesis disorders and PEX14 as the mutated gene', *Human Mutation*, 23(6), pp. 552-558.

Silverthorn, D.U. (2007) *Human Physiology: An Integrated Approach (Forth Edition)*. Benjamin Cummings; Pearson.

Singh, I., Lazo, O., Kalipada, P. and Singh, A.K. (1992) 'Phytanic acid [alpha]-oxidation in human cultured skin fibroblasts', *Biochimica et Biophysica Acta (BBA) - Molecular Basis of Disease*, 1180(2), pp. 221-224.

Skelin, M., Rupnik, M. and Cencic, A. (2010) 'Pancreatic beta cell lines and their applications in diabetes mellitus research', *ALTEX*, 27(2), pp. 105-13.

Sladek, R., Rocheleau, G., Rung, J., Dina, C., Shen, L., Serre, D., Boutin, P., Vincent, D., Belisle, A., Hadjadj, S., Balkau, B., Heude, B., Charpentier, G., Hudson, T.J., Montpetit, A., Pshezhetsky, A.V., Prentki, M., Posner, B.I., Balding, D.J., Meyre, D., Polychronakos, C. and Froguel, P. (2007) 'A genome-wide association study identifies novel risk loci for type 2 diabetes', *Nature*, 445(7130), pp. 881-885.

Snel, M., Jonker, J.T., Schoones, J., Lamb, H., de Roos, A., Pijl, H., Smit, J.W., Meinders, A.E. and Jazet, I.M. (2012) 'Ectopic fat and insulin resistance: pathophysiology and effect of diet and lifestyle interventions', *Int J Endocrinol*, 2012, p. 983814.

Steinberg, S.J., Wang, S.J., Kim, D.G., Mihalik, S.J. and Watkins, P.A. (1999) 'Human Very-Long-Chain Acyl-CoA Synthetase: Cloning, Topography, and Relevance to Branched-Chain Fatty Acid Metabolism', *Biochemical and Biophysical Research Communications*, 257(2), pp. 615-621.

Steinthorsdottir, V., Thorleifsson, G., Reynisdottir, I., Benediktsson, R., Jonsdottir, T., Walters, G.B., Styrkarsdottir, U., Gretarsdottir, S., Emilsson, V., Ghosh, S., Baker, A., Snorradottir, S., Bjarnason, H., Ng, M.C.Y., Hansen, T., Bagger, Y., Wilensky, R.L., Reilly,

M.P., Adeyemo, A., Chen, Y., Zhou, J., Gudnason, V., Chen, G., Huang, H., Lashley, K., Doumatey, A., So, W.-Y., Ma, R.C.Y., Andersen, G., Borch-Johnsen, K., Jorgensen, T., van Vliet-Ostaptchouk, J.V., Hofker, M.H., Wijmenga, C., Christiansen, C., Rader, D.J., Rotimi, C., Gurney, M., Chan, J.C.N., Pedersen, O., Sigurdsson, G., Gulcher, J.R., Thorsteinsdottir, U., Kong, A. and Stefansson, K. (2007) 'A variant in CDKAL1 influences insulin response and risk of type 2 diabetes', *Nat Genet*, 39(6), pp. 770-775.

Sun, Y., Ren, M., Gao, G.-q., Gong, B., Xin, W., Guo, H., Zhang, X.-j., Gao, L. and Zhao, J.-j. (2008) 'Chronic palmitate exposure inhibits AMPK[alpha] and decreases glucose-stimulated insulin secretion from [beta]-cells: modulation by fenofibrate', *Acta Pharmacol Sin*, 29(4), pp. 443-450.

Tanaka, A., Okumoto, K. and Fujiki, Y. (2003) 'cDNA cloning and characterization of the third isoform of human peroxin Pex11p', *Biochemical and Biophysical Research Communications*, 300(4), pp. 819-823.

Tenenbaum, A., Motro, M., Fisman, E.Z., Adler, Y., Shemesh, J., Tanne, D., Leor, J., Boyko, V., Schwammenthal, E. and Behar, S. (2005) 'Effect of bezafibrate on incidence of type 2 diabetes mellitus in obese patients', *Eur Heart J*, 26(19), pp. 2032-8.

Teramoto, T., Shirai, K., Daida, H. and Yamada, N. (2012) 'Effects of bezafibrate on lipid and glucose metabolism in dyslipidemic patients with diabetes: the J-BENEFIT study', *Cardiovasc Diabetol*, 11, p. 29.

The Wellcome Trust Case Control Consortium (2007) 'Genome-wide association study of 14,000 cases of seven common diseases and 3,000 shared controls', *Nature*, 447(7145), pp. 661-678.

Thomas, C., Mackey, M.M., Diaz, A.A. and Cox, D.P. (2009) 'Hydroxyl radical is produced via the Fenton reaction in submitochondrial particles under oxidative stress: implications for diseases associated with iron accumulation', *Redox Rep*, 14(3), pp. 102-8.

Thoms, S. and Erdmann, R. (2005) 'Dynamin-related proteins and Pex11 proteins in peroxisome division and proliferation', *FEBS Journal*, 272(20), pp. 5169-5181.

Thörn, K. and Bergsten, P. (2010) 'Fatty acid-induced oxidation and triglyceride formation is higher in insulin-producing MIN6 cells exposed to oleate compared to palmitate', *Journal of Cellular Biochemistry*, 111(2), pp. 497-507.

Tiedge, M., Lortz, S., Drinkgern, J. and Lenzen, S. (1997) 'Relation Between Antioxidant Enzyme Gene Expression and Antioxidative Defense Status of Insulin-Producing Cells', *Diabetes*, 46(11), pp. 1733-1742.

Titorenko, V.I. and Mullen, R.T. (2006) 'Peroxisome biogenesis: the peroxisomal endomembrane system and the role of the ER', *The Journal of Cell Biology*, 174(1), pp. 11-17.

Unger, R.H. (1997) 'How obesity causes diabetes in Zucker diabetic fatty rats', *Trends in Endocrinology and Metabolism*, 8(7), pp. 276-282.

Unger, R.H. and Zhou, Y.T. (2001) 'Lipotoxicity of beta-cells in obesity and in other causes of fatty acid spillover', *Diabetes*, 50(suppl 1), p. S118.

van Herpen, N.A. and Schrauwen-Hinderling, V.B. (2008) 'Lipid accumulation in non-adipose tissue and lipotoxicity', *Physiology & Behavior*, 94(2), pp. 231-241.

van Roermund, C.W.T., Tabak, H.F., van den Berg, M., Wanders, R.J.A. and Hettema, E.H. (2000) 'Pex11p Plays a Primary Role in Medium-Chain Fatty Acid Oxidation, a Process That Affects Peroxisome Number and Size in Saccharomyces cerevisiae', *The Journal of Cell Biology*, 150(3), pp. 489-498.

Van Veldhoven, P.P. (2010) 'Biochemistry and genetics of inherited disorders of peroxisomal fatty acid metabolism', *Journal of Lipid Research*, 51(10), pp. 2863-2895.

Verhoeven, N.M., Roe, D.S., Kok, R.M., Wanders, R.J.A., Jakobs, C. and Roe, C.R. (1998) 'Phytanic acid and pristanic acid are oxidized by sequential peroxisomal and mitochondrial reactions in cultured fibroblasts', *Journal of Lipid Research*, 39(1), pp. 66-74.

Verhoeven, N.M., Schor, D.S.M., ten Brink, H.J., Wanders, R.J.A. and Jakobs, C. (1997) 'Resolution of the Phytanic Acid [alpha]-Oxidation Pathway: Identification of Pristanal as Product of the Decarboxylation of 2-Hydroxyphytanoyl-CoA', *Biochemical and Biophysical Research Communications*, 237(1), pp. 33-36.

Wanders, R.J.A. (2004) 'Peroxisomes, lipid metabolism, and peroxisomal disorders', *Molecular Genetics and Metabolism*, 83(1-2), pp. 16-27.

Wanders, R.J.A., Ferdinandusse, S., Brites, P. and Kemp, S. (2010) 'Peroxisomes, lipid metabolism and lipotoxicity', *Biochimica et Biophysica Acta (BBA) - Molecular and Cell Biology of Lipids*, 1801(3), pp. 272-280.

Wanders, R.J.A. and Waterham, H.R. (2005) 'Peroxisomal disorders I: biochemistry and genetics of peroxisome biogenesis disorders', *Clinical Genetics*, 67(2), pp. 107-133.

Wanders, R.J.A. and Waterham, H.R. (2006) 'Biochemistry of mammalian peroxisomes revisited', *Annual Review of Biochemistry*, 75, pp. 295-332.

Watson, M.L., Macrae, K., Marley, A.E. and Hundal, H.S. (2011) 'Chronic Effects of Palmitate Overload on Nutrient-Induced Insulin Secretion and Autocrine Signalling in Pancreatic MIN6 Beta Cells', *PLoS ONE*, 6(10), p. e25975.

Welsh, N., Margulis, B., Borg, L.A., Wiklund, H.J., Saldeen, J., Flodstrom, M., Mello, M.A., Andersson, A., Pipeleers, D.G., Hellerstrom, C. and et al. (1995) 'Differences in the expression of heat-shock proteins and antioxidant enzymes between human and rodent pancreatic islets: implications for the pathogenesis of insulin-dependent diabetes mellitus', *Mol Med*, 1(7), pp. 806-20.

Weng, H., Ji, X., Naito, Y., Endo, K., Ma, X., Takahashi, R., Shen, C., Hirokawa, G., Fukushima, Y. and Iwai, N. (2013) 'Pex11alpha deficiency impairs peroxisome elongation and division and contributes to nonalcoholic fatty liver in mice', *Am J Physiol Endocrinol Metab*, 304(2), pp. E187-96.

WHO (1999) *Definition, Diagnosis and Classification of Diabetes Mellitus and its Complications. Part 1: Diagnosis and Classification of Diabetes Mellitus*. World Health Organization.

WHO (2006) *Definition and diagnosis of diabetes mellitus and intermediate hyperglycaemia: Report of a WHO/IDF consultation*. World Health Organization and International Diabetes Federation.

WHO (2013) *Diabetes Program*. Available at: http://www.who.int/diabetes/en/ (Accessed: 14/01/14).

Wild, S., Roglic, G., Green, A., Sicree, R. and King, H. (2004) 'Global Prevalence of Diabetes', *Diabetes Care*, 27(5), pp. 1047-1053.

Wilding, J.P. (2007) 'The importance of free fatty acids in the development of Type 2 diabetes', *Diabet Med*, 24(9), pp. 934-45.

Yamauchi, T., Kamon, J., Waki, H., Terauchi, Y., Kubota, N., Hara, K., Mori, Y., Ide, T., Murakami, K., Tsuboyama-Kasaoka, N., Ezaki, O., Akanuma, Y., Gavrilova, O., Vinson, C., Reitman, M.L., Kagechika, H., Shudo, K., Yoda, M., Nakano, Y., Tobe, K., Nagai, R., Kimura, S., Tomita, M., Froguel, P. and Kadowaki, T. (2001) 'The fat-derived hormone adiponectin reverses insulin resistance associated with both lipoatrophy and obesity', *Nat Med*, 7(8), pp. 941-946.

Yu, C., Chen, Y., Cline, G.W., Zhang, D., Zong, H., Wang, Y., Bergeron, R., Kim, J.K., Cushman, S.W., Cooney, G.J., Atcheson, B., White, M.F., Kraegen, E.W. and Shulman, G.I. (2002) 'Mechanism by Which Fatty Acids Inhibit Insulin Activation of Insulin Receptor Substrate-1 (IRS-1)-associated Phosphatidylinositol 3-Kinase Activity in Muscle', *Journal of Biological Chemistry*, 277(52), pp. 50230-50236.

Zeggini, E., Scott, L.J., Saxena, R., Voight, B.F., Marchini, J.L., Hu, T., de Bakker, P.I., Abecasis, G.R., Almgren, P., Andersen, G., Ardlie, K., Bostrom, K.B., Bergman, R.N., Bonnycastle, L.L., Borch-Johnsen, K., Burtt, N.P., Chen, H., Chines, P.S., Daly, M.J., Deodhar, P., Ding, C.J., Doney, A.S., Duren, W.L., Elliott, K.S., Erdos, M.R., Frayling, T.M., Freathy, R.M., Gianniny, L., Grallert, H., Grarup, N., Groves, C.J., Guiducci, C., Hansen, T., Herder, C., Hitman, G.A., Hughes, T.E., Isomaa, B., Jackson, A.U., Jorgensen, T., Kong, A., Kubalanza, K., Kuruvilla, F.G., Kuusisto, J., Langenberg, C., Lango, H., Lauritzen, T., Li, Y., Lindgren, C.M., Lyssenko, V., Marvelle, A.F., Meisinger, C., Midthjell, K., Mohlke, K.L., Morken, M.A., Morris, A.D., Narisu, N., Nilsson, P., Owen, K.R., Palmer, C.N., Payne, F., Perry, J.R., Pettersen, E., Platou, C., Prokopenko, I., Qi, L., Qin, L., Rayner, N.W., Rees, M., Roix, J.J., Sandbaek, A., Shields, B., Sjogren, M., Steinthorsdottir, V., Stringham, H.M., Swift, A.J., Thorleifsson, G., Thorsteinsdottir, U., Timpson, N.J., Tuomi, T., Tuomilehto, J., Walker, M., Watanabe, R.M., Weedon, M.N., Willer, C.J., Illig, T., Hveem, K., Hu, F.B., Laakso, M., Stefansson, K., Pedersen, O., Wareham, N.J., Barroso, I., Hattersley, A.T., Collins, F.S., Groop, L., McCarthy, M.I., Boehnke, M. and Altshuler, D. (2008) 'Meta-analysis of genome-wide association data and large-scale replication identifies additional susceptibility loci for type 2 diabetes', *Nat Genet*, 40(5), pp. 638-45.

Zeggini, E., Weedon, M.N., Lindgren, C.M., Frayling, T.M., Elliott, K.S., Lango, H., Timpson, N.J., Perry, J.R.B., Rayner, N.W., Freathy, R.M., Barrett, J.C., Shields, B., Morris, A.P., Ellard, S., Groves, C.J., Harries, L.W., Marchini, J.L., Owen, K.R., Knight, B., Cardon, L.R., Walker, M., Hitman, G.A., Morris, A.D., Doney, A.S.F., The Wellcome Trust Case Control, C., McCarthy, M.I. and Hattersley, A.T. (2007) 'Replication of Genome-Wide Association Signals in UK Samples Reveals Risk Loci for Type 2 Diabetes', *Science*, 316(5829), pp. 1336-1341.

Zeng, H.T., Fu, Y.C., Yu, W., Lin, J.M., Zhou, L., Liu, L. and Wang, W. (2013) 'SIRT1 prevents atherosclerosis via liverXreceptor and NFkappaB signaling in a U937 cell model', *Mol Med Rep*, 8(1), pp. 23-8.

Zhang, C.-Y., Baffy, G., Perret, P., Krauss, S., Peroni, O., Grujic, D., Hagen, T., Vidal-Puig, A.J., Boss, O., Kim, Y.-B., Zheng, X.X., Wheeler, M.B., Shulman, G.I., Chan, C.B. and Lowell, B.B. (2001) 'Uncoupling Protein-2 Negatively Regulates Insulin Secretion and Is a Major Link between Obesity, β Cell Dysfunction, and Type 2 Diabetes', *Cell*, 105(6), pp. 745-755.

Zhou, Y.P. and Grill, V. (1995) 'Long term exposure to fatty acids and ketones inhibits B-cell functions in human pancreatic islets of Langerhans', *J Clin Endocrinol Metab*, 80(5), pp. 1584-90.

Ziemke, F. and Mantzoros, C.S. (2010) 'Adiponectin in insulin resistance: lessons from translational research', *Am J Clin Nutr*, 91(1), pp. 258S-261.

Zimmet, P., Alberti, K.G.M.M. and Shaw, J. (2001) 'Global and societal implications of the diabetes epidemic', *Nature*, 414(6865), pp. 782-787.